TESIS DE LA UNIVERSIDAD DE ZARAGOZA

2013

133

Andersson Arias Aguilar

Complejos polinucleares de paladio y platino con el grupo difenilfosfanuro: Diseño, síntesis, caracterización y reactividad

Departamento
Química Inorgánica

Director/es
Fortuño Turmo, Consuelo

ISSN 2254-7606

Prensas de la Universidad
Universidad Zaragoza

Universidad Zaragoza
1542

Tesis Doctoral

COMPLEJOS POLINUCLEARES DE PALADIO Y PLATINO CON EL GRUPO DIFENILFOSFANURO: DISEÑO, SÍNTESIS, CARACTERIZACIÓN Y REACTIVIDAD

Autor

Andersson Arias Aguilar

Director/es

Fortuño Turmo, Consuelo

UNIVERSIDAD DE ZARAGOZA

Química Inorgánica

COMPLEJOS POLINUCLEARES DE PALADIO Y PLATINO CON EL GRUPO DIFENILFOSFANURO: DISEÑO, SÍNTESIS, CARACTERIZACIÓN Y REACTIVIDAD

Memoria presentada en la Facultad de Ciencias de la Universidad de Zaragoza para optar al grado de Doctor en Ciencias, Sección Químicas, por el Licenciado

Andersson Arias Aguilar

Apartado A

Esta Tesis Doctoral se presenta mediante un compendio de cinco trabajos publicados en revistas científicas con un índice de impacto incluido en la relación de revistas del *Journal Citation Reports*.

Las referencias de dichas publicaciones son las siguientes:

Título: “Formation of P-C Bond through Reductive Coupling between Bridging Phosphido and Benzoquinolinate Groups. Isolation of Complexes of the Pt(II)/Pt(IV)/Pt(II) Sequence”.
Autores: Andersson Arias, Juan Forniés, Consuelo Fortuño, Antonio Martín, Mario Latronico, Piero Mastrorilli, Stefano Todisco, Vito Gallo.
Revista: *Inorganic Chemistry* 2012, 51, 12682-12696. Factor de Impacto: 4.593; 5/43 de la categoría "Chemistry, Inorganic and Nuclear" de ISI WoK.

Título: “Oxidatively Induced P-O Bond Formation through Reductive Coupling between Phosphido and Acetylacetonate, 8-Hydroxyquinolinate, and Picolinate Groups”
Autores: Andersson Arias, Juan Forniés, Consuelo Fortuño, Antonio Martín, Piero Mastrorilli, Stefano Todisco, Mario Latronico, Vito Gallo.
Revista: *Inorganic Chemistry* 2013, 52, 5493-5506. Factor de Impacto: 4.593; 5/43 de la categoría "Chemistry, Inorganic and Nuclear" de ISI WoK.

Título: “Donor Behaviour of Anionic and Asymmetric Phosphanido Derivatives of Platinum and Palladium”
Autores: Andersson Arias, Juan Forniés, Consuelo Fortuño, Antonio Martín, Piero Mastrorilli, Vito Gallo, Mario Latronico, Stefano Todisco.
Revista: *European Journal of Inorganic Chemistry*, doi: 10.1002/ejic.20130088. Factor de Impacto: 3.120; 11/43 de la categoría "Chemistry, Inorganic and Nuclear" de ISI WoK.

Título: “Addition of Nucleophiles to Phosphanido Derivatives of Pt(III): Formation of P-C, P-N and P-O Bonds”
Autores: Andersson Arias, Juan Forniés, Consuelo Fortuño, Susana Ibáñez, Antonio Martín, Piero Mastrorilli, Vito Gallo, Stefano Todisco.
Revista: *Inorganic Chemistry*, doi: 10.1021/ic401689c. Factor de Impacto: 4.593; 5/43 de la categoría "Chemistry, Inorganic and Nuclear" de ISI WoK.

Título: “From a di- and trinuclear phosphanido fragment to tetra- and hexanuclear platinum(II) complexes”
Autores: Andersson Arias, Juan Forniés, Consuelo Fortuño, Antonio Martín,
Revista: *Inorganica Chimica Acta* 2013, 407, 189-196. Factor de Impacto: 1.687; 22/43 de la categoría "Chemistry, Inorganic and Nuclear" de ISI WoK.

Apartado B

CONSUELO FORTUÑO TURMO, Profesora Titular de Universidad del Departamento de Química Inorgánica de la Escuela de Ingeniería y Arquitectura de la Universidad de Zaragoza

CERTIFICA:

Que la presente Memoria titulada “COMPLEJOS POLINUCLEARES DE PALADIO Y PLATINO CON EL GRUPO DIFENILFOSFANURO: DISEÑO, SÍNTESIS, CARACTERIZACIÓN Y REACTIVIDAD” ha sido realizada en el Departamento de Química Inorgánica de la Universidad de Zaragoza y en el Instituto de Síntesis Química y Catálisis Homogénea (I.S.Q.C.H) bajo mi dirección, que se ajusta en su totalidad al proyecto de tesis aprobado en su momento y que cuenta con mi autorización para su presentación como Compendio de Publicaciones para que sea calificada como Tesis Doctoral.

Zaragoza, 1 de octubre de 2013.

Fdo: Consuelo Fortuño Turmo

Índice

Apartado C

Introducción general, presentación de los trabajos y justificación de su unidad temática

Los grupos dialquil y diarilfosfanuro, PR_2, han sido muy utilizados como ligandos en complejos de metales de transición.[1] Aunque se conocen ejemplos en los que el grupo fosfanuro se coordina únicamente a un centro metálico, es decir, actúa como ligando terminal[2-8] y otros en los que se enlaza como ligando puente entre tres centros metálicos,[9-19] el modo de coordinación usual de estos grupos es como ligando puente entre dos centros metálicos, $M(\mu\text{-}PR_2)_xM'$. Estos últimos sistemas presentan gran flexibilidad y pueden mantener los centros metálicos en un rango de distancias amplio y por tanto ángulos de enlace M–P–M' diferentes. De esta forma, se han reportado ángulos de enlace M–P–M en complejos con grupos fosfanuro puentes en un rango que abarca entre 65º [20] y 138º.[21]

La química de los complejos de metales de transición con ligandos fosfanuro puentes ha sido estudiada durante los últimos cincuenta años; estos grupos se consideraban generalmente como ligandos inertes capaces de formar complejos polinucleares y clústeres con reducida fragmentación, debido a que la estabilidad de los enlaces fósforo–metal permite conservar el sistema $M(\mu\text{-}PR_2)_xM'$ durante los diversos procesos de reacción. Aunque esto es cierto de forma habitual, desde inicios de la década de 1980 hay evidencia de casos de ruptura de enlaces P–M[22,23] e incluso de acoplamiento entre un grupo fosfanuro y otro ligando de la molécula;[24,25] hoy en día se reconocen estos ligandos como grupos capaces de presentar una variada reactividad.[1]

Las características especiales de los grupos fosfanuro –tendencia a actuar como puentes, notable flexibilidad y estabilidad general– han permitido el diseño y síntesis de complejos polinucleares con situaciones estructurales muy distintas como las que se recogen a continuación:

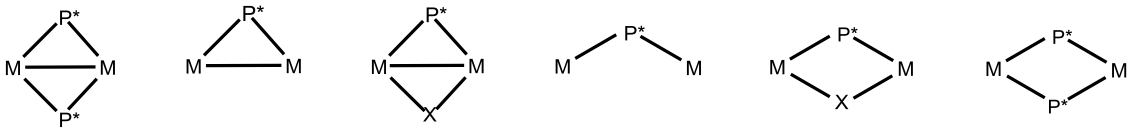

P* = PR_2

Esquema 1

Como cabe esperar, estas diferencias en los entornos químicos de los átomos de fósforo de los grupos fosfanuro puentes –dos grupos PR_2 actuando como puentes entre dos centros metálicos (Esquema 1, **A** y **F**), un solo grupo uniendo estos centros (**B** y **D**) o un grupo PR_2 y otro ligando actuando como puentes (**C** y **E**) – se ven reflejadas en los espectros de RMN de ^{31}P de estos complejos. De esta forma, desde que por primera vez se investigó la relación entre los desplazamientos químicos de ^{31}P de grupos fosfanuro puentes y su modo de coordinación en los complejos,[26] el análisis de datos de RMN de ^{31}P de derivados polinucleares de metales de transición con grupos PR_2 actuando como puentes[26-36] permitió obtener una primera conclusión al respecto: de forma general, los datos indican que los desplazamientos químicos correspondientes a grupos fosfanuro que unen dos centros metálicos que presentan enlace M–M (Esquema 1, **A** – **C**) aparecen a *campo bajo* (en un rango entre δ 400 y δ 50,

aproximadamente), mientras que los de grupos que unen dos centros sin enlace M–M (**D** – **F**) aparecen a *campo alto* (en un rango entre δ 50 y δ –200, aproximadamente); sin embargo, existen excepciones a esta correlación.[37-39]

A fecha de hoy, la gran cantidad de datos disponibles ha permitido relacionar los desplazamientos químicos no solo con la presencia o ausencia de enlace metal–metal, sino también con el número y la naturaleza de los grupos que actúan como puentes entre los dos centros. Así, los datos de RMN de ^{31}P han permitido observar una tendencia en los desplazamientos químicos en derivados con grupos difenilfosfanuro puentes (μ-PPh_2), tal como se muestra en el Esquema 1, en donde las señales correspondientes a sistemas de dos grupos difenilfosfanuro puentes entre dos centros metálicos que presentan enlace metal–metal (**A**) se encuentran a campo bajo, con valores mayores a δ 200; en un rango aproximado entre δ 200 y δ 50, se encuentran las señales de un grupo μ-PPh_2 entre dos centros metálicos que presentan enlace M–M, que puede actuar solo (**B**) o con otro ligando puente (**C**); a mayor campo, se ubican generalmente las señales correspondientes a un grupo difenilfosfanuro puente entre dos centros metálicos que no presentan enlace metal–metal, actuando solo (**D**) o con otro ligando puente (**E**); y finalmente, a alto campo se observan las señales correspondientes a un sistema de dos grupos difenilfosfanuro actuando como puentes entre dos centros metálicos que no presentan enlace M–M (**F**). Cabe destacar que estas "zonas" del espectro de RMN de ^{31}P respecto a las señales de grupos μ-PPh_2 entre dos centros metálicos se han establecido de forma empírica y que los límites entre ellas no son estrictos, por lo que debe tenerse cuidado al asignar señales de nuevos derivados con ligandos μ-PPh_2.

Dentro de los estudios realizados por nuestro grupo de investigación, la preparación *in situ* de los complejos *cis*-$[(C_6F_5)_2M(PPh_2)_2]^{2-}$ (M = Pd, Pt; Ph = C_6H_5)[40] ha permitido la síntesis de numerosos derivados polinucleares de paladio y platino (II) enlazados a través de grupos difenilfosfanuro que actúan como ligandos puentes entre, habitualmente, dos centros metálicos. Además, los grupos pentafluorofenilo (C_6F_5) unidos a los centros de paladio y platino suelen dar lugar a enlaces M–C que se mantienen durante los procesos de reacción, de manera que conservan su geometría *cis* en torno al centro metálico al que están coordinados, bloqueando así una parte de la esfera de coordinación del metal. Finalmente, estos ligandos pueden ser estudiados por espectroscopia de IR y RMN de ^{19}F, que aportan información muy valiosa y complementaria a la de RMN de ^{31}P, ayudando a la caracterización de los complejos.

Además de la síntesis y caracterización de derivados con ligandos fosfanuro puentes, se ha estudiado su reactividad. Así, una parte del trabajo llevado a cabo en nuestro grupo de investigación ha sido el estudio del comportamiento de algunos difenilfosfanuro-derivados bi y trinucleares frente a agentes oxidantes, tales como I_2 y sales de Ag(I). La química del platino y paladio en altos estados de oxidación está recibiendo mucha atención en los últimos años, debido a que estas especies pueden experimentar transformaciones que son difícilmente accesibles de otra forma. En concreto, además de los procesos redox Pd(0)/Pd(II) involucrados en transformaciones catalíticas y en síntesis orgánica estudiados durante las últimas cuatro

décadas,[41,42] los ciclos y secuencias Pd(II)/Pd(IV) han empezado a estudiarse profusamente en los últimos diez años.[43] La forma habitual de obtención de estos complejos de M(IV) es la oxidación de las especies de M(II) y es conocido que en el caso de complejos binucleares, este proceso de oxidación puede dar lugar a especies M(II),M(IV) o también a especies M(III),M(III).[44-50]

Las sales de plata (I) se encuentran entre los agentes oxidantes más usados, particularmente con complejos de metales de transición, siendo sus potenciales de oxidación dependientes de la naturaleza del disolvente usado, lo que puede hacerlas muy versátiles; sin embargo, su comportamiento no es directo o previsible, ya que además de actuar como agente oxidante, puede observarse también la abstracción de halogenuros o la unión del centro de Ag(I) a otros átomos de ligandos coordinados.[51] Finalmente, existen muchos ejemplos de formación de aductos en los que el centro de Ag(I) se coordina a uno o varios centros metálicos; en algunos casos, estos complejos con enlaces M–Ag pueden considerarse como intermedios en las reacciones de transferencia de electrones entre M y Ag^+.[52-54]

El estudio del comportamiento de fosfanuro-derivados binucleares sintetizados en nuestro grupo hacia sales de plata (I) se ha llevado a cabo sobre derivados de paladio y platino (II) de fórmula general $[(C_6F_5)_2Pt(\mu\text{-}PPh_2)_2ML_2]^{n-}$ (L_2 = $2C_6F_5$, n = 2;[55] L_2 = acac (acetilacetonato), n = 1;[56] L_2 = $2PPh_3$ (trifenilfosfano), n = 0;[17] L_2 = phen (1,10-fenantrolina), n = 0;[18] L_2 = dppm (metilenbis(difenilfosfano)), n = 0;[18]), obteniendo ya sea complejos binucleares oxidados de tipo M(III)–M(III) o aductos que presenten enlace M(II)–Ag(I), tal como se muestra en el Esquema 2. Para M = Pt, L = C_6F_5, n = 2, la adición de $AgClO_4$ (relación molar 1:2) produce un proceso de transferencia de electrones, formando Ag^0 y un complejo binuclear de Pt(III)–Pt(III) con enlace metal–metal de tipo **A** (Esquema 2).[55] Cabe destacar que en este complejo los dos centros metálicos oxidados presentan ambos un entorno de coordinación plano cuadrado, coplanares entre sí, y conteniendo el enlace Pt–Pt. Aunque existe un precedente de este tipo de complejos,[57] de forma general, los derivados binucleares de paladio y platino (III) encontrados en la bibliografía muestran los centros metálicos en un entorno octaédrico, con el enlace M–M perpendicular a los planos ecuatoriales de los centros metálicos.[46,48,49,57-68]

Para los fosfanuro-derivados con L_2 = acac, n = 1; con L_2 = phen, n = 0; y en el caso L_2 = dppm, n = 0, M = Pt, la adición de sales de Ag(I) da lugar a la formación de complejos de tipo **B** (Esquema 2), que adquieren una configuración de “libro abierto” para establecer uno o dos enlaces M(II)–Ag(I) (M = Pd, Pt).[18,56] Finalmente, para L_2 = $2PPh_3$, n = 0 y en el caso L_2 = dppm, n = 0, M = Pd, la reacción con sales de plata (I) produce complejos de tipo **C** (Esquema 2), en los que se observa que el enlace P–M(II) del fosfanuro-derivado es suficientemente básico como para formar un inusual enlace de 3c–2e con el centro de Ag(I).[17,18]

De los resultados obtenidos hasta el momento, se puede concluir que la adición de sales de plata (I) a fosfanuro-derivados binucleares de paladio y platino (II) produce complejos de tipo

A, **B** o **C**, dependiendo del ligando L_2; sin embargo, no es posible conocer de antemano si la compartición de electrones entre el complejo fosfanuro y el centro de Ag(I) producirá únicamente la coordinación del catión de la sal al fosfanuro-derivado (complejos de tipo **B** o **C**) o si este proceso desencadena la transferencia de electrones y la oxidación de ambos centros metálicos (complejos de tipo **A**), con formación de Ag^0.

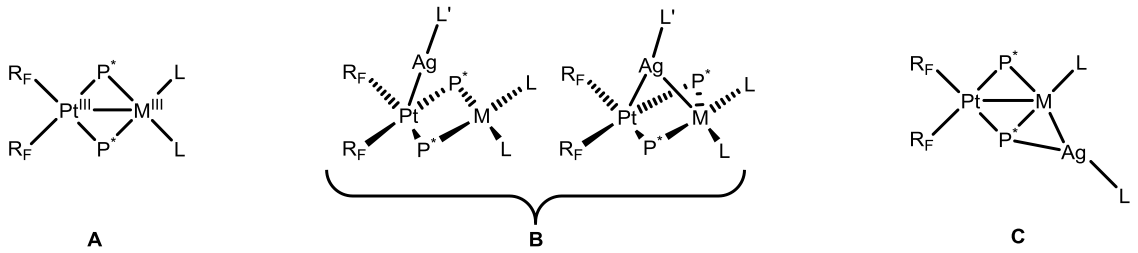

M = Pd, Pt
$R_F = C_6F_5$
P* = PPh_2

Esquema 2

Por otra parte, la adición de sales de plata (I) a fosfanuro-derivados trinucleares de platino (II) de fórmula general $[(C_6F_5)_2Pt(\mu\text{-}PPh_2)_2Pt(\mu\text{-}PPh_2)_2PtL_2]^{n-}$ ($L_2 = 2C_6F_5$, n = 2;[69] L_2 = acac, n = 1;[70] L_2 = phen, n = 0;[18] $L_2 = 2PPh_3$, n = 0;[18]) produce en todos los casos complejos de tipo **A** (Esquema 2), con dos centros de platino en estado de oxidación III y presentando enlace M–M. En ningún caso se observó la formación de posibles intermedios de tipo **B** o **C**, y además, el enlace Pt(III)–Pt(III) siempre se forma entre el átomo de Pt central y el Pt unido a los grupos C_6F_5; en ningún caso el centro metálico unido a los ligandos L_2 está involucrado en el enlace Pt–Pt.[18] Cuando la sal de plata (I) se añade sobre el derivado heterotrinuclear $[(C_6F_5)_2Pt(\mu\text{-}PPh_2)_2Pd(\mu\text{-}PPh_2)_2Pt(C_6F_5)_2]^{2-}$, el proceso de oxidación evoluciona con un llamativo acoplamiento entre dos grupos $\mu\text{-}PPh_2$ y formación de enlace P–P.[71]

Los halógenos X_2 son agentes oxidantes económicos, fácilmente purificables, ampliamente disponibles y solubles en una gran variedad de disolventes orgánicos. Su solubilidad en disolventes no polares permite, en forma general, desarrollar métodos sencillos para aislar de forma pura los productos organometálicos oxidados. Sin embargo, los halógenos no actúan únicamente como agentes oxidantes y es común que existan reacciones que compitan con la sola transferencia de electrones; incluso, durante un proceso de oxidación, los halógenos pueden no actuar solamente como electrófilos, sino que los halogenuros formados durante la reducción de halógenos pueden actuar como nucleófilos proclives a coordinarse a los centros metálicos del sustrato.[51]

Se ha estudiado la adición de I_2 sobre complejos binucleares de paladio y platino (II) con fórmula general $[(C_6F_5)_2M(\mu\text{-}PPh_2)_2M'L_2]^{n-}$ (L = C_6F_5, n = 2;[72] Esquema 3a. L = CH_3CN, n = 0;[73] Esquema 3b). El resultado final de estas reacciones son nuevos derivados de paladio y platino (II) que presentan un nuevo ligando: $Ph_2P\text{–}C_6F_5$. Este ligando es el resultado del acoplamiento reductor entre un grupo difenilfosfanuro puente y un grupo pentafluorofenilo, con formación de

enlace P–C. Hoy en día este proceso de formación de fosfano a partir de un grupo fosfanuro puente es un proceso ya establecido,[24,25,74-76] aunque menos común que el proceso inverso, el de formación de ligandos fosfanuro a través de activación térmica de enlaces P–C de fosfanos terciarios, que es una conocida vía de síntesis de fosfanuro-derivados.[25,77-86]

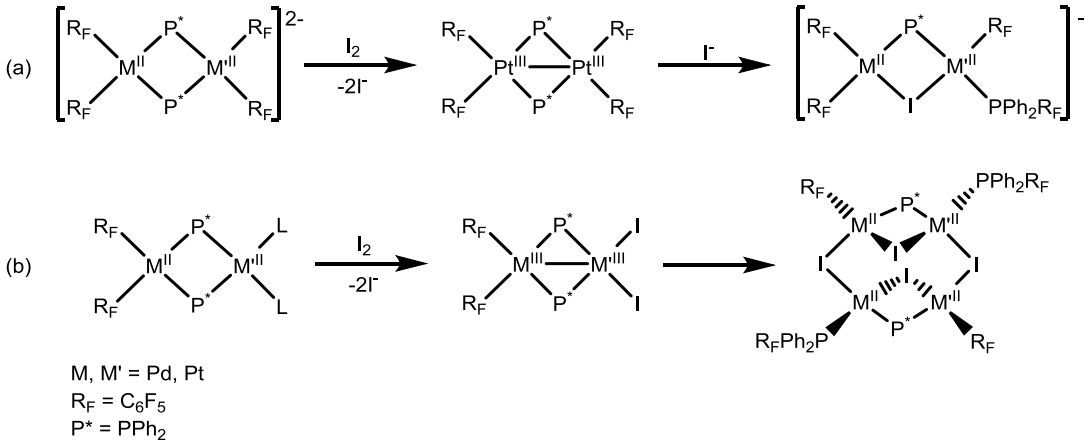

Esquema 3

En ambos casos ha sido posible aislar los intermedios de reacción, que corresponden a derivados de platino y/o paladio con estado de oxidación formal III y enlace metal–metal. De estos intermedios, el derivado simétrico $[(C_6F_5)_2Pt^{III}(\mu\text{-}PPh_2)_2Pt^{III}(C_6F_5)_2]$(Pt–Pt) (Esquema 3a) también se obtuvo mediante la oxidación del sustrato con una sal de plata (I).[55]

Finalmente, la adición de I_2 sobre fosfanuro-derivados trinucleares de fórmula general $[(C_6F_5)_2Pt(\mu\text{-}PPh_2)_2M(\mu\text{-}PPh_2)_2Pt(C_6F_5)_2]^{2-}$ (M = Pd, Pt) produce en ambos casos la formación nuevos ligandos fosfano. En el caso del complejo homonuclear de platino, al igual que para el complejo binuclear, la reacción con I_2 produce el acoplamiento entre un grupo difenilfosfanuro y uno pentafluorofenilo, con formación de enlace P–C (Esquema 4).[87] El intermedio de esta reacción, un complejo en el que dos centros metálicos presentan un estado de oxidación formal III y enlace metal–metal, también se ha obtenido previamente mediante la adición de una sal de plata (I) al sustrato.[69] Por otra parte, la adición de I_2 sobre el complejo heteronuclear produce una mezcla de dos productos isómeros, uno análogo al trinuclear de platino, con formación de enlace P–C y otro en el que el acoplamiento de dos grupos difenilfosfanuro produce el ligando tetrafenildifosfano, con formación de enlace P–P (Esquema 4).[70]

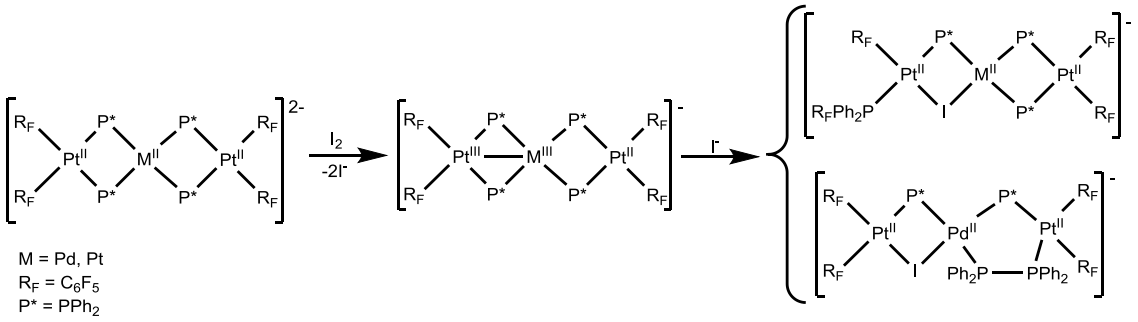

Esquema 4

De los estudios realizados hasta el momento se concluye que la adición de los agentes oxidantes I_2 y sales de plata (I) a fosfanuro-derivados de Pd/Pt(II) produce una transferencia de carga del sustrato al agente oxidante que puede ocasionar la oxidación de los centros metálicos, formando complejos bi y trinucleares insaturados con enlace Pt(III)–M(III) (M = Pd, Pt). En ocasiones, estos complejos no son suficientemente estables y pueden evolucionar, ya sea espontáneamente o inducidos por la presencia de un nucleófilo, mediante el acoplamiento reductor entre un grupo difenilfosfanuro y otro ligando –con formación de un ligando fosfano–, dando lugar a complejos con centros metálicos en estado de oxidación II. El predominio de cualquiera de estas posibilidades (transferencia de carga, oxidación o acoplamiento reductor) sobre las otras, depende tanto del agente oxidante empleado, así como del centro metálico (Pd o Pt) y de los ligandos unidos a estos, y aún no es posible conocer *a priori* cuál de los procesos se observará al realizar la adición sobre un determinado sustrato.

En este trabajo que se presenta como Tesis Doctoral nos hemos propuesto profundizar en los procesos de transformación del grupo difenilfosfanuro en fragmentos de tipo "M(μ-$PPh_2)_2$M'". Con este objeto, se ha llevado a cabo:

Diseño y la síntesis de nuevos derivados binucleares de Pd/Pt(II) con fórmula general $[(C_6F_5)_2M(\mu\text{-}PPh_2)_2M'(C\text{^}N]^-$, y estudiado su reactividad frente a I_2 (*Inorganic Chemistry* **2012**, *51*, 12682).

Diseño y la síntesis de nuevos derivados binucleares de Pd/Pt(II) con fórmula general $[(C_6F_5)_2M(\mu\text{-}PPh_2)_2M'(O\text{^}N]^-$, y estudiado su reactividad frente a I_2 (*Inorganic Chemistry* **2013**, *52*, 5493).

Estudio del comportamiento de los derivados anteriores de tipo $[(C_6F_5)_2M(\mu\text{-}PPh_2)_2M'(C\text{^}N]^-$ y $[(C_6F_5)_2M(\mu\text{-}PPh_2)_2M'(O\text{^}N]^-$ frente a la sal de plata (I) $[Ag(OClO_3)PPh_3]$ (*European Journal of Inorganic Chemistry* **2013**, doi: 10.1002/ejic.20130088).

Estudio de la adición de diferentes nucleófilos a los complejos $[(C_6F_5)_2Pt(\mu\text{-}PPh_2)_2Pt(C_6F_5)_2]$[55,72] y $[(C_6F_5)_2Pt(\mu\text{-}PPh_2)_2Pt(\mu\text{-}PPh_2)_2Pt(C_6F_5)_2]$[69] y comparado estos resultados con los obtenidos con el nucleófilo I^-[71,87] (*Inorganic Chemistry* **2013**, doi: 10.1021/ic401689c).

Finalmente, el desarrollo de las rutas sintéticas empleadas para la preparación de los nuevos complejos binucleares, también ha permitido la obtención de nuevos fosfanuro-derivados polinucleares de platino de alta nuclearidad y que confirman también la estabilidad de los enlaces P–M de fragmentos de tipo "$(C_6F_5)_2M(\mu\text{-}PPh_2)_2M$'" bajo diversas condiciones de reacción (*Inorganica Chimica Acta* **2013**, *407*, 189).

Como se acaba de exponer, los cinco trabajos presentados y mencionados anteriormente, continúan con una de las líneas de investigación de nuestro grupo. Los cinco trabajos constituyen una **unidad temática**, que es el diseño y síntesis de nuevos fosfanuro-derivados de paladio y platino y estudios de reactividad frente a agentes oxidantes y nucleófilos.

Apartado D

Copia de los trabajos publicados

Inorganic Chemistry

Article

pubs.acs.org/IC

Formation of P–C Bond through Reductive Coupling between Bridging Phosphido and Benzoquinolinate Groups. Isolation of Complexes of the Pt(II)/Pt(IV)/Pt(II) Sequence‡

Andersson Arias, Juan Forniés, Consuelo Fortuño,* and Antonio Martín

Departamento de Química Inorgánica, Instituto de Síntesis Química y Catálisis Homogénea, Universidad de Zaragoza—C.S.I.C., E-50009 Zaragoza, Spain

Mario Latronico, Piero Mastrorilli,* Stefano Todisco, and Vito Gallo

Dipartimento DICATECh del Politecnico di Bari and Istituto CNR-ICCOM, Via Orabona 4, I-70125 Bari, Italy

Supporting Information

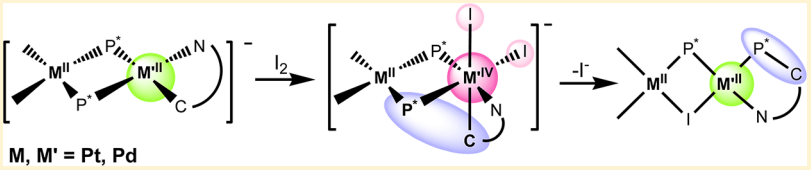

ABSTRACT: The rational synthesis of dinuclear asymmetric phosphanido derivatives of palladium and platinum(II), $[NBu_4][(R_F)_2M(\mu\text{-}PPh_2)_2M'(\kappa^2,N,C\text{-}C_{13}H_8N)]$ ($R_F = C_6F_5$; M = M′ = Pt, **1**; M = Pt, M′ = Pd, **2**; M = Pd, M′ = Pt, **3**; M = M′ = Pd, **4**), is described. Addition of I_2 to **1**–**4** gives complexes $[(R_F)_2M^{II}(\mu\text{-}PPh_2)(\mu\text{-}I)Pd^{II}\{PPh_2(C_{13}H_8N)\}]$ (M = M′ = Pt, **6**; M = Pt, M′ = Pd, **7**; M = M′ = Pd, **8**; M = Pd, M′ = Pt **10**) which contain the aminophosphane $PPh_2(C_{13}H_8N)$ ligand formed through a $Ph_2P/C^{\wedge}N$ reductive coupling on the mixed valence M(II)–M′(IV) $[NBu_4][(R_F)_2M^{II}(\mu\text{-}PPh_2)_2M'^{IV}(\kappa^2,N,C\text{-}C_{13}H_8N)I_2]$ complexes, which were identified for M^{II} = Pd, M'^{IV} = Pt (**9**), and isolated for M^{II} = Pt, M'^{IV} = Pt (**5**). Complex **5** showed an unusual dynamic behavior consisting in the exchange of two phenyl groups bonded to different P atoms, as well as a "through space" spin–spin coupling between *ortho*-F atoms of the pentafluorophenyl rings.

INTRODUCTION

Besides the well-established Pd(0)/Pd(II) redox-processes involved in a variety of palladium-catalyzed transformations and organic synthesis, Pd(II)/Pd(IV) cycles have been playing a complementary role in the past years.[2−19] Moreover, in addition to oxidation of Pd(II) precursors to Pd(IV) complexes, the formation of bimetallic Pd(III) complexes has been also reported.[2,20−24] The formal oxidation state +3 is not dominant either in platinum and in palladium chemistry, and although a quite large number of dinuclear derivatives of Pt(III) are known today,[25−34] only few bimetallic Pd(III) complexes have been reported.[35−38] In some cases the presence of a true bimetallic M(III)–M(III) complex or a M(II)–M(IV) one (B and D, respectively, in Chart 1) is still an open question.[39,40]

In the course of our current research on palladium or platinum phosphanido derivatives, we have reported the synthesis of type A (Chart 1) dinuclear complexes $[NBu_4]_2[(R_F)_2M(\mu\text{-}PPh_2)_2M'(R_F)_2]$ $R_F = C_6F_5$, M = M′ = Pd, Pt; M = Pt, M′ = Pd and their reactions with I_2 (1:1 molar ratio) which result in the formation of different types of complexes depending on the M′ (Pt or Pd) and on the reaction conditions. The B type diplatinum complex $[(R_F)_2Pt^{III}(\mu\text{-}PPh_2)_2Pt^{III}(R_F)_2]$[41,42] displaying a Pt(III)–Pt(III) bond is obtained through this reaction. Presumably, the bridging phosphanido ligands prevent the formation of a lantern type Pt(III)–Pt(III) compound (Chart 1C), which are by far more common in the context of Pt^{3+} dimers.[25−34] In no case we have previously observed that the oxidation of a Pt(II)–Pt(II) phosphanido complex with I_2 (1:1 molar ratio) occurs only for

Chart 1

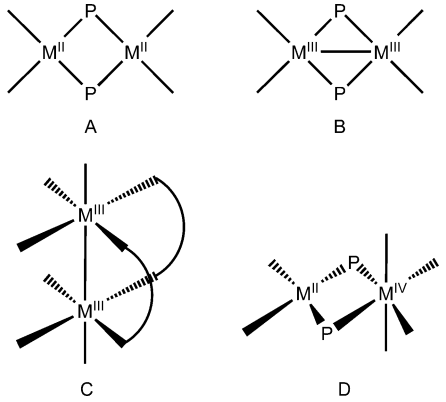

Received: June 19, 2012
Published: November 9, 2012

   dx.doi.org/10.1021/ic301298p | *Inorg. Chem.* 2012, 51, 12682–12696

Scheme 1

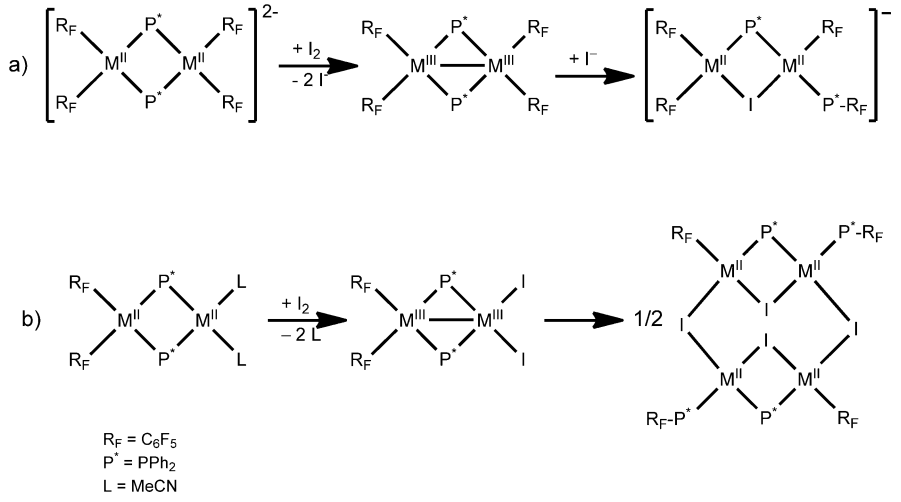

Scheme 2

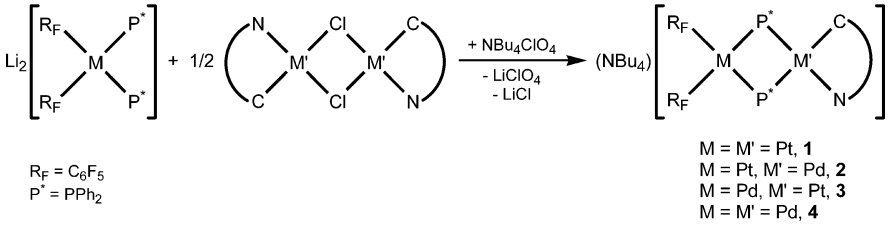

Table 1. $^{31}P\{^1H\}$ NMR Data of 1−10 in Deuteroacetone with δ in ppm, J in Hz

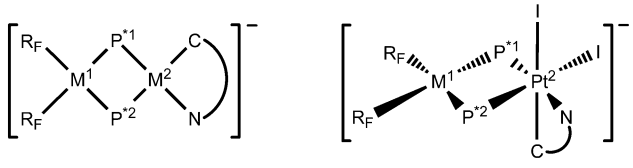

1-4 5, 9

6-8, 10 11

complex	δP^1	δP^2	$^2JP^1,P^2$	$^1JPt^1,P^1$	$^1JPt^2,P^1$	$^1JPt^1,P^2$	$^1JPt^2,P^2$	δPt^1	δPt^2
1	−107.9	−118.9	116	1937	2810	1646	1320	−3889[a]	−3717[a]
2	−78.8	−116.6	160	1806		1530		−3909	
3	−95.9	−111.7	160		2658		1213		−3738
4	−58.0	−107.0	204						
5	−115.5	−107.5	126	2032	1807	2189	1270	−3806[b]	−2917[b]
9	−97.7	−89.1	161		1680		1121		−2966
6	−11.4	14.2	2	1846	2513	37	4435	−4238	−4397
7	55.2	37.5	40	1864		97		−4315	
8	66.0	42.3	36						
10	7.9	18.6	2		2542		4307		−4416
11	−5.4	8.7	381		3317				n.d.

[a]$^2JPt-Pt$ = 541 Hz. [b]$^2JPt-Pt$ = ca. 100 Hz.

one of the metal centers forming a mixed valence Pt(II)−Pt(IV) compound (Chart 1D). The heterobinuclear complex M = Pt, M′ = Pd or the homobinuclear palladium derivative react with I_2 (1:1 molar ratio) forming $[NBu_4][(R_F)_2M(\mu\text{-}PPh_2)(\mu\text{-}I)M'(R_F)(PPh_2R_F)]$[42] which can be considered as the result of the oxidation of the binuclear M(II) to the unstable

dx.doi.org/10.1021/ic301298p | Inorg. Chem. 2012, 51, 12682−12696

Scheme 3

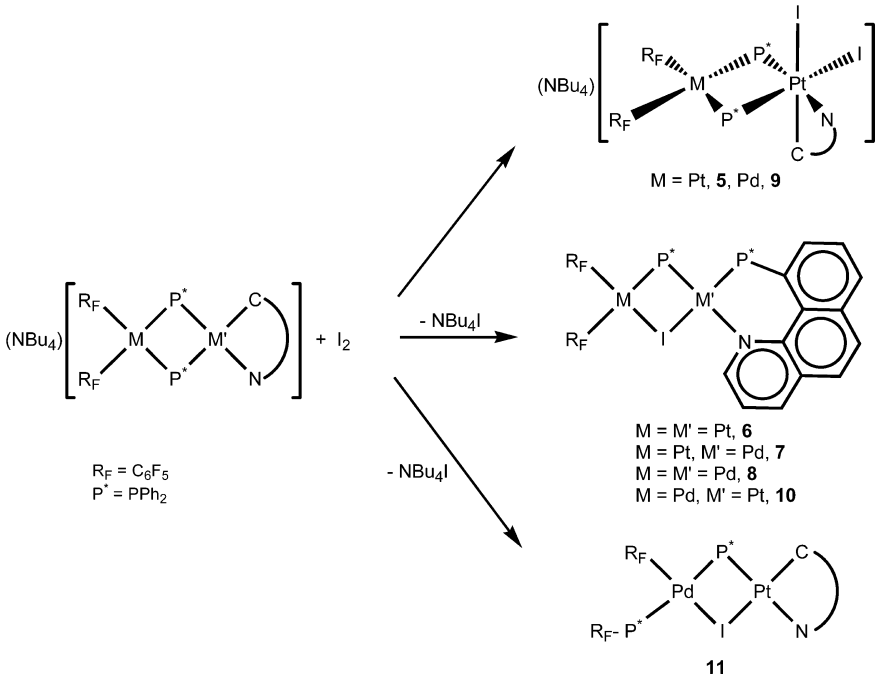

M(III)−M(III) which evolves rapidly, through a PPh_2/C_6F_5 reductive coupling, to the formation of the M(II)−M(II) compound. In fact the Pt(III)−Pt(III) derivative evolves, in the presence of I^-, to the corresponding Pt(II)−Pt(II) compound $[NBu_4][(R_F)_2Pt(\mu\text{-}PPh_2)(\mu\text{-}I)Pt(R_F)(PPh_2R_F)]$[42] (Scheme 1a).

A similar behavior has been observed in the reaction of the dinuclear neutral complexes $[(R_F)_2M(\mu\text{-}PPh_2)_2M'(CH_3CN)_2]$ with I_2 (Scheme 1b).[43,44] Addition of I_2 to these complexes produces the dinuclear Pt(III)−M(III) complexes $[(R_F)_2Pt^{III}(\mu\text{-}PPh_2)_2M^{III}I_2]$ (M = Pt, Pd) which evolve to the tetranuclear platinum and/or palladium(II) complexes $[M_4(\mu\text{-}PPh_2)_2(\mu\text{-}I)_4(R_F)_2(PPh_2R_F)_2]$, through a reductive coupling between a PPh_2 and a R_F groups and formation of the PPh_2R_F ligand (Scheme 1b).[44]

In this Article we report on the synthesis of the new asymmetric dinuclear phosphanido complexes of general formula $[NBu_4][(R_F)_2M(\mu\text{-}PPh_2)_2M'(\kappa^2,N,C\text{-}C_{13}H_8N)]$ (R_F = C_6F_5; $C_{13}H_8N$ = benzoquinolinate; M and M′ = Pd or Pt) and on the reactivity of these cyclometalated complexes with I_2.

RESULTS AND DISCUSSION

Synthesis of $[NBu_4][(R_F)_2M(\mu\text{-}PPh_2)_2M'(C\text{^}N)]$ (R_F = C_6F_5, C^N = Benzoquinolinate, M = M′ = Pt, 1; M = Pt, M′ = Pd, 2; M = Pd, M′ = Pt, 3; M = M′ = Pd, 4). The synthesis of the asymmetric dinuclear derivatives **1**−**4** was carried out by reacting *cis*-$Li_2[M(R_F)_2(PPh_2)_2]$[45] with the binuclear complex $[\{M'(\mu\text{-}Cl)(C\text{^}N)\}_2]$ (1:0.5 molar ratio) in THF (Scheme 2). From the corresponding mixtures, complexes **1**−**4** were isolated as yellow solids. The mononuclear phosphanido complexes behave as bidentate ligands causing the splitting of the $(\mu\text{-}Cl)_2$ bridging system and the displacement of the halide ligand in the binuclear C^N containing complex with formation of the asymmetric complexes **1**−**4**. The complexes were characterized by elemental analysis, HRMS, and multinuclear NMR spectroscopy. The IR spectra of complexes **1**−**4** in the solid state confirmed in all cases the presence of the relevant ligands and do not deserve insights. The HRMS(−) spectrograms of **1**−**4** showed in all cases intense peaks corresponding to $[M]^-$, with an isotope pattern superimposable to that calculated on the basis of the proposed formula.

The $^{31}P\{^1H\}$ NMR spectra of **1**−**4** showed two mutually coupled doublets (AX spin system) with ^{195}Pt satellites for complexes **1**−**3** (Table 1). The δP values in **1**−**4** range from −58.0 to −118.9 ppm. It has been established that usually the chemical shift decreases as the atomic number increases from top to bottom in a triad,[42,46] and in agreement with this, the chemical shifts increases passing from **1** (Pt_2) to **2**, **3** (PtPd), and **4** (Pd_2). The chemical shifts of P atoms in $M(\mu\text{-}PPh_2)_xM'$ frameworks without metal−metal bond appear at high field, and we have observed that δP in $M(\mu\text{-}PPh_2)M'$ usually appears at lower field than those of the doubly bridged $M(\mu\text{-}PPh_2)_2M'$ fragments.[47] The value of δ −58.0 is the highest one found for $M(\mu\text{-}PPh_2)_2M'$ systems and is close to those found in complexes containing single bridging $M(\mu\text{-}PPh_2)M'$ fragments without metal−metal bond.[48] The attributions of the coupling constants between P and Pt were unequivocally made by comparison of $^{31}P\{^1H\}$ and $^{195}Pt\{^1H\}$ spectra. As expected on the basis of the ligand *trans* to P, the lowest values of the $^1JPt,P$ (1320 Hz for **1** and 1213 Hz for **3**) were found for the coupling constants between P^2 and Pt^2 (P *trans* to benzoquinolinate C) while the highest ones (2810 Hz for **1** and 2658 Hz for **3**) were found for the $^1JPt^2,P^1$ (P *trans* to N).[43,49] The coupling constants between the P atoms and Pt^1 in complexes **1**−**2** range from 1530 to 1937 Hz.

The $^{195}Pt\{^1H\}$ NMR spectra of complexes **1**−**3** showed sharp signals for the Pt atoms bonded to benzoquinolinate (Pt^2) and broad multiplets, due to several couplings with unequivalent ^{19}F nuclei, for the Pt atoms bonded to pentafluorophenyl rings (Pt^1). The chemical shift of the Pt^1 was δ −3889 for **1** and δ −3909 for **2**, while those of the Pt^2 were δ −3717 for **1** and δ −3738 for **3** (Table 1). The geminal coupling constant between the two Pt atoms in **1** was 541 Hz.

dx.doi.org/10.1021/ic301298p | Inorg. Chem. 2012, 51, 12682−12696

The ^{19}F NMR spectra of complexes **1**−**4** recorded in deuteroacetone at 298 K showed in all cases different (often partially overlapped) signals for the *o*-F atoms (δ range −110 to −115 ppm), *m*-F atoms (δ range −166 to −167 ppm), and *p*-F atoms (δ range −168 to −169 ppm) of each ring, in agreement with the inequivalence of the two rings.

The partial overlapping of most homologous signals reflects the similarity of the environments of the two rings, while the equivalence of the *ortho* (and *meta*) fluorine atoms within each ring can be explained either by a free rotation about the Pt−C axis at 298 K or by an adopted conformation in solution having a mirror plane containing the skeleton of the molecule with the C_6F_5 rings perpendicular to this plane.

1D and 2D ^1H NMR spectra of **1**−**4** permitted the full assignment of all ^1H NMR signals. The four ^1H NMR spectra are almost superimposable, the main difference being the resonance of the M′−N−C*H*C proton (H2 in the numbering used in the Experimental Section) which falls at about 8.6 ppm when M′ was Pt and at about 8.4 ppm when the benzoquinolinate ligand was bound to Pd. The $^{13}C\{^1H\}$ NMR spectra of **1**−**4** showed clearly all signals due to tertiary carbons and are reported in the Supporting Information.

Reaction of 1−4 with I_2. Complexes **1**−**4** react with I_2 (1:1 molar ratio), and the resulting products depended on the respective starting materials and on the solvent in which the reactions were carried out (Scheme 3).

In a general procedure, a CH_2Cl_2 solution of I_2 was added dropwise to a CH_2Cl_2 solution of the dinuclear complexes $[NBu_4][(R_F)_2M(\mu\text{-}PPh_2)_2M'(C\text{^}N)]$ in 1:1 molar ratio at room temperature. For complex **1** the solution was stirred, at room temperature, for 20 h and by addition of *i*-PrOH, a mixture of the Pt(II)−Pt(IV) complexes $[NBu_4][(R_F)_2Pt^{II}(\mu\text{-}PPh_2)_2Pt^{IV}(C\text{^}N)I_2]$ (**5**) and $[(R_F)_2Pt^{II}(\mu\text{-}PPh_2)(\mu\text{-}I)\text{-}Pt^{II}\{PPh_2(C_{13}H_8N)\}]$ (**6**) was isolated. Complex **5** contains a Pt(II) and a Pt(IV) center with a *OC*-6−42 configuration (only one isomer of the pair is depicted in Scheme 3), and **6** is a dinuclear Pt(II)−Pt(II) derivative containing an aminophosphane group. The two metal centers are joined by two different bridging ligands, PPh_2^- and I^-. When the addition of I_2 to **1** was carried out in acetone, only the Pt(II),Pt(IV) complex **5** was obtained, suggesting that **5** might be a precursor of **6** and that the reductive coupling process is not favored in acetone. In fact, deuteroacetone solutions of **5** were stable (^{31}P NMR spectroscopy) for two weeks at room temperature whereas CD_2Cl_2 solutions of **5** evolved in the same period of time into a mixture of **5** and **6** (ca. 70% in **6**).

Complexes **2** (M = Pt, M′ = Pd) and **4** (M = M′ = Pd) react with I_2 under similar reaction conditions producing only the aminophosphane complexes $[(R_F)_2M^{II}(\mu\text{-}PPh_2)(\mu\text{-}I)\text{-}Pd^{II}\{PPh_2(C_{13}H_8N)\}]$ (M = Pt **7**, Pd **8**, Scheme 3). In an attempt to detect a Pt(II),Pd(IV) intermediate we carried out the addition of I_2 to complex **2** (1:1 molar ratio) in acetone solution at low temperature (213 K) obtaining, after evaporating the solution to dryness, an orange solid. The $^{31}P\{^1H\}$ NMR spectra in acetone at 213 K and at room temperature indicated this solid to be a mixture of mainly **7** and the tetranuclear species $[NBu_4]_2[\{(R_F)_2Pt(\mu\text{-}PPh_2)_2Pd(\mu\text{-}I)\}_2]$, described previously,[44] but signals assignable to a Pt(II)−Pd(IV) intermediate complex were not detected.

Finally, when a CH_2Cl_2 solution of I_2 was added to a CH_2Cl_2 solution of $[NBu_4][(R_F)_2Pd(\mu\text{-}PPh_2)_2Pt(C\text{^}N)]$ (**3**) (1:1 molar ratio) and stirred at room temperature for 20 h, and the resulting solution was evaporated to dryness, a yellow solid was isolated. Its $^{31}P\{^1H\}$ NMR spectrum in acetone indicated that this solid is a complex mixture of products in which $[NBu_4][(R_F)_2Pd^{II}(\mu\text{-}PPh_2)_2Pt^{IV}(C\text{^}N)I_2]$ (**9**), $[(R_F)_2Pd^{II}(\mu\text{-}PPh_2)(\mu\text{-}I)Pt^{II}\{PPh_2(C_{13}H_8N)\}]$ (**10**), and $[(R_F)(PPh_2R_F)\text{-}Pd^{II}(\mu\text{-}PPh_2)(\mu\text{-}I)Pt^{II}(C\text{^}N)]$ (**11**) could be identified (NMR spectroscopy) but not isolated as pure samples. All attempts to separate the mixture were unsuccessful.

Crystal Structures of 5′−8. Crystals of **5** suitable for X-ray studies could not be obtained. For this reason, $[N(PPh_3)_2]\text{-}[(R_F)_2Pt^{II}(\mu\text{-}PPh_2)_2Pt^{IV}(C\text{^}N)I_2]$ (**5′**) was prepared through two steps: (a) synthesis of $[N(PPh_3)_2][(R_F)_2Pt^{II}(\mu\text{-}PPh_2)_2Pt^{II}(C\text{^}N)]$, **1′**, in an analogous procedure than for **1** using $[N(PPh_3)_2]Cl$ instead of NBu_4ClO_4, and (b) the subsequent addition of I_2 to **1′**. The structures of compounds **5′**−**8** have been established by X-ray diffraction studies. Figures 1, 2, S1, and S2 show views of the corresponding complexes

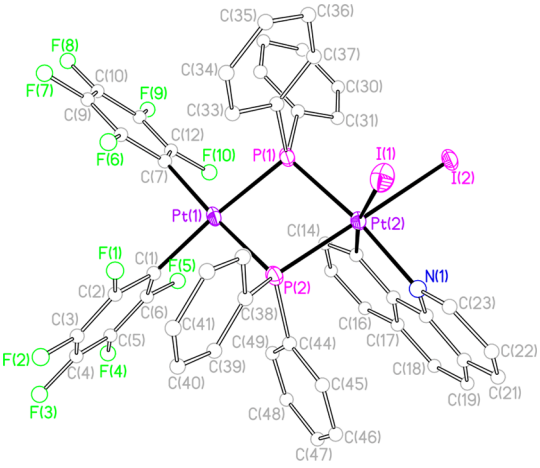

Figure 1. View of the molecular structure of the complex anion of $[N(PPh_3)_2][(R_F)_2Pt^{II}(\mu\text{-}PPh_2)_2Pt^{IV}(C\text{^}N)I_2]$ (**5′**).

and Tables 2, 3, S1, and S2 list their most relevant bond distances and angles. The crystal structure of **5′** confirms its dinuclear nature, with two platinum atoms bridged by two diphenylphosphanido ligands. The long intermetallic separation of 3.572(1) Å and the broad values of the Pt−P−Pt angles

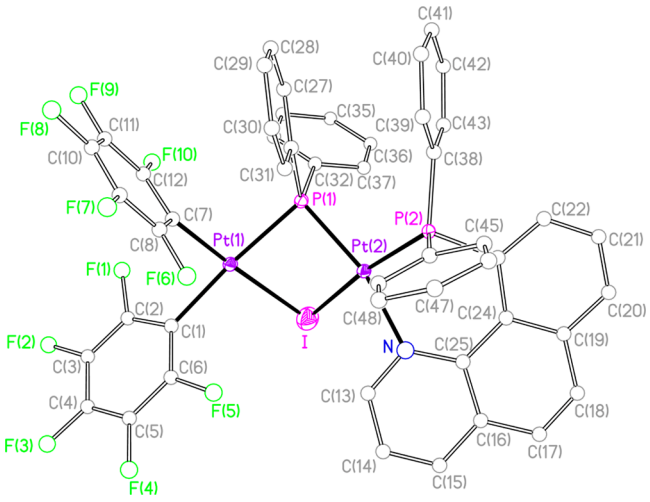

Figure 2. View of the molecular structure of the complex $[(R_F)_2Pt^{II}(\mu\text{-}PPh_2)(\mu\text{-}I)Pt^{II}\{PPh_2(C_{13}H_8N)\}]$ (**6**).

dx.doi.org/10.1021/ic301298p | *Inorg. Chem.* 2012, 51, 12682−12696

Table 2. Selected Bond Lengths (Å) and Angles (deg) for $[N(PPh_3)_2][(R_F)_2Pt^{II}(\mu\text{-}PPh_2)_2Pt^{IV}(C\text{^}N)I_2]\cdot Me_2CO\cdot 0.25n\text{-}C_6H_{14}$ ($5'\cdot Me_2CO\cdot 0.25n\text{-}C_6H_{14}$)

Pt(1)−C(1)	2.044(7)	Pt(1)−C(7)	2.064(6)	Pt(1)−P(2)	2.2990(18)
Pt(1)−P(1)	2.3033(17)	Pt(2)−C(13)	2.058(6)	Pt(2)−N(1)	2.138(5)
Pt(2)−P(1)	2.3407(17)	Pt(2)−P(2)	2.3837(18)	Pt(2)−I(1)	2.6913(5)
Pt(2)−I(2)	2.7556(5)				
C(1)−Pt(1)−C(7)	87.8(3)	C(1)−Pt(1)−P(2)	96.1(2)		
C(7)−Pt(1)−P(2)	175.66(17)	C(1)−Pt(1)−P(1)	175.42(19)		
C(7)−Pt(1)−P(1)	96.76(18)	P(2)−Pt(1)−P(1)	79.38(6)		
C(13)−Pt(2)−N(1)	80.6(2)	C(13)−Pt(2)−P(1)	94.56(19)		
N(1)−Pt(2)−P(1)	172.56(15)	C(13)−Pt(2)−P(2)	83.10(18)		
N(1)−Pt(2)−P(2)	96.76(15)	P(1)−Pt(2)−P(2)	76.93(6)		
C(13)−Pt(2)−I(1)	169.66(18)	N(1)−Pt(2)−I(1)	90.44(14)		
P(1)−Pt(2)−I(1)	94.82(4)	P(2)−Pt(2)−I(1)	103.27(4)		
C(13)−Pt(2)−I(2)	89.25(18)	N(1)−Pt(2)−I(2)	85.17(15)		
P(1)−Pt(2)−I(2)	100.52(4)	P(2)−Pt(2)−I(2)	171.68(4)		
I(1)−Pt(2)−I(2)	84.775(16)	Pt(1)−P(1)−Pt(2)	100.53(7)		
Pt(1)−P(2)−Pt(2)	99.38(7)				

Table 3. Selected Bond Lengths (Å) and Angles (deg) for $[(R_F)_2Pt^{II}(\mu\text{-}PPh_2)(\mu\text{-}I)Pt^{II}\{PPh_2(C_{13}H_8N)\}]$ (6)

Pt(1)−C(7)	2.008(7)	Pt(1)−C(1)	2.069(7)	Pt(1)−P(1)	2.2924(16)
Pt(1)−I	2.6762(6)	Pt(2)−N	2.138(5)	Pt(2)−P(2)	2.1938(16)
Pt(2)−P(1)	2.2730(16)	Pt(2)−I	2.6779(6)		
C(7)−Pt(1)−C(1)	88.8(3)	C(7)−Pt(1)−P(1)	94.56(18)		
C(1)−Pt(1)−P(1)	175.35(19)	C(7)−Pt(1)−I	176.08(18)		
C(1)−Pt(1)−I	94.31(18)	P(1)−Pt(1)−I	82.25(4)		
N−Pt(2)−P(2)	85.20(16)	N−Pt(2)−P(1)	165.52(17)		
P(2)−Pt(2)−P(1)	103.45(6)	N−Pt(2)−I	90.88(15)		
P(2)−Pt(2)−I	169.07(5)	P(1)−Pt(2)−I	82.57(4)		
Pt(1)−I−Pt(2)	74.880(16)	Pt(2)−P(1)−Pt(1)	90.95(6)		

(100.53(7)° and 99.38(7)°) discard any Pt···Pt interaction. The environment of Pt(1) is fairly typical for this metal in a formal oxidation state +2; that is, it lays in the center of a square planar environment formed by two mutually *cis* pentafluorophenyl ligands and the bridging phosphanido groups. On the other hand, the Pt(2) coordination sphere is octahedral as expected for a Pt^{IV} center. The two iodo ligands are mutually *cis*, with a *OC*-6−42 configuration for Pt(2) (see Figure 1).

Complexes **6**−**8** are isostructural, with a "*cis*-$M(C_6F_5)_2$" fragment (M = Pt in **6** and **7**, and M = Pd in **8**) and a "$M\{PPh_2(C_{13}H_8N)\}$" fragment (M = Pt in **6**, and M = Pd in **7** and **8**) held together through a double bridge formed by one iodo and one diphenylphosphanido ligands. Structural parameters are very similar in the three complexes (see Tables 3, S1, and S2) regardless of the nature of the metal. The metal center of the "*cis*-$M(C_6F_5)_2$" fragment lies in an essentially square planar environment, while the coordination sphere of the metal bonded to the aminophosphane group deviates significantly from planarity. This distortion is probably due to the strain imposed by the chelating coordination of the $PPh_2(C_{13}H_8N)$ ligand. The three structures confirm the coupling of the original diphenylphosphanido and benzoquinolinate ligands, with the formation of a P−C bond. The length of this new bond shows no appreciable differences with the other P−C(Ph) bonds formed by this phosphorus atom, P(2). The new chelate ligand and the metal atom form a non planar six-membered metallacycle. This is reflected in a distortion in the otherwise planar benzoquinolinate skeleton, which is warped, with N−C(25)−C(24)−C(23) torsion angles of 13.7(1)° for **6**, 13.5(1)° for **7**, and 12.7(1)° for **8**. The main difference resides in the intermetallic distance, which is longer for **6** (Pt(1)···Pt(2) = 3.255(1) Å) and very similar for the other two complexes (Pt−Pd = 3.081(1) Å in **7** and Pd(1)−Pd(2) = 3.078(1) Å in **8**). As a related effect, this difference is also found in the dihedral angle formed by the two planes defined by the metal centers and the bridging atoms bonded to them (plane P(1) M(1) I and plane P(1) M(2) I), which is broader in **6** (123.6(1)°) than in **7** or **8** (112.2(1)° in both cases).

Spectroscopic Properties. The NMR features of **5** were addressed in detail, as they were valuable for the study of the dynamic behavior in solution and for the mechanism of transformation into **6**.

The $^{31}P\{^1H\}$ NMR of **5** showed two doublets centered at δ −107.5 and δ −115.5, each flanked by three sets of ^{195}Pt satellites arising from isotopomers containing one or two ^{195}Pt atoms. Dipolar couplings (^1H NOESY) between protons of the benzoquinolinate ligand and protons of the phenyl ring A (i.e., one of the phenyls bonded to P2, as indicated by $^1H-^{31}P$ HMQC spectrum, Figure 3) permitted to assign the ^{31}P NMR signal at δ −107.5 to P2 and, therefore, the ^{31}P NMR signal at δ −115.5 to P1. Comparison with the $^{195}Pt\{^1H\}$ NMR spectrum permitted us to assign the direct Pt−P coupling constants. The values of $^1JPt^1-P^2$ and $^1JPt^1-P^1$ in **5** are 2189 and 2032 Hz, while those of the two $^1JPt(IV)-P$ were 1270 Hz ($^1JPt^2-P^2$) and 1807 Hz ($^1JPt^2-P^1$) (Table 1).

Our findings are in accord with literature data: in phosphane derivatives the Pt−P coupling constants in Pt(IV) derivatives are about two-thirds of that of the Pt(II) precursors,[50,51] and a value of 1801 Hz has been published for a $^1JPt(IV)-P$ coupling of a P atom *trans* to an I ligand in a phosphane derivative of platinum(IV).[50] Although values of 830 and 791 Hz for $^1JPt-P$ were reported in 1977 for two derivatives which were claimed

dx.doi.org/10.1021/ic301298p | *Inorg. Chem.* 2012, 51, 12682−12696

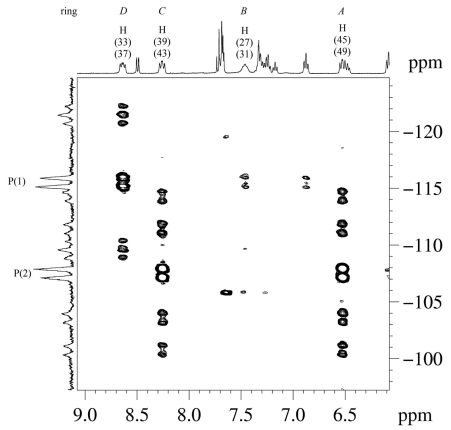

Figure 3. Low-field portion of the $^{1}H-^{31}P$ HMQC spectrum of **5** (400 MHz, C_3D_6O, 298 K).

to be Pt(IV) μ-PH_2 complexes,[52] a complete structural characterization of these complexes or subsequent data have not been reported later. As far as we know, complex **5** is the first platinum(IV) phosphanido derivative characterized unambiguously.

The ^{1}H NMR features of **5** were obtained by combining data extracted from $^{1}H-^{31}P$ HMQC, $^{1}H-^{195}Pt$ HMQC, ^{1}H NOESY, and ^{1}H COSY spectra. The attribution of all signals is reported in Figure S3 (the numbering of the hydrogen atoms coincides with that of the carbon atom to which they are bonded, taken from the solid state structure of **5′**, Chart 2).

Chart 2. Two Views of Complex 5 Showing the Labels for the Rings

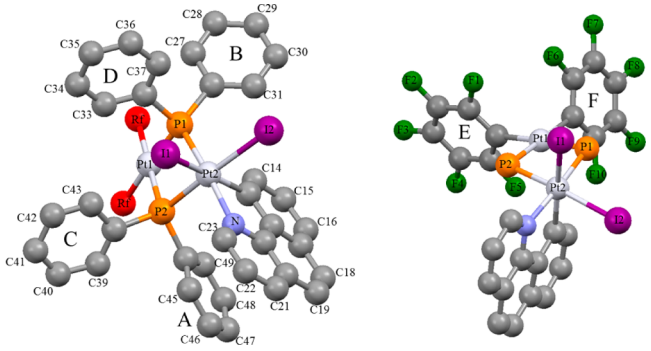

In particular, the attribution of the *ortho* protons of the phenyl rings was made on the basis of the $^{1}H-^{31}P$ HMQC spectrum (Figure 3) showing correlations (due to scalar coupling) between P1 and signals at δ_H 8.61 (H33/37) and δ_H 7.44 (H27/31) (*ortho* protons of phenyl rings D and B, respectively) as well as between P2 and signals at δ_H 8.23 (H39/43) and δ_H 6.50 (H45/49) (*ortho* protons of phenyl ring C and A, respectively). ^{1}H NOESY and ^{1}H COSY spectra permitted us to complete the assignment of all protons of the four phenyl rings. The attribution of the protons of the coordinated benzoquinolinate ligand was made on the basis of the $^{1}H-^{195}Pt$ HMQC spectrum (Figure 4) from which the protons scalar coupled to Pt2 could be identified. The analysis of ^{1}H NOESY and ^{1}H COSY spectra permitted us then to complete the assignment of all protons of the benzoquinolinate ligand. Signals due to H23 (δ 10.73), H14 (δ 9.63), and H21(δ 8.46) are well separated from each other, while the remaining

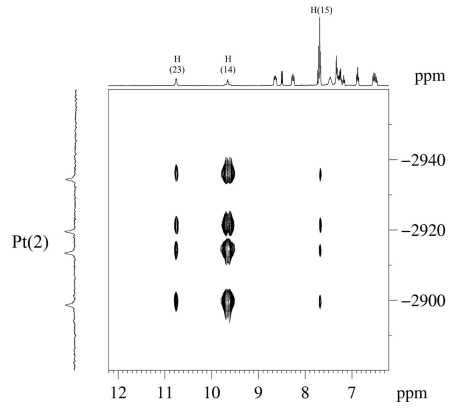

Figure 4. Low-field portion of the $^{1}H-^{195}Pt$ HMQC spectrum of **5** (400 MHz, C_3D_6O, 298 K).

five signals (H15, H16, H18, H19, and H22) are partially overlapped in the region ranging from δ 7.70 to δ 7.63. On passing from **1** to **5**, the ^{1}H NMR signals of the benzoquinolinate ring *trans* to I appear significantly shifted to low fields.

The ^{19}F NMR of **5** at 200 K showed 10 signals, one for each of the ^{19}F atoms of the two rings. The inequivalence of the two rings and of the two halves in each ring indicates that at low *T* the rotation of the pentafluorophenyl groups about the Pt−C bond is slow in the NMR time-scale and the structure in solution resembles that in the solid state. Combining the results of ^{19}F COSY, $^{19}F-^{1}H$ HOESY, and ^{19}F NOESY at various *T*'s permitted us to assign all ^{19}F atoms of **5** as shown in Figure 5 (the numbering is that of the solid state structure of **5′**).

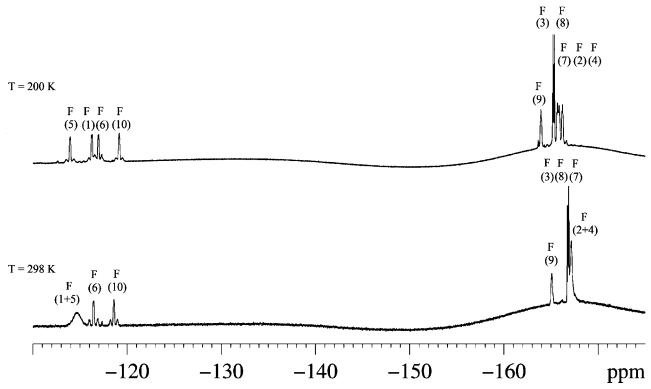

Figure 5. ^{19}F spectra of **5** (376 MHz, C_3D_6O).

At 298 K the signals of the *ortho* (F1 and F5) and of the *meta* (F2 and F4) fluorine atoms of ring E collapse into two very broad signals centered at δ −114.6 and δ −167.2, respectively, with the five signals of ring F (F6−10) remaining separated from each other.[53] This behavior indicates that, upon increasing the temperature from 200 to 298 K, ring E rotates (about the Pt1−C1 axis) with a frequency that averages the resonances of the two halves of the ring. On the other hand, even at 298 K, ring F rotates very slowly about the Pt1−C7 axis, so that the *o*-F and *m*-F still appear inequivalent. In accord to this view, the ^{19}F EXSY spectrum of **5** recorded at 298 K (Figure 6) showed intense cross peaks between the F6 and F10 (the *ortho*-F of ring *F*) as well as between the F7 and F9 (the *meta*-F of ring F), as a result of the exchange between the fluorine atoms upon

dx.doi.org/10.1021/ic301298p | *Inorg. Chem.* 2012, 51, 12682−12696

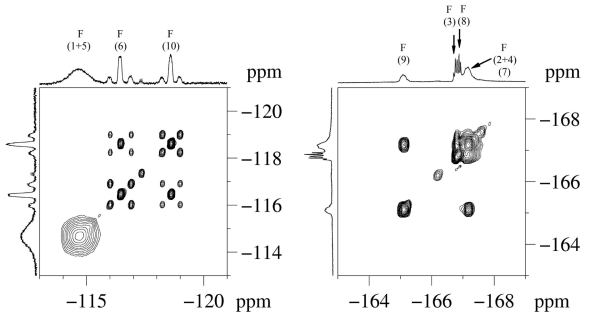

Figure 6. Two portions of the ^{19}F EXSY spectrum of **5** (376 MHz, C_3D_6O, 298 K).

rotation. VT ^{19}F NMR spectra for **5** allowed us to calculate the value of 57 kJ/mol for the activation free energy $\Delta G^{\ddagger}$ of rotation of the E ring of **5**.

The attribution of the ^{19}F signals to ring E or F was made on the basis of the correlations in the ^{19}F−^{1}H HOESY spectrum of **5** at 298 K (Figure 7, τ_m = 0.200 s). The ^{19}F−^{1}H HOESY

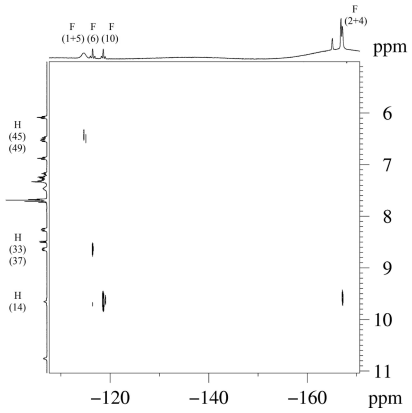

Figure 7. ^{19}F−^{1}H HOESY spectrum of **5** (376 MHz, C_3D_6O, 298 K).

experiment displays correlations deriving from the dinuclear coupling between fluorine atoms and protons in close spatial proximity, and in the case of **5** showed cross peaks between signals at δ_F −118.6 and δ_H 9.63 (H14) as well as between signals at δ_F −116.4 and δ_H 8.61 (*ortho* hydrogens of phenyl ring D, H33/37, Chart 3). Given that the fluorine atom closest to H14 is F10, one of the *ortho* fluorines of ring F (the distance in the crystal structure of **5′** is 2.79 Å) and the fluorine atom closest to H33/37 is F6 (d = 2.73 Å), we interpret these results admitting that the pentafluorophenyl ring displaying inequivalent *ortho*- and *meta*-fluorine atoms even at 298 K (*F* in Chart 2) is close to the phenyl ring D. These attributions are corroborated by a weak cross peak also present in the ^{19}F−^{1}H HOESY spectrum of **5** at 298 K between signals at δ_F −114.6 (F1/5) and δ_H 6.50 (*ortho* hydrogens of phenyl ring A, H45/49).

An interesting feature deduced from the ^{19}F COSY spectrum of **5** at 200 K (or at 273 K) is an intense cross peak between F5 (one of the *o*-F atoms of ring E) and F10, (one of the *o*-F atoms of ring F) (Figure 8). The scalar correlation between these six bonds away ^{19}F atoms belonging to different pentafluorophenyl rings in mutually *cis* position can be explained in terms of "through space" spin−spin couplings. In fact, the favorable spatial disposition of F5 and F10 (the F5−F10 distance in the solid state structure of **5′** is 2.98 Å) may

Chart 3

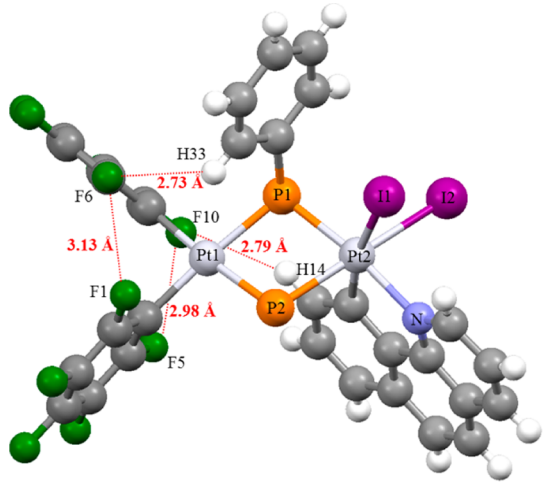

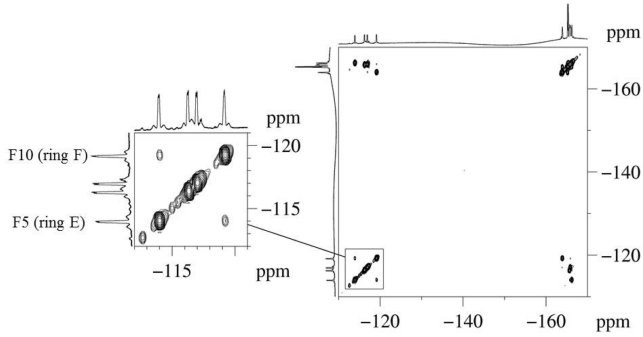

Figure 8. ^{19}F COSY spectrum of **5** (376 MHz, C_3D_6O, 200 K).

facilitate overlap interactions between filled orbitals of the F atoms, resulting in a no net bonding providing, nevertheless, a suitable pathway for transmitting spin information between the coupled nuclei.[54,55] An analogous "through space" coupling was observed also for the F1−F6 couple, whose distance in the solid state structure of **5′** is 3.13 Å. The existence of the "through space" coupling between F5 and F10 (as well as between F1 and F6) is corroborated by the presence, in the ^{19}F EXSY spectrum of **5** recorded at 200 K, of weak cross peaks between F5 and F10 (as well as between F1 and F6) confirming the spatial proximity of such pairs of ^{19}F atoms in solution at low *T*. Noteworthy, a weak "through space" coupling between *o*-F atoms belonging to different C_6F_5 rings was also observed by recording the ^{19}F COSY spectrum of **7** in deuteroacetone at 298 K (Figure S4).

The ^{195}Pt{^{1}H} NMR spectrum of **5** showed two signals, one at δ −3806, and the other at δ −2917. Of these, that at δ −3806 gives peaks broadened by multiple couplings with ^{19}F and is ascribed to Pt^{1}, bonded to pentafluorophenyl rings. The signal at δ −2917 is a sharp doublet of doublets (^{1}JPt^{2}−P 1270 and 1807 Hz) and is ascribed to the octahedral Pt^{2}(IV) atom. No geminal Pt−Pt coupling was visible (the half-height width of the signals was $\Delta\nu_{1/2}$ = 50 Hz). The deshielding of the Pt^{2} (+800 ppm) observed on passing from formal oxidation state +2 to +4 is in accord to the majority of literature data[56] but contrasts with what is found for the polysilylated compounds described by Tanaka, for which a strong shielding is observed upon Pt(II)→Pt(IV) oxidation.[57]

dx.doi.org/10.1021/ic301298p | *Inorg. Chem.* 2012, 51, 12682−12696

Multinuclear NMR spectra of complexes **6**−**10** are conclusive to establish their structure and are in accordance with the solid state study. All data extracted from the analysis of the spectra are collected in Table 1. For the aminophosphane complexes **6**−**8** and **10**, P^2 atoms appear at lower-field than those in the starting materials **1**−**4**, as a consequence of the transformation of the diphenylphosphanido ligand involved in a four-membered ring into an aminophosphane ligand, $PPh_2(C\hat{}N)$. Expectedly, the ^1JPt−P^2 values of **6** and **10** are larger, 4435 and 4307 Hz. It is well established that the P signals of "M(μ-PPh_2)(μ-X)M" (X = Cl, Br, I, OH) fragment in a saturated phosphanido bridged complex (without M−M bond) appear low-field shifted respect to the fragment M(μ-PPh_2)$_2$M in a saturated platinum or palladium derivative.[58−61] This is true for P^1 in **6**−**8** and **10** (see Table 1) compared with **1**−**4**. In the literature +50 ppm is considered roughly as the lowest limit of δP for the phosphanido group involved in four-membered rings in complexes without metal−metal bonds.[62] The values of δP^1 found for **7** and **8** (55.2 and 66.0 ppm) lie at the lower limit of this range, and $^2J P^1$−P^2 values are much smaller in **6** and **10** (2 Hz) than in **7** and **8** (40 and 36 Hz, respectively). It is also to note that the coupling of the P atom of the phosphane ligand with the Pt^1 center bonded to the C_6F_5 groups, $^3J Pt^1$−P^2, is observed, and this value is larger in the Pt−Pd complex **7** (97 Hz) than in the Pt−Pt one **6** (37 Hz). These three facts suggest some differences between **7**, **8** and **6**, **10** which may be related to the slightly smaller intermetallic distance in **7** and **8** with respect to **6**, as mentioned before.

The ^{19}F NMR spectra of **6**−**8** show three signals (2:2:1 intensity ratio) for each pentafluorophenyl ring, in agreement with the inequivalence of the two C_6F_5 groups, and indicate that in solution the two halves of each ring are equivalent, due to free rotation about the C−M bond. For **6**−**8**, one C_6F_5 ring rotates faster than the other, as evidenced by the difference in sharpness of the corresponding ^{19}F NMR signals. It is conceivable that the C_6F_5 ring *cis* to the bridging iodide suffers from less sterical hindrance than the C_6F_5 ring *cis* to the bridging diphenylphosphanide, thus rotating relatively faster and giving sharper ^{19}F NMR signals.

For the Pd(II)−Pt(IV) complex **9** analogous to **5** the bridging phosphanide ^{31}P resonances were found at δ −97.7 (P^1) and δ −89.1 (P^2) while the direct P−Pt coupling contants were 1121 Hz (^1JPt−P^2) and 1680 Hz (^1JPt−P^1) (Table 1). The ^{195}Pt NMR signal of **9**, obtained from the ^{1}H−^{195}Pt HMQC spectrum recorded on the mixture of **9**, **10**, and **11**, was found at δ −2966.

The identification of **11** from the NMR data as [(R_F)(PPh_2R_F)Pd^{II}(μ-PPh_2)(μ-I)Pt^{II}(C^N)] was easily achieved by comparing its spectra with the corresponding ones of the analogous [NBu_4][(R_F)(PPh_2R_F)Pd^{II}(μ-PPh_2)(μ-I)Pt^{II}(R_F)$_2$], prepared earlier in our laboratories.[42] The assignment of the Pt−N bond in *trans* position to the phosphanido group and not to the I ligand was made on the basis of the large value of ^1JPt−P^1 (3317 Hz) extracted from the spectrum. In this case, the ^{19}F NMR is also conclusive because signals due to the $PPh_2C_6F_5$ group appear in the spectrum well separate from those of Pd−C_6F_5.[42,43,49,63−65] ^{19}F NMR data are given in the Experimental Section. The ^{195}Pt NMR signal for complex **10** was found at δ −4416, by ^{1}H−^{195}Pt HMQC experiments recorded on the mixture of **9**, **10**, and **11**.

Mono- and bidimensional ^{1}H NMR spectra of **6**−**8** permitted the full assignment of all ^{1}H NMR signals. In these three cases the spectra display a similar pattern, and eight well separated signals are observed for the C^N part of the aminophosphane ligand. As a consequence of the formation of the P−C bond, the couplings between the P^2 atom and the hydrogen atom are observed in four of the eight signals. To distinguish the homonuclear from the heteronuclear scalar coupling ^{1}H{^{31}P} NMR experiments for complexes **6**−**8** were recorded. The data so obtained are reported in the Experimental Section.

DISCUSSION

The dinuclear Pt(II),Pt(IV) complex **5** is the result of the oxidative addition of I_2 to one of the platinum centers, the one containing the C^N ligand, in the dinuclear Pt(II),Pt(II) derivative **1**. In the oxidative addition of I_2, it is accepted that I_2 is usually activated heterolytically in an S_N2-like process,[51,66] which in the case of complex **1** could initially consist of the formation of the η^1-I_2 adduct **A**[67] (Scheme 4) followed by iodine dissociation and formation of the square pyramidal Pt(IV) intermediate **B**. The unsaturated intermediate **B** can

Scheme 4

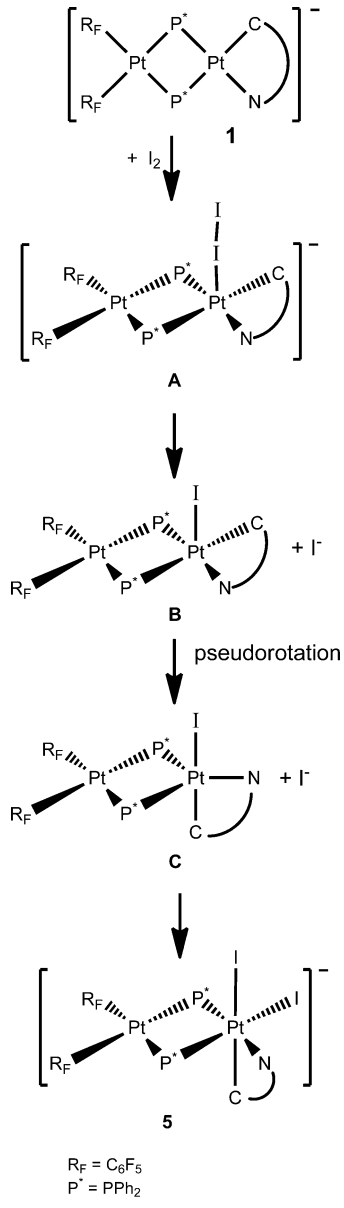

dx.doi.org/10.1021/ic301298p | Inorg. Chem. 2012, 51, 12682−12696

Scheme 5

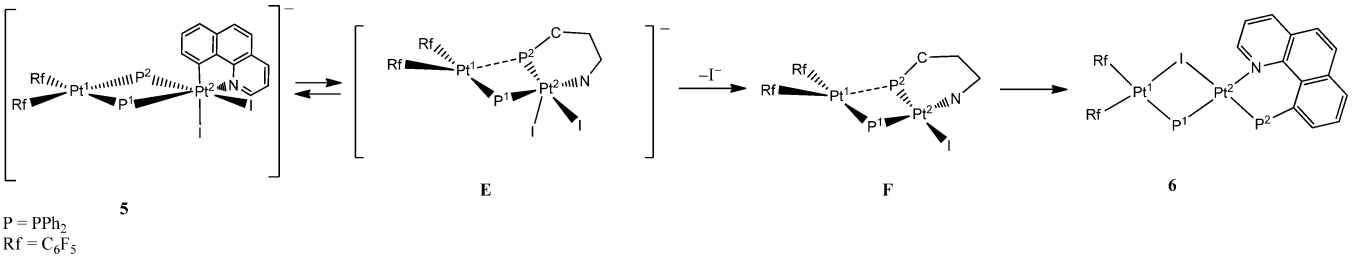

Scheme 6

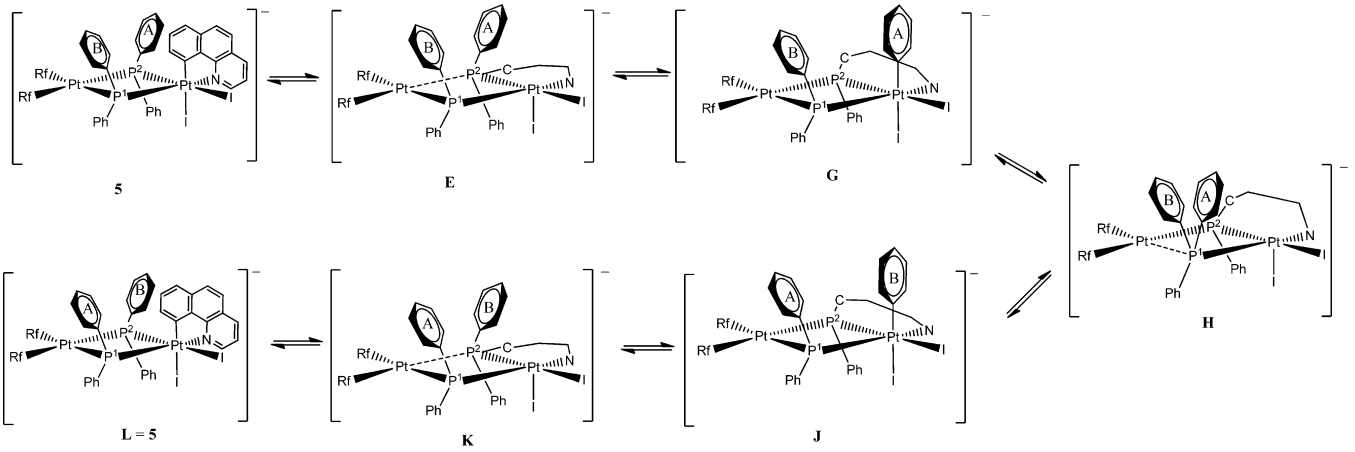

then rearrange via pseudorotation to the trigonal bipyramid intermediate **C** which, in turn, could uptake the anion I^- giving complex **5** as a result of the formal *cis*-addition (Scheme 4).

Obtaining the aminophosphane species **6** by leaving **5** in dichloromethane (or by carrying out the iodination of **1** in CH_2Cl_2) can be explained by the pathway shown in Scheme 5. Insertion of P^2 onto the Pt−C bond could give intermediate **E**, having a five-coordinate Pt^2. Intermediate **E** may then undergo iodide dissociation to give **F**, which affords **6** upon rupture of the P^2−Pt^1 bond, rotation about the P^1−Pt^2−N axis, and bridging coordination of the iodide bonded to Pt^2. Given that the reaction rate for a dissociative process is inhibited by the addition of an excess of the leaving group, we monitored by ^{31}P NMR the transformation of **5** into **6** in dichloromethane, with and without 5 equiv of $(NBu_4)I$. While the conversion of **5** into **6** was 25% after 64 h in the absence of external iodide, the solution containing **5** and $(NBu_4)I$ showed, after the same time, only signals of **5**.[68] The geometry of the five-coordinate Pt^2 in intermediate **E** could be in principle either trigonal bipyramid or square based pyramid. The analysis of the dynamics in solution of complex **5** revealed indicative in order to discriminate between the two geometries, favoring the square based pyramide one (*vide infra*). The ^1H EXSY spectrum of **5** at 298 K in deuteroacetone showed cross peaks between the signals at δ 6.05, 6.45, 6.50 with those at δ 6.85, 7.15, 7.44, respectively (Figure S5), indicating an exchange between the phenyl rings A and B, bonded to two different P atoms (A is bonded to P2 while B is bonded to P1). No evident exchange between protons belonging to C and D rings was observed, thus excluding the exchange of the two entire diphenylphosphanide groups. Such circumstance was confirmed by the absence of cross peaks in the $^{31}P\{^1H\}$ EXSY spectra of **5** at 298 K, recorded at various mixing times (from 0.100 to 0.800 s).

The observed exchange of rings A and B is not immediately rationalizable as it supposedly requires the shift of the phenyl ring A originally bonded to P2, first onto the Pt(IV) atom, and then onto P1, leaving fixed the P atoms. However, given that carbon insertion into μ-PPh_2−Pt bonds is not uncommon in diphenylphosphanido bridged Pt or Pd complexes[42,44,49,64,69−73] and that the systems under study do undergo such process in the reactions from **1**−**4** to **6**−**8** and **10**, we propose the mechanism reported in Scheme 6 to rationalize the observed ^1H NMR exchange. The fact that only rings A and B are involved in the exchange suggests that the dynamic process concerns only the half of the molecule containing the benzoquinolinate ligand, ring A and ring B (Chart 2).

Thus, as proposed in Scheme 5 for the **5** to **6** conversion, insertion of P^2 onto the Pt^2−C bond in **5** can give species **E** (Scheme 6). In acetone, species **E** may reform **5** by breaking of the P−C^N bond and formation of the Pt−C^N bond, or can give **G** by breaking of the P−Ph_A bond and formation of the Pt−Ph_A bond. The P−Ph_C bond cannot be involved in this process due to its unfavorable position that renders unlikely the shift of Ph_C to the apical coordination site of Pt(IV) (at least in a concerted way). The Ph_A bonded to Pt(IV) in **G** may migrate onto P^1 to give species **H** in which the pentacoordinated P^1 is bonded to three phenyl groups and the free coordination site on Pt is occupied by acetone. At this point, **H** may undergo breaking of the P−Ph_A bond or of the P−Ph_B bond (but not of the P−Ph_D bond) and formation of the Pt−Ph bond to give **G** or **J**, respectively. The path opposite to that which led from **5** to **H** can thus give first **K** and then **L** (identical to **E** and **5**, respectively, but with exchanged phenyl rings A and B). In the light of this finding, the square based pyramid geometry of the five-coordinate Pt^2 in complex **E** is the only one allowing the

dx.doi.org/10.1021/ic301298p | *Inorg. Chem.* 2012, 51, 12682−12696

exchange process involving phenyl rings A and B (with C and D rings not being exchanged).[71,72,74−76]

The mechanisms outlined in Schemes 5 and 6, besides explaining the **5** to **6** conversion and the observed exchange of phenyl rings A and B, may also account for the role of the solvent in the reactivity of **1** toward I_2. In fact, admitting that the stability of the intermediate **E** (which is anionic) increases with the polarity of the solvent, we can envision that species **E** slowly transforms into **F** (giving eventually **6**, Scheme 5) when the reaction is carried out in dichloromethane, whereas **E** isomerizes into **G** to start the exchange process depicted in Scheme 6 when dissolved in acetone.

The exchange between phenyl rings bonded to two different P atoms was observed (^{1}H EXSY in deuteroacetone at 298 K of the mixture containing a great amount of **9**) also for complex **9**, the Pd−Pt analogue of **5**.

Examples of polynuclear complexes in which the phosphane ligand adopts a μ^2-PR_3 coordination mode are well-known.[77−80] These complexes that show a pentacoordinated P atom provide a structural model as reaction intermediates in the oxidative addition processes of the P−C bond to a metal center to form phosphanido derivatives. In this work, species **E**, **H**, and **K** (Scheme 6) are proposed as intermediates in the inverse process: from phosphanido to a phosphane derivative.

The reaction products between equimolar amounts of **2** and I_2 in acetone at 213 K afforded, as mentioned before, **7** and $[NBu_4]_2[\{(R_F)_2Pt(\mu\text{-}PPh_2)_2Pd(\mu\text{-}I)\}_2]$. The presence of the tetranuclear derivative of platinum and palladium(II) showing the "$Pt(\mu\text{-}PPh_2)_2Pd$" fragment is explainable with a C−I reductive elimination from the Pd(IV) system in an intermediate similar to **5**. In addition, the reactions of **1** or **4** with I_2 did not produce in any case complexes containing the $PPh_2C_6F_5$ ligand, which could be the result of a P−C_6F_5 reductive coupling, but only compounds with the P−C^N ligand. This fact suggests that the initial oxidative addition takes place in the metal fragment which is bonded to the benzoquinolinate ligand, in accord to the mechanism shown in Scheme 4. Considering that the reaction of **1** (Pt−Pt) with I_2 in CH_2Cl_2 permitted us to isolate the oxidized complex **5**, and the aminophosphane derivative **6**, while only the aminophosphane derivative is obtained in the reaction of the homologous Pd−Pd derivative **4** with I_2 in the same conditions, it seems clear that the reductive coupling is faster on palladium derivatives. This result is not unexpected and parallels what was found for the addition of I_2 to complexes $[NBu_4]_2[(R_F)_2Pt(\mu\text{-}PPh_2)_2M(R_F)_2]$ (M = Pt, Pd). In these cases the isolated complexes $[NBu_4][(R_F)_2Pt(\mu\text{-}PPh_2)(\mu\text{-}I)M(R_F)(PPh_2R_F)]$ contained the ligand PPh_2R_F, as a consequence of a PPh_2 and C_6F_5 reductive coupling, but only for M = Pt the intermediate dinuclear Pt(III)−Pt(III) was observed and isolated. In complex **2** the C^N chelate ligand is bonded to a palladium center, the platinum atom is bonded to the C_6F_5 groups, and the oxidative addition occurs only on the palladium center. Finally, complex **3** shows the C^N chelate ligand bonded to a platinum center and the palladium atom bonded to the C_6F_5 groups and the identification of the complexes **9**, **10**, and **11** after reacting **3** with I_2 indicates that the oxidative addition of I_2 takes place in all likelihood on both metal centers. The oxidative addition to the Pt(II) center could produce **9** and **10** while the oxidative addition to Pd(II), and the subsequent reductive coupling of the PPh_2 and C_6F_5 groups on the intermediate and unstable Pd(IV) complex, could produce complex **11** with the $PPh_2C_6F_5$ ligand coordinated to the Pd(II) center.

Interestingly, although formation of C−C and C−X (X = halogen) bonds from M(IV) derivatives (M = Pt, Pd) is now well documented,[5,81−85] in our case the reductive coupling between a phosphanido bridge and the cyclometaled C,N ligand, with P−C bond formation, is observed.

It is worth commenting that the phosphanido ligands have been widely used as building blocks for the synthesis of a great variety of polynuclear palladium and platinum complexes due to their flexibility and to the stability of the M−P bonds, both facts being the main reasons of the retention of the polynuclear fragment $M(\mu\text{-}PR_2)_xM'$ (M, M′ = Pd, Pt) during the chemical reactions of phosphanido complexes.[86,87] However, nowadays, examples in which the polynuclear fragment $M(\mu\text{-}PR_2)_xM'$ evolves,[48,59,69,88−92] and the phosphanido ligand is transformed into another ligand[42,44,49,64,69−73,93−95] or is coordinated in a nonclassical bonding mode,[69,96−99] have already been reported. The process that produces **6** from **1** is the transformation of a phosphanido bridging ligand and a C^N chelate ligand into an aminophosphane group through a reductive coupling induced by oxidation. The formation of aminophosphane ligands had already been reported through a reductive elimination process on palladium(II) complexes leaving Pd(0) substrates.[100,101]

CONCLUDING REMARKS

The asymmetric homo- or heteronuclear complexes **1**−**4**, $[NBu_4][(R_F)_2M(\mu\text{-}PPh_2)_2M'(C_{13}H_8N)]$, were prepared by the adequate reactions of $Li_2[M(R_F)_2(PPh_2)_2]$ with $[\{M'(\mu\text{-}Cl)(C^N)\}_2]$. The addition of I_2 to these complexes resulted in the formation of a different type of complexes, the nature of which is mainly dependent on the type of binuclear compound used. In the case of the homodinuclear derivative **1**, M = M′ = Pt, it was possible to isolate the dinuclear Pt(II),Pt(IV) complex $[NBu_4][(R_F)_2Pt^{II}(\mu\text{-}PPh_2)_2Pt^{IV}(C^N)I_2]$ carrying out the reaction in acetone. For the other starting materials (**2**−**4**) and also for **1** when the reaction is carried out in CH_2Cl_2, the resulting compounds are M(II),M′(II) complexes which contain PPh_2−$C_{13}H_8N$ ligand as a result of the reductive coupling between a PPh_2 group and the benzoquinolinate ligand with formation of a P−C bond. The new resulting ligand remains coordinate chelated to one of the metal centers.

It seems also clear that the reductive coupling induced after addition of I_2 is faster on the palladium than on the platinum complexes and that it is also preferred on the metal center bonded to the C^N ligand than on the metal center bonded to the two C_6F_5 groups.

The identification of **9**−**11** obtained from **3** indicates that the oxidative addition of I_2 on the Pd center bonded to two pentafluorophenyl groups competes with the addition on the Pt center bonded to the C^N ligand.

It is also remarkable that while the oxidative addition of I_2 to these unsymmetrical complexes results initially in the formation of mixed-valence M(II),M′(IV) complexes (in some cases very unstable), the reaction of I_2 with the symmetric complexes $[NBu_4]_2[(R_F)_2M(\mu\text{-}PPh_2)_2M'(R_F)_2]$ results in the formation of M(III)−M′(III) derivatives.

Finally, in addition to the two well-known characteristics of phosphanido ligands frequently discussed since the chemistry of phosphanido complexes flourished (their flexibility, which allows them to support a great variety of structural situations, and the stability of M−P bond) a third characteristic has to be added today, the ability of the diphenylphosphanido group as a

very versatile ligand capable of stabilizing complexes of palladium or platinum in very different oxidation states: I, II, III, and IV.

EXPERIMENTAL SECTION

General Comments. C, H, and N analyses were performed with a Perkin-Elmer 2400 analyzer. IR spectra were recorded on a Perkin-Elmer Spectrum 100 FT-IR spectrometer. NMR spectra in solution were recorded on a Bruker AV 400 spectrometer with $SiMe_4$, $CFCl_3$, 85% H_3PO_4, and aqueous $[PtCl_6]^{2-}$ as external references for ^1H, ^{19}F, ^{31}P, and ^{195}Pt, respectively. The signal attributions and coupling constant assessment was made on the basis of a multinuclear NMR analysis of each compound including, besides 1D spectra, ^1H COSY, ^1H NOESY, $^1H-^{31}P$ HMQC, $^1H-^{195}Pt$ HMQC, ^{19}F COSY, $^{19}H-^1H$ HOESY, and ^{19}F NOESY experiments. Literature methods were used to prepare the starting materials *cis*-$[M(R_F)_2(PPh_2H)_2]$, M = Pd, Pt[45] and $[\{M(\mu\text{-Cl})(C\text{^}N)\}_2]$, M = Pd,[102] Pt.[103]

Synthesis of $[NBu_4][(R_F)_2M(\mu\text{-}PPh_2)_2M'(C\text{^}N)]$. *M = M′ = Pt*, ***1***. To a colorless solution of *cis*-$[Pt(C_6F_5)_2(PPh_2H)_2]$ (0.601 g, 0.667 mmol) in THF (10 mL) at −78 °C was added *n*-butyllitium (2.5 M in hexanes, 0.54 mL, 1.35 mmol) under an argon atmosphere. The resulting yellow solution was stirred for 15 min, and $[\{Pt(\mu\text{-Cl})(C\text{^}N)\}_2]$ (0.273 g, 0.334 mmol) was added. The suspension was allowed to reach room temperature, stirred for 20 h, and evaporated to dryness. CH_2Cl_2 (25 mL) was added to the resulting residue, and a solid was filtered through Celite. The CH_2Cl_2 solution was evaporated to dryness, and the residue was dissolved in ^{i}PrOH (ca. 30 mL). NBu_4ClO_4 (0.228 g, 0.667 mmol) was added to the solution, and **1** crystallized as a yellow solid, which was filtered, washed with ^{i}PrOH (3 × 1 mL), and dried, 0.873 g, 86% yield. Found: C, 51.35; H, 4.44; N, 1.93. $C_{65}F_{10}H_{64}N_2P_2Pt_2$ requires C, 51.52; H, 4.26; N, 1.85. HRMS(−), exact mass for the anion $[C_{49}H_{28}F_{10}NP_2Pt_2]^-$: 1272.0835. Measured *m/z*: 1272.0823 $(M)^-$.

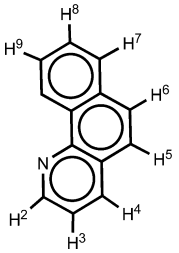

$^{31}P\{^1H\}$ NMR (161 MHz, 298 K, $(CD_3)_2CO$): δ −107.9 (d, $^2JP,P$ = 116 Hz, $^1JP1,Pt2$ = 2810 Hz, $^1JP1,Pt1$ = 1937 Hz, P1), −118.9 (d, $^2JP,P$ = 116 Hz, $^1JP2,Pt2$ = 1320 Hz, $^1JP2,Pt1$ = 1646 Hz, P2).

^{19}F NMR (376 MHz, 298 K, $(CD_3)_2CO$): δ −113.9 (m, 4 *o*-F, $^3JPt,F$ = ca. 330 Hz), −167.4 (ddd, 2 *m*-F, $^3JF,F$ = 25 Hz, $^3JF,F$ = 20 Hz, $^5JF,P$ = 9 Hz), −166.7 (2 *m*-F, ddd, 2 *m*-F, $^3JF,P$ = 25 Hz, $^3JF,F$ = 20 Hz, $^5JF,P$ = 11 Hz), −169.1 (t, 1 *p*-F, $^3JF,F$ = 20 Hz), −169.2 (t, 1 *p*-F, $^3JF,F$ = 20 Hz) ppm.

^1H NMR (400 MHz, 298 K, $(CD_3)_2CO$): 8.66 (m,1H, H2), 8.45 (dd, 1H, $^3JH,H$ = 8.0, $^4JH,H$ = 1.0 Hz, H4), 7.96 (m, 4H, *o*-Ph bonded to P1), 7.85 (m, 4H, *o*-Ph bonded to P2), 7.82 (d, 1H, $^3JH,H$ = 8.8 Hz, H6), 7.68 (d, 1H, $^3JH,H$ = 8.8 Hz, H5), 7.51 (dd, 1H, ^3JHH = 7.8 Hz, ^4JHH = 0.6 Hz, H7), 7.30 (d, 1H, $^3JH,H$ = 8.0 Hz, H3), 7.29 (d, 1H, $^3JH,H$ = 7.9 Hz, H9), from 7.20 to 7.03 (m, 13 H, overlapped *m*-Ph + *p*-Ph + H8), 3.49 (m 8H, NBu_4^+), 1.87 (m 8H, NBu_4^+), 1.48 (pseudosextet, 8H, $^3JH,H$ = 7.4 Hz, NBu_4^+), 1.02 (t, 12H, $^3JH,H$ = 7.4 Hz, NBu_4^+) ppm.

$^{195}Pt\{^1H\}$ NMR (86 MHz, 298 K, $(CD_3)_2CO$): δ −3717 (dd, $^1JPt2,P2$ = 1320 Hz, $^1JPt2,P1$ = 2810 Hz, $^2JPt,Pt$ = 541 Hz, Pt2), δ −3889 (m, $^1JPt1,P2$ = 1646 Hz, $^1JPt1,P1$ = 1937 Hz,Pt1).

M = Pt, M′ = Pd, ***2***. Complex **2** was prepared similarly from *cis*-$[Pt(C_6F_5)_2(PPh_2H)_2]$ (1.000 g, 1.110 mmol), *n*-butyllitium (2.5 M in hexanes, 0.89 mL, 2.22 mmol), $[\{Pd(\mu\text{-Cl})(C\text{^}N)\}_2]$ (0.355 g, 0.555 mmol), and NBu_4ClO_4 (0.380 g, 1.110 mmol) as a yellow solid, 1.177 g, 74% yield. Found: C, 54.49; H, 4.41; N, 1.89. $C_{65}F_{10}H_{64}N_2P_2PdPt$ requires C, 54.72; H, 4.52; N, 1.96. HRMS(−), exact mass for the anion $[C_{49}H_{28}F_{10}NP_2PdPt]^-$: 1184.0240. Measured *m/z*: 1184.0366 $(M)^-$.

$^{31}P\{^1H\}$ NMR (161 MHz, 298 K, $(CD_3)_2CO$): δ −78.8 (d, $^2JP,P$ = 160 Hz, $^1JP1,Pt2$ = 2648 Hz, P1), −116.6 (d, $^2JP,P$ = 160 Hz, $^1JP2,Pt1$ = 1530 Hz, P2).

^{19}F NMR (376 MHz, 298 K, $(CD_3)_2CO$): δ −113.8 (m, 4 *o*-F, $^3JPt,F$ = ca. 330 Hz), −167.4 (ddd, 2 *m*-F, $^3JF,F$ = 25 Hz, $^3JF,F$ = 20 Hz, $^5JF,P$ = 9 Hz), −167.7 (2 *m*-F, ddd, 2 *m*-F, $^3JF,P$ = 25 Hz, $^3JF,F$ = 20 Hz, $^5JF,P$ = 10 Hz), −169.17 (t, 1 *p*-F, $^3JF,F$ = 20 Hz), −169.24 (t, 1 *p*-F, $^3JF,F$ = 20 Hz) ppm.

^1H NMR (400 MHz, 298 K, $(CD_3)_2CO$): 8.41 (dd, 1H, $^3JH,H$ = 8.0, $^4JH,H$ = 1.0 Hz, H4), 8.36 (m,1H, H2), 7.93 (m, 4H, *o*-Ph bonded to P1), 7.82 (d, 1H, $^3JH,H$ = 8.6 Hz, H6), 7.79 (m, 4H, *o*-Ph bonded to P2), 7.70 (d, 1H, $^3JH,H$ = 8.6 Hz, H5), 7.50 (d, 1H, ^3JHH = 7.3 Hz, H7), 7.27 (d, 1H, $^3JH,H$ = 7.9 Hz, H3), 7.26 (d, 1H, $^3JH,H$ = 7.9 Hz, H9), from 7.17 to 7.00 (m, 13 H, overlapped *m*-Ph + *p*-Ph + H8), 3.49 (m 8H, NBu_4^+), 1.87 (m 8H, NBu_4^+), 1.48 (pseudosextet, 8H, $^3JH,H$ = 7.4 Hz, NBu_4^+), 1.02 (t, 12H, $^3JH,H$ = 7.4 Hz, NBu_4^+) ppm.

$^{195}Pt\{^1H\}$ NMR (86 MHz, 298 K, $(CD_3)_2CO$): δ −3909 (m, $^1JPt1,P2$ = 1530 Hz, $^1JPt1,P1$ = 1806 Hz, Pt1).

M = Pd, M′ = Pt, ***3***. Complex **3** was prepared similarly from *cis*-$[Pd(C_6F_5)_2(PPh_2H)_2]$ (0.400 g, 0.492 mmol), *n*-butyllitium (2.5 M in hexanes, 0.39 mL, 0.98 mmol), $[\{Pt(\mu\text{-Cl})(C\text{^}N)\}_2]$ (0.201 g, 0.246 mmol), and NBu_4ClO_4 (0.168 g, 0.492 mmol) as a yellow solid, 0.463 g, 66% yield. Found: C, 54.52; H, 4.63; N, 1.90. $C_{65}F_{10}H_{64}N_2P_2PdPt$ requires C, 54.72; H, 4.52; N, 1.96. HRMS(−), exact mass for the anion $[C_{49}H_{28}F_{10}NP_2PdPt]^-$: 1184.0240. Measured *m/z*: 1184.0334 $(M)^-$.

$^{31}P\{^1H\}$ NMR (161 MHz, 298 K, $(CD_3)_2CO$): δ −95.9 (d, $^2JP,P$ = 160 Hz, $^1JP1,Pt2$ = 2658 Hz, P1), −111.7 (d, $^2JP,P$ = 160 Hz, $^1JP2,Pt1$ = 1213 Hz, P2).

^{19}F NMR (376 MHz, 298 K, $(CD_3)_2CO$): δ −110.7 (m, 4 *o*-F), −166.3 (ddd, 2 *m*-F, $^3JF,F$ = 27 Hz, $^3JF,F$ = 20 Hz, $^5JF,P$ = 10 Hz), −166.6 (2 *m*-F, ddd, 2 *m*-F, $^3JF,P$ = 27 Hz, $^3JF,F$ = 20 Hz, $^5JF,P$ = 12 Hz), −168.0 (t, $^3JF,F$ = 20 Hz, 2 *p*-F overlapped) ppm.

^1H NMR (400 MHz, 298 K, $(CD_3)_2CO$): 8.62 (m,1H, H2), 8.45 (dd, 1H, $^3JH,H$ = 7.9, $^4JH,H$ = 1.3 Hz, H4), 7.94 (m, 4H, *o*-Ph bonded to P1), 7.84 (m, 4H, *o*-Ph bonded to P2), 7.83 (d, 1H, $^3JH,H$ = 8.8 Hz, H6), 7.68 (d, 1H, $^3JH,H$ = 8.8 Hz, H5), 7.52 (d, 1H, ^3JHH = 7.8 Hz, H7), 7.26 (d, 1H, $^3JH,H$ = 8.0 Hz, H3), 7.25 (d, 1H, $^3JH,H$ = 8.2 Hz, H9), from 7.18 to 7.03 (m, 13 H, overlapped *m*-Ph + *p*-Ph + H8), 3.49 (m 8H, NBu_4^+), 1.87 (m 8H, NBu_4^+), 1.48 (pseudosextet, 8H, $^3JH,H$ = 7.4 Hz, NBu_4^+), 1.02 (t, 12H, $^3JH,H$ = 7.4 Hz, NBu_4^+) ppm.

$^{195}Pt\{^1H\}$ NMR (86 MHz, 298 K, $(CD_3)_2CO$): δ −3738 (dd, $^1JPt,P2$ = 1213 Hz, $^1JPt,P1$ = 2658 Hz).

M = M′ = Pd, ***4***. Complex **4** was prepared similarly from *cis*-$[Pd(C_6F_5)_2(PPh_2H)_2]$ (0.432 g, 0.534 mmol), *n*-butyllitium (2.5 M in hexanes, 0.43 mL, 1.07 mmol), $[\{Pd(\mu\text{-Cl})(C\text{^}N)\}_2]$ (0.170 g, 0.267 mmol), and NBu_4ClO_4 (0.183 g, 0.534 mmol) as a yellow solid, 0.509 g, 72% yield. Found: C, 58.06; H, 4.80; N, 2.11. $C_{65}F_{10}H_{64}N_2P_2Pd_2$ requires C, 58.35; H, 4.82; N, 2.09. HRMS(−), exact mass for the anion $[C_{49}H_{28}F_{10}NP_2Pd_2]^-$: 1095.9637. Measured *m/z*: 1095.9626 $(M)^-$.

$^{31}P\{^1H\}$ NMR (161 MHz, 298 K, $(CD_3)_2CO$): δ −58.0 (d, $^2JP,P$ = 204 Hz, P1), −107.4 (d, $^2JP,P$ = 204 Hz, P2).

^{19}F NMR (376 MHz, 298 K, $(CD_3)_2CO$): δ −110.5 (m, 4 *o*-F), −166.3 (ddd, 2 *m*-F, $^3JF,F$ = 27 Hz, $^3JF,F$ = 20 Hz, $^5JF,P$ = 10 Hz), −166.6 (2 *m*-F, ddd, 2 *m*-F, $^3JF,P$ = 27 Hz, $^3JF,F$ = 20 Hz, $^5JF,P$ = 12 Hz), −168.0 (t, $^3JF,F$ = 20 Hz, 2 *p*-F overlapped) ppm.

^1H NMR (400 MHz, 298 K, $(CD_3)_2CO$): 8.40 (dd, 1H, $^3JH,H$ = 8.2 Hz, $^4JH,H$ = 0.9 Hz, H4), 8.35 (m, 1H, H2), 7.92 (m, 4H, *o*-Ph bonded to P1), 7.82 (d, 1H, $^3JH,H$ = 8.6 Hz, H6), 7.78 (m, 4H, *o*-Ph bonded to P2), 7.70 (d, 1H, $^3JH,H$ = 8.6 Hz, H5), 7.50 (d, 1H, ^3JHH = 7.6 Hz, H7), 7.25 (d, 1H, $^3JH,H$ = 8.0 Hz, H9), 7.24 (d, 1H, $^3JH,H$ = 7.9 Hz, H3), from 7.16 to 6.99 (m, 13 H, overlapped *m*-Ph + *p*-Ph + H8), 3.49 (m 8H, NBu_4^+), 1.87 (m 8H, NBu_4^+), 1.48 (pseudosextet, 8H, $^3JH,H$ = 7.4 Hz, NBu_4^+), 1.02 (t, 12H, $^3JH,H$ = 7.4 Hz, NBu_4^+) ppm.

dx.doi.org/10.1021/ic301298p | *Inorg. Chem.* 2012, 51, 12682−12696

Addition of I_2 to **1**. To a yellow solution of **1** (0.180 g, 0.118 mmol) in acetone (20 mL) was added I_2 (0.030 g, 0.118 mmol) in acetone (10 mL) dropwise. The solution was stirred at room temperature for 3.5 h, and the resulting red solution was evaporated to ca. 1 mL. *i*-PrOH (10 mL) was added, and **5** crystallized as a yellow solid which was filtered, washed with *i*-PrOH (2 × 1 mL), and air-dried, 0.175 g, 84% yield. Found: C, 43.73; H, 3.61; N, 1.63. $C_{65}F_{10}H_{64}I_2N_2P_2Pt_2$ requires C, 44.13; H, 3.65; N, 1.58. HRMS(−), exact mass for the anion $[C_{49}H_{28}F_{10}I_2P_2Pt_2]^-$: 1525.8924. Measured *m*/*z*: 1525.8911 $(M)^-$.

$[NBu_4][(R_F)_2Pt(\mu\text{-}PPh_2)_2Pt(C^\wedge N)I_2]$ (5). $^{31}P\{^1H\}$ NMR (161 MHz, 298 K, $(CD_3)_2CO$): δ −107.5 (d, $^2JP,P$ = 126 Hz, $^1JP2,Pt2$ = 1270 Hz, $^1JP2,Pt1$ = 2189 Hz, P2), −115.5 (d, $^2JP,P$ = 126 Hz, $^1JP1,Pt2$ = 1807 Hz, $^1JP1,Pt1$ = 2032 Hz, P1).

^{19}F NMR (376 MHz, 298 K, $(CD_3)_2CO$): δ −114.6 (very broad, 2F, F1+F5), −116.4 (1F, $^3JPt,F$ = 335 Hz, F6), −118.6 (1F, $^3JPt,F$ = 267 Hz, F10), −165.1 (1F, F9), −166.8 (t, 1 F, $^3JF,F$ = 19 Hz, F3), −166.9 (t, 1 F, $^3JF,F$ = 20 Hz, F8), from −167.0 to −166.3 (m, 3 F, F7 + F2 + F4) ppm.

^{19}F NMR (376 MHz, 200 K, $(CD_3)_2CO$): δ −113.9 (1F, $^3JPt,F$ = 302 Hz, F5), −116.2 (1F, $^3JPt,F$ = 237 Hz, F1), −116.9 (1F, $^3JPt,F$ = 230 Hz, F6), −119.1 (1F, $^3JPt,F$ = 252 Hz, F10), −163.9 (1F, F9), −165.2 (t, 1F, $^3JF,F$ = 20 Hz, F3), −165.3 (t, 1F, $^3JF,F$ = 20 Hz, F8), −165.7 (1F, F7), −165.9 (1F, F2), −166.2 (1F, F4) ppm.

^1H NMR (700 MHz, 298 K, $(CD_3)_2CO$): δ 10.73 (d, 1H, $^3JH,H$ = 5.2 Hz, H23), δ 9.64 (m, 1H, $^3JH,Pt$ = 39 Hz, H14), δ 8.61 (dd, 2H, $^3JH,H$ = 7.2 Hz, $^3JH,P$ = 11.3 Hz, H33/37), δ 8.46 (dd, 1H, $^4JH,H$ = 1.3, $^3JH,H$ = 7.8, H21), δ 8.23 (dd, 2H, $^3JH,H$ = 7.7 Hz, $^3JH,P$ = 10.6 Hz, H 39/43), δ 7.69 (d, 1H, $^3JH,H$ = 8.7 Hz, H18), δ 7.66 (partially overlapped dd, 1H, $^3JH,H$ = 5.2 Hz, $^3JH,H$ = 7.8, H 22), δ from 7.66 to 7.64 (m, 3H, H 15 + H16 + H19), δ 7.44 (broad m, 2H, H 27/31), δ 7.31 (d, 1H, $^3JH,H$ = 7.2, H 35), δ 7.29 (pseudo t, 2H, $^3JH,H$ = 7.2 Hz, H 34/H36), δ 7.26 (d, 1H, $^3JH,H$ = 7.2, H41), δ 7.21 (pseudo t, 2H, $^3JH,H$ = 7.7 Hz, H 40/H42), δ 7.15 (t, 1H, $^3JH,H$ = 7.1, H 29), δ 6.85 (pseudo t, 2H, $^3JH,H$ = 7.6 Hz, H 28/H30), δ 6.50 (dd, 2H, $^3JH,H$ = 8.3 Hz, $^3JH,P$ = 10.0 Hz, H 45/H49), δ 6.45 (t, 1H, $^3JH,H$ = 7.2, H47), δ 6.05 (pseudo t, 2H, $^3JH,H$ = 7.4 Hz, H 46/H48), 3.47 (m, 8H, NBu_4^+), 1.84 (m, 8H, NBu_4^+), 1.45 (pseudosextet, 8H, $^3JH,H$ = 7.4, NBu_4^+), 0.97 (t, 12H,$^3JH,H$ = 7.4, NBu_4^+) ppm.

$^{195}Pt\{^1H\}$ NMR (86 MHz, 298 K, $(CD_3)_2CO$): δ −2917 (dd, $^1JPt2,P2$ = 1270 Hz, $^1JPt2,P1$ = 1807 Hz, $^2JPt,Pt$ = 100 Hz, Pt2), δ −3806 (broad, Pt1).

To a yellow solution of **1** (0.281 g, 0.185 mmol) in CH_2Cl_2 (20 mL) was added dropwise I_2 (0.047 g, 0.185 mmol) in CH_2Cl_2 (10 mL). The solution was stirred at room temperature for 20 h, and the resulting orange solution was evaporated to ca. 1 mL. *i*-PrOH (10 mL) was added, and a yellow solid crystallized which was filtered, washed with *i*-PrOH (2 × 1 mL), and air-dried, 0.231 g. The solid was characterized by NMR spectroscopy as a mixture of **5** and **6**. The analysis of solids obtained from different preparations showed about 20−25% of **6** in the mixtures. A 0.202 g portion of a mixture was dissolved in 1 mL of CH_2Cl_2 and passed through a silica column (3 cm^2 × 15 cm) with CH_2Cl_2 as eluent, and the CH_2Cl_2 solution was evaporated to ca. 1 mL. *n*-Hexane (10 mL) was added, and **6** crystallized as a yellow solid, 0.085 g. Found: C, 41.77; H, 2.01; N, 1.01. $C_{49}F_{10}H_{28}INP_2Pt_2$ requires C, 42.04; H, 2.02; N, 1.00. HRMS(+), exact mass for $[C_{49}H_{28}F_{10}NP_2Pt]$: 1398.9868. Measured *m*/*z*: 1421.9502 $(M + Na)^+$.

$[(R_F)_2Pt(\mu\text{-}PPh_2)(\mu\text{-}I)Pt\{PPh_2(C_{13}H_8N)\}]$ (6). $^{31}P\{^1H\}$ NMR (161 MHz, 298 K, $(CD_3)_2CO$): δ −11.4 (d, $^2JP,P$ = 2 Hz, $^1JP1,Pt2$ = 2513 Hz, $^1JP1,Pt1$ = 1846 Hz, P1), 14.2 (d, $^2JP,P$ = 2 Hz, $^1JP2,Pt2$ = 4435 Hz, $^3JP2,Pt1$ = 37 Hz, P2) ppm.

^{19}F NMR (376 MHz, 298 K, $(CD_3)_2CO$): δ −115.2 (m, 2F, $^3JPt,F$ = 330 Hz, F1/5), −117.3 (m, 2F, $^3JPt,F$ = 536 Hz, F6/10), −165.2 (t, 1F, $^3JF,F$ = 19 Hz, F3), −166.2 (ddd, 2F, $^3JF,F$ = 22 Hz, $^3JF,F$ = 20 Hz, $^5JF,P$ = 9 Hz, F2/4), −167.4 (t, 1F, $^3JF,F$ = 19 Hz, F8), −167.5 (m, 2F, F7/9) ppm.

^1H NMR (400 MHz, 298 K, $(CD_3)_2CO$): 10.58 (broad d, 1H, $^3JH,H$ = 5.0 Hz, H13), 8.94 (dd, 1H, $^3JH,H$ = 8.0 Hz, $^4JH,H$ = 1.5 Hz, H15), 8.52 (d of pseudo t, 1H, $^3JH,H$ = 8.0 Hz, $^4JH,H$ = 1.2 Hz, H20), 8.32 (dd, 1H, $^3JH,H$ = 8.9 Hz, $^4JH,H$ = 1.6 Hz, H18), 8.18 (d, 1H, $^3JH,H$ = 8.9 Hz, H17), 8.07 (dd, 1H, $^3JH,H$ = 8.0 Hz, $^3JH,H$ = 5.2 Hz, H14), 7.98 (pseudo t of d, 1H, $^3JH,H$ = 7.8 Hz, $^4JH,P$ = 1.5 Hz, H21), 7.65 (ddd, 1H, $^3JH,H$ = 13.5 Hz, $^3JH,H$ = 7.5 Hz, $^3JH,P$ = 1.2 Hz, H22), from 7.65 to 7.52 (broad, 4H, H33, H37, H27, H31), from 7.52 to 7.41 (m, 6H, H39, H41, H43, H45, H47, H49), from 7.32 to 7.23 (m, 4H, overlapped H40/42 + H46/48), 7.22 (m, 2H, overlapped H29+H35), 7.07 (m, 4H, overlapped H28/30 + H34/36) ppm.

$^{195}Pt\{^1H\}$ NMR (86 MHz, 298 K, $(CD_3)_2CO$): δ −4238 (m, $^1JPt1,P1$ = 1846 Hz, $^3JPt1,F6/10$ = 536 Hz, $^3JPt1,F1/5$ = 330 Hz, Pt1), δ −4397 (dd, $^1JPt2,P2$ = 4435 Hz, $^1JPt2,P1$ = 2513 Hz, Pt2) ppm.

Addition of I_2 to **2** *and* **4**. To a yellow solution of **2** (0.204 g, 0.143 mmol) in CH_2Cl_2 (20 mL) was added dropwise I_2 (0.036 g, 0.143 mmol) in CH_2Cl_2 (10 mL). The solution was stirred at room temperature for 20 h, and the red solution was evaporated to ca. 1 mL. *i*-PrOH (10 mL) was added, and **7** crystallized as a yellow solid which was filtered, washed with *i*-PrOH (2 × 1 mL), and air-dried, 0.136 g, 72% yield. Found: C, 44.62; H, 2.00; N, 1.00. $C_{49}F_{10}H_{28}INP_2PdPt$ requires C, 44.89; H, 2.15; N, 1.07. HRMS(+), exact mass for $[C_{49}H_{28}F_{10}INP_2PdPt]$: 1310.9274. Measured *m*/*z*: 1333.9183 $(M + Na)^+$.

$[(R_F)_2Pt(\mu\text{-}PPh_2)(\mu\text{-}I)Pd\{PPh_2(C_{13}H_8N)\}]$ (7). $^{31}P\{^1H\}$ NMR (298 K, $(CD_3)_2CO$, 161 MHz): δ 55.2 (m, $^2JP,P$ = 40 Hz, $^1JP1,Pt$ = 1864 Hz, P1), 37.5 (d, $^2JP,P$ = 40 Hz, $^3JP2,Pt$ = 97 Hz, P2) ppm.

^{19}F NMR (376 MHz, 298 K, $(CD_3)_2CO$): δ −115.5 (m, 2F, $^3JPt,F$ = 319 Hz, F1/5), −116.2 (m, 2F, $^3JPt,F$ = 526 Hz, F6/10), −165.1 (t, 1F, $^3JF,F$ = 20 Hz, F3), −166.2 (ddd, 2F, $^3JF,F$ = 22 Hz, $^3JF,F$ = 20 Hz, $^5JF,P$ = 9 Hz, F2/4), −166.8 (t, 1F, $^3JF,F$ = 19 Hz, F8), −167.2 (m, 2F, F7/9) ppm.

^1H NMR (400 MHz, 298 K, $(CD_3)_2CO$): 10.56 (broad d, 1H, $^3JH,H$ = 4.8 Hz, H13), 8.83 (dd, 1H, $^3JH,H$ = 8.0 Hz, $^4JH,H$ = 1.5 Hz, H15), 8.49 (d of pseudo t, 1H, $^3JH,H$ = 8.0 Hz, $^4JH,H$ = 1.0 Hz, H20), 8.27 (dd, 1H, $^3JH,H$ = 8.7 Hz, $^4JH,H$ = 1.5 Hz, H18), 8.13 (d, 1H, $^3JH,H$ = 8.7 Hz, H17), 7.99 (dd, 1H, $^3JH,H$ = 8.0 Hz, $^3JH,H$ = 5.1 Hz, H14), 7.90 (ddd, 1H, $^3JH,H$ = 7.7 Hz, $^3JH,H$ = 7.8 Hz, $^4JH,P$ = 1.2 Hz, H21), 7.70 (ddd, 1H, $^3JH,H$ = 12.9 Hz, $^3JH,H$ = 7.6 Hz, $^3JH,P$ = 1.1 Hz, H22), from 7.60 to 7.45 (m, 10H, H27, H31, H33, H37, H39, H41, H43, H45, H47, H49), 7.30 (m, 4H, overlapped H40/42 + H46/48), 7.24 (m, 2H, overlapped H29+H35), 7.08 (m, 4H, overlapped H28/30 + H34/36) ppm.

$^{195}Pt\{^1H\}$ NMR (298 K, $(CD_3)_2CO$, 86 MHz): δ −4315 (dd, $^1JPt,P1$ = 1864 Hz, $^3JPt,P2$ = 97 Hz).

A similar procedure, using **4** (0.170 g, 0.127 mmol) and I_2 (0.032 g, 0.127 mmol), produces complex **8** as a yellow solid, 0.094 g, 60% yield. Solutions of **8** slowly became dark. Minor amounts of black palladium could be present in the samples of **8**. Found: C, 47.60; H, 2.20; N, 1.10. $C_{49}F_{10}H_{28}INP_2Pd_2$ requires C, 48.14; H, 2.31; N, 1.15. HRMS(+), exact mass for $[C_{49}H_{28}F_{10}INP_2Pd_2]$: 1222.8671. Measured: *m*/*z*: 1245.8558 $(M + Na)^+$.

$[(R_F)_2Pd(\mu\text{-}PPh_2)(\mu\text{-}I)Pd\{PPh_2(C_{13}H_8N)\}]$ (8). $^{31}P\{^1H\}$ NMR (161 MHz, 298 K, $(CD_3)_2CO$): δ 66.0 (m, $^2JP,P$ = 36 Hz, P1), 42.3 (d, $^2JP,P$ = 36 Hz, P2) ppm.

^{19}F NMR (376 MHz, 298 K, $(CD_3)_2CO$): δ −112.5 (very broad, 2F, F1/5), −113.6 (broad, 2F, F6/10), −164.3 (t, 1F, $^3JF,F$ = 20 Hz, F3), −165.2 (t of d, 1F, $^3JF,F$ = 20 Hz, $^4JF,F$ = 2 Hz, F8), −165.4 (ddd, 2F, $^3JF,F$ = 23 Hz, $^3JF,F$ = 19 Hz, $^5JF,P$ = 11 Hz, F2/4), −165.9 (dd, $^3JF,F$ = 24 Hz, $^3JF,F$ = 20 Hz, 2F, F7/9) ppm.

^1H NMR (400 MHz, 298 K, $(CD_3)_2CO$): 10.50 (broad d, 1H, $^3JH,H$ = 4.9 Hz, H13), 8.84 (dd, 1H, $^3JH,H$ = 8.0 Hz, $^4JH,H$ = 1.4 Hz, H15), 8.51 (d of pseudo t, 1H, $^3JH,H$ = 7.9 Hz, $^4JH,H$ = 1.2 Hz, H20), 8.29 (dd, 1H, $^3JH,H$ = 8.8 Hz, $^4JH,H$ = 1.4 Hz, H18), 8.15 (d, 1H, $^3JH,H$ = 8.8 Hz, H17), 8.00 (dd, 1H, $^3JH,H$ = 8.0 Hz, $^3JH,H$ = 5.1 Hz, H14), 7.95 (pseudo t of d, 1H, $^3JH,H$ = 7.8 Hz, $^4JH,P$ = 1.0 Hz, H21), 7.70 (ddd, 1H, $^3JH,H$ = 13.0 Hz, $^3JH,H$ = 7.5 Hz, $^3JH,P$ = 1.0 Hz, H22), from 7.64 to 7.39 (m, 10H, H27, H31, H33, H37, H39, H41, H43, H45, H47, H49), from 7.36 to 7.27 (m, 4H, overlapped H40/

42+H46/48), from 7.27 to 7.19 (m, 2H, overlapped H29+H35), from 7.14 to 7.01 (m, 4H, overlapped H28/30+H34/36) ppm.

Addition of I_2 to **3**. To a yellow solution of **3** (0.150 g, 0.105 mmol) in CH_2Cl_2 (10 mL) was added dropwise I_2 (0.027 g, 0.106 mmol) in CH_2Cl_2 (10 mL). The solution was stirred at room temperature for 20 h and evaporated to dryness to render a yellow solid. Its $^{31}P\{^1H\}$ NMR spectrum in acetone indicated that this solid is a complex mixture of products in which $[NBu_4][(R_F)_2Pd^{II}(\mu\text{-}PPh_2)_2Pt^{IV}(C\text{^}N)I_2]$ (**9**), $[(R_F)_2Pd^{II}(\mu\text{-}PPh_2)(\mu\text{-}I)Pt^{II}\{PPh_2(C_{13}H_8N)\}]$ (**10**), and $[(R_F)(PPh_2R_F)Pd^{II}(\mu\text{-}PPh_2)(\mu\text{-}I)Pt^{II}(C\text{^}N)]$ (**11**) could be identified (NMR spectroscopy) but not isolated as pure samples. All attempts to separate the mixture were unsuccessful.

Spectroscopic features of $[NBu_4][(R_F)_2Pd(\mu\text{-}PPh_2)_2Pt(C\text{^}N)I_2]$ (9). $^{31}P\{^1H\}$ NMR (161 MHz, 298 K, $(CD_3)_2CO$): δ −89.1 (broad d, $^2JP,P$ = 161 Hz, $^1JP2,Pt$ = 1121 Hz, P2), −97.7 (broad d, $^2JP,P$ = 161 Hz, $^1JP1,Pt$ = 1680 Hz, P1).

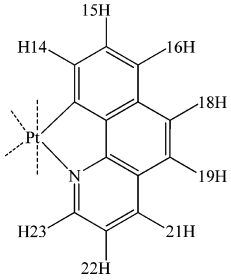

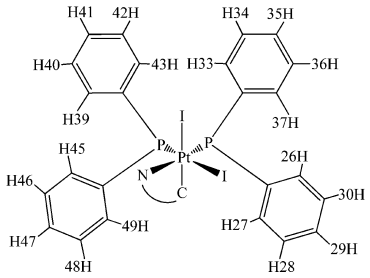

^1H NMR (400 MHz, 298 K, $(CD_3)_2CO$): δ 10.76 (m, 1H, H23), δ 9.47 (d, 1H, $^3JH,H$ = 6.5 Hz, $^3JH,Pt$ = 41 Hz, H14), δ 8.56 (dd, 2H, $^3JH,H$ = 7.3 Hz, $^3JH,P$ = 11.8 Hz, H33/37), δ 8.48 (d, 1H, $^3JH,H$ = 8.0, H21), δ 8.24 (dd, 2H, $^3JH,H$ = 8.2 Hz, $^3JH,P$ = 10.8 Hz, H 39/43), δ from 7.76 to 7.63 (overlapped, 5H, H15 + H16 + H18+ H19 + H22), δ 7.50 (pseudo t, 2H, $^3JH,H$ = 9.0 Hz, H 27/H31), δ from 7.33 to 7.14 (overlapped, 7H, H29 + H34 + H35 + H36 + H40 + H41 + H42), δ from 7.56 to 7.465 (partially overlapped, 3H, H 45 + H47 + H49), δ 6.10 (pseudo t, 2H, $^3JH,H$ = 7.8 Hz, H 46/H48), 3.50 (m, 8H, NBu_4^+), 1.86 (m, 8H, NBu_4^+), 1.48 (m, 8H, NBu_4^+), 1.02 (t, 12H, NBu_4^+) ppm.

$^{195}Pt\{^1H\}$ NMR (86 MHz, 298 K, $(CD_3)_2CO$): δ −2966 (dd, $^1JPt,P2$ = 1121 Hz, $^1JPt,P1$ = 1680 Hz).

X-ray Structure Determinations. Crystal data and other details of the structure analyses are presented in Table 4. Suitable crystals for X-ray diffraction studies were obtained by slow diffusion of *n*-hexane into concentrated solutions of the complexes in 3 mL of acetone (**5′**) or CH_2Cl_2 (**6**–**8**) at 5 °C. Crystals were mounted at the end of a quartz fiber. The radiation used in all cases was graphite monochromated Mo Kα (λ = 0.710 73 Å). X-ray intensity data were collected on an Oxford Diffraction Xcalibur diffractometer. The diffraction frames were integrated and corrected from absorption by using the CrysAlis RED program.[104] The structures were solved by Patterson and Fourier methods and refined by full-matrix least-squares on F^2 with SHELXL-97.[105] All non-hydrogen atoms were assigned anisotropic displacement parameters and refined without positional constraints. All hydrogen atoms were constrained to idealized geometries and assigned isotropic displacement parameters equal to

Table 4. Crystal Data and Structure Refinement for Complexes $[N(PPh_3)_2][(R_F)_2Pt^{II}(\mu\text{-}PPh_2)_2Pt^{IV}(C\text{^}N)I_2]\cdot Me_2CO\cdot 0.25n\text{-}C_6H_{14}$ (5′·Me_2CO·0.25*n*-C_6H_{14}), $[(R_F)_2Pt^{II}(\mu\text{-}PPh_2)(\mu\text{-}I)Pt^{II}\{PPh_2(C_{13}H_8N)\}]$ (6), $[(R_F)_2Pt^{II}(\mu\text{-}PPh_2)(\mu\text{-}I)Pd^{II}\{PPh_2(C_{13}H_8N)\}]\cdot n\text{-}C_6H_{14}\cdot 0.75CH_2Cl_2$ (7·*n*-C_6H_{14}·0.75CH_2Cl_2), and $[(R_F)_2Pd^{II}(\mu\text{-}PPh_2)(\mu\text{-}I)Pd^{II}\{PPh_2(C_{13}H_8N)\}]\cdot 0.75n\text{-}C_6H_{14}$ (8·0.75*n*-C_6H_{14})

	5′·Me_2CO·0.25*n*-C_6H_{14}	6	7·*n*-C_6H_{14}·0.75CH_2Cl_2	8·3CH_2Cl_2
formula	$C_{85}H_{58}F_{10}I_2N_2OP_4Pt_2\cdot Me_2CO\cdot 0.25n\text{-}C_6H_{14}$	$C_{49}H_{28}F_{10}INP_2Pt_2$	$C_{49}H_{28}F_{10}INP_2PdPt\cdot n\text{-}C_6H_{14}\cdot 0.75CH_2Cl_2$	$C_{49}H_{28}F_{10}INP_2Pd_2\cdot 0.75n\text{-}C_6H_{14}$
M_t [g mol^{-1}]	2144.82	1399.74	1460.92	1286.99
T [K]	100(1)	100(1)	100(1)	100(1)
λ [Å]	0.710 73	0.71073	0.710 73	0.710 73
cryst syst	triclinic	orthorhombic	monoclinic	monoclinic
space group	$P\bar{1}$	*Pbca*	$P2_1/c$	$P2_1/c$
a [Å]	10.3642(2)	11.7997(1)	17.2984(3)	17.1149(7)
b [Å]	19.8014(4)	20.9853(2)	13.6095(2)	13.7727(4)
c [Å]	20.3880(4)	34.6859(3)	22.9239(4)	22.9446(7)
α [deg]	88.4788(15)	90	90	90
β [deg]	81.7974(16)	90	96.7838(14)	97.294(3)
γ [deg]	80.0805(17)	90	90	90
V [Å^3]	4079.44(14)	8588.93(13)	5359.02(15)	5364.7(3)
Z	2	8	4	4
ρ [g cm^{-3}]	1.746	2.165	1.811	1.593
μ [mm^{-1}]	4.332	7.383	3.727	1.375
F(000)	2077	5264	2830	2526
2θ range [deg]	8.36–52.0	7.5–57.9	7.5–57.9	7.6–57.9
no. reflns collected	79857	50175	48264	58471
no. unique reflns	15993	10363	12672	12899
R(int)	0.0821	0.0267	0.0594	0.0569
final R indices [$I > 2\theta(I)$][a]				
R1	0.0482	0.0387	0.0349	0.0795
wR2	0.1254	0.1168	0.0590	0.2136
R indices (all data)				
R1	0.0620	0.0455	0.0683	0.1095
wR2	0.1304	0.1211	0.0621	0.2254
GOF on F^2[b]	1.010	1.061	1.018	1.068

[a] $R1 = \sum(|F_o| - |F_c|)/\sum|F_o|$. $wR_2 = [\sum w(F_o^2 - F_c^2)^2 / \sum w(F_o^2)^2]^{1/2}$. [b] $GOF = [\sum w(F_o^2 - F_c^2)^2/(n_{obs} - n_{param})]^{1/2}$.

dx.doi.org/10.1021/ic301298p | *Inorg. Chem.* 2012, 51, 12682–12696

1.2 times the U_{iso} values of their attached parent atoms (1.5 times for the methyl hydrogen atoms). Full-matrix least-squares refinement of these models against F^2 converged to final residual indices given in Table 4.

■ ASSOCIATED CONTENT

Ⓢ Supporting Information

Crystallographic data of **5′**·Me_2CO·0.25*n*-C_6H_{14}, **6**, **7**·*n*-C_6H_{14}·0.75CH_2Cl_2, and **8**·3CH_2Cl_2 (CIF format). NMR spectra, figures, tables, and HRMS spectrograms. This material is available free of charge via the Internet at http://pubs.acs.org.

■ AUTHOR INFORMATION

Corresponding Author

*E-mail: cfortuno@unizar.es (C.F.).

Notes

The authors declare no competing financial interest.

■ ACKNOWLEDGMENTS

This work was supported by the Spanish MICINN (Project CTQ2008-06669-C02-01) and the Gobierno de Aragón (Grupo Consolidado: Química Inorgánica y de los Compuestos Organometálicos). A.A. gratefully acknowledges MICINN for an FPU grant. COST Action CM0802 "PhoSciNet" and Italian MIUR (PRIN Project 2009LR88XR) are also acknowledged for financial support.

■ REFERENCES

(1) Forniés, F.; Fortuño, C.; Ibáñez, S.; Martín, A.; Mastrorilli, P.; Gallo, V. *Inorg. Chem.* **2011**, *50*, 10798−10809.

(2) Canty, A. J. *Dalton Trans.* **2009**, 10409−10417.

(3) Ball, N. D.; Kampf, J. W.; Sanford, M. S. *J. Am. Chem. Soc.* **2010**, *132*, 2878−2879.

(4) Kalyani, D.; Deprez, N. R.; Desai, L. V.; Sanford, M. S. *J. Am. Chem. Soc.* **2005**, *127*, 7330−7331.

(5) Belzen, R.; Elsevier, C. J.; Dedieu, A.; Veldman, N.; Spek, A. L. *Organometallics* **2003**, *22*, 722−736.

(6) Sehnal, P.; Taylor, R. J. K.; Fairlamb, I. J. S. *Chem. Rev.* **2010**, *110*, 824−889.

(7) Arnold, P. L.; Sanford, M. S.; Pearson, S. M. *J. Am. Chem. Soc.* **2009**, *131*, 13912−13913.

(8) Xu, L. M.; Li, B. J.; Yang, Z.; Shi, Z. J. *Chem. Soc. Rev.* **2010**, *39*, 712−733.

(9) Muñiz, K. *Angew. Chem., Int. Ed.* **2009**, *48*, 9412−9423.

(10) Ball, N. D.; Gary, J. B.; Ye, Y.; Sanford, M. S. *J. Am. Chem. Soc.* **2011**, *133*, 7577−7584.

(11) Morales Morales, D.; Redon, R.; Yung, C.; Jensen, C. M. *Chem. Commun.* **2000**, 1619−1620.

(12) Sunderman, A.; Uzan, O.; Martín, J. M. L. *Chem.—Eur. J.* **2001**, *7*, 1703−1711.

(13) Sjövall, S.; Wendt, O. F.; Andersson, C. *J. Chem. Soc., Dalton Trans.* **2002**, 1396−1400.

(14) Phan, N. T. S.; Van der Sluys, M.; Jones, C. W. *Adv. Synth. Catal.* **2006**, *348*, 609−679.

(15) Gerber, R.; Blacque, O.; Frech, C. M. *ChemCatChem* **2009**, *1*, 393−400.

(16) Shabashov, D.; Gaugulis, O. *J. Am. Chem. Soc.* **2010**, *132*, 3965−3972.

(17) Blacque, O.; Frech, C. M. *Chem.—Eur. J.* **2010**, *16*, 1521−1531.

(18) Zhang, H.; Lei, A. *Dalton Trans* **2011**, *40*, 8745−8754.

(19) Julia-Hernández, F.; Arcas, A.; Vicente, J. *Chem.—Eur. J.* **2012**, *18*, 7780−7786.

(20) Powers, D. C.; Geibel, M. A. L.; Klein, J. E. M. N.; Ritter, T. *J. Am. Chem. Soc.* **2009**, *131*, 17050−17051.

(21) Powers, D. C.; Benitez, D.; Tkatchouck, E.; Goddard, W. A., III; Ritter, T. *J. Am. Chem. Soc.* **2010**, *132*, 14092−14103.

(22) Ariafard, A.; Hyland, C. J. T.; Canty, A. J.; Sharma, M.; Yates, B. F. *Inorg. Chem.* **2011**, *50*, 6449−6457.

(23) Khusnutdinova, J. R.; Rath, N. P.; Mirica, L. M. *Angew. Chem., Int. Ed.* **2011**, *50*, 5532−5536.

(24) Martínez-Martínez, A. J.; Chicote, M. T.; Bautista, D.; Vicente, J. *Organometallics* **2012**, *31*, 3711−3719.

(25) Matsumoto, K.; Ochiai, M. *Coord. Chem. Rev.* **2002**, *231*, 229−238.

(26) Dick, A. R.; Kampf, J. W.; Sanford, M. S. *Organometallics* **2005**, *24*, 482−485.

(27) Ochiai, M.; Y-S., L.; Yamada, J.; Misawa, H.; Arai, S.; Matsumoto, K. *J. Am. Chem. Soc.* **2004**, *126*, 2536−2445.

(28) Iwatsuki, S.; Mizushima, C.; Morimoto, N.; Muranaka, S.; Ishihara, K.; Matsumoto, K. *Inorg. Chem.* **2005**, *44*, 8097−8104.

(29) Canty, A. J.; Gardiner, M. G.; Jones, R. C.; Rodemannn, T.; Sharma, M. *J. Am. Chem. Soc.* **2009**, *131*, 7236−7237.

(30) Whitfield, S. R.; Sanford, M. S. *Organometallics* **2008**, *27*, 1683−1689.

(31) Usón, R.; Forniés, J.; Tomás, M.; Casas, J. M.; Cotton, F. A.; Falvello, L. R.; Feng, X. *J. Am. Chem. Soc.* **1993**, *115*, 4145−4154.

(32) Anger, E.; Rudolph, M.; Shen, C.; Vanthuyne, N.; Toupet, L.; Roussel, C.; Autschbach, J.; Crassous, J.; Réau, R. *J. Am. Chem. Soc.* **2011**, *133*, 3800−3803.

(33) Romero, M. J.; Rodríguez, A.; Fernández, A.; López-Torres, M.; Vázquez-García, D.; Vila, J. M.; Fernández, J. J. *Polyhedron* **2011**, *30*, 2444−2450.

(34) Sicilia, V.; Forniés, F.; Casas, J. M.; Martín, A.; López, J. A.; Larraz, C.; Borja, P.; Ovejero, C.; Tordera, D.; Bolink, H. *Inorg. Chem.* **2012**, *51*, 3427−3435.

(35) Cotton, F. A.; Gu, J.; Murillo, C. A.; Timmons, D. J. *J. Am. Chem. Soc.* **1998**, *120*, 13280−13281.

(36) Cotton, F. A.; Koshevoy, I. O.; Lahuerta, P.; Murillo, C. A.; Sanau, M.; Ubeda, M. A. *J. Am. Chem. Soc.* **2006**, *128*, 13674−13675.

(37) Powers, D. C.; Ritter, T. *Nat. Chem.* **2009**, *1*, 302−309.

(38) Penno, D.; Estevan, F.; Fernández, E.; Hirva, P.; Lahuerta, P.; Sanaú, M.; Ubeda, M. A. *Organometallics* **2011**, *30*, 2083−2094.

(39) Deprez, N. R.; Sanford, M. S. *J. Am. Chem. Soc.* **2009**, *131*, 11234−11241.

(40) Ariafard, A.; Hyland, C. J. T.; Canty, A. J.; Sharma, M.; Brookes, N. J. *Inorg. Chem.* **2010**, *49*, 11249−11253.

(41) Alonso, E.; Casas, J. M.; Cotton, F. A.; Feng, X. J.; Forniés, J.; Fortuño, C.; Tomás, M. *Inorg. Chem.* **1999**, *38*, 5034−5040.

(42) Chaouche, N.; Forniés, J.; Fortuño, C.; Kribii, A.; Martín, A.; Karipidis, P.; Tsipis, A. C.; Tsipis, C. A. *Organometallics* **2004**, *23*, 1797−1810.

(43) Ara, I.; Chaouche, N.; Forniés, J.; Fortuño, C.; Kribii, A.; Martín, A. *Eur. J. Inorg. Chem.* **2005**, 3894−3901.

(44) Ara, I.; Chaouche, N.; Forniés, J.; Fortuño, C.; Kribii, A.; Tsipis, A. C. *Organometallics* **2006**, *25*, 1084−1091.

(45) Forniés, J.; Fortuño, C.; Navarro, R.; Martínez, F.; Welch, A. J. *J. Organomet. Chem.* **1990**, *394*, 643−658.

(46) Alonso, E.; Casas, J. M.; Forniés, J.; Fortuño, C.; Martín, A.; Orpen, A. G.; Tsipis, C. A.; Tsipis, A. C. *Organometallics* **2001**, *20*, 5571−5582.

(47) Alonso, E.; Forniés, J.; Fortuño, C.; Martín, A.; Orpen, A. G. *Organometallics* **2000**, *19*, 2690−2697.

(48) Alonso, E.; Forniés, J.; Fortuño, C.; Martín, A.; Orpen, A. G. *Organometallics* **2003**, *22*, 2723−2728.

(49) Ara, I.; Forniés, J.; Fortuño, C.; Ibáñez, S.; Martín, A.; Mastrorilli, P.; Gallo, V. *Inorg. Chem.* **2008**, *47*, 9069−9080.

(50) Bennett, M. A.; Bhargava, S. K.; Ke, M.; Willis, A. C. *Dalton Trans.* **2000**, 3537−3545.

(51) Yahav, A.; Goldberg, I.; Vigalok, A. *Organometallics* **2005**, *24*, 5654−5659.

(52) Ebsworth, E. A. V.; Ferrier, H. M.; Henner, B. J. L.; Rankin, D. W. H.; Reed, F. J. S.; Robertson, H. E.; Whitelock, J. D. *Angew. Chem., Int. Ed.* **1977**, *16*, 482−484.

(53) An overlap was observed between the *m*-F atoms of ring E, F2 and F4, and one of the *m*-F atoms of ring F, F7.

(54) Mallory, F. B. *J. Am. Chem. Soc.* **1973**, *95*, 7747−7752.
(55) Mallory, F. B.; Mallory, C. W.; Butler, K. E.; Levis, M. B.; Xia, A. Q.; Luzik, E. D.; Fredenburgh, L. E.; Ramanjulu, M. M.; Van, Q. N.; Francl, M. M.; Fredd, D. A.; Wray, C. C.; Hann., C.; Nerz-Stormes, M.; Carroll, P. J.; Chirlian, L. E. *J. Am. Chem. Soc.* **2000**, *122*, 4108−4116.
(56) Pregosin, P. S. *Coord. Chem. Rev.* **1982**, *44*, 247−291.
(57) Shimada, S.; Tanaka, M.; Honda, K. *J. Am. Chem. Soc.* **1995**, *117*, 8289−8290.
(58) Forniés, J.; Fortuño, C.; Gil, R.; Martín, A. *Inorg. Chem.* **2005**, *44*, 9534−9541.
(59) Alonso, E.; Forniés, J.; Fortuño, C.; Martín, A.; Rosair, G. M.; Welch, A. J. *Inorg. Chem.* **1997**, *36*, 4426−4431.
(60) Alonso, E.; Forniés, J.; Fortuño, C.; Tomás, M. *J. Chem. Soc., Dalton Trans.* **1995**, 3777−3784.
(61) Ara, I.; Chaouche, N.; Forniés, J.; Fortuño, C.; Kribii, A.; Tsipis, A. C.; Tsipis, C. A. *Inorg. Chim. Acta* **2005**, *358*, 1377−1385.
(62) Carty, A. J.; MacLaughlin, S. A.; Nucciarone, D. *Phosphorus-31 NMR Spectroscopy in Stereochemical Analysis*; VCH: Berlin, 1987.
(63) Falvello, L. R.; Forniés, J.; Fortuño, C.; Martín, A.; Martínez-Sariñena, A. P. *Organometallics* **1997**, *16*, 5849−5856.
(64) Forniés, J.; Fortuño, C.; Ibáñez, S.; Martín, A. *Inorg. Chem.* **2006**, *45*, 4850−4858.
(65) Forniés, J.; Fortuño, C.; Ibáñez, S.; Martín, A. *Inorg. Chem.* **2008**, *47*, 5978−5987.
(66) Nabavizadeh, S. M.; Amini, H.; Jame, F.; Khosraviolya, S.; Shahsavari, H. R.; Hosseini, F. N.; Rashidi, M. *J. Organomet. Chem.* **2012**, *698*, 53−61.
(67) Gossage, R. A.; Ryabov, A. D.; Spek, A. L.; Stufkens, D. J.; van Beek, J. A. M.; van Eldik, R.; van Koten, G. *J. Am. Chem. Soc.* **1999**, *121*, 2488−2497.
(68) In accord to the dissociative mechanism, while acetone solutions of **5** were found stable for weeks at room temperature, heating a $(CD_3)_2CO$ solution of **5** at 318 K resulted in a slow conversion into **6** (15% after three days).
(69) Chaouche, N.; Forniés, J.; Fortuño, C.; Kribii, A.; Martín, A. *J. Organomet. Chem.* **2007**, *692*, 1168−1172.
(70) Archambault, C.; Bender, R.; Braunstein, P.; Decian, A.; Fischer, J. *Chem. Commun.* **1996**, 2729−2730.
(71) Cabeza, J. A.; del Río, I.; Riera, V.; García-Granda, S.; Sanni, S. B. *Organometallics* **1997**, *16*, 1743−1748.
(72) Albinati, A.; Filippi, V.; Leoni, P.; Marchetti, L.; Pasquali, M.; Passarelli, V. *Chem. Commun.* **2005**, 2155−2157.
(73) Scriban, C.; Glueck, D. S.; Zakharov, L. N.; Kassel, W. S.; DiPasquale, A. G.; Golen, J. A.; Rheingold, A. L. *Organometallics* **2006**, *25*, 5757−5767.
(74) Kohl, S. W.; Heinemann, F. W.; Hummert, M.; Bauer, W.; Grohmann, A. *Chem.—Eur. J.* **2006**, *12*, 4313−4320.
(75) Li, B.; Xu, S.; Song, H.; Wang, B. *Eur. J. Inorg. Chem.* **2008**, 5494−5504.
(76) Nesterov, V.; Özbolat-Schön, A.; Schnakenburg, G.; Shi, L.; Cangönül, A.; van Gastel, M.; Neese, F.; Streubel, R. *Chem.—Asian J.* **2012**, *7*, 1708−1712.
(77) Welsch, S.; Nohra, B.; Peresypkina, E. V.; Lescop, C.; Scheer, M.; Réau, R. *Chem.—Eur. J.* **2009**, *15*, 4685−4703.
(78) Nohra, B.; Rodríguez-Sanz, E.; Lescop, C.; Réau, R. *Chem.—Eur. J.* **2008**, *14*, 3391−3403.
(79) Braunstein, P.; Boag, N. M. *Angew. Chem., Int. Ed.* **2001**, *40*, 2427−2433.
(80) Leca, F.; Sauthier, M.; Deborde, V.; Toupet, L.; Réau, R. *Chem.—Eur. J.* **2003**, *9*, 3785−3795.
(81) Oloo, W.; Zavalij, P. Y.; Zhang, J.; Khaskin, E.; Vedernikov, A. N. *J. Am. Chem. Soc.* **2010**, *132*, 14400−14402.
(82) Yahav-Levi, A.; Goldberg, I.; Vigalok, A.; Vedernikov, A. N. *Chem. Commun.* **2010**, *46*, 3324−3326.
(83) Ye, Y.; Ball, N. D.; Kampf, J. W.; Sanford, M. S. *J. Am. Chem. Soc.* **2010**, *132*, 14682−14687.
(84) Yahav-Levi, A.; Goldberg, I.; Vigalok, A. *J. Am. Chem. Soc.* **2006**, *128*, 8710−6711.
(85) Yahav-Levi, A.; Goldberg, I.; Vigalok, A.; Vedemikov, A. N. *J. Am. Chem. Soc.* **2008**, *130*, 724−731.
(86) Mastrorilli, P. *Eur. J. Inorg. Chem.* **2008**, 4835−4850.
(87) Berenguer, J. R.; Chaouche, N.; Forniés, J.; Fortuño, C.; Martín, A. *New J. Chem.* **2006**, *30*, 473−478.
(88) Alonso, E.; Forniés, J.; Fortuño, C.; Martín, A.; Orpen, A. G. *Chem. Commun.* **1996**, 231−232.
(89) Falvello, L. R.; Forniés, J.; Fortuño, C.; Durán, F.; Martín, A. *Organometallics* **2002**, *21*, 2226−2234.
(90) Bender, R.; Okio, C.; Welter, R.; Braunstein, P. *Dalton Trans.* **2009**, 4901−4907.
(91) Itazaki, M.; Nishihara, Y.; Osakada, K. *Organometallics* **2004**, *23*, 1610−1621.
(92) Leoni, P.; Manetti, S.; Pasquali, M.; Albinati, A. *Inorg. Chem.* **1996**, *35*, 6045−6052.
(93) Forniés, J.; Fortuño, C.; Ibáñez, S.; Martín, A.; Tsipis, A. C.; Tsipis, C. A. *Angew. Chem., Int. Ed.* **2005**, *44*, 2407−2410.
(94) Forniés, J.; Fortuño, C.; Ibáñez, S.; Martín, A.; Romero, P.; Mastrorilli, P.; Gallo, V. *Inorg. Chem.* **2011**, *50*, 285−298.
(95) Cristofani, S.; Leoni, P.; Pasquali, M.; Eisentraeger, F.; Albinati, A. *Organometallics* **2000**, *19*, 4589−4595.
(96) Bender, R.; Braunstein, P.; Dedieu, A.; Dusausoy, Y. *Angew. Chem., Int. Ed. Engl.* **1989**, *28*, 923−925.
(97) Leoni, P.; Pasquali, M.; Fortunelli, A.; Germano, G.; Albinati, A. *J. Am. Chem. Soc.* **1998**, *120*, 9564−9573.
(98) Leoni, P.; Marchetti, F.; Marchetti, L.; Passarelli, V. *Chem. Commun.* **2004**, 2346−2347.
(99) Alonso, E.; Forniés, F.; Fortuño, C.; Lledós, A.; Martín, A.; Nova, A. *Inorg. Chem.* **2009**, *48*, 7679−7690.
(100) Stepanova, V. A.; Dunina, V. V.; Smoliakova, I. P. *Organometallics* **2009**, *28*, 6546−6558.
(101) Stepanova, V. A.; Dunina, V. V.; Smoliakova, I. P. *J. Organomet. Chem.* **2011**, *696*, 871−878.
(102) Hartwell, G. E.; Lawrence, R. V.; Smas, M. J. *J. Chem. Soc., Chem. Commun.* **1970**, 912.
(103) Pregosin, P. S.; Wombacher, F.; Albinati, A.; Lianza, F. *J. Organomet. Chem.* **1991**, *418*, 249−267.
(104) *CrysAlisRED: Program for X-ray CCD Camera Data Reduction, Version 1.171.32.19*; Oxford Diffraction Ltd.: Oxford, U.K., 2008.
(105) Sheldrick, G. M. *SHELXL-97: A Program for Crystal Structure Determination*; University of Gottingen: Gottingen, Germany, 1997.

Inorganic Chemistry

Article

pubs.acs.org/IC

Oxidatively Induced P−O Bond Formation through Reductive Coupling between Phosphido and Acetylacetonate, 8-Hydroxyquinolinate, and Picolinate Groups†

Andersson Arias, Juan Forniés, Consuelo Fortuño,* and Antonio Martín

Departamento de Química Inorgánica, Instituto de Síntesis Química y Catálisis Homogénea, Universidad de Zaragoza-C.S.I.C., E-50009 Zaragoza, Spain

Piero Mastrorilli,* Stefano Todisco, Mario Latronico, and Vito Gallo

Dipartimento DICATECh del Politecnico di Bari and Istituto CNR-ICCOM, Via Orabona 4, I-70125 Bari, Italy

Supporting Information

ABSTRACT: The dinuclear anionic complexes $[NBu_4][(R_F)_2M^{II}(\mu\text{-}PPh_2)_2M'^{II}(N\text{^}O)]$ ($R_F = C_6F_5$. N^O = 8-hydroxyquinolinate, hq; M = M′ = Pt **1**; Pd **2**; M = Pt, M′ = Pd, **3**. N^O = *o*-picolinate, pic; M = Pt, M′ = Pt, **4**; Pd, **5**) are synthesized from the tetranuclear $[NBu_4]_2[\{(R_F)_2Pt(\mu\text{-}PPh_2)_2M(\mu\text{-}Cl)\}_2]$ by the elimination of the bridging Cl as AgCl in acetone, and coordination of the corresponding *N*,*O*-donor ligand (**1**, **4**, and **5**) or connecting the fragments "*cis*-$[(R_F)_2M(\mu\text{-}PPh_2)_2]^{2-}$" and "M′(N^O)" (**2** and **3**). The electrochemical oxidation of the anionic complexes **1**−**5** occurring under HRMS(+) conditions gave the cations $[(R_F)_2M(\mu\text{-}PPh_2)_2M'(N\text{^}O)]^+$, presumably endowed with a M(III),M′(III) core. The oxidative addition of I_2 to the 8-hydroxyquinolinate complexes **1**−**3** triggers a reductive coupling between a PPh_2 bridging ligand and the *N*,*O*-donor chelate ligand with formation of a P−O bond and ends up in complexes of platinum(II) or palladium(II) of formula $[(R_F)_2M^{II}(\mu\text{-}I)(\mu\text{-}PPh_2)M'^{II}(P,N\text{-}PPh_2hq)]$, M = M′ = Pt **7**, Pd **8**; M = Pt, M′ = Pd, **9**. Complexes **7**−**9** show a new $Ph_2P\text{-}OC_9H_6N$ (Ph_2P-hq) ligand bonded to the metal center in a *P*,*N*-chelate mode. Analogously, the addition of I_2 to solutions of the *o*-picolinate complexes **4** and **5** causes the reductive coupling between a PPh_2 bridging ligand and the starting *N*,*O*-donor chelate ligand with formation of a P−O bond, forming $Ph_2P\text{-}OC_6H_4NO$ (Ph_2P-pic). In these cases, the isolated derivatives $[NBu_4][(Ph_2P\text{-}pic)(R_F)Pt^{II}(\mu\text{-}I)(\mu\text{-}PPh_2)M^{II}(R_F)I]$ (M = Pt **10**, Pd **11**) are anionic, as a consequence of the coordination of the resulting new phosphane ligand (Ph_2P-pic) as monodentate *P*-donor, and a terminal iodo group to the M atom. The oxidative addition of I_2 to $[NBu_4][(R_F)_2Pt^{II}(\mu\text{-}PPh_2)_2Pt^{II}(acac)]$ (**6**) (acac = acetylacetonate) also results in a reductive coupling between the diphenylphosphanido and the acetylacetonate ligand with formation of a P−O bond and synthesis of the complex $[NBu_4][(R_F)_2Pt^{II}(\mu\text{-}I)(\mu\text{-}PPh_2)Pt^{II}(Ph_2P\text{-}acac)I]$ (**12**). The transformations of the starting complexes into the products containing the P−O ligands passes through mixed valence M(II),M′(IV) intermediates which were detected, for M = M′ = Pt, by spectroscopic and spectrometric measurements.

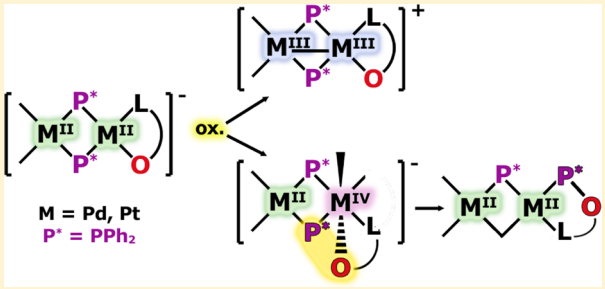

INTRODUCTION

Although the chemistry of platinum and palladium is usually studied in tandem and complexes in high oxidation states (III and IV) have been well recognized for platinum, the chemistry of palladium in oxidation states higher than (II) has been investigated in detail in the last 10 years.[2−10] These oxidized species easily undergo reductive elimination and play a key role as intermediates in some synthetic design.[11−18] The M(II)/M(IV) cycles can achieve transformations that are hardly accessible otherwise. The usual access to the M(IV) complexes is the oxidation of M(II) derivatives, and it is well established that the oxidation of dinuclear derivatives can afford M(III),M(III) or M(II),M(IV) complexes.[19−32]

In our current research on phosphanido derivatives, we have reported three types of palladium or platinum(II) dinuclear complexes $[(R_F)_2M(\mu\text{-}PPh_2)_2M'L_2]^{n-}$ ($R_F = C_6F_5$, M, M′ = Pt, Pd; L = R_F, *n* = 2, **A**; 2L = benzoquinolinate (C^N), *n* = 1, **B**; L = $NCCH_3$, *n* = 0, **C**). The two R_F groups bonded to a metal center in these complexes can act as terminal blocking ligands as well as provide adittional structural information (^{19}F NMR). The oxidation of these types of compounds with I_2 (Chart 1) has been reported.[33−35] In all cases, the oxidized intermediate

†Polynuclear Homo- or Heterometallic Palladium(II)−Platinum(II) Pentafluorophenyl Complexes Containing Bridging Diphenylphosphido Ligands. 31. For part 30, see ref 1.

Received: February 18, 2013
Published: April 18, 2013

   dx.doi.org/10.1021/ic4004005 | Inorg. Chem. 2013, 52, 5493−5506

Chart 1

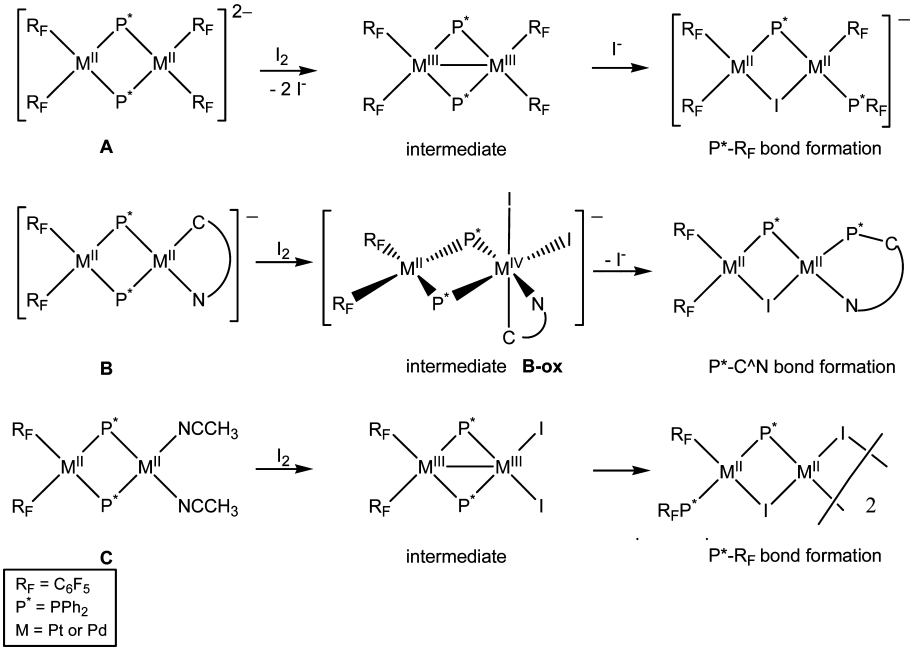

Chart 2

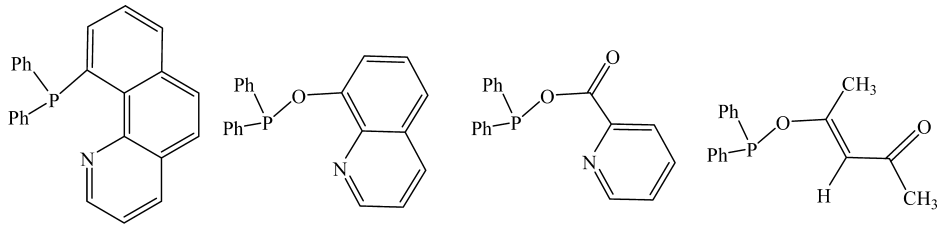

Scheme 1

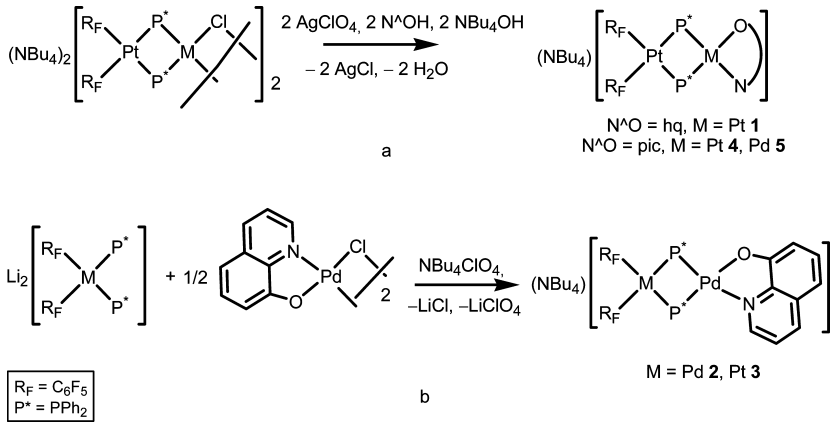

complexes evolve through a reductive coupling with formation of a P–C bond and new palladium(II) and platinum(II) derivatives. For complexes of type **A** (Chart 1), the reductive coupling between PPh_2 and C_6F_5 groups and formation of complexes containing the $PPh_2C_6F_5$ ligand was observed.[33] Only the platinum intermediate M(III),M(III) derivative, $[(R_F)_2Pt^{III}(\mu\text{-}PPh_2)_2Pt^{III}(R_F)_2]$(Pt–Pt), was stable enough, isolated and characterized.[33,36] For complexes of type **B**, the oxidation in the case of the Pt(II),Pt(II) derivative results in the formation of the diplatinum Pt(II),Pt(IV) $[NBu_4][(R_F)_2Pt^{II}(\mu\text{-}PPh_2)_2Pt^{IV}(C\text{^}N)I_2]$[34] (**B-ox**) complex which was stable enough and could be isolated and fully characterized. However, for the Pd(II),Pd(II) or the mixed Pt(II),Pd(II) complexes, the intermediates M(II),M(IV) could neither be isolated nor observed in solution, and the M(II),M(II) complexes containing the aminophosphane Ph_2P-bzq (P–C coupling, see Chart 2) were obtained. Finally, the formation of $Ph_2PC_6F_5$ was observed for the neutral complexes type **C** through the isolated and characterized intermediates of palladium or platinum(III) $[(R_F)_2Pt^{III}(\mu\text{-}PPh_2)_2M^{III}I_2]$(Pt-M) (M = Pt,

dx.doi.org/10.1021/ic4004005 | Inorg. Chem. 2013, 52, 5493–5506

Table 1. ^{31}P and ^{195}Pt NMR Data of 1−5 and 7−12 in Deuteroacetone at 298 K[a]

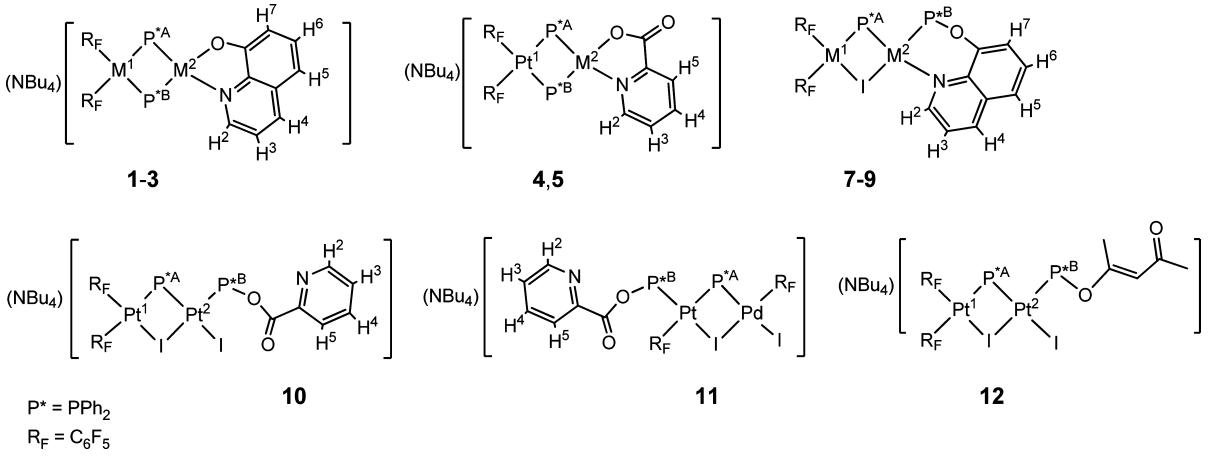

complex	δP^A	δP^B	$^2J_{P^A,P^B}$	$^1J_{P^A,Pt^1}$	$^1J_{P^A,Pt^2}$	$^1J_{P^B,Pt^1}$	$^1J_{P^B,Pt^2}$	δPt^1	δPt^2
1[b]	−137.2	−140.4	157	1892	2436	1876	2441	−3903	−3450
2	−100.4	−106.0	263						
3	−119.0	−124.5	216	1739		1719		−3901	
4[c]	−139.1	−141.6	160	1900	2420	1903	2532	−3911	−3542
5	−121.2	−125.6	220	1766		1737		−3905	
7[d]	−19.9	86.0		1903	2373	49	5025	−4250	−4420
8	55.4	122.9	32						
9	50.1	119.3	37	1928		119		−4317	
10[e]	−71.3	80.6		2005	2215		5179	−4045	−3572
10-hydr	−76.4	67.2	13	2042	2320		5019	−4050	−3520
11	−45.8	84.6	8	1654			5088	−4436	
12[f]	−88.5	81.6	21	2030	2291	29	5216	−4020	−3500

[a] δ in ppm, J in Hz. [b] $^2J_{Pt1,Pt2}$ = 289 Hz. [c] $^2J_{Pt1,Pt2}$ = 284 Hz. [d] $^2J_{Pt1,Pt2}$ = 1220 Hz. [e] $^2J_{Pt1,Pt2}$ = 1280 Hz. [f] $^2J_{Pt1,Pt2}$ = 1283 Hz.

Pd).[35] The analysis of the results indicated that (i) the reductive coupling is usually preferred on a palladium rather than on a platinum center; (ii) the coupling between PPh_2 and benzoquinolinate groups are preferred to the coupling between PPh_2 and C_6F_5 groups; (iii) in the iodo derivatives, the coupling between PPh_2 and I to form iodophosphane has not yet been observed.

In this paper we report on the synthesis of new dinuclear anionic phosphanido derivatives of platinum and palladium(II) containing 8-hydroxyquinolinate or *o*-picolinate as ligands, and the reaction of the complexes $[NBu_4][(R_F)_2Pt(\mu\text{-}PPh_2)_2M^{II}(L\text{-}L')]$ [M = Pt, Pd; L-L′ = 8-hydroxyquinolinate (hq), *o*-picolinate (pic) or acetylacetonate (acac)] with I_2.

RESULTS AND DISCUSSION

Synthesis of $[NBu_4][(R_F)_2M(\mu\text{-}PPh_2)_2M'(N\text{^}O)]$ (R_F = C_6F_5. N^O = 8-hydroxyquinolinate (hq), M = M′ = Pt, 1; Pd, 2; M = Pt, M′ = Pd, 3) and $[NBu_4][(R_F)_2Pt(\mu\text{-}PPh_2)_2M(N\text{^}O)]$ (R_F = C_6F_5. N^O = picolinate (pic), M = Pt 4; Pd, 5). The synthesis of the asymmetric complexes **1**, **4**, and **5** (Scheme 1a) was carried out by elimination of the bridging chloro ligands as AgCl from the corresponding tetranuclear derivatives $[NBu_4]_2[\{(R_F)_2Pt(\mu\text{-}PPh_2)_2M(\mu\text{-}Cl)\}_2]$,[37] and treatment of the resulting species with the corresponding N^O-donor ligand. Complexes **2** and **3** were obtained by reacting the anion *cis*-$[Pt(R_F)_2(PPh_2)_2]^{2-}$[37] with the binuclear $[\{Pd(\mu\text{-}Cl)(N\text{^}O)\}_2]$ complexes. The anionic moiety behaves as a diphosphane ligand and produces the displacement of the bridging chloro ligand in the binuclear derivative (Scheme 1b). This type of displacement is rather frequent when dinuclear palladium or platinum halido complexes are reacted with bidentate chelating ligands.[35,38−43] The IR spectra of complexes **1**−**5** in the solid state confirmed the presence of the ligands in the respective complexes. These were characterized by elemental analysis, high resolution mass spectrometry, and NMR spectroscopy. The ^{19}F NMR spectra of the complexes were recorded in deuteroacetone, and the relevant data are collected in Experimental Section. In these complexes, the two pentafluorophenyl groups are inequivalent, but the chemical environments of the two rings are very similar and some ^{19}F nuclei were almost isochronous. The $^{31}P\{^1H\}$ NMR spectra are more informative. In all cases, the two inequivalent P atoms appear at high fields (in the range −100 to −145 ppm) as expected for a "$M(\mu\text{-}PPh_2)_2M$" (M = Pt, Pd) fragment without a metal−metal bond.[44−46] As previously noted,[47] the phosphanido ^{31}P NMR signals appear at lower field when Pd atoms were present in the molecule. The assignment of the proper signal to each of the phosphanido P atoms (Table 1) was made on the basis of the $^1H-^{31}P$ HMQC and ^1H NOESY spectra. In fact, once assigned the *ortho* protons of the phenyl rings bonded to the P atoms by means of the $^1H-^{31}P$ HMQC, the position of the PPh_2 group was established thanks to the NOE contact between the *ortho* protons of the phenyls and the N−C-*H* protons of the N^O ligand. The attribution of the coupling constants between P and Pt was made by comparison of $^{31}P\{^1H\}$ and $^{195}Pt\{^1H\}$ spectra. The $^{195}Pt\{^1H\}$ spectra of **1**, **3**, **4**, **5** showed broad multiplets at ca. δ −3900 for the Pt^1 atoms bonded to the pentafluorophenyl rings. For **1** and **4**, the $^{195}Pt\{^1H\}$ spectra showed also sharp signals at δ −3450 (**1**) or δ −3542 (**4**) for the Pt^2 atom bonded to the N^O ligand (Table

dx.doi.org/10.1021/ic4004005 | Inorg. Chem. 2013, 52, 5493−5506

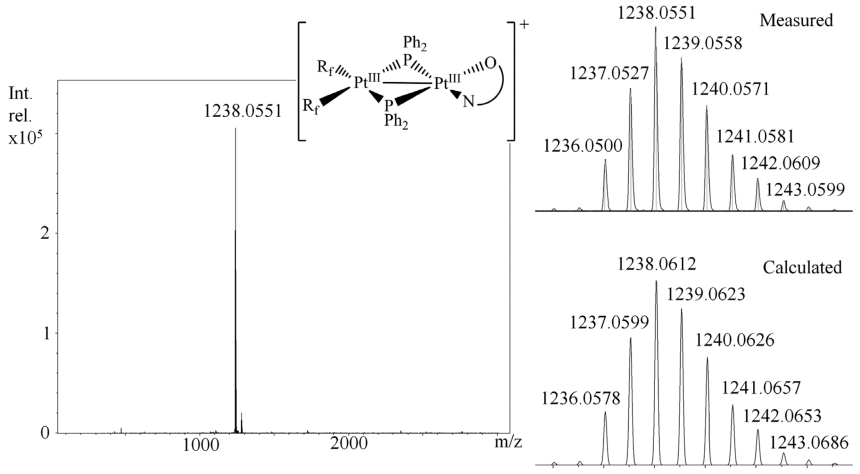

Figure 1. HRMS(+) spectrogram of **1** in MeCN showing the peak corresponding to the cation $[(R_F)_2Pt(\mu\text{-}PPh_2)_2Pt(hq)]^+$. The error between calculated and observed isotopic patterns is 5.3 ppm.

Scheme 2

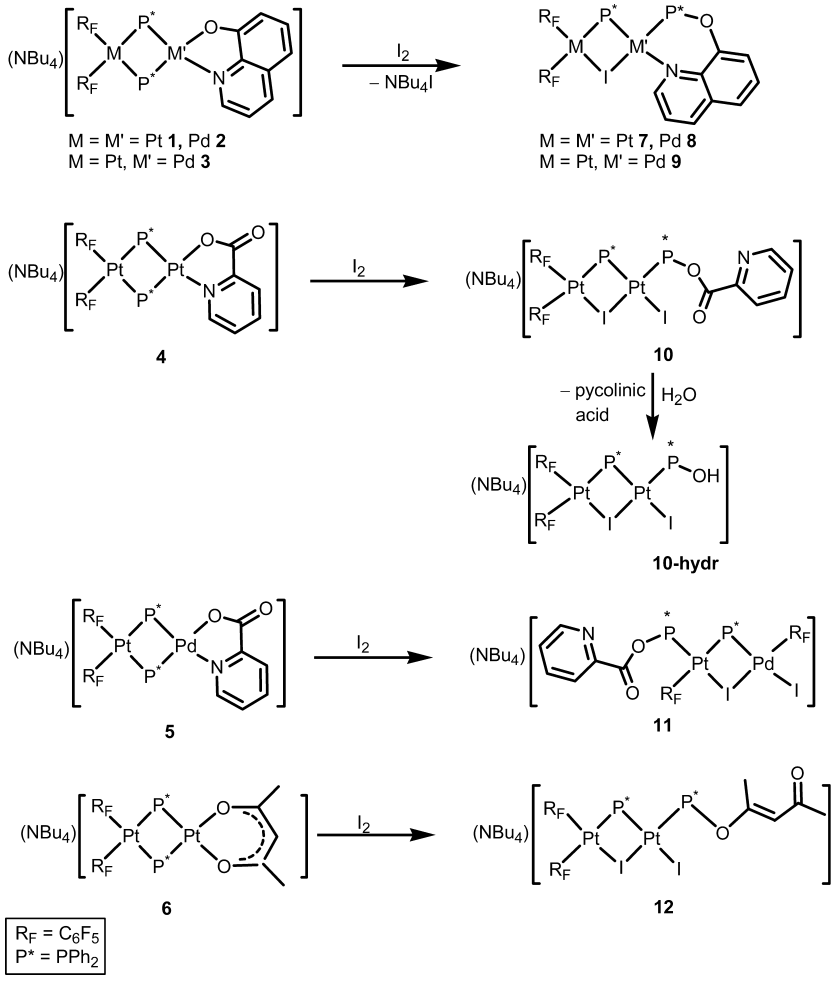

1). The geminal coupling constants between the two Pt atoms in these complexes were 289 and 284 Hz, respectively. The full assignment of all ^{1}H NMR signals was made by means of 1D and 2D ^{1}H NMR spectra and is reported in the Experimental Section.

The HRMS(−) analysis of the anionic complexes **1**−**5** showed the peaks corresponding to their formulas. Given that the electrospray ionization source can act as an electrochemical cell capable to assist redox processes,[48,49] we tested the possibility to oxidize electrochemically the anionic complexes **1**−**5** by submitting them to HRMS(+) analysis in positive mode. In the conditions detailed in the Experimental Section, the five monoanions were smoothly oxidized and the HRMS(+) spectrograms showed intense peaks ascribable to

dx.doi.org/10.1021/ic4004005 | Inorg. Chem. 2013, 52, 5493−5506

the corresponding monocationic complexes deriving from loss of two electrons. This suggests that an electrochemical oxidation of **1**−**5** occurs to give probably the corresponding M(III),M′(III) species of the general formula $[(R_F)_2M^{III}(\mu\text{-}PPh_2)_2M'^{III}(L_2)]^+$(Pt−Pt) ($L_2$ = N^O). Figure 1 shows the HRMS(+) spectrogram of **1**, which could be due to the cation $[(R_F)_2Pt^{III}(\mu\text{-}PPh_2)_2Pt^{III}(hq)]^+$(Pt−Pt).[50] The tendency of **1**−**5** to undergo an electrochemical oxidation was found less marked in the case of the mixed metal Pt−Pd complexes **3** and **5**, with respect to **1**, **2**, and **4**, as indicated by the relative intensities of the ion currents due to the oxidized species.[51]

Reaction of $[NBu_4][(R_F)_2M(\mu\text{-}PPh_2)_2M'(L\text{-}L')]$ with I_2. The addition of I_2 to CH_2Cl_2 solutions of complexes $[NBu_4][(R_F)_2M(\mu\text{-}PPh_2)_2M'(L\text{-}L')]$ (L-L′ = hq, **1**−**3**; pic, **4**, **5**; acac, **6**[39]) in a 1:1 molar ratio afforded complexes **7**−**12** with structures depending on the L-L′ ligand and/or the metal cores (Scheme 2). All products **7**−**12** have a common core constituted by a M-P-M′-I four-membered ring and a coordinated Ph_2P-hq, Ph_2P-pic, or Ph_2P-acac ligand (see Chart 2), which are the result of the PPh_2/L-L′ coupling with P−O bond formation (Scheme 2). Complexes **7**−**12** are nonplanar binuclear derivatives endowed with large M···M (M = Pt, Pd) distances as expected for 32 VEC saturated complexes. As we will comment below, the formation of these ligands is the consequence of a reductive coupling induced by I_2 oxidation. The ligand Ph_2P-hq is coordinated to the metal centers in **7**−**9** as chelating, while Ph_2P-pic and Ph_2P-acac act as monodentate (κ-*P*) in complexes **10**−**12**, and the binuclear anion contains also a terminal iodide ligand. Complex **10** was very sensitive to moisture and in solution of wet solvents quantitatively hydrolyses to give **10-hydr** (Scheme 2). In addition, the reaction which produces complex **11** is more complicated since migration of one C_6F_5 group from Pt to Pd occurred.

The HRMS(+) spectrograms of the neutral products **7**−**9** showed intense peaks due to $[M + Na]^+$ adducts, while HRMS(−) analysis of **10**−**12** (for which the complexes are anionic) showed peaks due to $[M]^-$.

The molecular structures of **7**, **9**, **11**, and **12** were established by X-ray diffraction studies. Figures 234−5 show molecular drawings of complexes 7 and **9** and of the anionic parts of complexes **11** and **12**, while Tables 234−5 list the most

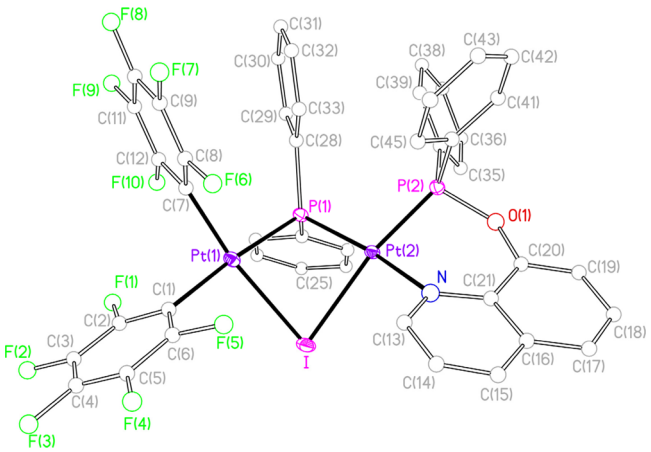

Figure 2. View of the molecular structure of the complex $[(C_6F_5)_2Pt(\mu\text{-}I)(\mu\text{-}PPh_2)Pt(P,N\text{-}Ph_2P\text{-}hq)]$ $2Me_2CO$ ($7{\cdot}2Me_2CO$). Solvent molecules are omitted for clarity.

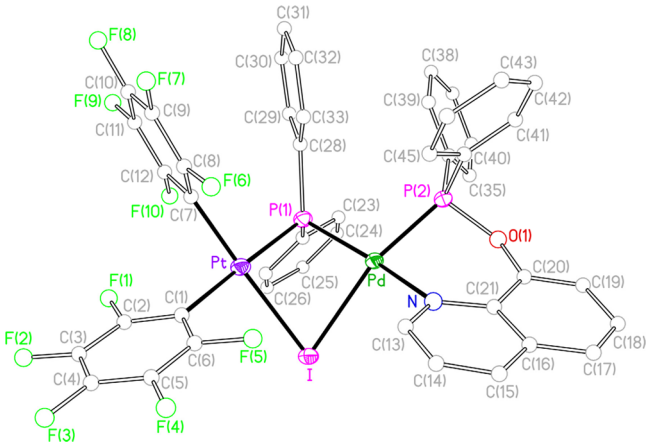

Figure 3. View of the molecular structure of the complex $[(C_6F_5)_2Pt(\mu\text{-}I)(\mu\text{-}PPh_2)Pd(P,N\text{-}Ph_2P\text{-}hq)]$ $Me_2CO{\cdot}0.25n\text{-}C_6H_{14}$ ($9{\cdot}Me_2CO{\cdot}0.25n\text{-}C_6H_{14}$). Solvent molecules are omitted for clarity.

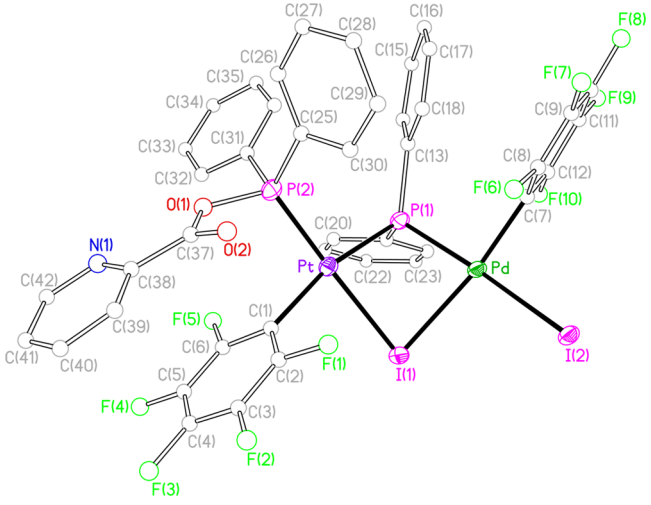

Figure 4. View of the molecular structure of the anion of the complex $[NBu_4][(Ph_2P\text{-}pic)(C_6F_5)Pt(\mu\text{-}I)(\mu\text{-}PPh_2)Pd(C_6F_5)I]$ CH_2Cl_2 ($11{\cdot}CH_2Cl_2$). Solvent molecules are omitted for clarity.

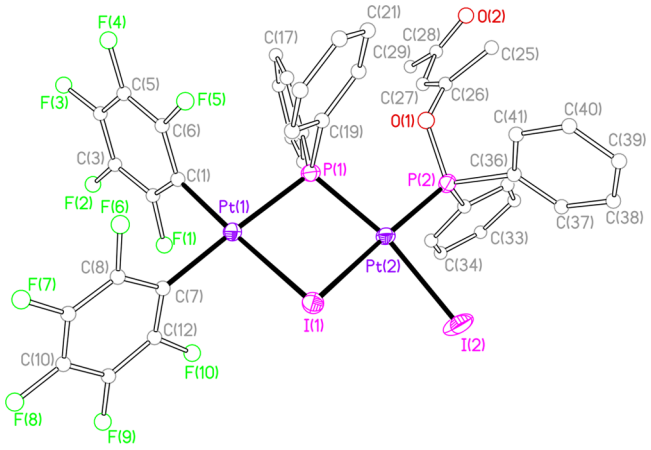

Figure 5. View of the molecular structure of the anion of the complex $[NBu_4][(C_6F_5)_2Pt(\mu\text{-}I)(\mu\text{-}PPh_2)PtI(Ph_2P\text{-}acac)]$ (**12**).

relevant bond distances and angles for the respective complexes. The crystal structures confirm the dinuclear nature of the complexes. In all cases, the core contains the "Pt(μ-

dx.doi.org/10.1021/ic4004005 | Inorg. Chem. 2013, 52, 5493−5506

Table 2. Selected Bond Lengths (Å) and Angles (°) for $[(C_6F_5)_2Pt(\mu\text{-}I)(\mu\text{-}PPh_2)Pt(P,N\text{-}PPh_2hq)]\cdot 2Me_2CO$ ($7\cdot 2Me_2CO$)

Pt(1)–C(7)	2.005(3)	Pt(1)–C(1)	2.077(3)	Pt(1)–P(1)	2.2853(7)
Pt(1)–I	2.6743(2)	Pt(2)–N	2.149(2)	Pt(2)–P(2)	2.1763(7)
Pt(2)–P(1)	2.2673(7)	Pt(2)–I	2.6971(2)	P(2)–O(1)	1.627(2)
C(7)–Pt(1)–C(1)	90.62(11)	C(7)–Pt(1)–P(1)	94.48(8)		
C(1)–Pt(1)–P(1)	174.77(9)	C(7)–Pt(1)–I	169.61(8)		
C(1)–Pt(1)–I	93.29(8)	P(1)–Pt(1)–I	81.862(19)		
N–Pt(2)–P(2)	86.07(7)	N–Pt(2)–P(1)	166.75(7)		
P(2)–Pt(2)–P(1)	102.48(3)	N–Pt(2)–I	92.06(6)		
P(2)–Pt(2)–I	167.74(2)	P(1)–Pt(2)–I	81.675(19)		
Pt(1)–I–Pt(2)	75.979(6)	Pt(2)–P(1)–Pt(1)	93.14(3)		

Table 3. Selected Bond Lengths (Å) and Angles (°) for $[(C_6F_5)_2Pt(\mu\text{-}I)(\mu\text{-}PPh_2)Pd(P,N\text{-}PPh_2hq)]\cdot Me_2CO\cdot 0.25n\text{-}C_6H_{14}$ ($9\cdot Me_2CO\cdot 0.25n\text{-}C_6H_{14}$)

Pt–C(7)	2.013(3)	Pt–C(1)	2.080(3)	Pt–P(1)	2.2790(9)
Pt–I	2.6788(2)	Pt–Pd	3.1421(3)	Pd–N	2.175(3)
Pd–P(2)	2.2015(8)	Pd–P(1)	2.2641(8)	Pd–I	2.7464(3)
P(2)–O(1)	1.640(2)				
C(7)–Pt–C(1)	88.84(13)	C(7)–Pt–P(1)	92.56(10)		
C(1)–Pt–P(1)	178.19(9)	C(7)–Pt–I	177.87(10)		
C(1)–Pt–I	93.25(9)	P(1)–Pt–I	85.34(2)		
C(7)–Pt–Pd	122.49(10)	C(1)–Pt–Pd	132.15(9)		
P(1)–Pt–Pd	46.05(2)	I–Pt–Pd	55.619(6)		
N–Pd–P(2)	84.49(7)	N–Pd–P(1)	165.31(8)		
P(2)–Pd–P(1)	102.57(3)	N–Pd–I	92.90(7)		
P(2)–Pd–I	162.74(2)	P(1)–Pd–I	84.04(2)		
N–Pd–Pt	121.07(7)	P(2)–Pd–Pt	141.04(2)		
P(1)–Pd–Pt	46.44(2)	I–Pd–Pt	53.608(6)		
Pt–I–Pd	70.773(7)	Pd–P(1)–Pt	87.52(3)		

Table 4. Selected Bond Lengths (Å) and Angles (°) for $[NBu_4][(PPh_2\text{-}pic)(C_6F_5)Pt(\mu\text{-}I)(\mu\text{-}PPh_2)Pd(C_6F_5)I]\cdot CH_2Cl_2$ ($11\cdot CH_2Cl_2$)

Pt–C(1)	2.059(4)	Pt–P(2)	2.2074(8)	Pt–P(1)	2.3292(9)
Pt–I(1)	2.6855(2)	Pd–C(7)	2.024(4)	Pd–P(1)	2.2629(8)
Pd–I(2)	2.6807(3)	Pd–I(1)	2.6919(3)	P(2)–O(1)	1.660(3)
C(1)–Pt–P(2)	94.29(10)	C(1)–Pt–P(1)	165.62(10)		
P(2)–Pt–P(1)	99.60(3)	C(1)–Pt–I(1)	86.85(9)		
P(2)–Pt–I(1)	177.76(2)	P(1)–Pt–I(1)	79.39(2)		
C(7)–Pd–P(1)	92.83(10)	C(7)–Pd–I(2)	90.29(10)		
P(1)–Pd–I(2)	176.05(3)	C(7)–Pd–I(1)	172.20(11)		
P(1)–Pd–I(1)	80.40(2)	I(2)–Pd–I(1)	96.315(10)		
Pt–I(1)–Pd	79.463(8)	Pd–P(1)–Pt	96.91(3)		

Table 5. Selected Bond Lengths (Å) and Angles (°) for $[NBu_4][(C_6F_5)_2Pt(\mu\text{-}I)(\mu\text{-}PPh_2)PtI(PPh_2\text{-}acac)]$ (12)

Pt(1)–C(1)	2.018(7)	Pt(1)–C(7)	2.078(7)	Pt(1)–P(1)	2.308(2)
Pt(1)–I(1)	2.653(1)	Pt(2)–P(1)	2.300(2)	Pt(2)–P(2)	2.198(2)
Pt(2)–I(1)	2.674(1)	Pt(2)–I(2)	2.688(1)	P(2)–O(1)	1.621(5)
C((1)–Pt((1)–C(7)	88.2(3)	C((1)–Pt((1)–P(1)	95.26(19)		
C(7)–Pt((1)–P(1)	175.93(18)	C(1)–Pt((1)–I((1)	176.44(17)		
C(7)–Pt(1)–I(1)	94.68(18)	P(1)–Pt(1)–I(1)	81.98(5)		
P(2)–Pt(2)–P(1)	100.18(7)	P(2)–Pt(2)–I(1)	173.31(5)		
P(1)–Pt(2)–I(1)	81.64(5)	P2)–Pt(2)–I(2)	89.53(5)		
P(1)–Pt(2)–I(2)	169.51(4)	I(1)–Pt(2)–I(2)	89.17(3)		
Pt(1)–I(1)–Pt(2)	85.06(4)	Pt(2)–P(1)–Pt((1)	102.85(7)		

$PPh_2)(\mu\text{-}I)M$" fragment, being M = Pt for **7** and **12**, and M = Pd for **9** and **11**. The intermetallic distances (3.306(1) Å for **7**, 3.142(1) Å for **9**, 3.437(1) Å for **11**, and 3.601(2) Å for **12**) are in agreement with the absence of a M–M bond, as expected for these saturated (32 VEC) complexes. The metal atoms lie in the center of square planes, each plane sharing an edge. The core formed by the two metals and the two bridging atoms is not planar, and the value of the dihedral angle formed by the coordination planes is 53.08(2)° for **7**, 57.52(2)° for **9**, 50.77(2)° for **11**, and 31.93(3)° for **12**. All these structural parameters, along the variability found in the values of the Pt–I–M and Pt–P–M angles, are in agreement with the well-

dx.doi.org/10.1021/ic4004005 | Inorg. Chem. 2013, 52, 5493–5506

known flexibility of the "Pt(μ-PPh_2)(μ-I)M" central fragment.[33,35,42,52−54]

In complexes **7**, **9** (neutral), and **12** (anionic) the two pentafluorophenyl ligands retain the mutually *cis* disposition to a Pt atom. The other metal atom, Pt(2) in **7**, Pd in **9**, and Pt(2) in **12**, completes its coordination sphere with the formed Ph_2P-hq ligand which is coordinated in a *P*,*N*-chelate mode (complexes **7** and **9**), while in complex **12**, the Ph_2P-acac ligand formed in the course of the reaction acts as a monodentate P-donor ligand and the iodide which is present in the mixture completes the coordination environment of Pt(2). Within the acac fragment the sequence of distances C(26)−C(27) 1.337(9), C(27)−C(28) 1.470(9), C(26)−O(1) 1.362(7), and C(28)−O(2) 1.212(8) is different from those of a typical acac ligand,[42,55] as is to be expected according to its rather different bonding situation of this moiety (Chart 2). Finally, in complex **11**, one of the pentafluorophenyl groups has migrated from the Pt to the Pd atom, and the Pt center completes the coordination environment with the P atom of the formed phosphane Ph_2P-pic while an iodo ligand completes the coordination sphere of the Pd.

Spectroscopic Properties. The $^{31}P\{^1H\}$ NMR spectra of **7**−**12** in deuteroacetone solution show the signal due to the P atom of the new phosphinito ligand (Ph_2P-hq, Ph_2P-pic, Ph_2P-acac) at low field (see Table 1), in the 80.6−122.9 δ range. It is well established that in complexes without a metal−metal bond the signal due to the P atom of phosphanido ligand involved in a "M(μ-X)(μ-PPh_2)M" fragment (X = halide) appears at lower field than the signals due to the "M(μ-PPh_2)$_2$M" fragment.[53,54,56,57] The phosphanido ligands in complexes **7**−**12**, containing a "M(μ-I)(μ-PPh_2)M" fragment, appears at lower fields (55.4 to −88.5 ppm) than the starting material, −100.4 to −139.1 ppm. The relationship between δ(μ-P) values and the M-(μ-P)-M angle in bridging phosphanido complexes has long been known.[47] In addition, in complexes **7**, **9**, **11**, and **12** the four atoms M, M′, (μ-I) and (μ-P) are not coplanar in the solid state, and the deviation from the planarity of these four atoms could be related with the dihedral angle α formed by the two planes (μ-P), M, (μ-I) and (μ-P), M′, (μ-I). Noteworthy, in **7**−**12** the δ(μ-^{31}P) range is wide and the δ(μ-^{31}P) values can be related with the structural disposition of the four M, (μ-I), (μ-P), M atoms, i.e., with the planarity of the "M(μ-I)(μ-P)M′" fragment. Table 6 collects data of this α angle for **7**, **9**, **11**, and **12**, as well as for complexes [$(R_F)_2$M(μ-I)(μ-PPh_2)M′(*P*,*N*-Ph_2P-bzq)] (M, M′ = Pt, **13a**, M = Pt, M′ = Pd, **13b**, M, M′ = Pd, **13c**) reported previously,[34] along with the values of their δ(μ-^{31}P). All complexes collected in Table 6 contain the "M(μ-I)(μ-PPh_2)M" fragment, and it is apparent that the increase of value of δ(μ-^{31}P) is related to a larger value of α.

Table 6. δ(μ-P) Values (ppm) and Dihedral Angle α (°) in complexes with the fragment "M(μ-P)(μ-I)M′"

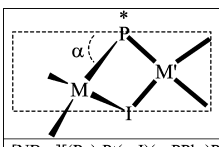	δ(μ-P)	α	Ref.
[NBu_4][$(R_F)_2$Pt(μ-I)(μ-PPh_2)Pt(Ph_2P-acac)I], **12**	−90.1	31.93(3)	this work
[NBu_4][(R_F)(Ph_2P-pic)Pt(μ-I)(μ-PPh_2)Pd(R_F)I], **11**	−47	50.77(2)	this work
[$(R_F)_2$Pt(μ-I)(μ-PPh_2)Pt(*P*,*N*-Ph_2P-hq)], **7**	−21	53.08(2)	this work
[$(R_F)_2$Pt(μ-I)(μ-PPh_2)Pt(*P*,*N*-Ph_2P-bzq)], **13a**	−10.9	56	[34]
[$(R_F)_2$Pt(μ-I)(μ-PPh_2)Pd(*P*,*N*-Ph_2P-hq)], **9**	48.2	57.52(2)	this work
[$(R_F)_2$Pt(μ-I)(μ-PPh_2)Pd(*P*,*N*-Ph_2P-bzq)], **13b**	55.6	68	[34]
[$(R_F)_2$Pd(μ-I)(μ-PPh_2)Pd(*P*,*N*-Ph_2P-bzq)], **13c**	66.6	68	[34]

The ^{19}F NMR spectra of **7**−**12** in deuteroacetone solution show in all cases two signals due to the *o*-F atoms (2:2 intensity ratio), two signals due to the *m*-F atoms (2:2 intensity ratio), and two signals due to the *p*-F atoms (1:1 intensity ratio). This pattern is in agreement with the presence of two inequivalent C_6F_5 groups and indicates that the two halves within each C_6F_5 ring become equivalent in solution. Moreover, *o*- and *m*-F atoms of the R_F rings in *trans* position with respect to P show additional ^{19}F−^{31}P couplings. All data are collected in the Experimental Section. The ^{1}H NMR (1D and 2D) spectra of **7**−**12** show the signals due to the N^O ligands, phenyl groups and the possible counterion (NBu_4^+) in the proper intensity ratio. The spectra confirm the stoichiometry of the complexes. The signals due to the N^O-groups in complexes **1**−**5** and those due to the OR part of the phosphinito ligand PPh_2OR in **7**−**12** deserve some attention. The signal due to H^2 (see Table 1 for atom numbering) in N^O-chelate shifts significantly downfield when passing from the starting complexes **1**−**5** to the products **7**−**11**. The formation of the P−O bond causes broadening of the ^{1}H signals which experience a (small) P−H coupling, as confirmed by ^{1}H−^{31}P HMQC and $^1H\{^{31}P\}$ NMR experiments. The ^{1}H NMR spectrum of **12** in deuteroacetone solution shows two signals for the two inequivalent CH_3 groups and a signal, a doublet ($^4J_{P,H}$ = 2 Hz), for the C*H* proton of the acac group. The ^{1}H−^{31}P HMQC of **12** showed cross peaks between the phosphinito P and both the C═C−C*H*$_3$ and the C*H* protons.

The $^{195}Pt\{^1H\}$ spectra of **7** and **9**−**12** showed broad multiplets in the −4020 to −4436 ppm range for the Pt^1 atoms. For **7**, **10**, and **12** the $^{195}Pt\{^1H\}$ spectra showed also sharp signals at δ −4420 (**7**), δ −3572 (**10**), δ −3500 (**12**) for the Pt^2 atom (Table 1). The geminal coupling constants between the two Pt atoms in these complexes ranged from 1220 to 1283 Hz, values four times higher than those of the respective starting complexes (289 Hz for **1** and 284 Hz for **4**). This effect is presumably due to the substitution of a μ-PPh_2 by a μ-I on passing from reagents to products.

Reductive Coupling Between PPh_2 and hq, pic, or acac. Considering our previous experience,[33−35,42,54,58] the synthesis of the bimetallic complexes **7**−**12** could, in all likelihood, be the result of an initial oxidation of the diphosphanido dinuclear complexes **1**−**5** by means of I_2 in dichloromethane at room temperature, followed by a reductive coupling between one of the bridging PPh_2 and the corresponding *O*-donor chelate ligand. The addition of I_2 could give either a M(II),M(IV) complex or a binuclear M(III)-M(III) derivative (Chart 1), which would evolve through a P−O reductive coupling to the corresponding Pt(II),Pt(II) final phosphinito complex. In order to gain insights into the mechanism of formation of **7**−**12** and to discriminate between a M(II),M(IV) and a M(III)-M(III) intermediate (Chart 1), we monitored the reaction between **1** and I_2 in conditions that hopefully could guarantee the detection of the intermediate. Thus, knowing that for the analogous benzoquinolinate phosphanido M(II),M′(IV) complexes the reductive coupling leading to P^C bond formation was hampered in acetone with the diplatinum species, allowing the isolation of the Pt(II),Pt(IV) intermediate,[34] and given that such Pt(II),Pt(IV) intermediate was quite stable even in dichloromethane in the presence of an excess of iodide, we

dx.doi.org/10.1021/ic4004005 | Inorg. Chem. 2013, 52, 5493−5506

monitored the reactions of **1**, **4**, and **6** with I_2 in acetone-d_6 at 268 K, in the presence of 4 equiv of NBu_4I. In these conditions, 3 equiv of iodine were necessary to convert **1** into a new species **1-ox** (>90%), the spectroscopic and spectrometric features of which indicated as the Pt(II),Pt(IV) intermediate depicted in Scheme 3. HRMS-MS/MS and ^{195}Pt NMR data were

Scheme 3. Proposed Pathway for the 1 to 7 Transformation

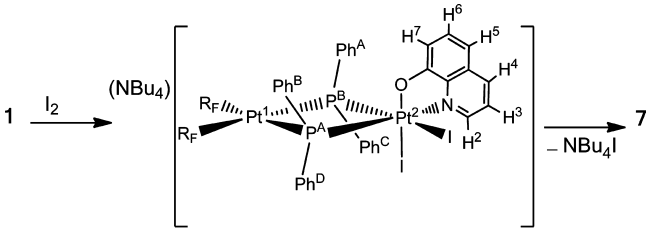

diagnostic for the characterization of **1-ox** as the product of I_2 addition to **1** having a square planar Pt(II) atom bridged by two PPh_2 ligands to an octahedral Pt(IV) atom. In fact, **1-ox** showed at the HRMS(−) analysis an intense peak at m/z 1491.8630 with an isotope pattern superimposable to that of $[\mathbf{1}+2\ I]^-$ (calculated mass = 1491.8712 Da).[59] MS/MS analysis of the peak at m/z 1491.8630 showed fragmentation with loss of I_2, suggesting that the two iodide ligands are in a mutual *cis* position. As to the ^{195}Pt{^{1}H} NMR, we have shown that, for phosphanido complexes, a metal oxidation from +2 to +3 (affording square planar dinuclear species endowed with a Pt(III)−Pt(III) bond) results in a strong ^{195}Pt shielding,[42] whereas metal oxidation from +2 to +4 (affording Pt(II),Pt(IV) dinuclear species) results in a strong ^{195}Pt deshielding.[34]

The ^{195}Pt{^{1}H} spectrum of **1-ox** showed two signals centered at δ −2385 and δ −3774 (Table 7). Of this, the first one is a sharp doublet of doublets (with satellites stemming from the isotopomer having two ^{195}Pt atoms, $^2J_{Pt,Pt}$ = 316 Hz) ascribable to the Pt atom not bonded to the C_6F_5 rings (Pt^2). The deshielding of more than 1000 ppm undergone by Pt^2 on passing from **1** (δ −3450) to **1-ox** (δ −2835) indicates that Pt^2 of **1-ox** is an octahedral Pt(IV). The signal at δ −3774 is a multiplet broadened due to multiple ^{195}Pt−^{19}F couplings and is ascribed to the Pt(II) atom bonded to the C_6F_5 rings (Pt^1), which did not change significantly on passing from **1** (δ_{Pt1} −3903) to **1-ox**.

Complex **1-ox** was characterized in the ^{31}P NMR by two mutually coupled signals at δ −107.5 and δ −84.3, ($^2J_{P,P}$ = 116 Hz). Perusal of multinuclear NMR data indicates that the structure of **1-ox** was that depicted in Scheme 3, with the coordination sites of the octahedral Pt^2(IV) occupied by a iodide and the nitrogen of the hq ligand in the plane containing the two Pt and the two P atoms; the other I and the hq oxygen in the apical positions. Such a structure is analogous to that of **B-ox**, the intermediate formed by addition of I_2 to the benzoquinolinate complex **B** (Chart 1),[34] with the oxygen in place of carbon in the coordination sphere of Pt^2, and for which the XRD structure is known.

The stability of **1-ox** in acetone in the presence of iodide suggests that the mechanism of **1** to **7** transformation (Scheme 3) can be similar to that proposed in our previous work,[34] where a P−C bond formation through reductive coupling between bridging phosphanido and benzoquinolinate groups occurred.[60]

Monitoring in a NMR tube the reaction between **1** and I_2 in acetone-d_6 (in the absence of NBu_4I and with a 1:1 I_2:**1** molar ratio) at 298 K revealed that, immediately after the mixing of the reactants, the mixture contained mainly **1-ox** (plus traces of **1** and **7**) and that, after 48 h, **1-ox** transformed into **7** in ca. 61% spectroscopic yields. The ^{31}P{^{1}H} spectrum of the mixture after 48 h showed also signals ascribable to two species: the tetranuclear Pt(II) complex $[NBu_4]_2[\{(R_F)_2Pt(\mu\text{-}PPh_2)_2Pt(\mu\text{-}I)\}_2]$[35] (ca. 15%) and the iododiphenylphosphane complex $NBu_4[(R_F)_2Pt(\mu\text{-}PPh_2)(\mu\text{-}I)Pt(PPh_2I)I]$ (ca. 21%) featuring signals at δ_P 13.4 ($^2J_{P,P}$ = 10 Hz; $^1J_{Pt,P}$ = 4852 Hz) and δ_P −63.1 ($^2J_{P,P}$ = 10 Hz; $^1J_{Pt,P}$ = 1980 Hz, $^1J_{Pt,P}$ = 2194 Hz). This latter species accounts for the peak at m/z = 1474.7291 (exact mass for the proposed formula = 1474.7306 Da) found in the HRMS(−) spectrogram of the reaction mixture. The MS/MS spectrogram obtained by fragmentation of the m/z = 1474.7291 ion showed only a peak at m/z = 1162.7902 corresponding to the loss of the iododiphenylphosphane.[61] Unfortunately, all attempts to isolate **1-ox** in the state of purity were unsuccessful.

The monitoring at 268 K of the reaction of **4** with I_2 (3 equiv) in the presence of NBu_4I (4 equiv) in acetone-d_6 allowed us to detect, immediately after the mixing of reactants, an intermediate, **4-ox** (Scheme 4), having a structure similar to **1-ox**. The ^{31}P NMR signals of the Pt(II),Pt(IV) complex **4-ox** were found at δ −99.5 (P^A) and δ −77.5 (P^B), while the chemical shift of the octahedral Pt^2(IV) was δ −2501 ppm (Table 7). The HRMS(−) analysis of the solution containing **4-ox** showed an intense signal at m/z = 1469.8500 corresponding to $[\mathbf{4} + 2\ I]^-$ whose fragmentation at the MS/MS analysis consisted of the loss of I_2 with formation of the ion at m/z = 1216.0178. On standing in acetone-d_6 solution at 268 K, **4-ox** slowly reacted to give **10** (after 15 h the mixture contained ca. 35% of **10** and 50% of **4-ox**).[62]

Interestingly, carrying out the monitoring of **4** plus 1 equiv I_2 (without external iodide) in anhydrous thf at 298 K, revealed

Table 7. ^{31}P and ^{195}Pt NMR Data of Intermediates Detected by Monitoring the Reactions of 1, 4, and 6 with I_2 in Deuteroacetone at 268 K[a]

complex	δP^A	δP^B	$^2J_{P^A,P^B}$	$^1J_{P^A,Pt^1}$	$^1J_{P^A,Pt^2}$	$^1J_{P^B,Pt^1}$	$^1J_{P^B,Pt^2}$	δPt^1	δPt^2
B-ox[b]	−115.5	−107.5	126	2032	1807	2189	1270	−3806[c]	−2917[c]
1-ox	−107.5	−84.3	116	2101	1545	2130	1226	−3774[d]	−2385[d]
4-ox	−99.5	−77.5	119	2088	1544	2125	1184	−3810[e]	−2501[e]
10*[g]	−20.4	93.1	15	1906	2257	110	4993	nd	nd
6-ox-*cis*	−73.4	−81.6	102	2126	1641	2140	1260	−3746	−2024[h]
6-ox-*trans*	−88.5			2160	1570			−3746	−2834[i]

[a] δ in ppm, J in Hz. See Schemes 3−5 for numbering. [b] At 298 K, from ref 34. [c] $^1J_{Pt^1,Pt^2}$ = ca. 100 Hz. [d] $^2J_{Pt^1,Pt^2}$ = 316 Hz. [e] $^2J_{Pt^1,Pt^2}$ = 386 Hz. [g] In thf at 298 K. [h] $^2J_{Pt^1,Pt^2}$ = 225 Hz. [i] $^2J_{Pt^1,Pt^2}$ = 360 Hz

dx.doi.org/10.1021/ic4004005 | Inorg. Chem. 2013, 52, 5493−5506

Scheme 4. Proposed Pathway for the 4 to 10 Transformation

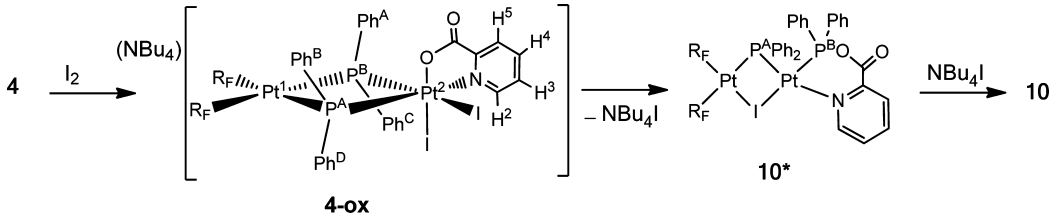

Scheme 5. Proposed Pathway for the 6 to 12 Transformation

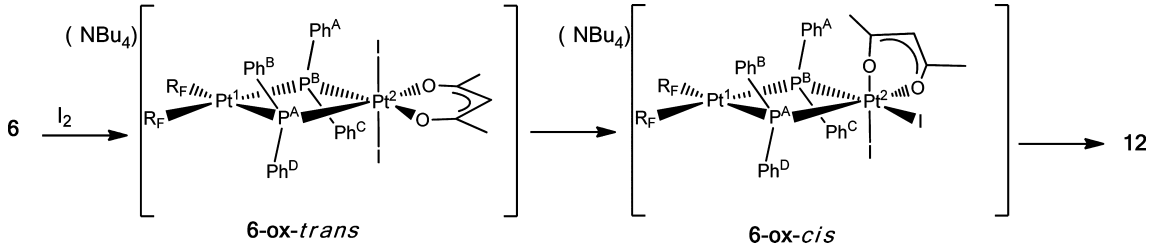

the immediate formation of **4-ox** which progressively transformed into an intermediate, **10***, exhibiting $^{31}P\{^1H\}$ NMR signals at δ_P 93.1 ($^1J_{Pt,P}$ = 4993 Hz) and δ_P −20.4 ($^1J_{Pt,P}$ = 2257 Hz, $^1J_{Pt,P}$ = 1906 Hz) which, in turn, evolved within 1 h into **10**. The similarity of ^{31}P NMR features between **10*** and **7** suggests that the intermediate **10*** might have the structure depicted in Scheme 4, analogous to **7**. The obtainment of **10** as final product from **10*** might therefore be the result of iodide displacement of the coordinated N on Pt^2 (Scheme 4).

Different from the cases of **1** and **4**, the NMR monitoring of the reaction of **6** with 3 equiv of I_2 and in the presence of 4 equiv of NBu_4I at 268 K showed the transformation of **6** into two new species in ca. 60:40 molar ratio. The $^{31}P\{^1H\}$ spectrum of the reaction mixture showed two mutually coupled doublets at δ −73.4 (P^A) and δ −81.6 (P^B), ascribable to a Pt(II),Pt(IV) species, **6-ox**-*cis* (Scheme 5), analogous to **1-ox** (and **4-ox**) along with a singlet at δ −88.5 flanked by two sets of satellites ($J_{P,Pt}$ = 2160 and 1570 Hz). This signal was presumably due to a Pt(II),Pt(IV) species (**6-ox**-*trans*, Scheme 5) having two iodide ligands in mutual *trans* position, in order to justify the symmetry of the molecule evidenced by the NMR data. Accordingly, the $^{195}Pt\{^1H\}$ spectrum of the mixture showed a doublet of doublets at δ −2024 ascribed (by comparison of the P−Pt coupling constants) to the Pt^2(IV) of **6-ox**-*cis*; a triplet at δ −2834 ($J_{P,Pt}$ = 1570 Hz) assigned to the Pt^2(IV) of **6-ox**-*trans*; a broad multiplet at δ −3746 ascribed to the overlapping of the signals due to the Pt^1(II) of **6-ox**-*cis* and **6-ox**-*trans*.

On standing at 268 K, the complex **6-ox**-*trans* quantitatively transformed into **6-ox**-*cis*,[63] which was stable at least for one week in solution at 268 K, allowing us to detect the HRMS(−) signal due to the anion of **6-ox** at m/z = 1446.8716 (calculated mass = 1446.8708 Da). The MS/MS study of the ion at m/z = 1446.8716 showed that it fragmented with a loss of I_2, giving the ion at m/z = 1193.0649.

The Pt(II),Pt(IV) complex **6-ox**-*cis* did not evolve to **12** under these conditions (i.e., deuteroacetone solvent and excess of iodide) even at 298 K. In fact, the $^{31}P\{^1H\}$ spectrum of the reaction mixture recorded after 3 days at 298 K showed only signals of **6-ox**-*cis* along with weak peaks due to $(R_F)_2Pt(\mu\text{-}PPh_2)(\mu\text{-}I)Pt(PPh_2)I$ and other unidentified species. Carrying out the NMR monitoring of the reaction of **6** with I_2 in acetone-d_6 without external iodide and at 298 K revealed the immediate formation of **6-ox**-*cis* and **6-ox**-*trans* which, within 15 min, rapidly evolved to **12**.

With all this information the synthesis of complexes **7**−**12** could be understood through a similar process observed earlier[34] for the benzoquinolinate derivatives: addition of I_2 to **1**−**6** derivatives gives a dinuclear intermediate with both diphenylphosphanido groups bridging two metal centers, one of them in oxidation state II and the other one in oxidation state IV. The dissociation of a I^- group gives an unsaturated oxidized metal from which the coupling between a bridging PPh_2 and the O-donor ligand forms the new ligand with P−O bond formation. Taking into account that we have isolated the Pt(II),Pt(IV) intermediate $[NBu_4][(R_F)_2Pt^{II}(\mu\text{-}PPh_2)_2Pt^{IV}(C\text{^}N)I_2]$[34] (**B-ox**) and all attempts to achieve pure samples of the Pt(II),Pt(IV) intermediates, **1-ox** and **4-ox**, were unsuccessful, the processes forming Ph_2P-L ligand seem to be easier for Ph_2P-hq, Ph_2P-pic, and Ph_2P-acac (formation of P−O bond) than for Ph_2P-bzq (formation of P−C bond). It is to note that the oxidized intermediates have been detected only for platinum complex, and it is in agreement with the fact that M(IV)-iodo derivatives are usual for platinum but scarce for palladium derivatives.[13,64−66] The processes described here imply a M−P and M−O bond cleavage and a P−O bond formation and result in a formation of PPh_2(O^N) or PPh_2(O^O) (Chart 2) from a bridging phosphanido complex and can be considered as an intermediate step for the transition metal-mediated P−C/O exchange at bound phosphane ligands.[67]

Although complexes **7**−**12** can be isolated as pure solids, the coupling between the PPh_2 group and the O-donor ligand is not the only process which takes place in the reaction. The study shows that unidentified species, formed from side reactions, are present and that the iododiphenylphosphane complex $NBu_4[(R_F)_2Pt(\mu\text{-}PPh_2)(\mu\text{-}I)Pt(PPh_2I)I]$ and the tetranuclear derivatives of platinum or palladium(II) $[NBu_4]_2[\{(R_F)_2Pt(\mu\text{-}PPh_2)_2M(\mu\text{-}I)\}_2]$,[35] which could be the result of other type of reductive coupling of ligands, are identified in solution in some of the processes. The iododiphenylphosphane complex might derive from the P−I reductive coupling on the M(II),M(IV) intermediates. The $[NBu_4]_2[\{(R_F)_2Pt(\mu\text{-}PPh_2)_2M(\mu\text{-}I)\}_2]$ complexes[35] show two

dx.doi.org/10.1021/ic4004005 | Inorg. Chem. 2013, 52, 5493−5506

"$(R_F)_2Pt^{II}(\mu\text{-}PPh_2)_2M^{II}$" fragments joined by two I^- groups, i.e., after addition of I_2, the phosphanido groups are still acting as bridging ligands maintaining the polynuclear fragment and behaving as a spectator. The evolution of high oxidation state complexes of palladium and platinum through several paths of reductive coupling is not surprising, and even on phosphanido derivatives we observed the formation of a mixture of products resulting of the P−C and P−P reductive couplings on trinuclear phosphanido complex.[58]

CONCLUSIONS

The bridging phosphanido ligand, in anionic derivatives of palladium and platinum(II), is not only used as a way for maintaining the molecular architecture. The transformation of bridging phosphanido ligands into phosphane is now well established.[33−35,42,54,68−72] The addition of I_2 to anionic phosphanido derivatives of palladium and platinum(II) with *O*-donor ligands facilitated the formation of P−O bonds resulting in the phosphane ligands Ph_2P-hq, in complexes **7**−**9**, Ph_2P-pic, in complexes **10** and **11**, and Ph_2P-acac in complex **12**. The process takes place through the intermediate M(II),M(IV) complexes which evolve to undergo easy reductive coupling reactions. In no case was observed the formation of $PPh_2C_6F_5$ from the starting anionic complexes. The oxidation of these diphenylphosphanido complexes allows the identification of intermediates, in some cases stable enough to be isolated and fully characterized, in formal oxidation states Pt(III)(square-planar)-Pt(III)(square-planar) or Pt(II)(square-planar)-Pt(IV)(octahedral). Both type of complexes seem to be not too different, and in fact the formation of the Pt(II),Pt(IV) derivatives can be considered as formed by the addition of two I^- ligands to the same metal center of the dinuclear Pt(III)−Pt(III) compounds. The high oxidation state intermediates observed in the described reactions could provide opportunities for achieving distinct and complementary reactivity of the phosphanido complexes. This reactivity paves the way for the synthesis of specific ligands through two steps: (a) synthesis of the adequate starting material by a formal coordination of a chelate L-L′ ligand (*O*-donor group) to the "$(R_F)_2Pt^{II}(\mu\text{-}PPh_2)_2M^{II}$" fragment and (b) oxidation of this new phosphanido complex which induces the formation of a P−L bond providing the designed new ligand Ph_2P-LL′.

EXPERIMENTAL SECTION

General Comments. C, H, and N analyses were performed with a Perkin-Elmer 2400 analyzer. IR spectra were recorded on a Perkin-Elmer Spectrum 100 FT-IR spectrometer. NMR spectra in solution were recorded on Bruker Avance 400 spectrometers with $SiMe_4$, $CFCl_3$, 85% H_3PO_4, and aqueous $[PtCl_6]^{2-}$ as external references for ^1H, ^{19}F, ^{31}P, and ^{195}Pt, respectively. High resolution mass spectrometry (HRMS) and MS/MS analyses were performed using a time-of-flight mass spectrometer equipped with an electrospray ion source (Bruker micrOTOF-Q II). The analyses were carried out in positive and in negative ion modes. The samples were introduced as acetonitrile solutions by continuous infusion with the aid of a syringe pump at a flow-rate of 180 μL/h. The instrument was operated at end plate offset −500 V and capillary −4500 V. Nebulizer pressure was 0.3 bar (N_2) and the drying gas (N_2) flow 4 L/min. Drying gas temperature was set at 453 K. The software used for the simulations is Bruker Daltonics Data Analysis (version 4.0). For all described HRMS peaks, the isotope patterns were superimposable to those calculated on the basis of the proposed formulas. Literature methods were used to prepare the starting materials *cis*-$[M(R_F)_2(PPh_2H)_2]$ (M = Pd, Pt),[37] $[NBu_4]_2[\{(R_F)_2Pt(\mu\text{-}PPh_2)_2M(\mu\text{-}Cl)\}_2]$ (M = Pd, Pt),[37] $[\{Pd(\mu\text{-}Cl)(hq)\}_2]$,[73] $[NBu_4][(R_F)_2Pt(\mu\text{-}PPh_2)_2Pt(acac)]$ (**6**).[39]

Synthesis of $[NBu_4][(R_F)_2M(\mu\text{-}PPh_2)_2M'(hq)]$. *M* = *M*′ = *Pt*, ***1***. $AgClO_4$ (0.118 g, 0.570 mmol) was added to a colorless solution of $[NBu_4]_2[\{(R_F)_2Pt(\mu\text{-}PPh_2)_2Pt(\mu\text{-}Cl)\}_2]$ (0.783 g, 0.285 mmol) in acetone (25 mL). The mixture was stirred in the dark for 1 h. 8-Hydroxyquinoline (0.083 g, 0.570 mmol) was added and stirred for 30 min. NBu_4OH (1 M in methanol, 0.6 mL, 0.6 mmol) was added, and after 30 min the mixture was filtered through Celite. The yellow solution was evaporated to ca. 2 mL and *i*-PrOH (ca. 15 mL) was added. Complex **1** crystallized as a yellow solid which was filtered, washed with cold *i*-PrOH (3 × 1 mL), and dried. Yield: 0.553 g, 65%. Found: C, 49.59; H, 4.47; N, 1.82. $C_{61}H_{62}F_{10}N_2OP_2Pt_2$ requires C, 49.46; H, 4.22; N, 1.89. HRMS(−), exact mass for the anion $[C_{45}H_{26}F_{10}NOP_2Pt_2]^-$: 1238.0622; measured: *m*/*z*: 1238.0623 $(M)^-$. ^1H NMR (298 K, $(CD_3)_2CO$, 400 MHz): δ 8.33 (d, 1H, H^4, 8.4 Hz), 8.12 (broad, 1H, H^2), 8.00 (dd, 4H, *o*-Ph bonded to P^A, 10.5 Hz, 7.6 Hz), 7.92 (pseudo t, 4H, *o*-Ph bonded to P^B, 9.1 Hz), 7.41 (pseudo t, 1H, H^6, 7.4 Hz), 7.28−7.13 (m, 13 H, overlapped H^3, *m*-Ph, *p*-Ph), 6.88 (d, 1H, H^5, 7.9 Hz), 6.82 (d, 1H, H^7, 7.9 Hz), 3.49 (m, 8H, NBu_4^+), 1.87 (m, 8H, NBu_4^+), 1.49 (pseudo sextet, 8H, 7.4 Hz, NBu_4^+), 1.03 (t, 12H, 7.4 Hz, NBu_4^+) ppm. ^{19}F NMR (298 K, $(CD_3)_2CO$, 376.5 MHz): δ −114.8 (m, 4 *o*-F, $^3J_{F,Pt}$ = ca. 330 Hz), −168.3 (m, 4 *m*-F), −167.3 (m, 2 *p*-F).

M = *M*′ = *Pd*, ***2***. *n*-Butyllitium (2.5 M in hexanes, 0.50 mL, 1.25 mmol) was added to a colorless solution of *cis*-$[Pd(C_6F_5)_2(PPh_2H)_2]$ (0.500 g, 0.615 mmol) in thf (15 mL) under an argon atmosphere at −78 °C. The yellow solution was stirred for 15 min and $[\{Pd(\mu\text{-}Cl)(8\text{-}hq)\}_2]$ (0.176 g, 0.308 mmol) was added. The suspension was allowed to reach room temperature, stirred for 20 h, and evaporated to dryness. CH_2Cl_2 (25 mL) was added to the resulting residue, and a solid was filtered through Celite. The CH_2Cl_2 solution was evaporated to dryness, and the residue was dissolved in *i*-PrOH (ca. 35 mL). NBu_4ClO_4 (0.212 g, 0.617 mmol) was added to the solution and **2** started to crystallize. The solution was evaporated to ca. 20 mL and left in the freezer for 4 h. **2** crystallized as a yellow solid, which was filtered, washed with cold *i*-PrOH (3 × 1 mL), and dried, 0.362 g, 45% yield. Found: C, 56.59; H, 4.73; N, 2.13. $C_{61}H_{62}F_{10}N_2OP_2Pd_2$ requires C, 56.19; H, 4.79; N, 2.15. HRMS(−), exact mass for the anion $[C_{45}H_{26}F_{10}NOP_2Pd_2]^-$: 1061.9399; measured: *m*/*z*: 1061.9428 $(M)^-$. ^1H NMR (298 K, $(CD_3)_2CO$, 400 MHz): δ 8.20 (d, 1H, H^4, 8.3 Hz), 7.99 (dd, 4H, *o*-Ph bonded to P^A, 10.4 Hz, 7.7 Hz), 7.91 (dd, 4H, *o*-Ph bonded to P^B, 10.1 Hz, 7.8 Hz), 7.63 (broad, 1H, H^2), 7.32 (pseudo t, 1H, H^6, 8.1 Hz), 7.25 (t, 2H, *p*-Ph bonded to P^B, 6.7 Hz), 7.23 (t, 2H, *p*-Ph bonded to P^A, 6.7 Hz), 7.18 (t, 4H, *m*-Ph bonded to P^B, 7.4 Hz), 7.12 (t, 4H, *m*-Ph bonded to P^A, 7.2 Hz), 7.07 (dd, 1H, H^3, 7.9 Hz, 4.8 Hz), 6.81 (d, 1H, H^5, 7.9 Hz), 6.72 (d, 1H, H^7, 7.9 Hz), 3.49 (m, 8H, NBu_4^+), 1.87 (m, 8H, NBu_4^+), 1.49 (pseudo sextet, 8H, 7.4 Hz, NBu_4^+), 1.03 (t, 12H, 7.4 Hz, NBu_4^+) ppm. ^{19}F NMR (298 K, $(CD_3)_2CO$, 376.5 MHz): δ −111.5 (m, 2 *o*-F), −111.7 (2 *o*-F), −167.0 (m, 4 *m*-F), −166.2 (m, 1 *p*-F), −166.3 (m, 1 *p*-F).

M = *Pt*, *M*′ = *Pd*, ***3***. Complex **3** was prepared similarly to **2** from *cis*-$[Pt(C_6F_5)_2(PPh_2H)_2]$ (0.610 g, 0.676 mmol), *n*-butyllitium (2.5 M in hexane, 0.54 mL, 1.35 mmol), $[\{Pd(\mu\text{-}Cl)(8\text{-}hq)\}_2]$ (0.193 g, 0.337 mmol) and NBu_4ClO_4 (0.231 g, 0.676 mmol) as a yellow solid. 0.478 g, 51% yield. Found: C, 52.70; H, 4.43; N, 1.96. $C_{61}H_{62}F_{10}N_2OP_2PdPt$ requires C, 52.61; H, 4.49; N, 2.01. HRMS(−), exact mass for the anion $[C_{45}H_{26}F_{10}NOP_2PdPt]^-$: 1150.0005; measured: *m*/*z*: 1149.9899 $(M)^-$. ^1H NMR (298 K, $(CD_3)_2CO$, 400 MHz): δ 8.21 (d, 1H, H^4, 8.3 Hz), 8.01 (pseudo t, 4H, *o*-Ph bonded to P^A, 8.8 Hz), 7.92 (dd, 4H, *o*-Ph bonded to P^B, 9.1 Hz), 7.70 (broad, 1H, H^2), 7.32 (pseudo t, 1H, H^6, 8.0 Hz), 7.29−7.08 (m, 13 H, overlapped H^3, *m*-Ph, *p*-Ph), 6.82 (d, 1H, H^5, 7.9 Hz), 6.73 (d, 1H, H^7, 7.9 Hz), 3.49 (m, 8H, NBu_4^+), 1.87 (m, 8H, NBu_4^+), 1.49 (pseudo sextet, 8H, 7.4 Hz, NBu_4^+), 1.03 (t, 12H, 7.4 Hz, NBu_4^+) ppm. ^{19}F NMR (298 K, $(CD_3)_2CO$, 376.5 MHz): δ −114.7 (m, 2 *o*-F, $^3J_{F,Pt}$ = 324 Hz), −115.0 (m, 2 *o*-F, $^3J_{F,Pt}$ = 330 Hz), −168.1 (m, 4 *m*-F), −167.3 (m, 2 *p*-F) ppm.

Synthesis of $[NBu_4][(R_F)_2Pt(\mu\text{-}PPh_2)_2M(pic)]$. *M* = *Pt*, ***4***. Complex **4** was prepared similarly to **1** from $[NBu_4]_2[\{(R_F)_2Pt(\mu\text{-}PPh_2)_2Pt(\mu\text{-}Cl)\}_2]$ (0.362 g, 0.132 mmol), $AgClO_4$ (0.055 g, 0.264 mmol), picolinic acid (0.032 g, 0.264 mmol), and NBu_4OH (1 M in methanol, 0.3 mL, 0.300 mmol) as a white solid. Yield: 0.217 g, 57%.

dx.doi.org/10.1021/ic4004005 | *Inorg. Chem.* 2013, 52, 5493−5506

Found: C, 47.34; H, 3.61; N 1.90. $C_{58}H_{60}F_{10}N_2P_2Pt_2$ requires C, 47.74; H, 4.14; N, 1.92. HRMS(−), exact mass for the anion $[C_{42}H_{24}F_{10}NO_2P_2Pt_2]^-$: 1216.0415; measured: *m*/*z*: 1216.0350 $(M)^-$. ^{1}H NMR (298 K, $(CD_3)_2CO$, 400 MHz): δ 8.16 (pseudo td, 1H, H^4, 7.5 Hz, 1.3 Hz), 8.08 (d, 1H, H^5, 7.5 Hz), 8.02 (d, 1H, H^2, 5.0 Hz), 7.90 (pseudo t, 4H, *o*-Ph bonded to P^A, 8.8 Hz), 7.88 (pseudo t, 4H, *o*-Ph bonded to P^B, 8.8 Hz), 7.47 (dd, 1H, H^2, 7.5 Hz, 5.9 Hz), 7.32−7.15 (m, 12 H, *m*-Ph, *p*-Ph), 3.49 (m, 8H, NBu_4^+), 1.87 (m, 8H, NBu_4^+), 1.49 (pseudo sextet, 8H, 7.4 Hz, NBu_4^+), 1.03 (t, 12H, 7.4 Hz, NBu_4^+) ppm. ^{19}F NMR (298 K, $(CD_3)_2CO$, 376.5 MHz): δ −115.0 (m, 2 *o*-F, $^3J_{F,Pt}$ = 323 Hz), −115.1 (m, 2 *o*-F, $^3J_{F,Pt}$ = 325 Hz), −168.0 (m, 4 *m*-F), −167.2 (m, 2 *p*-F) ppm.

M = *Pd*, ***5***. Complex **5** was prepared similarly to **1** from $[NBu_4]_2[\{(R_F)_2Pt(\mu\text{-}PPh_2)_2Pd(\mu\text{-}Cl)\}_2]$ (0.200 g, 0.078 mmol), $AgClO_4$ (0.032 g, 0.156 mmol), picolinic acid (0.019 g, 0.156 mmol), and NBu_4OH (1 M in methanol, 0.16 mL, 0.160 mmol) as a yellow solid 0.135 g, 63% yield. Found: C, 50.72; H, 4.26; N, 2.26. $C_{58}H_{60}F_{10}N_2P_2Pt_2PdPt$ requires C, 50.83; H, 4.41; N, 2.04. HRMS(−), exact mass for the anion $[C_{42}H_{24}F_{10}NO_2P_2PtPd]^-$: 1127.9787; measured: *m*/*z*: 1127.9741 $(M)^-$. ^{1}H NMR (298 K, $(CD_3)_2CO$, 400 MHz): δ 8.10 (d, 1H, H^5, 7.6 Hz), δ 8.04 (pseudo t, 1H, H^4, 7.6 Hz), 7.93 (m, 4H, *o*-Ph bonded to P^A, overlapped), 7.89 (m, 4H, *o*-Ph bonded to P^B, overlapped), 7.64 (d, 1H, H^2, 4.1 Hz), 7.37−7.14 (m, 13 H, *m*-Ph, *p*-Ph, H^3), 3.49 (m, 8H, NBu_4^+), 1.87 (m, 8H, NBu_4^+), 1.49 (pseudo sextet, 8H, 7.4 Hz, NBu_4^+), 1.03 (t, 12H, 7.4 Hz, NBu_4^+) ppm. ^{19}F NMR (298 K, $(CD_3)_2CO$, 376.5 MHz): δ −115.0 (m, 2 *o*-F, $^3J_{F,Pt}$ = ca. 325 Hz), −115.1 (m, 2 *o*-F, $^3J_{F,Pt}$ = ca. 335 Hz), −167.1 (m, 4 *m*-F), −167.7 (m, 1 *p*-F), −167.8 (m, 1 *p*-F) ppm.

Synthesis of $[(R_F)_2M(\mu\text{-}I)(\mu\text{-}PPh_2)M'(P,O\text{-}PPh_2hq)]$. *M* = *M′* = *Pt*, ***7***. I_2 (0.029 g, 0.114 mmol) in CH_2Cl_2 (10 mL) was added dropwise to a yellow solution of **1** (0.169 g, 0.114 mmol) in CH_2Cl_2 (5 mL). The solution was stirred at room temperature for 20 h, and the orange solution was evaporated to ca. 1 mL. *i*-PrOH (10 mL) was added, stirred for 30 min, and left in the freezer for 4 h. Complex **7** crystallized as a yellow solid which was filtered, washed with cold *i*-PrOH (2 × 1 mL), and dried. Yield: 0.098 g, 63%. Found: C, 39.27; H, 1.96; N, 1.16. $C_{45}H_{26}F_{10}INOP_2Pt_2$ requires C, 39.58; H, 1.92; N, 1.03. HRMS(+), measured: *m*/*z*: 1387.9561 $[M + Na]^+$, exact mass: 1387.9554; ^{1}H NMR (298 K, $(CD_3)_2CO$, 400 MHz): δ 10.53 (broad d, 1H, H^2, 4.9 Hz), 8.97 (d, 1H, H^4, 8.4 Hz), 8.05 (d, 1H, H^5, 8.0 Hz, overlapped), 8.03 (m, 1H, H^3, overlapped), 7.88 (d, 1H, H^7, 8.0 Hz), 7.81 (pseudo t, 1H, H^6, 8.0 Hz), 7.65−7.52 (m, 6H, *o*-Ph bonded to P^B, *p*-Ph bonded to P^B), 7.46−7.34 (m, 8H, *o*-Ph bonded to P^A, *m*-Ph bonded to P^B), 7.27 (t, 2H, *p*-Ph bonded to P^A, 7.5 Hz), 7.09 (pseudo t, 4H, *m*-Ph bonded to P^A, 7.5 Hz) ppm. ^{19}F NMR (298 K, $(CD_3)_2CO$, 376.5 MHz): δ −115.4 (m, 2 *o*-F of the R_F *trans* to P, $^3J_{F,Pt}$ = 336 Hz, $^3J_{F,F} = {}^3J_{F,P}$ = 18 Hz), −117.5 (d, 2 *o*-F of the R_F *trans* to I, $^3J_{F,Pt}$ = 528 Hz, $^3J_{F,F}$ = 27 Hz), −165.1 (t, 1 *p*-F of the R_F *trans* to P, $^3J_{F,F}$ = 19 Hz), −166.1 (td, 2 *m*-F of the R_F *trans* to P, $^3J_{F,F}$ = 19 Hz, $^5J_{F,P}$ = 9 Hz), −167.2 (t, 1 *p*-F of the R_F *trans* to I, $^3J_{F,F}$ = 19 Hz), −167.5 (m, 2 *m*-F of the R_F *trans* to I, $^4J_{F,Pt}$ = 130 Hz, $^3J_{F,F}$ = 19 Hz, $^3J_{F,F}$ = 27 Hz) ppm.

M = *M′* = *Pd*, ***8***. I_2 (0.039 g, 0.157 mmol) in CH_2Cl_2 (10 mL) was added dropwise to a yellow solution of **2** (0.204 g, 0.157 mmol) in CH_2Cl_2 (5 mL), and the resulting mixture was stirred at room temperature for 20 h. The red solution was evaporated to ca. 1 mL, passed through a silica column (ca. 15 cm ×3 cm^2) and eluted with CH_2Cl_2. The red solution (ca. 50 mL) was evaporated to ca. 1 mL, Et_2O (30 mL), and hexane (ca. 2 mL) was added and left in the freezer for 4 h. A red solid, **8**, was filtered, washed with cold *n*-hexane (2 × 1 mL), and dried. 0.040 g, 21% yield. Solutions of **8** slowly became dark. Minor amounts of black palladium could be present in the samples of **8**. Found: C, 44.34; H, 2.40; N, 1.18. $C_{45}H_{26}F_{10}INOP_2Pd_2$ requires C, 45.48; H, 2.21; N, 1.18. HRMS(+), measured: *m*/*z*: 1211.8283 $[M + Na]^+$, exact mass: 1211.8359; ^{1}H NMR (298 K, $(CD_3)_2CO$, 400 MHz): δ 10.46 (broad d, 1H, H^2, 4.9 Hz), 8.88 (dd, 1H, H^4, 8.3 Hz, 1.4 Hz), 8.00 (dd, 1H, H^3, 8.3 Hz, 5.0 Hz), 7.98 (d, 1H, H^5, 8.0 Hz, 1.4 Hz), 7.82 (ddd, 1H, H^7, 7.7 Hz, 1.3 Hz, 0.7 Hz), 7.75 (pseudo t, 1H, H^6, 8.0 Hz), 7.64 (t, 2H, *p*-Ph bonded to P^B, 7.3 Hz), 7.54 (dd, 4H, *o*-Ph bonded to P^B, 12.4 Hz, 8.2 Hz) 7.44 (ddd, 4H, *m*-Ph bonded to P^B, 8.2 Hz, 7.3 Hz, 3.4 Hz), 7.36−7.29 (m, 6H, *p*-Ph bonded to P^A, *o*-Ph bonded to P^A), 7.11 (ddd, 4H, *m*-Ph bonded to P^A, 8.0 Hz, 7.5 Hz, 2.2 Hz) ppm. ^{19}F NMR (298 K, $(CD_3)_2CO$, 376.5 MHz): δ −112.6 (m, 2 *o*-F of the R_F *trans* to P, $^3J_{F,F}$ = 31 Hz), −113.8 (m, 2 *o*-F of the R_F *trans* to I, $^3J_{F,F}$ = 24 Hz), −164.2 (t, 1 *p*-F of the R_F *trans* to P, $^3J_{F,F}$ = 19 Hz), −165.1 (td, 1 *p*-F of the R_F *trans* to I, $^3J_{F,F}$ = 19 Hz, $^4J_{F,F}$ = 2 Hz), −165.3 (ddd, 2 *m*-F of the R_F *trans* to P, $^3J_{F,F}$ = 31 Hz, $^3J_{F,F}$ = 19 Hz, $^5J_{F,P}$ = 11 Hz), −165.9 (dd, 1 *m*-F of the R_F *trans* to I, $^3J_{F,F}$ = 24 Hz, $^3J_{F,F}$ = 19 Hz) ppm.

M = *Pt*, *M′* = *Pd*, ***9***. Complex **9** was prepared similarly to **8** from **3** (0.203 g, 0.145 mmol) and I_2 (0.037 g, 0.145 mmol) as a orange solid. 0.052 g, 28% yield. Found: C, 42.14; H, 2.24; N, 1.34 $C_{45}H_{26}F_{10}INOP_2PdPt$ requires C, 42.32; H, 2.05; N, 1.10. HRMS(+), measured: *m*/*z*: 1299.8893 $[M + Na]^+$, exact mass: 1299.8937; ^{1}H NMR (298 K, $(CD_3)_2CO$, 400 MHz): δ 10.49 (broad d, 1H, H^2, 4.3 Hz), 8.89 (d, 1H, H^4, 8.3 Hz), 8.03−7.96 (m, 2H, H^3 + H^5), 7.82 (d, 1H, H^7, 7.3 Hz), 7.75 (pseudo t, 1H, H^6, 7.7 Hz), 7.66 (t, 2H, *p*-Ph bonded to P^B, 7.1 Hz), 7.57−7.43 (m, 8H, *o*-Ph bonded to P^B, *m*-Ph bonded to P^B), 7.36−7.26 (m, 6H, *p*-Ph bonded to P^A, *o*-Ph bonded to P^A), 7.11 (pseudo t, 4H, *m*-Ph bonded to P^A, 7.3 Hz) ppm. ^{19}F NMR (298 K, $(CD_3)_2CO$, 376.5 MHz): δ −115.8 (m, 2 *o*-F of the R_F *trans* to P, $^3J_{F,Pt}$ = 336 Hz, $^3J_{F,F} = {}^3J_{F,P}$ = 18 Hz), −117.9 (d, 2 *o*-F of the R_F *trans* to I, $^3J_{F,Pt}$ = 515 Hz, $^3J_{F,F}$ = 27 Hz), −164.9 (t, 1 *p*-F of the R_F *trans* to P, $^3J_{F,F}$ = 20 Hz), −166.1 (td, 2 *m*-F of the R_F *trans* to P, $^3J_{F,F}$ = 20 Hz, $^5J_{F,P}$ = 9 Hz), −166.7 (t, 1 *p*-F of the R_F *trans* to I, $^3J_{F,F}$ = 19 Hz), −167.2 (m, 2 *m*-F of the R_F *trans* to I, $^4J_{F,Pt}$ = 168 Hz, $^3J_{F,F}$ = 19 Hz, $^3J_{F,F}$ = 27 Hz) ppm.

Reaction of ***4*** *with* I_2. I_2 (0.030 g, 0.118 mmol) was added to a yellow solution of **4** (0.173 g, 0.118 mmol) in anhydrous CH_2Cl_2 (10 mL), and the resulting mixture was stirred under argon at room temperature for 20 h. The resulting solution was evaporated to ca. 3 mL, anhydrous *n*-hexane (10 mL) was added, and a yellow oil was formed. The liquors were eliminated, and the yellow oil was stirred with anhydrous *n*-hexane (5 mL) for 30 min affording a yellow solid. The *n*-hexane was eliminated, and the solid was dried in a vacuum. The $^{31}P\{^1H\}$NMR spectrum of this yellow solid showed to be a mixture of $[NBu_4][(R_F)_2Pt(\mu\text{-}I)(\mu\text{-}PPh_2)Pt(PPh_2\text{-}pic)I]$, **10**, and $[NBu_4][(R_F)_2Pt(\mu\text{-}I)(\mu\text{-}PPh_2)Pt(PPh_2OH)I]$, **10-hydr**, and satisfactory analysis of **10** could in no case be obtained. Recrystallization of this mixture from wet acetone and *i*-PrOH (1 mL/5 mL) afforded **10-hydr** which was filtered, washed with cold *i*-PrOH (2 × 0.5 mL), and dried. **10-hydr**. Yield: 0.111 g, 54%. Found: C, 38.81; H, 3.31; N, 0.98. $C_{52}H_{57}F_{10}I_2NOP_2Pt_2$ requires C, 38.84; H, 3.57; N, 0.87.

10. HRMS(−), exact mass for the anion $[C_{42}H_{24}F_{10}NI_2O_2P_2Pt_2]^-$: 1469.8504 Da; measured: *m*/*z*: 1469.8517 $(M)^-$. ^{1}H NMR (298 K, $(CD_3)_2CO$, 400 MHz): δ 8.62 (broad d, 1H, H^2, 4.3 Hz), 8.01 (dd, 4H, *o*-Ph bonded to P^B, 7.1 Hz, 8.5 Hz), 7.84−7.77 (m, 5H, *o*-Ph bonded to P^A, H^4), 7.58−7.39 (m, 8H, *p*-Ph bonded to P^B, *m*-Ph bonded to P^B, H^3, H^5), 7.10 (t, 2H, *p*-Ph bonded to P^A, 6.9 Hz), 7.00 (pseudo t, 4H, *m*-Ph bonded to P^A, 7.3 Hz), 3.49 (m, 8H, NBu_4^+), 1.87 (m, 8H, NBu_4^+), 1.49 (pseudo sextet, 8H, 7.4 Hz, NBu_4^+), 1.03 (t, 12H, 7.4 Hz, NBu_4^+) ppm. ^{19}F NMR (298 K, $(CD_3)_2CO$, 376.5 MHz): δ −114.9 (pseudo t, 2 *o*-F of the R_F *trans* to P, $^3J_{F,Pt}$ = 340 Hz, $^3J_{F,F} = {}^3J_{F,P}$ = 19 Hz), −116.4 (d, 2 *o*-F of the R_F *trans* to I, $^3J_{F,Pt}$ = 505 Hz, $^3J_{F,F}$ = 30 Hz), −166.5 (t, 1 *p*-F of the R_F *trans* to P, $^3J_{F,F}$ = 19 Hz), −166.9 (m, 2 *m*-F of the R_F *trans* to P, $^3J_{F,F}$ = 20 Hz, $^5J_{F,P}$ = 10 Hz), −168.3 (pseudo t, 2 *m*-F of the R_F *trans* to I, $^4J_{F,Pt}$ = 138 Hz, mean $^3J_{F,F}$ = 24 Hz) −168.7 (t, 1 *p*-F of the R_F *trans* to I, $^3J_{F,F}$ = 19 Hz) ppm.

10-hydr. HRMS(−), exact mass for the anion $[C_{36}H_{21}F_{10}I_2OP_2Pt_2]^-$: 1364.8289; measured: *m*/*z*: 1364.8294 $(M)^-$. ^{1}H NMR (298 K, $(CD_3)_2CO$, 400 MHz): δ 7.96 (dd, 4H, *o*-Ph bonded to P^A, 10.4 Hz, 7.9 Hz), δ 7.81 (dd, 4H, *o*-Ph bonded to P^B, 12.4 Hz, 8.0 Hz), 7.54 (s, PO*H*, detected from ^{1}H EXSY spectrum, by its exchange with H_2O), 7.52 (t, 2H, *p*-Ph bonded to P^B, 7.4 Hz), 7.45 (pseudo t, 4H, *m*-Ph bonded to P^B, 7.4 Hz), 7.22 (t, 6H, *p*-Ph bonded to P^A, 7.2 Hz) 7.13 (pseudo t, 4H, *m*-Ph bonded to P^A, 7.2 Hz), 3.49 (m, 8H, NBu_4^+), 1.87 (m, 8H, NBu_4^+), 1.49 (pseudo sextet, 8H, 7.4

dx.doi.org/10.1021/ic4004005 | *Inorg. Chem.* 2013, 52, 5493−5506

Hz, NBu_4^+), 1.03 (t, 12H, 7.4 Hz, NBu_4^+) ppm. ^{19}F NMR (298 K, $(CD_3)_2CO$, 376.5 MHz): δ −115.2 (pseudo t, 2 *o*-F of the R_F *trans* to P, $^3J_{F,Pt}$ = 345 Hz, $^3J_{F,F}$ = $^3J_{F,P}$ = 19 Hz), −116.7 (d, 2 *o*-F of the R_F *trans* to I, $^3J_{F,Pt}$ = 503 Hz, $^3J_{F,F}$ = 29 Hz), −166.7 (t, 1 *p*-F of the R_F *trans* to P, $^3J_{F,F}$ = 19 Hz), −167.0 (td, 2 *m*-F of the R_F *trans* to P, $^3J_{F,F}$ = 19 Hz, $^5J_{F,P}$ = 9 Hz), −168.2 (pseudo t, 2 *m*-F of the R_F *trans* to I, $^4J_{F,Pt}$ = 136 Hz, mean $^3J_{F,F}$ = 24 Hz) −169.0 (t, 1 *p*-F of the R_F *trans* to I, $^3J_{F,F}$ = 19 Hz) ppm.

Synthesis of [NBu4][(PPh2-pic)(RF)Pt(μ-I)(μ-PPh2)Pd(RF)I], 11. I_2 (0.037 g, 0.146 mmol) in CH_2Cl_2 (10 mL) was added dropwise to a yellow solution of **5** (0.200 g, 0.146 mmol) in CH_2Cl_2 (5 mL). The solution was stirred under nitrogen at room temperature for 20 h and then evaporated to dryness. The solid residue was recrystallized from acetone/*i*-PrOH (1 mL/5 mL). Complex **11** crystallized as a yellow solid which was filtered, washed with cold *i*-PrOH (2 × 0.5 mL), and dried. 0.125 g, 53% yield. Found: C, 42.29; H, 3.65; N, 1.88. $C_{58}H_{60}F_{10}I_2N_2O_2P_2PdPt$ requires C, 42.89; H, 3.72; N, 1.72. HRMS(−), exact mass for the anion $[C_{42}H_{24}F_{10}I_2NO_2P_2PdPt]^-$: 1381.7887 Da; measured: *m*/*z*: 1381.7895 $(M)^-$. ^1H NMR (298 K, $(CD_3)_2CO$, 400 MHz): δ 8.60 (broad d, 1H, H^2, 3.9 Hz), 7.89−7.79 (m, 6H, *o*-Ph bonded to P^B, H^4, H^5), 7.64−7.54 (m, 3H, *p*-Ph bonded to P^B, H^3), 7.51−7.38 (m, 8H, *o*-Ph bonded to P^A, *m*-Ph bonded to P^B), 7.06 (t, 2H, *p*-Ph bonded to P^A, 7.2 Hz), 6.88 (pseudo t, 4H, *m*-Ph bonded to P^A, 7.1 Hz), 3.49 (m, 8H, NBu_4^+), 1.87 (m, 8H, NBu_4^+), 1.49 (pseudo sextet, 8H, 7.4 Hz, NBu_4^+), 1.03 (t, 12H, 7.4 Hz, NBu_4^+) ppm. ^{19}F NMR (298 K, $(CD_3)_2CO$, 376.5 MHz): δ −112.2 (d, 2 *o*-F of the R_F *trans* to I, $^3J_{F,F}$ = 28 Hz), −115.5 (dd, 2 *o*-F of the R_F *trans* to P, $^3J_{F,Pt}$ = 256 Hz, $^3J_{F,F}$ = 24 Hz, $^4J_{F,P}$ = 17 Hz), −164.9 (t, 1 *p*-F of the R_F *trans* to P, $^3J_{F,F}$ = 19 Hz), −166.1 (m, 2 *m*-F of the R_F *trans* to P, $^3J_{F,F}$ = 24 Hz, $^3J_{F,F}$ = 19 Hz), −167.0 to −167.3 (m, 1 *p*-F of the R_F *trans* to I, 2 *m*-F of the R_F *trans* to I) ppm.

Synthesis of [NBu4][(RF)2Pt(μ-I)(μ-PPh2)PtI(Ph2P-acac)] (12). I_2 (0.035 g, 0.140 mmol) in CH_2Cl_2 (10 mL) was added dropwise to a colorless solution of $[NBu_4][(R_F)_2Pt(\mu\text{-}PPh_2)_2Pt(O,O'\text{-acac})]$ (**6**) (0.201 g, 0.140 mmol) in CH_2Cl_2 (20 mL), and the resulting mixture was stirred at room temperature for 20 h. The obtained yellow solution was evaporated to ca. 2 mL, $CHCl_3$ (8 mL) was added, and evaporated to ca. 6 mL. The mixture was stirred for 30 min, and **12** crystallized as a yellow solid which was filtered, washed with cold $CHCl_3$ (2× 1 mL), and dried. 0.168 g, 69% yield. Found: C, 40.26; H, 3.82; N, 1.18. $C_{57}H_{63}F_{10}I_2NO_2P_2Pt_2$ requires C, 40.51; H, 3.76; N, 0.83. HRMS(−), exact mass for the anion $[C_{41}H_{27}F_{10}I_2O_2P_2Pt_2]^-$: 1446.870 Da; measured: *m*/*z*: 1446.8720 $(M)^-$. ^1H NMR (298 K, $(CD_3)_2CO$, 400 MHz): δ 7.98 (dd, 4H, *o*-Ph bonded to P^A, 10.8 Hz, 8.5 Hz), 7.66 (dd, 4H, *o*-Ph bonded to P^B, 12.2 Hz, 7.3 Hz), 7.58 (t, 2H, *p*-Ph bonded to P^B, 6.9 Hz), 7.49 (pseudo t, 4H, *m*-Ph bonded to P^B, 7.3 Hz), 7.36−7.22 (m, 6H, *p*-Ph bonded to P^A, *m*-Ph bonded to P^A) 4.96 (d, 1H, C*H*, 2.0 Hz), 3.49 (m, 8H, NBu_4^+), 1.87 (m, 8H, NBu_4^+), 1.72 (s, 3H, (O═C)-C*H*$_3$)), 1.49 (pseudo sextet, 8H, 7.4 Hz, NBu_4^+), 1.40 (s, 3H, C═C−C*H*$_3$), 1.03 (t, 12H, 7.4 Hz, NBu_4^+) ppm. ^{19}F NMR (298 K, $(CD_3)_2CO$, 376.5 MHz): δ −115.3 (m, 2 *o*-F of the R_F *trans* to P, $^3J_{F,Pt}$ = 340 Hz, $^3J_{F,F}$ = $^3J_{F,P}$ = 18 Hz), −116.9 (d, 2 *o*-F of the R_F *trans* to I, $^3J_{F,Pt}$ = 497 Hz, $^3J_{F,F}$ = 29 Hz), −166.5 (t, 1 *p*-F of the R_F *trans* to P, $^3J_{F,F}$ = 19 Hz), −166.9 (td, 2 *m*-F of the R_F *trans* to P, $^3J_{F,F}$ = 19 Hz, $^5J_{F,P}$ = 9 Hz), −168.1 (pseudo t, 2 *m*-F of the R_F *trans* to I, $^4J_{F,Pt}$ = 137 Hz, mean $^3J_{F,F}$ = 24 Hz) −168.7 (t, 1 *p*-F of the R_F *trans* to I, $^3J_{F,F}$ = 19 Hz) ppm.

NMR Monitoring of the Reaction Solutions. An NMR tube kept at 268 K was charged with an acetone-d_6 solution of **1** (0.030 g, 0.024 mmol in 0.5 mL), solid NBu_4I (0.037 mg, 0.100 mmol), and solid I_2 (18 mg, 0.072 mmol) and vigorously shaken. The resulting red solution was put in the NMR probe precooled at 268 K, and multinuclear NMR spectra were recorded. The mixture revealed the immediate formation of **1-ox** that, under these conditions, was found stable at 268 K for at least one week. The same procedure was followed for (i) the monitoring of the reaction between **1** (0.030 g, 0.024 mmol in 0.5 mL), and solid I_2 (6.1 mg, 0.024 mmol) in acetone-d_6 at 298 K, which showed the transformation of **1-ox** into **7**; (ii) the monitoring of the reaction between **4** (0.030 g, 0.025 mmol in 0.5 mL), solid NBu_4I (0.037 mg, 0.100 mmol), and solid I_2 (18 mg, 0.072 mmol) in acetone-d_6 at 268 K, which showed the formation of **4-ox**; (iii) the monitoring of the reaction between **4** (0.030 g, 0.025 mmol in 0.5 mL), and solid I_2 (6.4 mg, 0.025 mmol) in anhydrous thf at 298 K, which showed the transformation of **4-ox** into **10**; (iv) the monitoring of the reaction between **6** (0.030 g, 0.025 mmol in 0.5 mL), solid NBu_4I (0.037 mg, 0.100 mmol), and solid I_2 (18 mg, 0.072 mmol) in acetone-d_6 at 268 K, which showed the formation of **6-ox**-*cis* and -*trans*; (v) the monitoring of the reaction between **6** (0.030 g, 0.025 mmol in 0.5 mL) and solid I_2 (6.4 mg, 0.025 mmol) in acetone-d_6 at 298 K, which showed the transformation of **6-ox** into **12**.

X-ray Structure Determinations. Crystal data and other details of the structure analyses are presented in Table S1. Suitable crystals for X-ray diffraction studies were obtained by slow diffusion of *n*-hexane into concentrated solutions of the complexes in 3 mL of Me_2CO or CH_2Cl_2. Crystals were mounted at the end of a quartz fiber. The radiation used in all cases was graphite monochromated $Mo_{K\alpha}$ (λ = 0.71073 Å). For **7**, **9**, and **11**, X-ray intensity data were collected on an Oxford Diffraction Xcalibur diffractometer. The diffraction frames were integrated and corrected from absorption by using the CrysAlis RED program.[74] For **12**, diffraction measurements were made on an Enraf-Nonius CAD-4 diffractometer. Diffracted intensities were measured in a hemisphere of reciprocal space. Three check reflections remeasured after every 300 ordinary reflections showed no decay of the diffracted intensities over the period of data collection. An absorption correction was applied based on 548 azimuthal scan data.

The structures were solved by Patterson and Fourier methods and refined by full-matrix least-squares on F^2 with SHELXL-97.[75] All non-hydrogen atoms were assigned anisotropic displacement parameters and refined without positional constraints, except as noted below. All hydrogen atoms were constrained to idealized geometries and assigned isotropic displacement parameters equal to 1.2 times the U_{iso} values of their attached parent atoms (1.5 times for the methyl hydrogen atoms). In the structures of **7**·2Me_2CO and **9**·Me_2CO·0.25*n*-C_6H_{14}, restraints were applied in the geometry of the acetone solvent and *n*-hexane molecules respectively. In the structure of **12**, the tetrabutylammonium cation was found to be very badly disordered, with two positions sharing some of the carbon atoms of the butyl "branches"; moreover, some of the nonshared carbon atoms are also disordered over two positions. Partial occupancy assignments and restraints in the geometry were used for this moiety. Full-matrix least-squares refinement of these models against F^2 converged to final residual indices given in Table S1.

■ ASSOCIATED CONTENT

Ⓢ Supporting Information

Crystallographic data of **7**·2Me_2CO, **9**·Me_2CO·0.25*n*-C_6H_{14}, **11**·CH_2Cl_2, and **12** (CIF format); NMR spectra of **1**−**5**, **7**, **10**−**12**, **1-ox**, **4-ox**, **6-ox**; HRMS spectrograms of **1**−**5**, **7**−**12**, **1-ox**, **4-ox**, **6-ox**. This material is available free of charge via Internet at http://pubs.acs.org

■ AUTHOR INFORMATION

Corresponding Author

*E-mail: cfortuno@unizar.es (C.F.); p.mastrorilli@poliba.it (P.M.).

Notes

The authors declare no competing financial interest.

■ ACKNOWLEDGMENTS

This work was supported by the Spanish MICINN (Project CTQ2008-06669-C02-01), the Ministerio de Economía y Competitividad (Project CTQ2012-35251), and the Cobierno de Aragón (Grupo de Consolidado: Química Inorgánica y de los Compuestos Organometálicos). A.A. gratefully acknowledges MICINN for a FPU grant. Italian MIUR (PRIN project n. 2009LR88XR) is also acknowledged for financial support.

REFERENCES

(1) Forniés, J.; Fortuño, C.; Ibáñez, S.; Martín, A.; Mastrorilli, P.; Gallo, V.; Tsipis, A. *Inorg. Chem.* **2013**, *52*, 1942−1953.
(2) Xu, L. M.; Li, B. J.; Yang, Z.; Shi, Z. J. *Chem. Soc. Rev.* **2010**, *39*, 712−733.
(3) Sehnal, P.; Taylor, R. J. K.; Fairlamb, I. J. S. *Chem. Rev.* **2010**, *110*, 824−889.
(4) Lyons, T. W.; Sanford, M. S. *Chem. Rev.* **2010**, *110*, 1147−1169.
(5) Canty, A. J. *Dalton Trans.* **2009**, 10409−10417.
(6) Khusnutdinova, J. R.; Rath, N. P.; Mirica, L. M. *J. Am. Chem. Soc.* **2010**, *132*, 7303−7305.
(7) Crespo, M.; Anderson, C. M.; Kfoury, N.; Font-Bardia, M.; Calvet, T. *Organometallics* **2012**, *31*, 4401−4404.
(8) Tang, F.; Zhang, Y.; Rath, N. P.; Mirica, L. M. *Organometallics* **2012**, *31*, 6690−6696.
(9) Julia-Hernández, F.; Arcas, A.; Vicente, J. *Chem.—Eur. J.* **2012**, *18*, 7780−7786.
(10) Zhang, H.; Lei, A. *Dalton Trans* **2011**, *40*, 8745−8754.
(11) Ball, N. D.; Gary, J. B.; Ye, Y.; Sanford, M. S. *J. Am. Chem. Soc.* **2011**, *133*, 7577−7584.
(12) Sierra, D.; Cao, P.; Cabrera, J.; Padilla, R.; Rominger, F.; Limbach, M. *Organometallics* **2011**, *30*, 1885−1895.
(13) Vicente, J.; Arcas, A.; Juliá-Hernández, F.; Bautista, D. *Inorg. Chem.* **2011**, *50*, 5339−5341.
(14) Lanci, M. P.; Remy, M. S.; Lao, D. B.; Sanford, M. S.; Mayer, J. M. *Organometallics* **2011**, *30*, 3704−3707.
(15) Yahav-Levi, A.; Goldberg, I.; Vigalok, A.; Vedernikov, A. N. *Chem. Commun.* **2010**, *46*, 3324−3326.
(16) Vicente, J.; Arcas, A.; Juliá-Hernández, F.; Bautista, D. *Angew. Chem., Int. Ed.* **2011**, *50*, 6896−6899.
(17) Zhao, X.; Dong, V. M. *Angew. Chem., Int. Ed.* **2011**, *50*, 932−934.
(18) Racowski, J. M.; Gary, J. B.; Sanford, M. S. *Angew. Chem., Int. Ed.* **2012**, *51*, 3414−3417.
(19) Ariafard, A.; Hyland, C. J. T.; Canty, A. J.; Sharma, M.; Brookes, N. J. *Inorg. Chem.* **2010**, *49*, 11249−11253.
(20) Ariafard, A.; Hyland, C. J. T.; Canty, A. J.; Sharma, M.; Yates, B. F. *Inorg. Chem.* **2011**, *50*, 6449−6457.
(21) Deprez, N. R.; Sanford, M. S. *J. Am. Chem. Soc.* **2009**, *131*, 11234−11241.
(22) Penno, D.; Estevan, F.; Fernández, E.; Hirva, P.; Lahuerta, P.; Sanaú, M.; Ubeda, M. A. *Organometallics* **2011**, *30*, 2083−2094.
(23) Powers, D. C.; Ritter, T. *Nat. Chem.* **2009**, *1*, 302−309.
(24) Matsumoto, K.; Ochiai, M. *Coord. Chem. Rev.* **2002**, *231*, 229−238.
(25) Canty, A. J.; Gardiner, M. G.; Jones, R. C.; Rodemannn, T.; Sharma, M. *J. Am. Chem. Soc.* **2009**, *131*, 7236−7237.
(26) Whitfield, S. R.; Sanford, M. S. *Organometallics* **2008**, *27*, 1683−1689.
(27) Powers, D. C.; Lee, E.; Ariafard, A.; Sanford, M. S.; Yates, B. F.; Canty, A. J.; Ritter, T. *J. Am. Chem. Soc.* **2012**, *134*, 12002−12009.
(28) Powers, D. C.; Ritter, T. *Acc. Chem. Res.* **2012**, *45*, 840−850.
(29) Hickman, A. J.; Sanford, M. S. *Nature* **2012**, *484*, 177−185.
(30) Wilson, J. J.; Lippard, S. J. *Inorg. Chem.* **2012**, *51*, 9852−9864.
(31) Sicilia, V.; Forniés, J.; Casas, J. M.; Martín, A.; López, J. A.; Larraz, C.; Borja, P.; Ovejero, C.; Tordera, D.; Bolink, H. *Inorg. Chem.* **2012**, *51*, 3427−3435.
(32) Ibáñez, S.; Estevan, F.; Hirva, P.; Sanaú, M.; Ubeda, M. A. *Organometallics* **2012**, *31*, 8098−8108.
(33) Chaouche, N.; Forniés, J.; Fortuño, C.; Kribii, A.; Martín, A.; Karipidis, P.; Tsipis, A. C.; Tsipis, C. A. *Organometallics* **2004**, *23*, 1797−1810.
(34) Arias, A.; Forniés, J.; Fortuño, C.; Martín, A.; Latronico, M.; Mastrorilli, P.; Todisco, S.; Gallo, V. *Inorg. Chem.* **2012**, *51*, 12682−12696.
(35) Ara, I.; Chaouche, N.; Forniés, J.; Fortuño, C.; Kribii, A.; Tsipis, A. C. *Organometallics* **2006**, *25*, 1084−1091.
(36) Alonso, E.; Casas, J. M.; Cotton, F. A.; Feng, X. J.; Forniés, J.; Fortuño, C.; Tomás, M. *Inorg. Chem.* **1999**, *38*, 5034−5040.
(37) Forniés, J.; Fortuño, C.; Navarro, R.; Martínez, F.; Welch, A. J. *J. Organomet. Chem.* **1990**, *394*, 643−658.
(38) Alonso, E.; Forniés, J.; Fortuño, C.; Tomás, M. *J. Chem. Soc., Dalton Trans.* **1995**, 3777−3784.
(39) Alonso, E.; Forniés, J.; Fortuño, C.; Martín, A.; Orpen, A. G. *Organometallics* **2003**, *22*, 5011−5019.
(40) Ara, I.; Chaouche, N.; Forniés, J.; Fortuño, C.; Kribii, A.; Martín, A. *Eur. J. Inorg. Chem.* **2005**, 3894−3901.
(41) Berenguer, J. R.; Chaouche, N.; Forniés, J.; Fortuño, C.; Martín, A. *New J. Chem.* **2006**, *30*, 473−478.
(42) Ara, I.; Forniés, J.; Fortuño, C.; Ibáñez, S.; Martín, A.; Mastrorilli, P.; Gallo, V. *Inorg. Chem.* **2008**, *47*, 9069−9080.
(43) Forniés, J.; Fortuño, C.; Ibáñez, S.; Martín, A.; Mastrorilli, P.; Gallo, V. *Inorg. Chem.* **2011**, *50*, 10798−10809.
(44) Alonso, E.; Casas, J. M.; Forniés, J.; Fortuño, C.; Martín, A.; Orpen, A. G.; Tsipis, C. A.; Tsipis, A. C. *Organometallics* **2001**, *20*, 5571−5582.
(45) Falvello, L. R.; Forniés, J.; Fortuño, C.; Durán, F.; Martín, A. *Organometallics* **2002**, *21*, 2226−2234.
(46) Mastrorilli, P. *Eur. J. Inorg. Chem.* **2008**, 4835−4850.
(47) Carty, A. J.; MacLaughlin, S. A.; Nucciarone, D. *Phosphorus-31 NMR Spectroscopy in Stereochemical Analysis*; VCH: New York, 1987.
(48) de la Mora, J. F.; Van Berkel, G. J.; Enke, C. G.; Cole, R. B.; Martinez-Sanchez, M.; Fenn, J. B. *J. Mass Spectrom.* **2000**, *35*, 939−952.
(49) Kebarle, P. *J. Mass Spectrom.* **2000**, *35*, 804−817.
(50) The HRMS(+) peak is compatible also with a Pt(II))Pt(IV) formulation of the oxidised cations, but this would be in contrast with the tendency of Pt(IV) to give almost invariably octahedral six-coordinated species. On the other hand, phosphanido bridged Pt(III) Pt(III) systems endowed with a metal bond have long been known: refs 35, 36, 42−44.
(51) The HRMS(+) analyses of **1**−**5** were all carried out using acetonitrile solutions of the complexes having approximately the same molar concentration.
(52) Bender, R.; Okio, C.; Welter, R.; Braunstein, P. *Dalton Trans.* **2009**, 4901−4907.
(53) Ara, I.; Chaouche, N.; Forniés, J.; Fortuño, C.; Kribii, A.; Tsipis, A. C.; Tsipis, C. A. *Inorg. Chim. Acta* **2005**, *358*, 1377−1385.
(54) Forniés, J.; Fortuño, C.; Ibáñez, S.; Martín, A. *Inorg. Chem.* **2006**, *45*, 4850−4858.
(55) De Pascali, S. A.; Papadia, P.; Capoccia, S.; Marchiò, L.; Lanfranchi, M.; Ciccarese, A.; Fanizzi, F. P. *Dalton Trans.* **2009**, 7786−7795.
(56) Alonso, E.; Forniés, J.; Fortuño, C.; Martín, A.; Rosair, G. M.; Welch, A. J. *Inorg. Chem.* **1997**, *36*, 4426−4431.
(57) Forniés, J.; Fortuño, C.; Gil, R.; Martín, A. *Inorg. Chem.* **2005**, *44*, 9534−9541.
(58) Forniés, J.; Fortuño, C.; Ibáñez, S.; Martín, A. *Inorg. Chem.* **2008**, *47*, 5978−5987.
(59) Throughout the paper, the calculated (exact mass) and the experimental (accurate) *m*/*z* values have been compared considering the principal ion (which gives the most intense peak) of the isotope pattern.
(60) A different behaviour between the benzoquinolinate and the 8-hydroxyquinolinate systems was found comparing the dynamics in solution of **B-ox** with that of **1-ox**: while in the case of **B-ox** the exchange between two phenyl rings bonded to different P atoms was observed at 298 K in acetone-d_6,[34] in the case of **1-ox** no exchanges were observed by ^{1}H NOESY experiments carried out in the same conditions. A rationale for this different behaviour may be the different strength of the P-O vs P-C bond, the former being more stable, which manifests itself in an irreversible P-O bond formation (8-hydroxyquinolinate system) in contrast to the reversible P-C bond formation (benzoquinolinate system).
(61) An example of coordinated PPh_2I arising from reaction of a phosphanido bridged dirhenium complex with I_2 is reported in: Flörke, U.; Haupt, H.-J. *Acta Crystallogr.* **1991**, *C47*, 1535−1537. while a PPh_2I Nb complex is described in: Antiñolo, A.; García-Yuste, S.;

dx.doi.org/10.1021/ic4004005 | *Inorg. Chem.* 2013, 52, 5493−5506

Otero, A.; Pérez-Flores, J. C.; Reguillo-Carmona, R.; Rodríguez, A. M.; Villaseñor, E. *Organometallics* **2006**, *25*, 1310−1316.
(62) The iododiphenylphosphane complex $NBu_4[(R_F)_2Pt(\mu\text{-}PPh_2)(\mu\text{-}I)Pt(PPh_2I)I]$ accounted for the remaining 15%.
(63) A related irreversible trans to cis isomerization of a diiodoPt(IV) complex has been described in Yahav, A.; Goldberg, I.; Vigalok, A. *Organometallics* **2005**, *24*, 5654−5659.
(64) Yahav-Levi, A.; Goldberg, I.; Vigalok, A.; Vedemikov, A. N. *J. Am. Chem. Soc.* **2008**, *130*, 724−731.
(65) Yahav, A.; Goldberg, I.; Vigalok, A. *Organometallics* **2005**, *24*, 5654−5659.
(66) Yagyu, T.; Ohashi, J.; Maeda, M. *Organometallics* **2007**, *26*, 2383−2391.
(67) Macgregor, S. A. *Chem. Soc. Rev.* **2007**, *36*, 67−76.
(68) Archambault, C.; Bender, R.; Braunstein, P.; Decian, A.; Fischer, J. *Chem. Commun.* **1996**, 2729−2730.
(69) Cabeza, J. A.; del Río, I.; Riera, V.; García-Granda, S.; Sanni, S. B. *Organometallics* **1997**, *16*, 1743−1748.
(70) Albinati, A.; Filippi, V.; Leoni, P.; Marchetti, L.; Pasquali, M.; Passarelli, V. *Chem. Commun.* **2005**, 2155−2157.
(71) Chaouche, N.; Forniés, J.; Fortuño, C.; Kribii, A.; Martín, A. *J. Organomet. Chem.* **2007**, *692*, 1168−1172.
(72) Forniés, J.; Fortuño, C.; Ibáñez, S.; Martín, A.; Tsipis, A. C.; Tsipis, C. A. *Angew. Chem., Int. Ed.* **2005**, *44*, 2407−2410.
(73) Hartwell, G. E.; Lawrence, R. V.; Smas, M. J. *J. Chem. Soc., Chem. Commun.* **1970**, 912.
(74) *CrysAlisRED, Program for X-ray CCD Camera Data Reduction*, Version 1.171.32.19; Oxford Diffraction Ltd.: Oxford, UK, 2008.
(75) Sheldrick, G. M. *SHELXL-97 A Program for Crystal Structure Determination*; University of Gottingen: Germany, 1997.

EurJIC European Journal of Inorganic Chemistry
ChemPubSoc Europe
FULL PAPER

DOI:10.1002/ejic.201300808

Donor Behaviour of Anionic and Asymmetric Phosphanido Derivatives of Platinum and Palladium[‡]

Andersson Arias,[a] Juan Forniés,[a] Consuelo Fortuño,*[a] Antonio Martín,[a] Piero Mastrorilli,*[b] Vito Gallo,[b] Mario Latronico,[b] and Stefano Todisco[b]

Dedicated to Professor A. Laguna on the occasion of his 65th birthday

Keywords: Metal–metal interactions / P ligands / Palladium / Platinum / Structure elucidation

The reactions of $[Ag(OClO_3)(PPh_3)]$ with $[NBu_4][(C_6F_5)_2Pt(\mu\text{-}PPh_2)_2M(hq)]$, $[NBu_4][(C_6F_5)_2Pt(\mu\text{-}PPh_2)_2M(bq)]$, $[NBu_4][(C_6F_5)_2Pt(\mu\text{-}PPh_2)_2M(pic)]$ and $[NBu_4][(C_6F_5)_2Pt(\mu\text{-}PPh_2)_2Pt(C_6F_5)(tht)]$ (M = Pt, Pd; hq = 8-hydroxyquinolinate, bq = benzoquinolinate, pic = picolinate, tht = tetrahydrothiophene) afford the corresponding neutral adducts $[(C_6F_5)_2Pt(\mu\text{-}PPh_2)_2(\mu\text{-}AgPPh_3)M(bq)]$ (M = Pt, **1**; Pd, **2**), $[(C_6F_5)_2Pt(\mu\text{-}PPh_2)_2(\mu\text{-}AgPPh_3)M(hq)]$ (M = Pt, **3**; Pd, **4**) $[(C_6F_5)_2Pt(\mu\text{-}PPh_2)_2(\mu\text{-}AgPPh_3)Pt(C_6F_5)(tht)]$ (**5**) and $[(C_6F_5)_2Pt(\mu\text{-}PPh_2)_2M(pic\text{-}AgPPh_3)]$ (M = Pt, **6**; Pd, **7**) as yellow solids. The XRD structures of **1**–**5**, in which a $[AgPPh_3]^+$ moiety bridges the metal centres, were confirmed in solution at low temperature. At room temperature, a dynamic process for the $[AgPPh_3]^+$ moiety, which passes from the top to the bottom part of the molecules **1**–**5**, was ascertained. For **6** and **7**, the XRD analyses revealed structures in which the $[AgPPh_3]^+$ moiety is linked to the picolinate oxygen atom bonded to the M centre; however, although such a structure was confirmed in solution for the Pt–Pd species **7**, the stable form of the Pt–Pt species **6** in solution is that with the $[AgPPh_3]^+$ moiety bridging the metal centres.

Introduction

Since the first complexes with platinum–silver bonds were structurally characterized during the 1980s,[1–8] the number and study of complexes with metallophilic bonds has considerably grown.[9–31] Attractive M–M′ interactions behave as a powerful tool in the formation of polynuclear systems with special topologies and electronic properties. A particular case of this type of interaction is the Pt^{II}–Ag^{I} bond (d^8–s^0), which is often referred to as a platinum–silver dative bond. Although a typical entry to these complexes is the straightforward addition of a silver(I) salt or complex to a square-planar d^8 platinum complex, in some cases the expected Pt–Ag adducts do not form, and the reaction evolves with halogen (or pseudohalogen) abstraction by the platinum(II) centre.[5,32] In other cases, electron transfer processes occur, and the platinum–silver complex is an unstable intermediate that gives rise to an intramolecular redox reaction consisting of oxidation of the platinum centres and formation of metallic silver.[33–35]

In the course of our current research on platinum and palladium diphenylphosphanido derivatives, we have studied the behaviour of dinuclear complexes of the general formula $[(C_6F_5)_2M(\mu\text{-}PPh_2)_2M(L)(L')]^n$ (M = Pt, Pd) towards Ag^{I}. The results were strongly dependant on the L ligands, which are bonded to the Pt/Pd metal centres, and are summarized in Scheme 1 in which the white arrows indicate the part of the substrate that acts as a donor.

In the simplest cases, the dinuclear phosphanido complexes act as monodentate (Scheme 1, type **A** and **B** donors) or bidentate chelating (Scheme 1, type **C**) metal donor ligands towards the silver centre, and the final complexes display one or two M–Ag (M = Pt, Pd) bonds[36–38] for each dinuclear fragment. In a few other cases, a very unusual 3c–2e interaction between the M^{II}–(μ-P) bond of the phosphanido complex and the Ag^{I} centre is formed[38,39] (the dinuclear fragment acts as a type **D** donor, Scheme 1). In some cases, the reaction proceeds either with the elimination of AgX (X = Cl, Br, C_6F_5) from the palladium– and platinum–silver complexes[36,37,40,41] (Scheme 1, type **E**) or with the oxidation of the platinum(II) centre to plati-

[‡] Polynuclear Homo- or Heterometallic Palladium(II)–Platinum(II) Pentafluorophenyl Complexes Containing Bridging Diphenylphosphido Ligands, 33. Part 32: ref.[72]

[a] Departamento de Química Inorgánica, Instituto de Síntesis Química y Catálisis Homogénea-ISQCH, Universidad de Zaragoza-C.S.I.C.,
50009 Zaragoza, Spain
http://platinum.unizar.es
[b] Dipartimento DICATECh del Politecnico di Bari and Istituto CNR-ICCOM,
Via Orabona 4, 70125 Bari, Italy
http://www.dicatech.poliba.it/index.php?id=80&idp=208&ruolo=

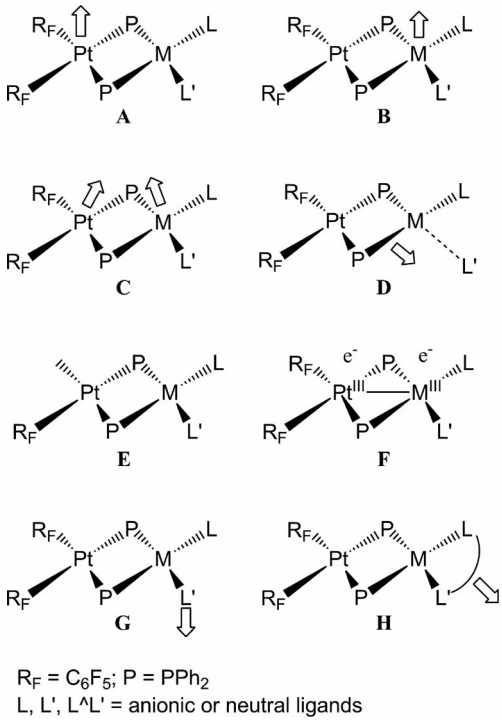

Scheme 1.

num(III) (Scheme 1, type **F**) and the consequent formation of metallic silver.[38,42–44] Finally, an example has been reported in which the L–L′ ligand of $[Ag_2\{Pt_2(\mu\text{-}PPh_2)_2(C_6F_5)_2(acac)\}_2]$ (acac = acetylacetonate) acts as donor towards the silver atom (Scheme 1, type **G** and **H**).[36] In our experience, the results obtained so far in these types of reactions indicate that it is impossible to predict the behaviour of a particular complex towards Ag^I.

Recently, we have reported the reactions of I_2 with $[NBu_4][(C_6F_5)_2Pt^{II}(\mu\text{-}PPh_2)_2M^{II}(C\text{^}N)]$[45] and $[NBu_4][(C_6F_5)_2Pt^{II}(\mu\text{-}PPh_2)_2M^{II}(O\text{^}N)]$[46] [M = Pt, Pd; C^N = benzoquinolinate (bq); O^N = 8-hydroxyquinolinate (hq), picolinate (pic)], which contain dinuclear asymmetric anionic complexes and a chelate ligand. In all cases, the addition of molecular I_2 to the complexes resulted in oxidation of the metal centre and the formation of M^{II}–M^{IV} intermediates, which evolved through a PPh_2/C^N or PPh_2/O^N reductive coupling with the formation of new M^{II}–M^{II} compounds.

In this paper, we report the results obtained in the reactions of anionic complexes of platinum(II) and palladium(II) containing benzoquinolinate, 8-hydroxyquinolinate, tetrahydrothiophene (tht) and picolinate ligands with $[AgPPh_3(OClO_3)]$; these reactions were performed to establish the type of complex (**A**–**H**, Scheme 1) obtained when the different dinuclear phosphanido platinum or palladium fragments are reacted with Ag^I salts.

Results

Synthesis and Solid-State Structures

The addition of $[Ag(OClO_3)(PPh_3)]$ to CH_2Cl_2 solutions of $[NBu_4][(C_6F_5)_2Pt(\mu\text{-}PPh_2)_2M(hq)]$,[46] $[NBu_4][(C_6F_5)_2Pt(\mu\text{-}PPh_2)_2M(bq)]$,[45] $[NBu_4][(C_6F_5)_2Pt(\mu\text{-}PPh_2)_2M(pic)]$[46] (M = Pt, Pd) and $[NBu_4][(C_6F_5)_2Pt(\mu\text{-}PPh_2)_2Pt(C_6F_5)(tht)]$[47] results in the formation of the corresponding neutral adducts $[(C_6F_5)_2Pt(\mu\text{-}PPh_2)_2(\mu\text{-}AgPPh_3)M(bq)]$ (M = Pt, **1**; Pd, **2**), $[(C_6F_5)_2Pt(\mu\text{-}PPh_2)_2(\mu\text{-}AgPPh_3)M(hq)]$ (M = Pt, **3**; Pd, **4**), $[(C_6F_5)_2Pt(\mu\text{-}PPh_2)_2(\mu\text{-}AgPPh_3)Pt(C_6F_5)(tht)]$ (**5**) and $[(C_6F_5)_2Pt(\mu\text{-}PPh_2)_2M(pic\text{-}AgPPh_3)]$ (M = Pt, **6**; Pd, **7**) as yellow solids (Scheme 2).

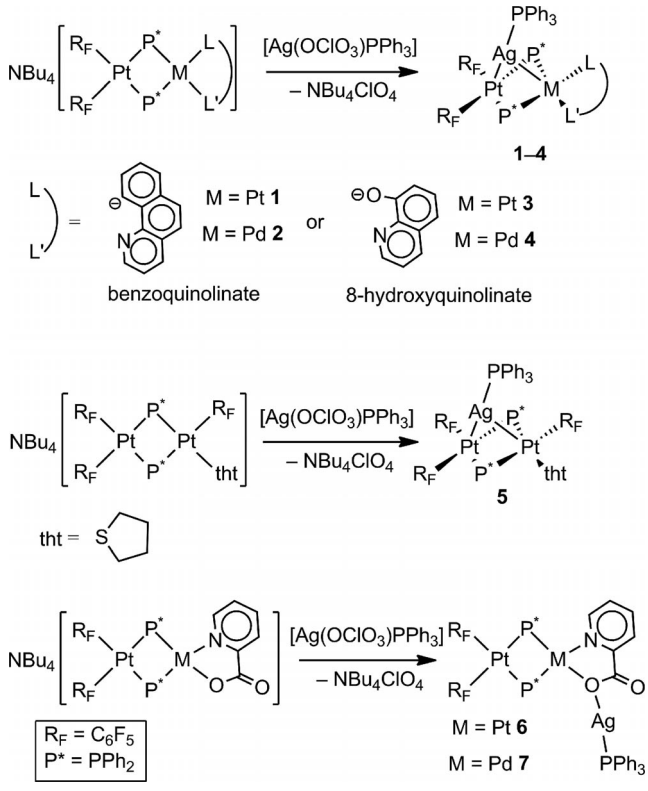

Scheme 2.

The structures of **1** and **3**–**7** were established by X-ray diffraction studies. Figures 1–6 show views of the corre-

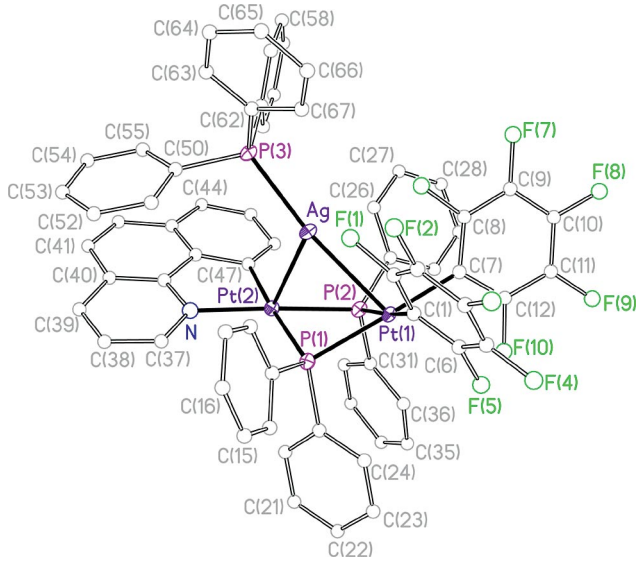

Figure 1. View of the molecular structure of **1**.

sponding complexes, and Tables 1–6 list relevant bond lengths and angles. The six studied compounds are trinuclear PtMAg (M = Pt, Pd) complexes; however, although **1**, **3**, **4** and **5** display two M–Ag bonds and show a **C**-type structure (Scheme 1), complexes **6** and **7** do not display M–Ag bonds, and the ilver centre is bonded to one of the oxygen atoms of the picolinate ligand (Scheme 1, type **G**).

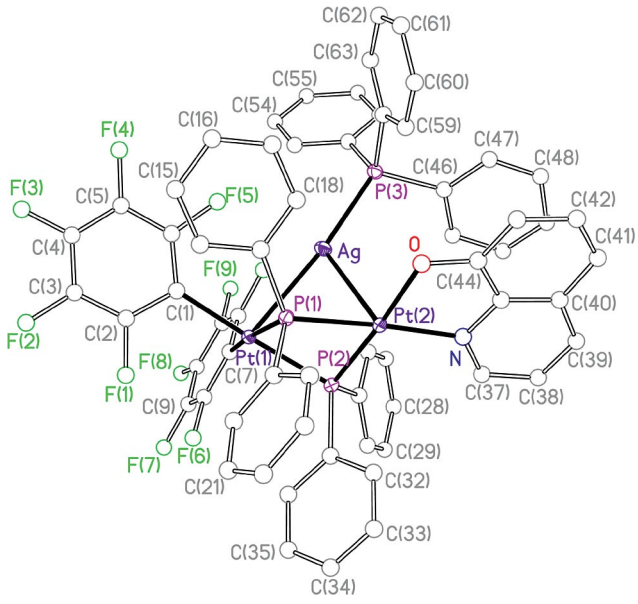

Figure 2. View of the molecular structure of **3**.

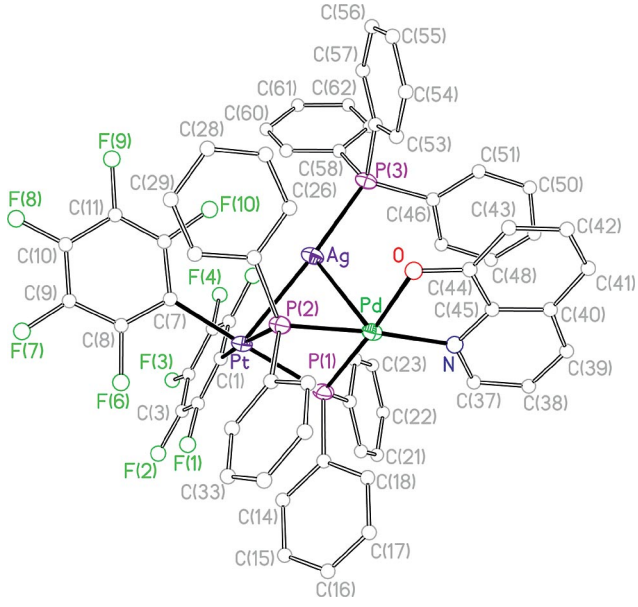

Figure 3. View of the molecular structure of **4**.

The structures of **1**, **3**, **4** and **5** are similar. In all four cases, the complexes can be regarded as the union of two subunits: "$(C_6F_5)_2Pt(\mu\text{-}PPh_2)_2M(E\text{^}N)$" (M = Pt, Pd; E = C, O) and "$AgPPh_3$" through Pt–Ag and Pd–Ag bonds. The Pt or Pd atoms are at the centres of square-planar coordination environments, which share an edge formed by the P atoms of the two phosphanide bridging ligands. One of the

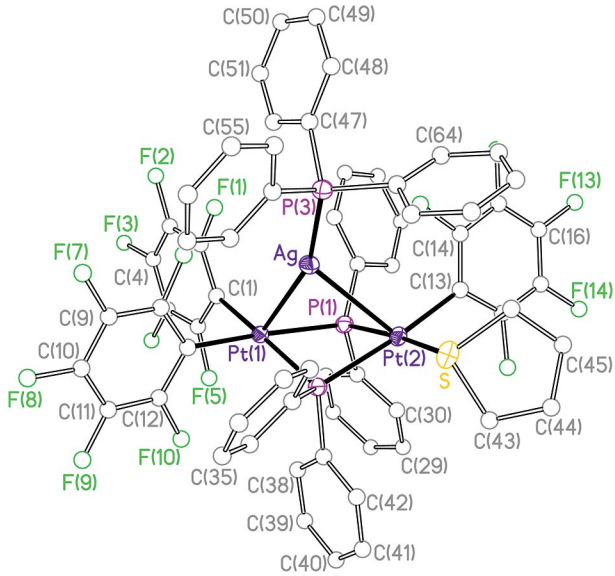

Figure 4. View of the molecular structure **5**.

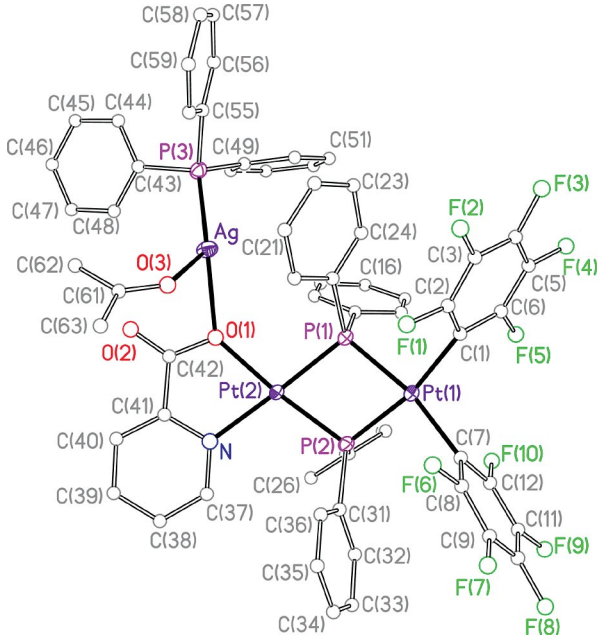

Figure 5. View of the molecular structure of **6′**.

metal atoms, Pt in all cases, completes its coordination sphere with two C atoms of the two mutually *cis* pentafluorophenyl ligands. The other metal centre [Pt(2) in **1** and **3** or Pd in **4**] is bonded to a planar bidentate C^N (benzoquinolinate, **1**) or O^N (8-hydroxyquinolinate, **3** and **4**) ligand coordinated in a chelate mode. In **1**, **3** and **4**, the chelate ligands are coplanar with the best Pt(2) or Pd coordination plane. In **5**, the Pt(2) atom completes its coordination sphere with a pentafluorophenyl ligand and a neutral tetrahydrothiophene ligand. The Pt···Pt or Pt···Pd distances, which range from 3.408(1) to 3.472(1) Å, are long enough to discard any interactions between the Pt and Pd centres.[48–53] In each complex, the dihedral angles between

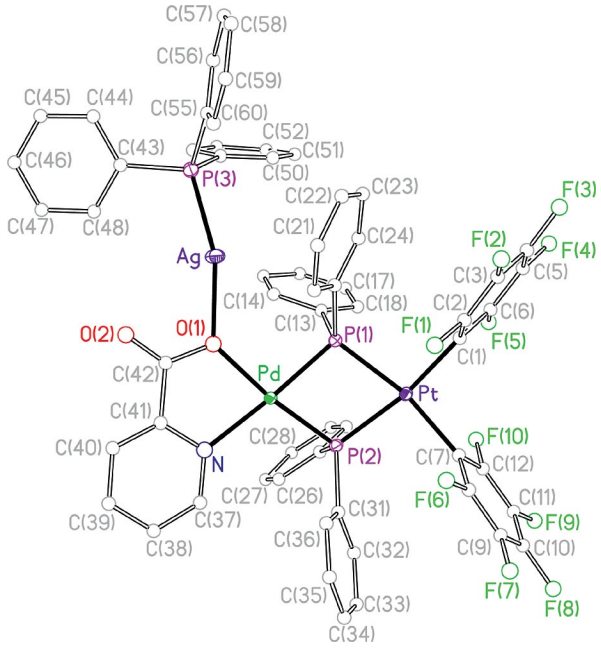

Figure 6. View of the molecular structure of **7**·CH_2Cl_2. The solvent molecule has been omitted for clarity.

Table 1. Selected bond lengths [Å] and angles [°] for **1**.

Pt(1)–C(7)	2.070(3)	Pt(1)–C(1)	2.088(3)
Pt(1)–P(2)	2.2984(8)	Pt(1)–P(1)	2.3225(9)
Pt(1)–Ag	2.8426(3)	Pt(2)–C(47)	2.052(3)
Pt(2)–N	2.092(3)	Pt(2)–P(2)	2.2787(9)
Pt(2)–P(1)	2.3870(9)	Pt(2)–Ag	2.8188(3)
Ag–P(3)	2.4321(9)		
C(7)–Pt(1)–C(1)	87.11(12)	C(7)–Pt(1)–P(2)	94.12(9)
C(1)–Pt(1)–P(2)	174.75(9)	C(7)–Pt(1)–P(1)	170.02(9)
C(1)–Pt(1)–P(1)	102.87(9)	P(2)–Pt(1)–P(1)	75.95(3)
C(47)–Pt(2)–N	80.64(12)	C(47)–Pt(2)–P(2)	101.14(9)
N–Pt(2)–P(2)	177.65(9)	C(47)–Pt(2)–P(1)	176.05(9)
N–Pt(2)–P(1)	103.19(8)	P(2)–Pt(2)–P(1)	75.06(3)
P(3)–Ag–Pt(2)	116.61(2)	P(3)–Ag–Pt(1)	168.35(2)
Pt(2)–Ag–Pt(1)	74.885(7)		

Table 2. Selected bond lengths [Å] and angles [°] for **3**.

Pt(1)–C(1)	2.0682(18)	Pt(1)–C(7)	2.0700(19)
Pt(1)–P(1)	2.3063(5)	Pt(1)–P(2)	2.3074(5)
Pt(1)–Ag	2.8163(2)	Pt(2)–O	2.0781(13)
Pt(2)–N	2.0875(16)	Pt(2)–P(2)	2.2757(5)
Pt(2)–P(1)	2.2907(5)	Pt(2)–Ag	2.8337(2)
Ag–P(3)	2.4086(5)		
C(1)–Pt(1)–C(7)	87.36(7)	C(1)–Pt(1)–P(1)	99.26(5)
C(7)–Pt(1)–P(1)	171.49(6)	C(1)–Pt(1)–P(2)	174.02(5)
C(7)–Pt(1)–P(2)	98.57(5)	P(1)–Pt(1)–P(2)	74.759(17)
O–Pt(2)–N	80.30(6)	O–Pt(2)–P(2)	176.24(4)
N–Pt(2)–P(2)	103.12(5)	O–Pt(2)–P(1)	101.02(4)
N–Pt(2)–P(1)	176.03(5)	P(2)–Pt(2)–P(1)	75.668(17)
P(3)–Ag–Pt(1)	168.784(14)	P(3)–Ag–Pt(2)	115.922(13)
Pt(1)–Ag–Pt(2)	74.505(4)		

the best least-squares planes of both Pt centres (**1**, **3** and **5**) or the Pt and Pd centres (**4**) are 40.7(1), 39.9(1), 39.9(1) and 35.7(1)° (for **1**, **3**, **4** and **5**, respectively) and result in an "open-book" framework. The silver centre is located in the inner side of the book and is bonded to the two Pt atoms

Table 3. Selected bond lengths [Å] and angles [°] for **4**.

Pt–C(7)	2.057(7)	Pt–C(1)	2.087(8)
Pt–P(2)	2.303(2)	Pt–P(1)	2.305(2)
Pt–Ag	2.7723(7)	Pd–O	2.076(5)
Pd–N	2.093(6)	Pd–P(1)	2.291(2)
Pd–P(2)	2.292(2)	Pd–Ag	2.8458(9)
Ag–P(3)	2.407(2)		
C(7)–Pt–C(1)	86.2(3)	C(7)–Pt–P(2)	99.8(2)
C(1)–Pt–P(2)	172.4(2)	C(7)–Pt–P(1)	175.4(2)
C(1)–Pt–P(1)	98.4(2)	P(2)–Pt–P(1)	75.58(7)
O–Pd–N	80.6(2)	O–Pd–P(1)	175.97(16)
N–Pd–P(1)	103.02(19)	O–Pd–P(2)	100.52(16)
N–Pd–P(2)	174.8(2)	P(1)–Pd–P(2)	76.05(8)
P(3)–Ag–Pt	170.57(6)	P(3)–Ag–Pd	113.09(6)
Pt–Ag–Pd	74.68(2)		

Table 4. Selected bond lengths [Å] and angles [°] for **5**.

Pt(1)–C(7)	2.069(3)	Pt(1)–C(1)	2.086(4)
Pt(1)–P(2)	2.3140(9)	Pt(1)–P(1)	2.3144(9)
Pt(1)–Ag	2.7517(3)	Pt(2)–C(13)	2.068(3)
Pt(2)–P(1)	2.2953(10)	Pt(2)–P(2)	2.3276(9)
Pt(2)–S	2.3623(10)	Pt(2)–Ag	2.8889(3)
Ag–P(3)	2.4041(15)		
C(7)–Pt(1)–C(1)	89.44(13)	C(7)–Pt(1)–P(2)	96.08(9)
C(1)–Pt(1)–P(2)	171.68(10)	C(7)–Pt(1)–P(1)	171.64(10)
C(1)–Pt(1)–P(1)	98.74(9)	P(2)–Pt(1)–P(1)	75.98(3)
C(13)–Pt(2)–P(1)	92.86(11)	C(13)–Pt(2)–P(2)	168.93(11)
P(1)–Pt(2)–P(2)	76.08(3)	C(13)–Pt(2)–S	94.56(11)
P(1)–Pt(2)–S	172.40(3)	P(2)–Pt(2)–S	96.50(3)
P(3)–Ag–Pt(1)	161.15(3)	P(3)–Ag–Pt(2)	122.77(2)
Pt(1)–Ag–Pt(2)	75.951(8)		

Table 5. Selected bond lengths [Å] and angles [°] for **6′**.

Pt(1)–C(7)	2.072(3)	Pt(1)–C(1)	2.080(3)
Pt(1)–P(1)	2.2889(8)	Pt(1)–P(2)	2.2944(8)
Pt(2)–O(1)	2.114(2)	Pt(2)–N	2.129(3)
Pt(2)–P(2)	2.2500(8)	Pt(2)–P(1)	2.2656(8)
Ag–O(1)	2.307(2)	Ag–P(3)	2.3608(9)
Ag–O(3)	2.424(2)	O(2)–C(42)	1.228(4)
C(7)–Pt(1)–C(1)	97.14(12)	C(7)–Pt(1)–P(1)	167.79(9)
C(1)–Pt(1)–P(1)	94.57(9)	C(7)–Pt(1)–P(2)	94.15(9)
C(1)–Pt(1)–P(2)	167.89(9)	P(1)–Pt(1)–P(2)	73.93(3)
O(1)–Pt(2)–N	77.97(9)	O(1)–Pt(2)–P(2)	174.15(6)
N–Pt(2)–P(2)	107.25(7)	O(1)–Pt(2)–P(1)	99.66(6)
N–Pt(2)–P(1)	176.73(7)	P(2)–Pt(2)–P(1)	75.23(3)
O(1)–Ag–P(3)	140.55(6)	O(1)–Ag–O(3)	80.78(8)
P(3)–Ag–O(3)	132.98(7)		

Table 6. Selected bond lengths [Å] and angles [°] for **7**·CH_2Cl_2.

Pt–C(1)	2.066(2)	Pt–C(7)	2.070(2)
Pt–P(1)	2.2786(6)	Pt–P(2)	2.2921(6)
Pd–O(1)	2.1161(15)	Pd–N	2.164(2)
Pd–P(1)	2.2638(6)	Pd–P(2)	2.2677(6)
Ag–O(1)	2.2192(16)	Ag–P(3)	2.3622(6)
O(1)–C(42)	1.298(3)	O(2)–C(42)	1.226(3)
C(1)–Pt–C(7)	95.20(9)	C(1)–Pt–P(1)	96.00(6)
C(7)–Pt–P(1)	167.98(7)	C(1)–Pt–P(2)	168.18(6)
C(7)–Pt–P(2)	94.24(7)	P(1)–Pt–P(2)	74.11(2)
O(1)–Pd–N	77.93(7)	O(1)–Pd–P(1)	98.10(5)
N–Pd–P(1)	175.96(5)	O(1)–Pd–P(2)	172.91(5)
N–Pd–P(2)	109.13(5)	P(1)–Pd–P(2)	74.86(2)
O(1)–Ag–P(3)	150.77(5)		

or to the Pt and Pd atoms. The Pt/Pd–Ag bond lengths are in the range 2.7723(7)–2.8889(3) Å (see Tables 1–4), which are similar to the bond lengths in other complexes with analogous Pt^{II}–Ag^{I} bonds.[14,17,29,38,54] The silver centre of each complex completes its trigonal coordination environment with the phosphorus atom of the triphenylphosphane ligand. The Pt, M (Pt or Pd), Ag and P(3) atoms are coplanar, the trigonal environment of the Ag atom is unsymmetrical, and the Pt(1)–Ag–P(3) angle [161.15(3)–170.57(6)°, see Tables 1–4] is greater than the Pt(2)/Pd–Ag–P(3) angle [113.09(6)–122.72(4)°, see Tables 1–4]. The difference between these two angles for **1**, **3** and **4** is ca. 55°, whereas this value is lower in **5** (38°). Thus, the "$AgPPh_3$" fragment coordinates to the dinuclear platinum fragment in an asymmetric way and leans toward the planar chelate ligand (**1**, **3** and **4**), which is the less-crowded region. For **5**, the two ligands bonded to Pt(2) are C_6F_5 and tetrahydrothiophene, the environment of Pt(2) is more encumbered than in **1**, **3** and **4**, and the difference between the values of the two Pt–Ag–P(3) angles is minor. Finally, in **1**, **3**, **4** and **5**, some short *o*-F–Ag distances are present in the 2.774(2)–3.001(2) Å range, which indicate the existence of *o*-F···Ag dative contacts in the solid state.[14,55]

Crystals of **1**, **3**, **4**, **5** and **7** suitable for X-ray studies were grown in CH_2Cl_2 solutions, but we were unable to grow crystals of **6** in CH_2Cl_2 solutions. Crystals of **6** were grown in acetone, and the crystals obtained were **6** with an additional acetone molecule coordinated to the silver centre (in the following **6′**). Therefore, the structures of **6′** and **7** are very similar (at least the main structural facts) but with a different environment of the Ag centres.

The structures of **6′** and **7** are different from the structure of **1**, **3**, **4** and **5**. Figures 5 and 6 show views of **6′** and **7**, and Tables 5 and 6 list relevant bond lengths and angles. Although the complexes are also the result of the interactions between the $[(C_6F_5)_2Pt(\mu\text{-}PPh_2)_2M(pic)]^-$ anion and the $[AgPPh_3]^+$ cation, both fragments are exclusively connected through a Ag–O(1) bond and no Pt or Pd···Ag interactions are observed. No interactions between the other oxygen atom of the picolinate ligand O(2) are observed in either case [the Ag–O(2) distance is 2.961(2) Å in **6′** and 2.962(2) Å in **7**]. As we have commented before, the silver environment is different in each complex. In **6′** the silver centre is three-coordinate because of the presence of a molecule of acetone as a ligand and displays a nearly planar T-shaped distorted environment with angles of 140.55(6) [P(3)–Ag–O(1)], 132.98(7) [P(3)–Ag–O(3)] and 80.78(8)° [O(1)–Ag–O(3)]. The silver centre is 0.299(1) Å out of the plane defined by P(3), O(1) and O(3). The silver centre in **7** is dicoordinated, and the P(3)–Ag–O(1) angle is 150.77(5)°. The Ag–O(1) distances are different [2.307(2) Å in **6′** and 2.219(2) Å in **7**] probably because of the different coordination number of the silver centre in the two complexes. The coordination environment of O(1) is planar in both cases, and the sums of the bond angles around the O(1) atom are 359.97 and 359.33°, respectively. The Ag–P(3) distances are similar in both complexes [2.3608(9) and 2.3622(6) Å, respectively] and slightly shorter than the Ag–P(3) distances in **1** and **3**–**5** (Tables 1–4). Concerning the structure of the rest of the molecule, that is, the "$(C_6F_5)_2Pt(\mu\text{-}PPh_2)_2$-Pd(pic)" fragments, they are similar to the analogous fragment present in **1**, **3** and **4**. Thus, the two metal square-planar coordination environments share an edge defined by the two P atoms of the PPh_2 ligands, and the dihedral angles between the best least-square planes of the Pt and Pd atoms are 29.1(1) (M = Pt, **6′**) and 30.2(1)° (M = Pd, **7**), that is, these fragments can be also described as an "open-book" framework with very similar interplanar angles. Although one should think that the "open-book" structure is favoured to facilitate the Pt–Ag interactions, the structures of **6′** and **7** demonstrate that the Pt–Ag interactions do not seem to play a decisive role in this fact.

Solution Behaviour

The solution behaviour of the Ag^{I} adducts **1**–**7** was studied by multinuclear NMR spectroscopy at various temperatures, and the ^{31}P and ^{195}Pt NMR features of **1**–**7** are collected in Table 7. In all cases, the $^{31}P\{^1H\}$ NMR spectra of **1**–**7** at 298 K showed two mutually coupled doublets in the region δ = –125 to –60 ppm owing to the bridging phosphanides P^1 and P^2 (see Table 7), along with a complex signal at lower fields (δ = 4–16 ppm) ascribable to the Ag-bonded PPh_3 ligand. The chemical shifts of P^1 and P^2 are typical for bridging PPh_2 groups involved in four-membered P–M–P–M rings that do not subtend metal–metal bonds.[56] The $^2J_{P,P}$ coupling constants are higher for the Pt–Pd systems than for the Pt–Pt ones, and the signal attributed to the Ag-bonded P^3Ph_3 ligand consists of the superimposition of the doublets owing to coupling of P^3 with ^{107}Ag and ^{109}Ag nuclei. The ^{31}P–^{107}Ag coupling constants range from 629 to 713 Hz, whereas those between ^{31}P and ^{109}Ag range from 723 to 822 Hz.

All ^{31}P NMR signals are quite broad at room temperature owing to unresolved small couplings with the ^{19}F atoms of the pentafluorophenyl rings as well as to dynamic processes.

The $^{195}Pt\{^1H\}$ NMR spectra of **1**–**4** showed very broad signals for the platinum atom bonded to the C_6F_5 rings (Pt^1) owing to multiple couplings with ^{19}F and $^{107/109}Ag$ atoms. The signals of the other platinum atom (Pt^2) were sharper and fell at δ = –3426 and –3177 ppm for **1** and **3**, respectively. The $^{195}Pt\{^1H\}$ NMR spectrum of **1** at 268 K is shown in Figure 7 and shows the very broad signal at δ = –3337 ppm, ascribed to Pt^1, and the complex pattern of the Pt^2 signal owing to the coupling of $^{195}Pt^2$ nuclei with ^{31}P (2378, 1089 and 280 Hz), $^{107/109}Ag$ (227 and 261 Hz) and $^{195}Pt^1$ nuclei (ca. 400 Hz).

The ^{195}Pt NMR signals of **5** were smoothly obtained by recording a ^{19}F–^{195}Pt heteronuclear multiple quantum coherence (HMQC) spectrum at low temperature (Figure 8) and exploiting the scalar coupling of each Pt atom with a *o*-F atom of the pentafluorophenyl ring. The Pt^1 chemical shift (δ = –3337 ppm) is similar to those of the other complexes described in this study, whereas the chemical shift of

Pt^2 (δ = –3655 ppm) was high-field shifted with respect to those of the corresponding Pt^2 atoms bearing bq (δ = –3426 ppm) or hq (δ = –3177 ppm) ligands (Table 7). A comparison of the ^{195}Pt chemical shifts of the starting materials (Pt^1 δ = ca. –3900 ppm, Pt^2 δ = –3450 to –3717 ppm for **1**–**4**;[45,46] Pt^1 δ = –3821 ppm, Pt^2 δ = –3911 ppm for **5**) with those of the adducts **1**–**5** shows that in all cases the addition of the $[AgPPh_3]^+$ group resulted in a strong deshielding of the ^{195}Pt centre, in accord with the donor behaviour of the Pt atoms in molecules with Pt–Ag bonds.

As far as the picolinate complexes are concerned, the ^{195}Pt NMR signals of **6** were found (at 243 K) at δ = –3335 (Pt^1) and–3275 ppm (Pt^2), whereas the ^{195}Pt NMR signal of **7** was found (at 243 K) at δ = –3920 ppm (Pt^1). The great difference in chemical shift between Pt^1 of **7** and Pt^1 of **1**–**5** suggests that the chemical environment around Pt^1 in **7** is different from those in **1**–**5**. This is quite reasonable if the solution structure of **7** is analogous to that obtained from XRD studies for **7**, that is, if the $[AgPPh_3]^+$ moiety is bonded to the picolinate oxygen atom. The ^{195}Pt chemical

Table 7. ^{31}P and ^{195}Pt NMR parameters[a] of **1**–**10** in CD_2Cl_2 solution (T = 298 K).

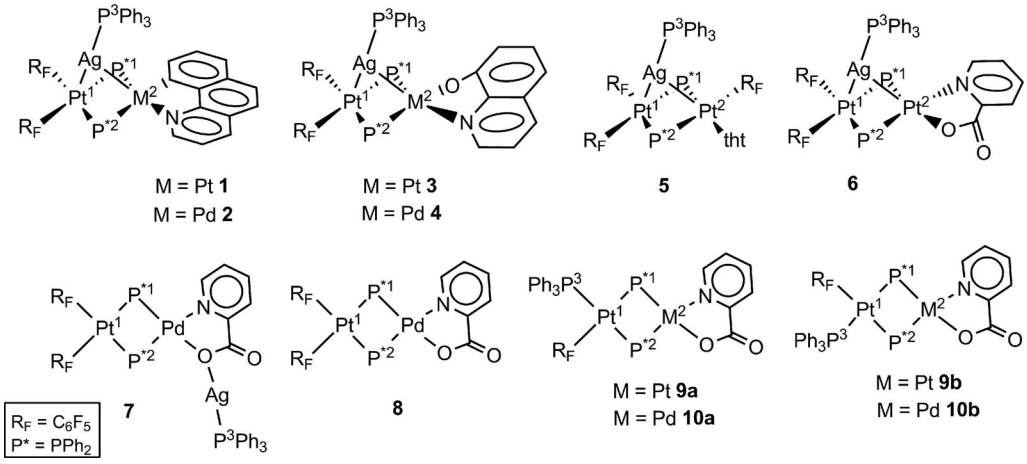

Complex	δP^1	δP^2	δP^3	$^1J_{P^3,^{107}Ag}$	$^1J_{P^3,^{109}Ag}$	$^2J_{P^1,P^2}$	$^1J_{P^1,Pt^1}$	$^1J_{P^1,Pt^2}$	$^1J_{P^2,Pt^1}$	$^1J_{P^2,Pt^2}$	δPt^1	δPt^2
1	–88.0	–93.3	4.0	630	726	57	1478	2378	1254	1089	–3337[b]	–3426[b]
2	–60.2	–98.3	7.5	629	723	86	1359	–	1184	–	–3315	–
3	–124.5	–119.7	8.8	653	752	100	1465	2094	1506	2070	–3351[c]	–3177[c]
4	–104.7	–102.4	11.8	667	772	150	1387	–	1436	–	–3438	–
5[c]	–110.6	–125.2	7.7	701	806	81	1423	2031	1292	1412	–3337	–3655
6	–122.2	–127.1	9.2	664	764	102	1481	2271	1473	2113	–3335[d]	–3275[d]
7	–108.5	–111.3	16.6	713	822	193	1644	–	1613	–	–3920[d]	–
8[e]	–121.5	–125.6		–	–	220	1766	–	1737	–	–3905	–
9a	–135.2	–126.2	22.0[f]	–	–	160	1773	2635	1964	2752	–4200	–3502
9b	–134.2	–146.2	22.8[g]	–	–	164	1979	2800	1661	2470	–4200	–3541
10a	–114.6	–110.5	19.9[h]	–	–	213	1666	–	1776	–	–4240	–
10b	–116.2	–127.2	20.1[i]	–	–	221	1822	–	1614	–	–4250	–

[a] δ in ppm, J in Hz. [b] $^1J_{Pt^2,Ag} \approx 250$ Hz, $^2J_{Pt^1,Pt^2} \approx 400$ Hz, $^2J_{P^3,Pt^2} = 280$ Hz; T = 268 K. [c] At 213 K. [d] At 243 K. [e] From ref.[46] [f] $J_{P^3,P^2} = 349$ Hz; $J_{P^3,Pt} = 2255$ Hz. [g] $J_{P^3,P^1} = 345$ Hz; $J_{P^3,Pt} = 2245$ Hz. [h] $J_{P^3,P^2} = 326$ Hz; $J_{P^3,Pt} = 2304$ Hz. [i] $J_{P^3,P^1} = 336$ Hz; $J_{P^3,Pt} = 2298$ Hz.

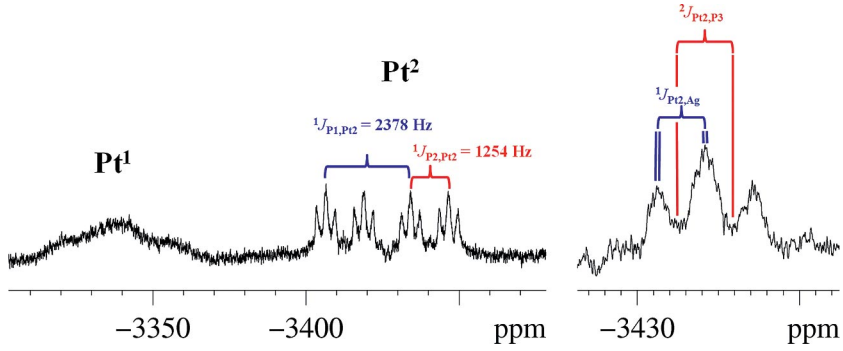

Figure 7. $^{195}Pt\{^1H\}$ NMR spectrum of **1** (CD_2Cl_2, 268 K).

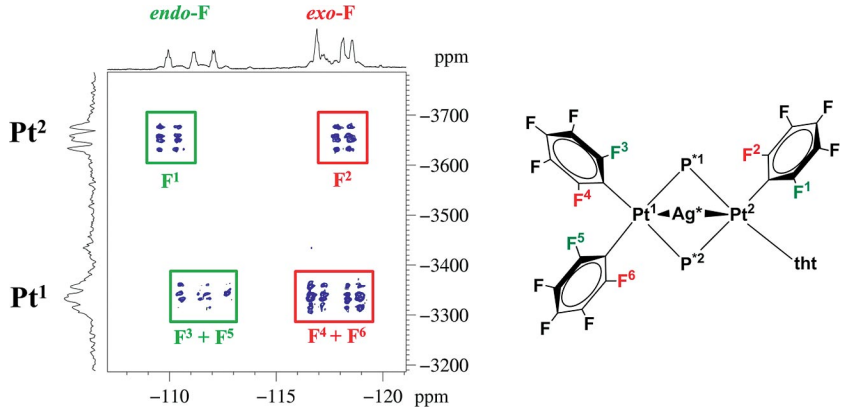

Figure 8. Portion of the ^{19}F–^{195}Pt HMQC spectrum of **5** (*ortho*-F region). ^{195}Pt decoupling was not applied during acquisition. Ag* = $Ag(PPh_3)$; P* = PPh_2. Solvent: CD_2Cl_2; T = 213 K.

shift of $[(C_6F_5)_2Pt(\mu\text{-}PPh_2)_2Pd(N\text{^}O\text{-}pic)]$ (**8**, the precursor of **7**), in which the Pt atom displays a chemical environment similar to that of **7**, falls at δ = –3905 ppm (Table 7).[57]

The chemical shift for Pt^1 for **6** is expected at $\delta \approx$ –3900 ppm if the $[AgPPh_3]^+$ moiety is bonded to the picolinate oxygen atom and $\delta \approx$ –3300 ppm if the $[AgPPh_3]^+$ moiety bridges the platinum atoms. The found values of δ = –3335 ppm for Pt^1 and δ = –3275 ppm for Pt^2 suggest that the solution structure of **6** is similar to those of **1**–**5**, that is, it has a bridging $[AgPPh_3]^+$ moiety. This hypothesis has been confirmed by the variable-temperature (VT) ^1H and ^{19}F NMR solution spectra of **6**, vide infra.[58]

The ^1H NMR analysis of **1**–**7** was performed by VT ^1H NMR, ^1H–^{31}P HMQC, ^1H COSY and ^1H NOESY–EXSY experiments.

The ^1H NMR spectrum of **1** at 298 K showed sharp signals for the protons of the benzoquinolinate and PPh_3 ligands, together with very broad signals near the baseline for the protons of the μ-PPh_2 ligands. The ^1H NMR features exhibited by **1** are indicative of a dynamic process. As ascertained by a ^1H exchange spectroscopy (EXSY) experiment (Figure 9), only the signals of the benzoquinolinate protons are not affected by such a process.

At 268 K, the phenyl protons of the μ-PPh_2 ligands started to emerge from the baseline and became sharp at 238 K. The attribution of all protons of the molecule was made on the basis of the ^1H COSY and ^1H NOESY experiments and is reported in the Experimental Section. At 268 K, the ^1H–^{31}P HMQC spectrum showed only cross-peaks between P^3 and the *ortho* protons of the PPh_3 ligand. The phenyl ring bonded to the bridging phosphanides are inequivalent at or below 268 K: for example, the phenyl rings Ph^A and Ph^B bonded to P^1 gave signals for the *ortho*-H at δ = 7.89 and 7.28 ppm, respectively, whereas the phenyl rings Ph^C and Ph^D bonded to P^2 gave signals for the *ortho*-H at δ = 7.80 and 7.34 ppm, respectively [the attribution of *ortho*-H signals to each phenyl ring was made on the basis of the ^{19}F–^1H heteronuclear Overhauser effect (HOESY) spectrum at 268 K, vide infra].

The ^1H EXSY spectrum of **1** at 268 K (Figure 10) showed exchange cross-peaks between the protons of Ph^A and those of Ph^B as well as between Ph^C and Ph^D (Scheme 3). Such exchanges can be explained in terms of a dynamic process consisting of the motion of the $[AgPPh_3]^+$ moiety, which passes from the top to the bottom part of

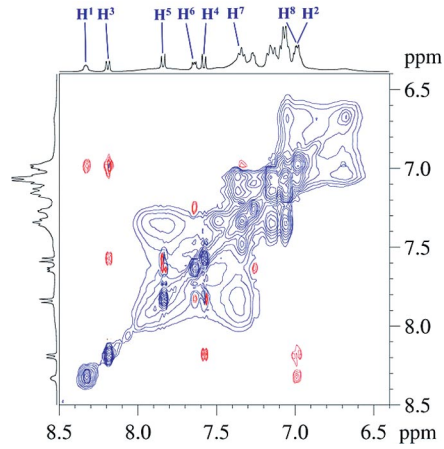

Figure 9. Portion of the ^1H EXSY spectrum of **1** at 298 K (CD_2Cl_2).

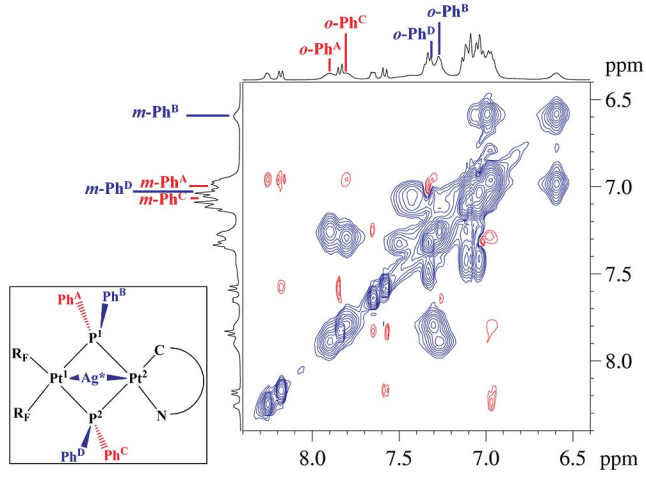

Figure 10. Portion of the ^1H EXSY spectrum of **1** showing the Ph^A/Ph^B and Ph^C/Ph^D exchanges (CD_2Cl_2, 268 K). Ag* = $Ag(PPh_3)$.

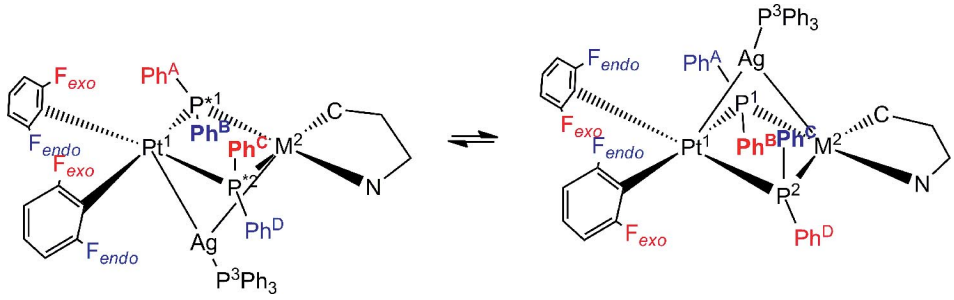

Scheme 3. Plausible dynamic process explaining the exchange of phenyl rings bonded to the μ-P atoms of **1** through the rupture of Ag–$M^{1/2}$ bonds. The same process also occurs for **2**–**5**.

the complex, as shown in Scheme 3. The proposed dynamic process can be held responsible for the absence of cross-peaks in the ^1H–^{31}P HMQC spectrum at 268 K between $P^{1/2}$ and the phenyl rings $Ph^{A–D}$.

The ^1H NMR features of **2** are similar to those of **1**, which indicates that the $[AgPPh_3]^+$ moiety in **2** also displays dynamic behaviour. In addition to the signals of the 8-hydroxyquinolinate and PPh_3 ligands, the ^1H NMR spectra of **3** and **4** at 298 K showed one set of signals for the phenyl rings bonded to P^1 and one set for the phenyl rings bonded to P^2. The chemical equivalence of the Ph rings bonded to the same μ-P atom, notwithstanding the asymmetry induced by the presence of the bridging $[AgPPh_3]^+$ moiety, suggests that for the 8-hydroxyquinolinate adducts **3** and **4**, the $AgPPh_3$ motion shown in Scheme 3 is very fast on the NMR timescale. At 213 K, all signals became broad, presumably because for these complexes the motion of the $AgPPh_3$ remains fast also at low *T*.

The behaviour of **5** was similar to that of **1** and **2**, in the sense that only the tht and PPh_3 protons were distinguishable in the ^1H NMR spectra at 298 K, whereas sharp signals that permitted differentiation of the protons bonded to the four phenyl rings were present in the low *T* (213 K) ^1H NMR spectrum. The ^1H EXSY spectrum at 213 K revealed that the phenyl rings bonded to the same P atom still exchange with each other, which indicates that, for **5**, the $AgPPh_3$ motion is fast at 298 K and slow (but not blocked) at 213 K.

In addition to the signals attributable to the picolinate protons, the ^1H NMR spectrum of **6** at 298 K showed one set of signals for the protons of the phenyl rings bonded to P^1 and one set of signals for the protons of the phenyl rings bonded to P^2. These phenyl protons became very broad at 200 K, which suggests that a solution structure with the $AgPPh_3$ moiety bonded to the picolinate oxygen atom is unlikely. Conversely, a structure similar to those of **1**–**5** (i.e., with the bridging $[AgPPh_3]^+$ moiety) is more plausible. The alleged dynamic behaviour exhibited by **6** is analogous to that exhibited by **3** and **4**, that is, it is characterized by a very fast movement of the $AgPPh_3$ moiety from the top to the bottom part of the molecule at room temperature and a fast motion at low *T*.

In addition to the signals attributable to the picolinate protons, the ^1H NMR spectrum of **7** at 298 K showed one set of signals for the protons of the phenyl rings bonded to P^1 and one set of signals for the protons of the phenyl rings bonded to P^2. These signals became broader at 203 K but did not split into four sets of phenyl signals, one for each Ph ring bonded to μ-P.

The ^1H EXSY spectrum of **7** at 298 K revealed exchange between the phenyl rings bonded to P^1 and the phenyl rings bonded to P^2, which indicates a dynamic behaviour different from that observed for **1**–**6**. The most plausible explanation is the exchange of position of the N and O atoms bonded to Pd possibly by detachment and rebinding of the O–$AgPPh_3$ bond, as shown in Scheme 4.

The fluxionality of the pic-O–$AgPPh_3$ moiety was confirmed by the ^{31}P EXSY spectrum at 298 K and the ^{19}F EXSY spectra, which showed exchange between P^1 and P^2 and between the two C_6F_5 rings, respectively.[59]

The ^{19}F NMR spectra of **1**–**7** are in agreement with the occurrence of the specific dynamic processes described above, as the pentafluorophenyl rings are almost perpendicular to the coordination plane of the Pt atom to which they are bonded and their rotation is already hindered at room temperature. The following discussion is restricted to the diagnostic *ortho*-F atoms, and a full assignment of all ^{19}F signal (at 298 K and low *T*) is reported in the Experimental Section. At 200 K, the *ortho*-F atoms of **1** give four signals at δ = –111.1, –111.9, –117.2 and –118.0 ppm with $^3J_{F,Pt}$

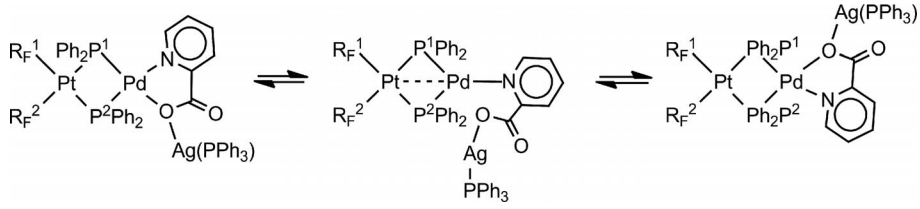

Scheme 4. Plausible dynamic process explaining the exchange in solution for **7** of μ-P^1Ph_2 with μ-P^2Ph_2 and of R_F^1 with R_F^2.

coupling constants of 440, 415, 275 and 255 Hz, respectively. At 298 K, two broad signals at δ = –111.8 and –117.5 ppm were observed. As the $AgPPh_3$ motion is slowed down (or even blocked) at 200 K, the four observed signals at that temperature can be ascribed to the four inequivalent F atoms of the C_6F_5 rings, two *endo* F atoms (on the same side as the $AgPPh_3$ bridge, δ = –117.2 and –118.0 ppm) and two *exo* F atoms (on the opposite site with respect to the $AgPPh_3$ bridge, δ = –111.1 and –111.9 ppm).

At 298 K, the $AgPPh_3$ motion becomes fast, and as a result, all signals broaden and two broad peaks are observed, one for the *endo* F atoms, and the other for the *exo* F atoms. The attribution of the signals at δ = –117.2 and –118.0 ppm (or δ = –111.1 and –111.9 ppm) of **1** to *o*-F of different C_6F_5 rings was made on the basis of the ^{19}F EXSY spectrum at 268 K, which showed exchange cross-peaks between the signals at δ = –117.6 and –111.6 ppm and between the signals at δ = –118.2 and –112.1 ppm (Figure 11).

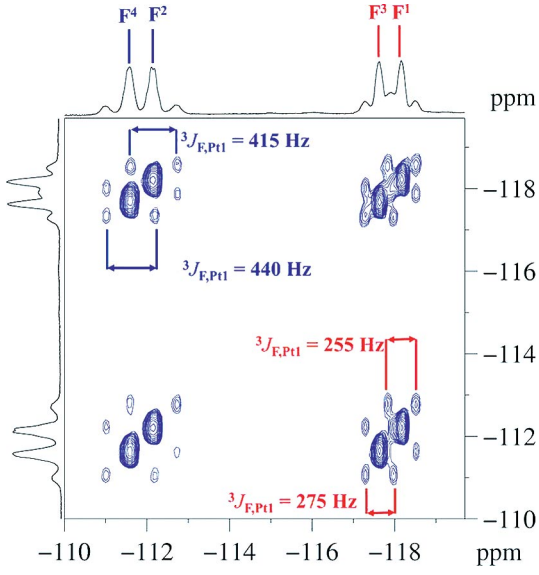

Figure 11. Portion of the ^{19}F EXSY spectrum of **1** showing the *ortho*-F region (CD_2Cl_2, 268 K, τ_m = 0.600 s).

The *exo* or *endo* position of the *o*-F atoms was ascertained by the ^{19}F–^{1}H HOESY spectrum at 238 K, which showed intense cross-peaks between the ^{19}F NMR signals at δ = –111.1 and –111.9 ppm with the ^{1}H signals at δ = 7.13 ppm, attributed to the phenyl rings bonded to P^3 (^{1}H–^{31}P HMQC), which indicates that the *o*-F signals at δ = –111.1 and –111.9 ppm lie on the same side of the $AgPPh_3$ moiety (i.e., they are in *endo* positions). These attributions indicate that the *endo* *o*-F atoms are characterized by a $^{3}J_{F,Pt}$ coupling constant that is sensibly higher than those of the *exo* ones (compare 440 and 415 Hz for the *endo* *o*-F atom with 275 and 255 Hz for the *exo* *o*-F atom). Differences in the coupling constants for *o*-F atoms of C_6F_5 rings bonded to Pt atoms have already been reported in many complexes.[14,60,61]

Interestingly, the ^{19}F–^{1}H HOESY spectrum at 268 K (Figure 12), a temperature at which the NOEs were enhanced with respect to those at 238 K and the *exo*-F/*endo*-F exchanges were frequent, showed NOE contacts between the signals of the *ortho* phenyl protons at δ_H = 7.80 ppm and the *ortho*-F atom at δ_F = –111.6 and –117.6 ppm (as well as between the signals of the *ortho* phenyl protons at δ_H = 7.89 ppm and the *ortho*-F atom at δ_F = –112.1 and –118.2 ppm), which indicates that the fluorine atoms at δ_F = –112.1 and –118.2 ppm belong to the C_6F_5 ring *cis* to P^1 (bearing the phenyl ring to which the *o*-H atoms at δ_H = 7.89 ppm belong), whereas the fluorine atoms at δ_F = –111.6 and –117.6 ppm belong to the C_6F_5 ring *cis* to P^2 (bearing the phenyl ring to which the *o*-H atoms at δ_H = 7.80 ppm belong). As the *o*-H atom at δ_H = 7.80 ppm showed a NOE contact with H^1 of the benzoquinolinate ligand, it can be inferred that the phenyl ring to which the *o*-H atoms at δ_H = 7.89 ppm belong is Ph^A and, consequently, that *o*-H at δ_H = 7.80 ppm belongs to Ph^C (see sketches in Figure 12).

A similar behaviour was observed for **2**.

In the case of **3**, in which the $AgPPh_3$ motion was very fast at 298 K and still fast at 200 K, the ^{19}F NMR spectra at 298 K showed two signals, each of which is attributed to the *o*-F atoms belonging to the same C_6F_5 ring. At 200 K, the spectrum showed three peaks: two broad signals at δ = –113.6 and –114.5 ppm with $^{3}J_{F,Pt}$ coupling constants of 630 and 626 Hz, respectively, ascribable to two *endo* *o*-F atoms (on the basis of the large $^{3}J_{F,Pt}$ value), plus a broad signal centred at δ = –118.0 ppm owing to the partial overlap of the remaining two *o*-F signals.

The ^{19}F NMR spectrum of **4** at 298 K is similar to that of **3** at the same temperature, and in this case also shows two sharp (averaged) resonances for the *o*-F atoms of the two C_6F_5 rings at δ = –115.9 and –116.4 ppm. At 200 K, the signals broadened but did not resolve into four different peaks.

The ^{19}F NMR spectrum of **5** is more complicated owing to the presence of three pentafluorophenyl rings, which are affected by the $AgPPh_3$ fluxionality. Thus, two very broad signals are present in the ^{19}F NMR spectrum at 298 K, ascribable to *endo* or *exo* *o*-F atoms, whereas six resolved signals centred at δ = –109.9, –111.1, –112.1, –116.9, –118.2 and –118.5 ppm were present in the ^{19}F NMR spectrum at 200 K.

In the ^{19}F NMR spectrum of the Pt–Pt complex **6** at 298 K, the signals of the *o*-F atoms in *endo* and *exo* positions were isochronous and gave rise to a peak at δ = –118.5 ppm,[62] whereas the spectrum recorded at 200 K showed four distinct peaks, two for the *endo* *o*-F atom at δ = –111.4 and –112.2 ppm with $^{3}J_{F,Pt}$ coupling constants of 443 and 435 Hz, respectively, and two for the *exo* *o*-F atom at δ = –117.4 and –118.3 ppm with $^{3}J_{F,Pt}$ coupling constants of 252 and 255 Hz, respectively. The appearance of four peaks is difficult to reconcile with the solid-state structure, which has the $AgPPh_3$ moiety bonded to the picolinate oxygen atom but is perfectly compatible with the proposed solution structure with the bridging $AgPPh_3$ moiety.

Finally, the ^{19}F NMR spectrum of **7** at 298 K showed two signals attributable to the *o*-F atoms of the two C_6F_5 rings, which broadened at 200 K. This behaviour is in ac-

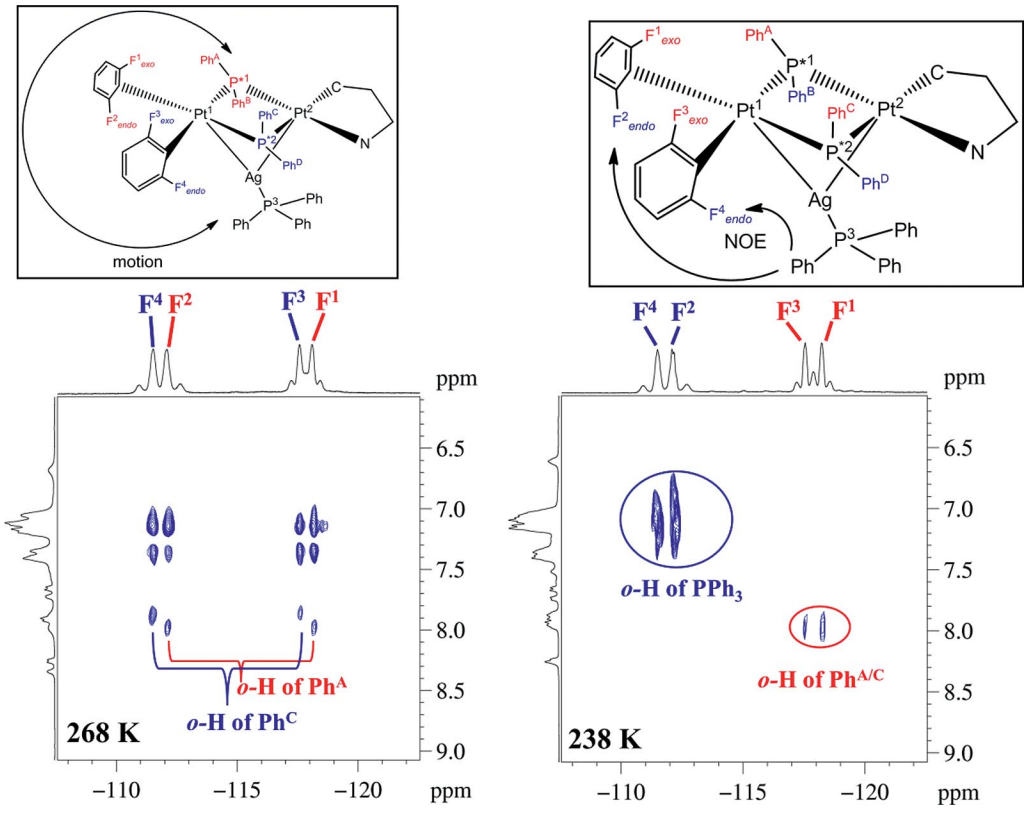

Figure 12. Portion of the ^{19}F–^{1}H HOESY spectrum of **1** (CD_2Cl_2, 238 K, τ_m = 0.500 s) showing the correlation between the *endo* *o*-F atom (δ = –111.1 and –111.9 ppm) and the *ortho* protons of PPh_3 (δ = 7.13 ppm). Left: T = 268 K, τ_m = 0.200 s; right: T = 238 K, τ_m = 0.500 s.

cord with a structure of **7** in solution with the *O*-bound $AgPPh_3$ moiety, analogous to that found in the solid state.

Discussion

The structural study of the trinuclear AgMPt derivatives demonstrates that most of them, **1**–**5**, show a **C**-type (Scheme 1) structure in the solid state, whereas the picolinate derivatives **6** and **7** adopt a **G**-type (Scheme 1) structure in the solid state. Notably, the hydroxyquinolinate complexes **3** and **4** (**C**-type, Scheme 1) have an oxygen atom bonded to the Pt or Pd atoms, which could act as a donor towards the $AgPPh_3$ fragment as in **6** and **7** (**G**-type, Scheme 1). The slight changes to the ligands within the starting materials imply different structures of the trinuclear AgMPt derivatives.

The NMR study of **1**–**5** revealed that in all cases the solution structures are analogous to those found in the solid state; the $AgPPh_3$ moiety bridges the two metal centres, and the $AgPPh_3$ moiety passes from one side of the molecule to the other, possibly by rupture and reformation of the Ag–$M^{1/2}$ bonds. This motion is fast for the 8-hydroxyquinolinate and tht complexes **3**–**5** even at low temperature, whereas it can be significantly slowed down for the benzoquinolinate complexes **1** and **2**.

The behaviour of the picolinate complexes **6** and **7** in solution can be rationalized if it is assumed that the structures with either bridging or oxygen-bonded $AgPPh_3$ moieties are possible in solution (Scheme 5). For the Pt–Pt species **6**, the stable form in solution is that with a bridging (and dynamic) $AgPPh_3$ moiety, which is equilibrium *b* (Scheme 5) shifted to the right. On the other hand, for the Pt–Pd species **7**, the stable form in solution is the one with an oxygen-bonded $AgPPh_3$ moiety, that is, equilibrium *b* (Scheme 5) is shifted to the left. These facts indicate the very small difference in energy between the Pt–Ag–M and the Pt–M–O–Ag types of adducts in these picolinate complexes and is also in keeping with the lower number of complexes with Pd–Ag than with Pt–Ag bonds.[9,14,30,63–65]

Complex **7** shows a peculiar behaviour in solution that is explained with the proposal shown in Scheme 4. The breaking of the Pd–O bond in **7** implies the formation of an unsaturated (30 valence electrons) derivative with a Pt–Pd bond. This unsaturated species is fully comparable with the isolated and well-characterized dinuclear $[(C_6F_5)_2Pt(\mu\text{-}PPh_2)_2Pd(PPh_3)]$[40] and in agreement with the formation of metal–metal bonds induced by the elimination of ligands in phosphanido derivatives, a well-established process.[41,48] Palladium complexes are more labile than the corresponding platinum derivatives, and the breaking of the Pd–O bond in **7** (Scheme 4) has to be easier than the breaking of the Pt–O bond in **6**; therefore, the observed equivalence between P^1 and P^2 (and the two R_F groups) is accomplished only for the palladium derivative **7**. In agreement with this,

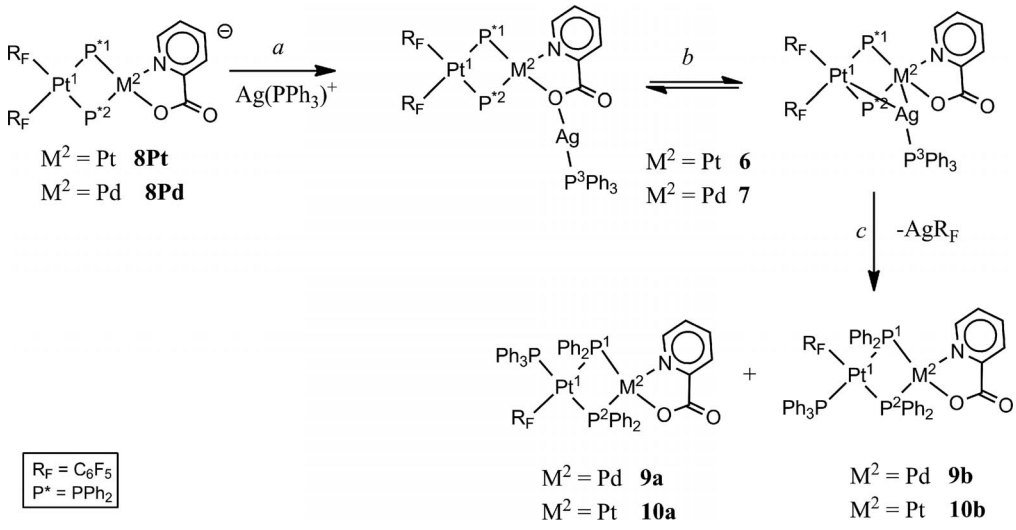

Scheme 5. Solution behaviour of picolinate complexes.

we have reported that the elimination of the L ligand from [$(R_F)_2Pt(\mu\text{-}PPh_2)_2MLL'$]" complexes (M = Pt, Pd) requires softer conditions for palladium than for platinum and in some cases the process takes place only when M = Pd.[38,40,52]

Finally, the M–Ag (M = Pt, Pd) adducts are usually unstable and decompose in solution, and for this reason the characterization in solution is performed with freshly prepared solutions. In both cases, prolonged dissolution (24 h) resulted in the decomposition of the silver adducts (reaction *c* in Scheme 5) with formation of **9** and **10**, in which one of the pentafluorophenyl rings has been replaced by a PPh_3 ligand, that is, adducts **6** and **7** behave as intermediates to afford complexes of type **E** (Scheme 1).[36,66,67] The ^{31}P and ^{195}Pt NMR features of **9**–**10** are reported in Table 7.

Concluding Remarks

Despite the well-recognized ability of Ag^+ to act as an oxidant,[35] in no case is the oxidation of these Pt–Pt or Pt–Pd substrates to produce type **F** complexes observed. Considering the occurrence of such a type of oxidation processes with Ag^+ with dianionic[43] or neutral starting materials,[38] it seems that the charge of the dinuclear phosphanido fragment does not play an important role in the facilitation of the Ag^+-promoted oxidation of platinum substrates. The solid-state X-ray diffraction study shows that, in the adducts **1**–**5**, the dinuclear starting materials act as a donor towards the silver centre and forms two M–Ag bonds (M = Pt, Pd), whereas in **6′** and **7**, the silver centre is bonded to the dinuclear fragment through the O atom of the picolinate group, which is already bonded to the M centre.

The NMR study indicates that the structures of **1**–**5** and **7** in solution are the same as those in the solid state. Moreover, the M–Ag (M = Pt, Pd) bonds in **1**–**5** are not maintained in solution at room temperature as a dynamic process operates. For the benzoquinolinate adducts **1** and **2**, such a dynamic process can be slowed down at low temperatures. Complex **6** is peculiar: the NMR spectroscopic data indicate that in solution the silver centre is bonded to the two platinum donor centres as in **1**–**5**.

Finally, it is remarkable that although **6′** and **7** display the same structure in the solid state, in which both moieties are connected through an Ag–O bond, all the NMR spectroscopic data for **6** are compatible with a structure in which the Pt and Ag moieties are connected through Pt–Ag interactions, as for complexes **1**–**5**, whereas in **7** the NMR spectroscopic data are fully compatible with the solid-state structure. All these results point to the very similar stabilization energy of both types of isomers: Pt–Ag–Pt or Pt–O–Ag.

In general, it is difficult to establish a priori the type of complexes that will be obtained when different dinuclear phosphanido platinum or palladium fragments react with Ag^+, and the final product is the result of a delicate balance between the electronic properties of the basic centres and the structural parameters.

Experimental Section

General Procedures and Materials: C, H and N analyses were performed with a Perkin–Elmer 2400 CHNS/O Series II microanalyzer. IR spectra were recorded with a Perkin–Elmer Spectrum 100 FTIR spectrophotometer in the range 4000–250 cm^{-1}. Solution NMR spectra were recorded with Bruker Avance 400 spectrometers with $SiMe_4$, $CFCl_3$, 85% H_3PO_4 and aqueous $[PtCl_6]^{2-}$ as external references for ^1H, ^{19}F, ^{31}P and ^{195}Pt, respectively. Literature methods were used to prepare the starting materials [$Ag(OClO_3)(PPh_3)$],[68] [NBu_4][$(C_6F_5)_2Pt(\mu\text{-}PPh_2)_2M(hq)$],[46] [$NBu_4$][$(C_6F_5)_2Pt(\mu\text{-}PPh_2)_2M(bq)$][45] and [$NBu_4$][$(C_6F_5)_2Pt(\mu\text{-}PPh_2)_2M(C_6F_5)(tht)$][47] (M = Pd or Pt).

Caution: Perchlorate salts of metal complexes with organic ligands are potentially explosive. Only small amounts of materials should be prepared and these should be handled with great caution.

[$(C_6F_5)_2Pt(\mu\text{-}PPh_2)_2(\mu\text{-}AgPPh_3)Pt(bq)$] (1): [$Ag(OClO_3)(PPh_3)$] (0.078 g, 0.166 mmol) was added to a yellow solution of

$[NBu_4][(C_6F_5)_2Pt(\mu\text{-}PPh_2)_2Pt(bq)]$ (0.251 g, 0.166 mmol) in CH_2Cl_2 (10 mL). The solution became darker, and the mixture was stirred for 30 min in air. The solution was evaporated to dryness, and Et_2O (15 mL) was added to the residue. The white solid (NBu_4ClO_4) was removed by filtration, and the resulting solution was evaporated to ca. 1 mL. *n*-Hexane (10 mL) was added, and **1** crystallized as a yellow solid, which was filtered, washed with hexane (2× 2 mL) and air-dried, yield 0.127 g, 46%. $C_{67}H_{43}AgF_{10}NP_3Pt_2$ (1643.03): calcd. C 48.98, H 2.64, N 0.85; found C 49.05, H 2.54, N 0.70. ^{1}H NMR (400 MHz, 298 K, CD_2Cl_2): the ^{1}H signals of phenyl rings bonded to μ-P atoms are very broad near the baseline owing to dynamic processes. The ^{1}H signals of the coordinated benzoquinolinate and PPh_3 are δ = 8.33 (br., 1 H, H^1), 8.19 (d, 1 H, $^3J_{H,H}$ = 8.1 Hz, H^3), 7.84 (d, 1 H, J = 8.8 Hz, H^5), 7.64 (m, 1 H, H^6), 7.58 (d, 1 H, J = 8.8 Hz, H^4), 7.34 (pseudo-t, 1 H, J = 6.7 Hz, H^8), 7.27 (br., 1 H, H^7), 7.20–6.93 (m, 16 H, overlapped Ph–P^3, H^2) ppm. ^{1}H NMR (400 MHz, 238 K, CD_2Cl_2): δ = 8.30–8.21 (m, 2 H, H^1, H^3), 7.95 (partially overlapped pseudo-t, 2 H, J = 8.2 Hz, *o*-Ph^A–P^1), 7.92 (partially overlapped d, 1 H, J = 8.8 Hz, H^5), 7.87 (partially overlapped pseudo-t, 2 H, *o*-Ph^C–P^2), 7.74 (d, 1 H, J = 6.7 Hz, H^6), 7.66 (d, 1 H, J = 8.7 Hz, H^4), 7.44–7.31 (m, 5 H, *o*-Ph^D, *o*-Ph^C, H^8), 7.25 (br., 1 H, H^7), 7.21–6.97 (m, 26 H, Ph–P^3, 2 *m*-Ph^A, 2 *m*-Ph^D, 2 *m*-Ph^C, 4 *p*-Ph, H^2) 6.61 (br., 2 H, *m*-Ph^B) ppm. ^{19}F NMR (376 MHz, 298 K, CD_2Cl_2): δ = –111.8 (v br., 2 *endo o*-F), –117.5 (v br., 2 *exo o*-F), –164.5 to –165.0 (m, 6 F, *m*-F, *p*-F) ppm. ^{19}F NMR (376 MHz, 200 K, CD_2Cl_2): δ = –111.1 (br., $^3J_{F,Pt}$ = 440 Hz, 1 *endo o*-F^4), –111.9 (br., $^3J_{F,Pt}$ = 415 Hz, 1 *endo o*-F^2), –117.2 (br., $^3J_{F,Pt}$ = 275 Hz, 1 *exo o*-F^3), –118.0 (br., $^3J_{F,Pt}$ = 255 Hz, 1 *exo o*-F^1),–162.5 to –163.9 (m, 6 F, *m*-F, *p*-F) ppm.

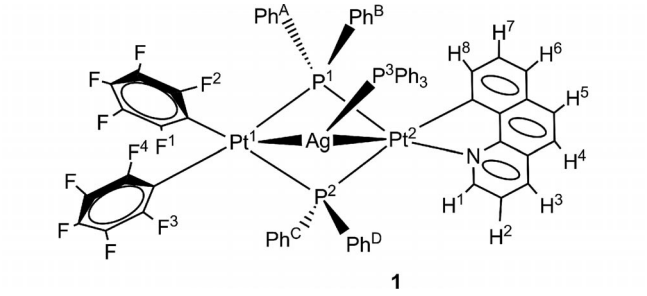

1

Synthesis of 2–7: These complexes were prepared in an analogous procedure to that described for complex **1**.

2: $[Ag(OClO_3)(PPh_3)]$ (0.052 g, 0.111 mmol) and $[NBu_4][(C_6F_5)_2Pt(\mu\text{-}PPh_2)_2Pd(bq)]$ (0.158 g, 0.111 mmol), yield 0.049 g, 24%. $C_{67}H_{43}AgF_{10}NP_3PdPt$ (1554.34): calcd. C 51.77, H 2.79, N 0.90; found C 51.46, H 2.71, N 0.94. ^{1}H NMR (400 MHz, 298 K, CD_2Cl_2): the ^{1}H signals of the phenyl rings bonded to P atoms are very broad near the baseline owing to dynamic processes. The ^{1}H signals of the coordinated benzoquinolinate ligand are δ = 8.16 (dd, 1 H, J = 8.1 Hz, J = 1.4 Hz, H^3), 8.11 (b, 1 H, H^1), 7.80 (d, 1 H, J = 8.7 Hz, H^5), 7.60 (partially overlapped d, 1 H, J = 7.7 Hz, H^6), 7.58 (partially overlapped d, 1 H, J = 8.7 Hz, H^4), 7.14 (overlapped, 1 H, H^7), 6.98 (overlapped H^8, H^2) ppm. ^{19}F NMR (376 MHz, 298 K, CD_2Cl_2): δ = –112.6 (v br., 2 *o*-F), –118.0 (v br., 2 *o*-F),–164.5 to –164.9 (m, 6 F, *m*-F, *p*-F) ppm. ^{19}F NMR (376 MHz, 200 K, CD_2Cl_2): δ = –112.2 (br., $^3J_{F,Pt}$ = 450 Hz, 1 *endo o*-F), –112.7 (br., $^3J_{F,Pt}$ = 440 Hz, 1 *endo o*-F), –117.6 (br., $^3J_{F,Pt}$ = 248 Hz, 1 *exo o*-F), –118.5 (br., $^3J_{F,Pt}$ = 253 Hz, 1 *exo o*-F),–162.4 to –164.1 (m, 6 F, *m*-F, *p*-F) ppm.

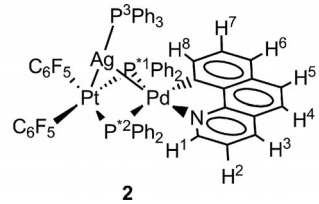

2

3: $[Ag(OClO_3)(PPh_3)]$ (0.032 g, 0.067 mmol) and $[NBu_4][(C_6F_5)_2Pt(\mu\text{-}PPh_2)_2Pt(hq)]$ (0.100 g, 0.067 mmol), yield 0.079 g, 74%. $C_{63}H_{41}AgF_{10}NOP_3Pt_2$ (1608.97): calcd. C 47.03, H 2.57, N 0.87; found C 47.34, H 2.70, N 0.96. ^{1}H NMR [298 K, $(CD_3)_2CO$, 400 MHz]: δ = 8.57 (d, 1 H, J = 8.2 Hz, H^3), 8.12 (br., 1 H, H^1), 7.92 (dd, 4 H, J = 11.5 Hz, J = 7.3 Hz, *o*-Ph–P^1), 7.78 (dd, 4 H, J = 11.3 Hz, J = 7.5 Hz, *o*-Ph–P^2), 7.65 (pseudo-t, 1 H, J = 7.8 Hz, H^5), 7.60–7.31 (m, 16 H, H^2, Ph–P^3), 7.31–7.17 (m, 5 H, *p*-Ph–P^2, *p*-Ph–P^1, H^4), 7.11 (pseudo-t, 4 H, J = 7.5 Hz, *m*-Ph–P^2), 7.01 (pseudo-t, 4 H, J = 7.3 Hz, *m*-Ph–P^1), 7.15 (d, 1 H, J = 7.9 Hz, H^6), ppm. ^{19}F NMR [298 K, $(CD_3)_2CO$, 376.5 MHz]: δ = –115.4 (m, $^3J_{F,Pt}$ = 346 Hz, 2 *o*-F), –115.7 (m, $^3J_{F,Pt}$ = 352 Hz, 2 *o*-F),–164.8 to –165.4 (m, 6 *m*-F, *p*-F) ppm. ^{19}F NMR (200 K, CD_2Cl_2, 376.5 MHz): δ = –113.6 (br., $^3J_{F,Pt}$ = 630 Hz, 1 *o*-F), –114.5 (br., $^3J_{F,Pt}$ = 626 Hz, 1 *o*-F),–118.0 (br., 2 *o*-F), –163.0 (t, $^3J_{F,F}$ = 20 Hz, 1 *p*-F), –163.2 (t, $^3J_{F,F}$ = 20 Hz, 1 *p*-F), –163.7 (br., 4 *m*-F).

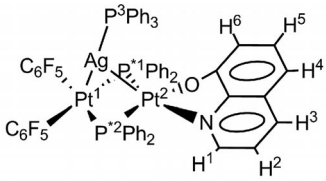

3

4: $[Ag(OClO_3)(PPh_3)]$ (0.034 g, 0.072 mmol) and $[NBu_4][(C_6F_5)_2Pt(\mu\text{-}PPh_2)_2Pd(hq)]$ (0.100 g, 0.072 mmol), yield 0.050 g, 46%. $C_{63}H_{41}AgF_{10}NOP_3PdPt$ (1520.28): calcd. C 49.77, H 2.72, N 0.92; found C 49.98, H 2.82, N 0.90. ^{1}H NMR (298 K, CD_2Cl_2, 400 MHz): δ = 8.17 (d, 1 H, J = 8.2 Hz, H^3), 7.84 (dd, 4 H, J = 10.3 Hz, J = 7.4 Hz, *o*-Ph–P^1), 7.71 (dd, 4 H, J = 10.5 Hz, J = 7.3 Hz, *o*-Ph–P^2), 7.50 (br., 1 H, H^1), 7.45 (dd, 1 H, H^5), 7.06–6.98 (m, 5 H, *m*-Ph–P^2, H^4), 6.92 (pseudo-t, 4 H, J = 7.4 Hz, *m*-Ph–P^1), 7.09 (t, 2 H, 7.4 Hz, *p*-Ph–P^1), 7.30–7.14 (m, 18 H, H^6, Ph–P^3, *p*-Ph–P^2), 6.96 (partially overlapped dd, 1 H, J = 8.3 Hz, J = 4.8 Hz, H^2) ppm. ^{19}F NMR (298 K, CD_2Cl_2, 376.5 MHz): δ = –115.9 (m, 2 *o*-F, $^3J_{F,Pt}$ = 352 Hz), –116.4 (m, $^3J_{F,Pt}$ = 354 Hz, 2 *o*-F), –164.0 to –164.9 (m, 6 F, *m*-F, *p*-F) ppm. ^{19}F NMR (200 K, CD_2Cl_2, 376.5 MHz): δ = –116.0 (v br., $^3J_{F,Pt} \approx$ 350 Hz, 2 *o*-F), –117.0 (v br., $^3J_{F,Pt} \approx$ 340 Hz, 2 *o*-F), –163.3 (m, 2 *p*-F), –163.9 (br., 4 *m*-F).

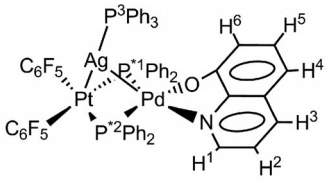

4

5: $[Ag(OClO_3)(PPh_3)]$ (0.040 g, 0.085 mmol) and $[NBu_4][(C_6F_5)_2Pt(\mu\text{-}PPh_2)_2Pt(C_6F_5)tht]$ (0.135 g, 0.085 mmol), yield 0.086 g, 59%. $C_{64}H_{43}AgF_{15}P_3Pt_2S$ (1720.04): calcd. C 44.69, H 2.52; found C 44.44, H 2.31. ^{1}H NMR (400 MHz, 298 K, CD_2Cl_2): the ^{1}H signals of phenyl rings bonded to μ-P atoms are very broad near the baseline owing to dynamic processes. The ^{1}H signals of the coordinated

tht and PPh_3 ligands are δ = 7.63–6.78 (m, PPh_3), 2.74 (br., 4 H, CH_2S) 1.74 (br., 4 H, CH_2CH_2S) ppm. ^{1}H NMR (400 MHz, 213 K, CD_2Cl_2): δ = 7.64–6.61 (m, Ph), 2.92 (br., 2 H, CH_2S), 2.68 (br., 2 H, CH_2S), 1.81 (br., 2 H, CH_2CH_2S), 1.63 (br., 2 H, CH_2CH_2S). ^{1}H–^{31}P HMQC and ^{1}H NOESY (213 K): δ = 7.58 (*o*-Ph–P^1), 7.52 (*o*-Ph–P^3), 7.50 (*o*-Ph–P^2), 7.44 (*m*-Ph–P^3), 7.22 (*o*-Ph–P^2), 7.05 (*m*-Ph–P^2), 7.00 (*m*-Ph–P^1), 6.94 (*o*-Ph–P^1), 6.71 (*m*-Ph–P^2), 6.65 (*m*-Ph–P^1) ppm. ^{19}F NMR (376 MHz, 298 K, CD_2Cl_2): δ = 108.4–119.7 (v br., 6 F, *o*-F), –161.7 (t, $J_{F,F}$ = 24.0 Hz, 1 *p*-F), –162.7 (br., 2 *m*-F), –163.3 (t, $J_{F,F}$ = 19.8 Hz, 1 *p*-F), –163.8 (t, $J_{F,F}$ = 19.9 Hz, 1 *p*-F), –164.0 (pseudo-t, $J_{F,F} \approx$ 24 Hz, 2 *m*-F), –164.3 (pseudo-t, $J_{F,F} \approx$ 20 Hz, 2 *m*-F) ppm. ^{19}F NMR (376 MHz, 228 K, CD_2Cl_2): δ = –109.9 (br., $^3J_{F,Pt}$ = 280 Hz, 1 *o*-F C_6F_5–Pt^2), –111.1 (br., $^3J_{F,Pt}$ = 400 Hz, *endo o*-F C_6F_5–Pt^1), –112.1 (br., $^3J_{F,Pt}$ = 409 Hz, *endo o*-F C_6F_5–Pt^1), –116.9 (br., $^3J_{F,Pt}$ = 219 Hz, *exo o*-F C_6F_5–Pt^1), –118.2 (br., $^3J_{F,Pt}$ = 310 Hz, 1 *o*-F C_6F_5–Pt^2), –118.5 (br., $^3J_{F,Pt}$ = 205 Hz, *exo o*-F C_6F_5–Pt^1), –161.6 (t, $J_{F,F}$ = 20.4 Hz, 1 *p*-F), –162.1 (br., 1 *m*-F),–162.7 to –163.1 (m, 2 F, *p*-F, *m*-F), –163.2 to –163.8 (m, 4 F, 1 *p*-F, 3 *m*-F), –164.1 (br., 1 *m*-F) ppm.

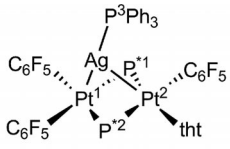

5

6: $[Ag(OClO_3)(PPh_3)]$ (0.041 g, 0.087 mmol) and $[NBu_4][(C_6F_5)_2Pt(\mu\text{-}PPh_2)_2Pt(pic)]$ (0.125 g, 0.086 mmol), yield 0.068 g, 47%. $C_{60}H_{39}AgF_{10}NO_2P_3Pt_2$ (1586.92): calcd. C 45.41, H 2.48, N 0.88; found C 45.75, H 2.43, N 0.82. ^{1}H NMR (400 MHz, 268 K, CD_2Cl_2): δ = 8.25 (d, 1 H, J = 7.6 Hz, H^4), 8.18 (pseudo-td, 1 H, J = 7.6 Hz, J = 1.3 Hz, H^3), 7.75 (br., 1 H, H^1), 7.66 (m, 4 H, *o*-Ph–P^2), 7.62 (m, 4 H, *o*-Ph–P^1), 7.41–7.31 (m, 15 H, overlapped Ph–P^3), 7.25–7.19 (m, 3 H, *p*-Ph–P^1, H^2), 7.11 (t, 2 H, J = 7.4 Hz, *p*-Ph–P^2), 7.02 (pseudo-t, 2 H, J = 7.4 Hz, *m*-Ph–P^1), 6.90 (pseudo-t, 2 H, J = 7.4 Hz, *m*-Ph–P^2) ppm. ^{19}F NMR (376 MHz, 298 K, CD_2Cl_2): δ = –115.9 to –116.3 (overlapped, 4 *o*-F), –163.5 (t, $J_{F,F}$ = 19.7 Hz, 1 *p*-F), –163.6 (t, $J_{F,F}$ = 19.7 Hz, 1 *p*-F), –164.1 (m, 2 *m*-F), –164.3 (m, 2 *m*-F) ppm. ^{19}F NMR (376 MHz, 200 K, CD_2Cl_2): δ = –116.1 (m, $^3J_{F,Pt}$ = 348 Hz, 2 *o*-F), –116.5 ($^3J_{F,Pt}$ = 342 Hz, 2 *o*-F), –165.2 (t, $J_{F,F}$ = 19.2 Hz, 1 *p*-F), –165.4 (t, $J_{F,F}$ = 18.0 Hz, 1 *p*-F), –165.5 to –165.7 (m, 4 *m*-F) ppm.

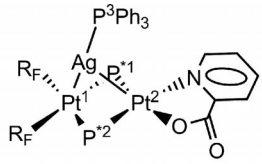

6

7: $[Ag(OClO_3)(PPh_3)]$ (0.043 g, 0.092 mmol) and $[NBu_4][(C_6F_5)_2Pt(\mu\text{-}PPh_2)_2Pd(pic)]$ (0.125 g, 0.091 mmol), yield 0.050 g, 36%. $C_{60}H_{39}AgF_{10}NO_2P_3PdPt$ (1498.23): calcd. C 48.10, H 2.62, N 0.93; found C 48.33, H 2.46, N 1.0. ^{1}H NMR (400 MHz, 298 K, CD_2Cl_2): δ = 8.21 (d, 1 H, J = 7.6 Hz, H^4), 7.93 (pseudo-td, 1 H, J = 7.6 Hz, $J_{H,H}$ = 1.5 Hz, H^3), 7.82–7.72 (m, 8 H, *o*-Ph–P^2, *o*-Ph–P^1), 7.49 (t, 3 H, J = 7.6 Hz, *p*-Ph–P^3), 7.40 (partially overlapped d, 1 H, J = 5.3 Hz, H^1), 7.36 (pseudo-t, 6 H, J = 7.4 Hz, *m*-Ph–P^3), 7.29–7.18 (m, 9 H, *p*-Ph–P^1, *o*-Ph–P^3, H^2), 7.14 (pseudo-t, 4 H, J = 7.1 Hz, *m*-Ph–P^1), 6.93 (m, 6 H, *m*-Ph, *p*-Ph–P^2) ppm. ^{19}F NMR (376 MHz, 298 K, CD_2Cl_2): δ = –116.0 (m, $^3J_{F,Pt}$ = 348 Hz, 2 *o*-F), –116.5 (m, $^3J_{F,Pt}$ = 339 Hz, 2 *o*-F), –165.2 (t, $J_{F,F}$ = 19.7 Hz, 1 *p*-F), –165.3 to –165.7 (m, 2 *m*-F, 1 *p*-F) ppm.

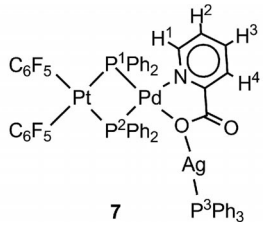

7

X-ray Structure Determinations: The crystal data and other details of the structure analyses are presented in Table 8. Suitable crystals

Table 8. Crystal data and structure refinement for **1**, **3**, **4**, **5**, **6′** and **7**·CH_2Cl_2.

	1	**3**	**4**	**5**	**6′**	**7**·CH_2Cl_2
Formula	$C_{67}H_{43}AgF_{10}NP_3Pt_2$	$C_{63}H_{41}AgF_{10}NOP_3Pt_2$	$C_{63}H_{41}AgF_{10}NOP_3PtPd$	$C_{64}H_{43}AgF_{15}P_3Pt_2S$	$C_{63}H_{45}AgF_{10}NO_3P_3Pt_2$	$C_{60}H_{39}AgF_{10}NO_2P_3PtPd{\cdot}CH_2Cl_2$
M_t	1642.98	1608.93	1520.2	1583.12	1644.96	1720.00
Crystal system	monoclinic	monoclinic	monoclinic	monoclinic	monoclinic	monoclinic
Space group	$P2_1/n$	$P2_1/c$	$P2_1/n$	$P2_1/n$	$P2_1/c$	$P2_1/c$
a [Å]	13.4528(1)	13.4548(1)	13.3626(4)	19.7022(5)	13.1699(5)	12.6659(1)
b [Å]	20.6793(2)	19.6485(1)	19.6328(6)	15.1324(4)	15.0418(6)	15.5784(2)
c [Å]	20.3291(1)	21.8278(2)	21.8979(8)	19.8324(6)	29.6249(12)	29.5594(3)
β [°]	97.4556(7)	107.785(1)	107.689(4)	101.748(3)	102.4160(10)	101.313(1)
V [Å^3]	5607.63(7)	5494.76(7)	5473.2(3)	5789.0(3)	5731.4(4)	5737.63(10)
Z	4	4	4	4	4	4
D_c [g cm^{-3}]	1.946	1.945	1.845	1.973	1.906	1.833
T [K]	100(1)	100(1)	100(1)	100(1)	100(1)	100(1)
μ [mm^{-1}]	5.490	5.599	3.396	5.366	5.372	3.335
F(000)	3160	3088	2960	3304	3168	3080
2θ range [°]	7.4–57.8	8.3–64.5	8.3–56.8	8.3–64.6	3.1–57.3	8.2–57.7
Collected reflections	61145	54446	93375	47258	37437	63461
Unique reflections	13354	17914	13045	18458	13407	13546
R_{int}	0.0256	0.0173	0.0950	0.0288	0.0236	0.0260
R_1, wR_2[a] [$I > 2\sigma(I)$]	0.0255, 0.0565	0.0203, 0.0470	0.0573, 0.1316	0.0326, 0.0701	0.0253, 0.0571	0.0213, 0.0488
R_1, wR_2[a] (all data)	0.0325, 0.0582	0.0267, 0.0479	0.1030, 0.1411	0.0534, 0.0731	0.0308, 0.0595	0.0289, 0.0497
GOF (F^2)[b]	1.036	1.044	1.018	1.007	1.055	1.029

[a] $R_1 = \Sigma(|F_o| - |F_c|)/\Sigma|F_o|$, $wR2 = [\Sigma w(F_o^2 - F_c^2)^2/\Sigma w(F_o^2)^2]^{1/2}$. [b] Goodness-of-fit = $[\Sigma w(F_o^2 - F_c^2)^2/(n_{obs} - n_{param})]^{1/2}$.

for X-ray diffraction studies were obtained by slow diffusion of *n*-hexane into concentrated solutions of the complexes in CH_2Cl_2 (3 mL; **1**, **3**, **4**, **5** and **7**·CH_2Cl_2) or Me_2CO (3 mL; **6′**). Crystals were mounted at the end of quartz fibres. The radiation used in all cases was graphite-monochromated Mo-K_α (λ = 0.71073 Å). For **1**, **3**, **4**, **5** and **7**·CH_2Cl_2, the X-ray intensity data were collected with an Oxford Diffraction Xcalibur diffractometer. The diffraction frames were integrated and corrected for absorption by using the CrysAlis RED software.[69] For **6′**, the X-ray intensity data were collected with an Oxford Diffraction Bruker Smart CCD diffractometer. The diffraction frames were integrated and corrected for absorption by using the APEX II software.[70] The structures were solved by Patterson and Fourier methods and refined by full-matrix least-squares on F^2 with SHELXL-97.[71] All non-hydrogen atoms were assigned anisotropic displacement parameters and refined without positional constraints. All hydrogen atoms were constrained to idealized geometries and assigned isotropic displacement parameters equal to 1.2 times the U_{iso} values of their attached parent atoms. Full-matrix least-squares refinement against F^2 converged to the final residual indices given in Table 8.

CCDC-947475 (for **1**), -947476 (for **3**), -947477 (for **4**), -947478 (for **5**), -947479 (for **6′**) and -947480 (for **7**·CH_2Cl_2) contain the supplementary crystallographic data for this paper. These data can be obtained free of charge from The Cambridge Crystallographic Data Centre via www.ccdc.cam.ac.uk/data_request/cif.

Acknowledgments

This work was supported by the Spanish Ministerio de Ciencia e Innovación (MICINN), DGPTC/FEDER (project number CTQ2008-06669-C02-01/BQU), Ministerio de Economía y Competitividad (MINECO)/FEDER (project number CTQ2012-35251) and the Gobierno de Aragón (Grupo Consolidado E21: Química Inorgánica y de los Compuestos Organometálicos). A. A. gratefully acknowledges MICINN for an FPU grant. The Italian Ministero dell'Università e della Ricerca (MIUR) (PRIN project number 2009LR88XR) is also acknowledged for financial support.

[1] B. Lippert, D. Neugebauer, *Inorg. Chem.* **1982**, *21*, 451–452.
[2] R. Usón, J. Forniés, M. Tomás, F. A. Cotton, L. R. Falvello, *J. Am. Chem. Soc.* **1984**, *106*, 2482–2483.
[3] A. Albinati, K. H. Dahmen, A. Togni, L. M. Venanzi, *Angew. Chem.* **1985**, *97*, 760; *Angew. Chem. Int. Ed. Engl.* **1985**, *24*, 766–767.
[4] R. Usón, J. Forniés, M. Tomás, J. M. Casas, F. A. Cotton, L. R. Falvello, *J. Am. Chem. Soc.* **1985**, *107*, 2556–2557.
[5] R. Usón, J. Forniés, B. Menjón, F. A. Cotton, L. R. Falvello, M. Tomás, *Inorg. Chem.* **1985**, *24*, 4651–4656.
[6] A. Albinati, F. Demartin, L. M. Venanzi, M. K. Wolfer, *Angew. Chem.* **1988**, *100*, 571; *Angew. Chem. Int. Ed. Engl.* **1988**, *27*, 563.
[7] G. Douglas, M. C. Jennings, L. Manojlovic-Muir, Puddephatt, *Inorg. Chem.* **1988**, *27*, 4516–4520.
[8] F. D. Rochon, R. M. Melanson, *Acta Crystallogr. Sect. C: Cryst. Struct. Commun.* **1988**, *44*, 474–477.
[9] J. Bauer, H. Braunschweig, R. D. Dewhurst, *Chem. Rev.* **2012**, *112*, 4329–4346.
[10] M. J. Katz, K. Sakai, D. B. Leznoff, *Chem. Soc. Rev.* **2008**, *37*, 1884–1895.
[11] S. Sculfort, P. Braunstein, *Chem. Soc. Rev.* **2011**, *40*, 2741–2760.
[12] V. W.-W. Yam, E. C.-C. Cheng, *Chem. Soc. Rev.* **2008**, *37*, 1806–1813.
[13] A. Díez, E. Lalinde, M. T. Moreno, *Coord. Chem. Rev.* **2011**, *255*, 2426–2447.
[14] J. Forniés, A. Martín, in: *Metal Clusters in Chemistry*, vol. 1 (Eds.: P. Braunstein, L. A. Oro, P. R. Raithby), Wiley-VCH, Weinheim, Germany, **1999**, p. 417–443, and references cited therein.
[15] T. Yamaguchi, F. Yamazaki, T. Ito, *J. Am. Chem. Soc.* **1999**, *121*, 7405–7406.
[16] M. Kim, T. J. Taylor, F. P. Gabbai, *J. Am. Chem. Soc.* **2008**, *130*, 6332–6333.
[17] M.-E. Moret, P. Chen, *J. Am. Chem. Soc.* **2009**, *131*, 5675–5690.
[18] M. J. A. Johnson, P. K. Gantzel, C. P. Kubiak, *Organometallics* **2002**, *21*, 3831–3832.
[19] E. J. Fernández, A. Laguna, J. M. Lopez-de-Luzuriaga, *Dalton Trans.* **2007**, 1969–1981.
[20] J. Forniés, S. Fuertes, A. Martín, V. Sicilia, B. Gil, E. Lalinde, *Dalton Trans.* **2009**, 2224–2234.
[21] L. R. Falvello, J. Forniés, R. Garde, A. García, E. Lalinde, M. T. Moreno, A. Steiner, M. Tomás, I. Usón, *Inorg. Chem.* **2006**, *45*, 2543–2552.
[22] J. R. Stork, M. M. Olmsread, J. C. Fettinger, A. L. Balch, *Inorg. Chem.* **2006**, *45*, 849–857.
[23] F. H. Liu, W. Z. Chen, D. Q. Wang, *Dalton Trans.* **2006**, 3015–3024.
[24] N. Oberbeckmann-Winter, X. Morise, P. Braunstein, R. Welter, *Inorg. Chem.* **2005**, *44*, 1391–1403.
[25] L. R. Falvello, J. Forniés, E. Lalinde, B. Menjón, M. A. García-Monforte, M. T. Moreno, M. Tomás, *Chem. Commun.* **2007**, 3838–3840.
[26] D. E. Janzen, L. F. Mehne, D. G. VanDerveer, G. J. Grant, *Inorg. Chem.* **2005**, *44*, 8182–8184.
[27] G. Kampf, P. J. S. Miguel, M. Willermann, A. Schneider, B. Lippert, *Chem. Eur. J.* **2008**, *14*, 6882–6891.
[28] H.-B. Song, Z.-Z. Zhang, Z. Hui, C.-M. Che, T. C. W. Mak, *Inorg. Chem.* **2002**, *41*, 3146–3154.
[29] J. Forniés, S. Ibáñez, E. Lalinde, A. Martín, M. T. Moreno, A. C. Tsipis, *Dalton Trans.* **2012**, *41*, 3439–3451.
[30] V. Sicilia, F. Forniés, S. Fuertes, A. Martín, *Inorg. Chem.* **2012**, *51*, 10581–10589.
[31] M. Ma, A. Sidiropoulos, L. Ralte, A. Stasch, C. Jones, *Chem. Commun.* **2013**, *49*, 48–50.
[32] N. Oberbeckmann-Winter, P. Braunstein, R. Welter, *Organometallics* **2004**, *23*, 6311–6318.
[33] B. Lippert, H. Schollhorn, U. Thewalt, *Inorg. Chem.* **1987**, *26*, 1736–1741.
[34] L. M. Rendina, T. W. Hambley, *Platinum*, in: *Comprehensive Coordination Chemistry II*, vol. 6: *Transition Metal Groups 9–12* (Eds.: J. A. McCleverty, T. J. Meyer), Elsevier, San Diego, **2004**.
[35] N. G. Connelly, W. E. Geiger, *Chem. Rev.* **1996**, *96*, 877–910.
[36] E. Alonso, J. Forniés, C. Fortuño, A. Martín, A. G. Orpen, *Organometallics* **2003**, *22*, 5011–5019.
[37] J. Forniés, C. Fortuño, S. Ibáñez, A. Martín, *Inorg. Chem.* **2008**, *47*, 5978–5987.
[38] J. Forniés, C. Fortuño, S. Ibáñez, A. Martín, P. Mastrorilli, V. Gallo, *Inorg. Chem.* **2011**, *50*, 10798–10809.
[39] E. Alonso, J. Forniés, C. Fortuño, A. Lledós, A. Martín, A. Nova, *Inorg. Chem.* **2009**, *48*, 7679–7690.
[40] L. R. Falvello, J. Forniés, C. Fortuño, F. Martínez, *Inorg. Chem.* **1994**, *33*, 6242–6246.
[41] J. Forniés, C. Fortuño, R. Gil, A. Martín, *Inorg. Chem.* **2005**, *44*, 9534–9541.
[42] J. Forniés, C. Fortuño, S. Ibáñez, A. Martín, A. C. Tsipis, C. A. Tsipis, *Angew. Chem.* **2005**, *117*, 2459; *Angew. Chem. Int. Ed.* **2005**, *44*, 2407–2410.
[43] E. Alonso, J. M. Casas, F. A. Cotton, X. J. Feng, J. Forniés, C. Fortuño, M. Tomás, *Inorg. Chem.* **1999**, *38*, 5034–5040.
[44] E. Alonso, J. M. Casas, J. Forniés, C. Fortuño, A. Martín, A. G. Orpen, C. A. Tsipis, A. C. Tsipis, *Organometallics* **2001**, *20*, 5571–5582.

[45] A. Arias, F. Forniés, C. Fortuño, A. Martín, M. Latronico, P. Mastrorilli, S. Todisco, V. Gallo, *Inorg. Chem.* **2012**, *51*, 12628–12696.
[46] A. Arias, F. Forniés, C. Fortuño, A. Martín, P. Mastrorilli, M. Latronico, S. Todisco, V. Gallo, *Inorg. Chem.* **2013**, *52*, 5493–5506.
[47] J. Forniés, C. Fortuño, R. Navarro, F. Martínez, A. J. Welch, *J. Organomet. Chem.* **1990**, *394*, 643–658.
[48] F. Forniés, C. Fortuño, S. Ibáñez, A. Martín, P. Mastrorilli, V. Gallo, A. Tsipis, *Inorg. Chem.* **2013**, *52*, 1942–1953.
[49] E. Alonso, J. Forniés, C. Fortuño, A. Martín, A. G. Orpen, *Organometallics* **2001**, *20*, 850–859.
[50] F. Forniés, C. Fortuño, S. Ibáñez, A. Martín, *Inorg. Chem.* **2006**, *45*, 4850–4858.
[51] I. Ara, N. Chaouche, J. Forniés, C. Fortuño, A. Kribii, A. C. Tsipis, *Organometallics* **2006**, *25*, 1084–1091.
[52] N. Chaouche, J. Forniés, C. Fortuño, A. Kribii, A. Martín, *J. Organomet. Chem.* **2007**, *692*, 1168–1172.
[53] J. Forniés, C. Fortuño, S. Ibáñez, A. Martín, P. Romero, P. Mastrorilli, V. Gallo, *Inorg. Chem.* **2011**, *50*, 285–298.
[54] L. R. Falvello, J. Forniés, C. Fortuño, F. Durán, A. Martín, *Organometallics* **2002**, *21*, 2226–2234.
[55] A. Martín, U. Belío, S. Fuertes, V. Sicilia, *Eur. J. Inorg. Chem.* **2013**, 2231–2247.
[56] P. Mastrorilli, *Eur. J. Inorg. Chem.* **2008**, 4835–4850.
[57] The homologous picolinate Pt–Pt complex displays a chemical shift of –3911 ppm for the ^{195}Pt atom bonded to two C_6F_5 and two μ-PPh_2 ligands; see ref.[46].
[58] The extraction of ^{195}Pt–$^{107/109}$Ag couplings, which was possible only for Pt^2 of complex **1**, is impossible for Pt^1 signals, owing to their broadness, see Figure 7, and is a very hard task for the Pt^2 signals of **3**, **5** and **6** because the coupling constant merges with signal width.
[59] For comparison, the ^{1}H EXSY, ^{31}P EXSY and ^{19}F EXSY spectra of **6** at 298 K did not show any exchange cross-peaks.
[60] J. M. Casas, F. Forniés, A. Martín, B. Menjón, M. Tomás, *Polyhedron* **1996**, *15*, 3599–3604.
[61] F. Forniés, S. Ibáñez, A. Martín, M. Sanz, J. R. Berenguer, E. Lalinde, J. Torroba, *Organometallics* **2006**, *25*, 4331–4340.
[62] The *meta*- and *para*-F atoms of the two C_6F_5 rings gave distinguishable signals, see Experimental Section.
[63] F. Kessler, N. Szesni, C. Maaß, C. Hohberger, B. Weibert, H. Fischer, *J. Organomet. Chem.* **2007**, *692*, 3005–3018.
[64] P. Braunstein, C. Frison, N. Oberbeckmann-Winter, X. Morise, A. Messaoudi, M. Bénard, M.-M. Rohmer, R. Welter, *Angew. Chem.* **2004**, *116*, 6246; *Angew. Chem. Int. Ed.* **2004**, *43*, 6120–6125.
[65] Y. Liu, K. H. Lee, J. J. Vittal, T. S. A. Hor, *J. Chem. Soc., Dalton Trans.* **2002**, 2747–2751.
[66] F. Forniés, F. Martínez, R. Navarro, E. Urriolabeitía, *Organometallics* **1996**, *15*, 1813–1819.
[67] R. Usón, F. Forniés, M. Tomás, I. Ara, J. M. Casas, A. Martín, *J. Chem. Soc., Dalton Trans.* **1991**, 2253–2264.
[68] F. A. Cotton, L. R. Falvello, R. Usón, J. Forniés, M. Tomás, J. M. Casas, I. Ara, *Inorg. Chem.* **1987**, *26*, 1366–1370.
[69] *CrysAlisRED*, *Program for X-ray CCD camera data reduction*, version 1.171.32.19, Oxford Diffraction Ltd., Oxford, UK, **2008**.
[70] *APEX2*, v. 2009.7-0, **2009**, Bruker AXS, Madison, WI.
[71] G. M. Sheldrick, *Acta Crystallogr., Sect. A* **2008**, *64*, 112–122.
[72] A. Arias, F. Forniés, C. Fortuño, A. Martín, *Inorg. Chim. Acta* **2013**, *407*, 189–196.

Received: June 27, 2013
Published Online: ■

Heterometallic Complexes

Keywords: Metal–metal interactions / P ligands / Palladium / Platinum / Structure elucidation

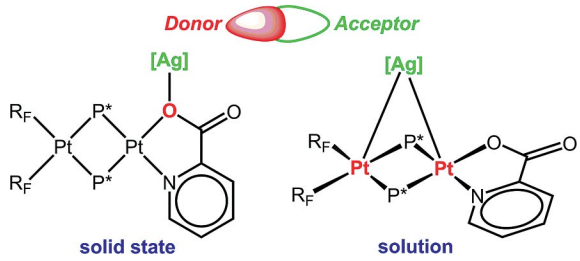

The trinuclear adducts $[(C_6F_5)_2Pt(\mu\text{-}PPh_2)_2M(L–L')(AgPPh_3)]$ (M = Pt, Pd) are synthesized as yellow solids. In these adducts, the $[AgPPh_3]$ moiety bridges the metal centres and is also linked to the picolinate oxygen atom. The dynamic behaviour of the adducts is studied.

Inorganic Chemistry

Article

pubs.acs.org/IC

Addition of Nucleophiles to Phosphanido Derivatives of Pt(III): Formation of P−C, P−N, and P−O Bonds

Andersson Arias, Juan Forniés, Consuelo Fortuño,* Susana Ibáñez, and Antonio Martín

Departamento de Química Inorgánica, Instituto de Síntesis Química y Catálisis Homogénea-ISQCH, Universidad de Zaragoza-C.S.I.C., E-50009 Zaragoza, Spain

Piero Mastrorilli,* Vito Gallo, and Stefano Todisco

Dipartimento DICATECh del Politecnico di Bari and Istituto CNR-ICCOM, Via Orabona 4, I-70125 Bari, Italy

S *Supporting Information*

ABSTRACT: The reactivity of the dinuclear platinum(III) derivative $[(R_F)_2Pt^{III}(\mu\text{-}PPh_2)_2Pt^{III}(R_F)_2]$*(Pt−Pt)* ($R_F = C_6F_5$) (**1**) toward OH^-, N_3^-, and NCO^- was studied. The coordination of these nucleophiles to a metal center evolves with reductive coupling or reductive elimination between a bridging diphenylphosphanido group and OH^-, N_3^-, and NCO^- or C_6F_5 groups and formation of P−O, P−N, or P−C bonds. The addition of OH^- to **1** evolves with a reductive coupling with the incoming ligand, formation of a P−O bond, and the synthesis of $[NBu_4]_2[(R_F)_2Pt^{II}(\mu\text{-}OPPh_2)(\mu\text{-}PPh_2)\text{-}Pt^{II}(R_F)_2]$ (**3**). The addition of N_3^- takes place through two ways: (a) formation of the P−N bond and reductive elimination of PPh_2N_3 yielding $[NBu_4]_2[(R_F)_2Pt^{II}(\mu\text{-}N_3)(\mu\text{-}PPh_2)Pt^{II}(R_F)_2]$ (**4a**) and (b) formation of the P−C bond and reductive coupling with one of the C_6F_5 groups yielding $[NBu_4][(R_F)_2Pt^{II}(\mu\text{-}N_3)(\mu\text{-}PPh_2)Pt^{II}(R_F)(PPh_2R_F)]$ (**4b**). Analogous behavior was shown in the addition of NCO^- to **1** which afforded $[NBu_4]_2[(R_F)_2Pt^{II}(\mu\text{-}NCO)(\mu\text{-}PPh_2)Pt^{II}(R_F)_2]$ (**5a**) and $[NBu_4][(R_F)_2Pt^{II}(\mu\text{-}NCO)(\mu\text{-}PPh_2)Pt^{II}(R_F)(PPh_2R_F)]$ (**5b**). In the reaction of the trinuclear complex $[(R_F)_2Pt^{III}(\mu\text{-}PPh_2)_2Pt^{III}(\mu\text{-}PPh_2)_2Pt^{II}(R_F)_2]$*(Pt^{III}−Pt^{III})* (**2**) with OH^- or N_3^-, the coordination of the nucleophile takes place selectively at the central platinum(III) center, and the PPh_2/OH^- or PPh_2/N_3^- reductive coupling yields the trinuclear $[NBu_4]_2[(R_F)_2Pt^{II}(\mu\text{-}Ph_2PO)(\mu\text{-}PPh_2)Pt^{II}(\mu\text{-}PPh_2)_2Pt^{II}(R_F)_2]$ (**6**) and $[NBu_4]\text{-}[(R_F)_2Pt^1(\mu_3\text{-}Ph_2PNPPh_2)(\mu\text{-}PPh_2)Pt^2(\mu\text{-}PPh_2)Pt^3(R_F)_2]$*(Pt^2−Pt^3)* (**7**). Complex **7** is fluxional in solution, and an equilibrium consisting of Pt−Pt bond migration was ascertained by ^{31}P EXSY experiments.

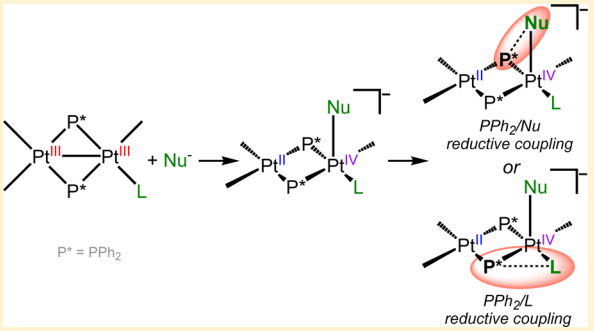

INTRODUCTION

Oxidation of platinum(II) and palladium(II) derivatives is the usual way to prepare complexes in high oxidation states (III and IV) which undergo easy reductive elimination processes which produce new M(II)/M(IV)/M(II) or M(II)/M_2(III)/M(II) cycles and provide transformations that are difficult to achieve otherwise. Despite the fact that platinum and palladium chemistry display rather similar trends in reactivity, the unambiguous characterization and isolation of dinuclear Pd(III) and mononuclear Pd(IV) intermediates in these cycles have been carried out only in the past 10 years.[1−18]

In the course of our current research on diphenylphosphanido derivatives of palladium(II) and platinum(II), we have reported (Scheme 1) that complexes of the type $[(R_F)_2M(\mu\text{-}PPh_2)_2M'XL]^{n-}$ (type **A**, $R_F = C_6F_5$) add I_2 affording new complexes $[(R_F)_2M(\mu\text{-}PPh_2)(\mu\text{-}I)M'(PPh_2X)L]^{(n-1)-}$ showing (a) the "$M(\mu\text{-}PPh_2)(\mu\text{-}I)M'$" fragment; (b) a new PPh_2X ligand, and (c) both metal centers in formal oxidation state (II).[19−22] Thus, oxidative addition of I_2 to the dinuclear phosphanido complexes of M(II) (type **A**) is followed by a reductive coupling process between a diphenylphosphanido bridged ligand and a pentafluorophenyl, benzo[*h*]quinolinate (bzq), 8-hydroxyquinolinate (hq), piccolinate (pic), or acetylacetonate (acac) groups with formation of P−C and P−O bonds (Scheme 1).

Scheme 1

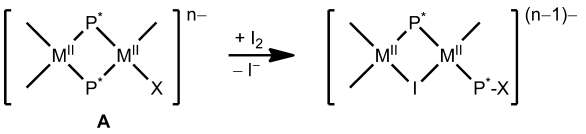

These reductive couplings have been demonstrated to take place either via the dinuclear M(III)−M′(III) (type **B**) or from the mixed oxidation state M(II),M′(IV) (type **C**) intermediates (Scheme 2).[20−23] It has been concluded that both the

Received: July 2, 2013

   dx.doi.org/10.1021/ic401689c | *Inorg. Chem.* XXXX, XXX, XXX−XXX

Scheme 2

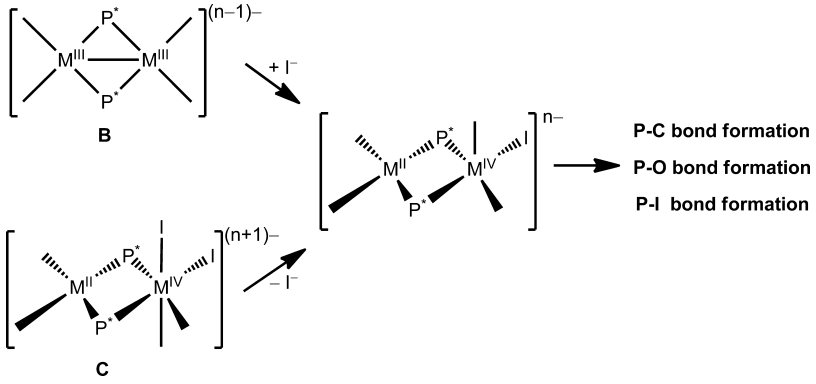

Scheme 3

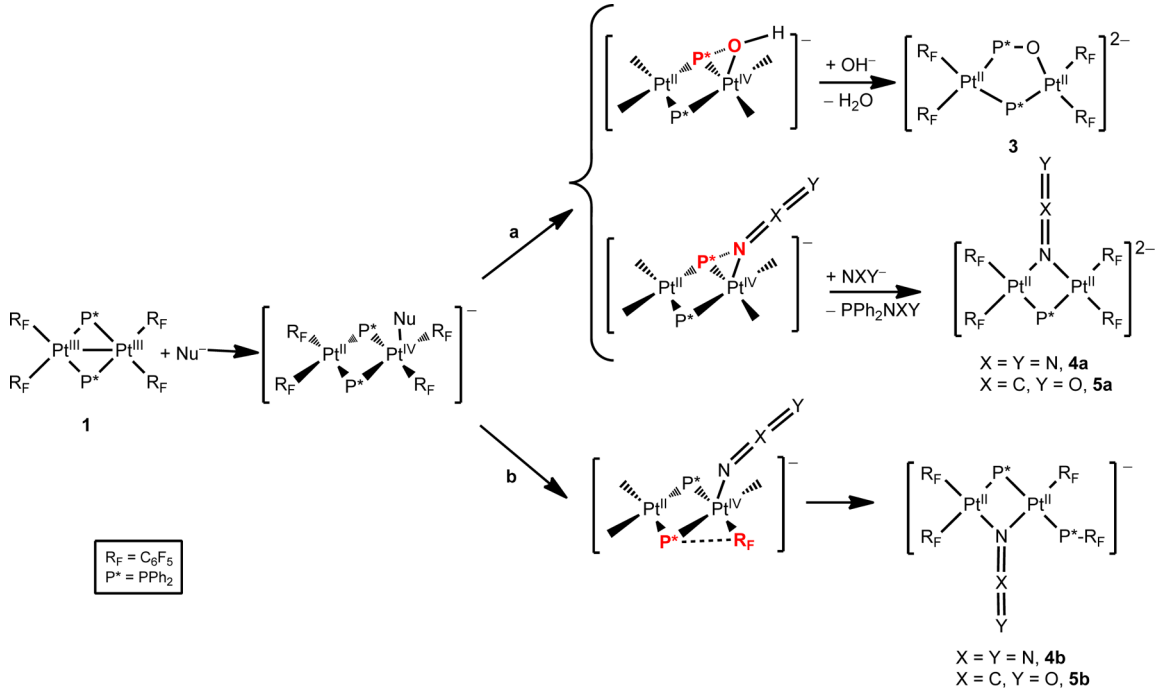

coordination of I^- to the M(III)−M′(III) type **B** complex[19,24,25] or the elimination of a I^- group from the M(II),M′(IV) type **C** complex[21,22] produces the unsaturated M(II),M′(IV) intermediate which evolves through a PPh_2/X reductive coupling with formation of P−C and P−O bonds. In this way complexes with $PPh_2C_6F_5$,[19,20,24−27] PPh_2bzq,[21] PPh_2hq,[22] PPh_2pic,[22] and PPh_2acac[22] ligands could be isolated. We have also identified in solution complexes with diphenyliodophosphine as a result of the reductive coupling between a diphenylphosphanido bridging ligand and the incoming ligand, the iodide group, with formation of a P−I bond.[22] Besides these studies, very little is known about the behavior of the M(III), M(III) phosphanido complexes and their role on the PPh_2/X reductive coupling.

Therefore, we have studied the reaction of several nucleophiles X^- with $[(R_F)_2Pt^{III}(\mu\text{-}PPh_2)_2Pt^{III}(R_F)_2]$*(Pt−Pt)* (**1**) and $[(R_F)_2Pt^{III}(\mu\text{-}PPh_2)_2Pt^{III}(\mu\text{-}PPh_2)_2Pt^{II}(R_F)_2]$*(Pt^{III}−Pt^{III})* (**2**) (smoothly obtained by Ag^+ oxidation of $[NBu_4]_2[(R_F)_2Pt^{II}(\mu\text{-}PPh_2)_2Pt^{II}(R_F)_2]$, and $[NBu_4]_2[(R_F)_2Pt^{II}(\mu\text{-}PPh_2)_2Pt^{II}(\mu\text{-}PPh_2)_2Pt^{II}(R_F)_2]$, respectively) in order to establish the ability of these two complexes to produce PPh_2/X reductive coupling and to ascertain the nature of the final Pt(II) complexes.

RESULTS AND DISCUSSION

Reaction of $[(R_F)_2Pt^{III}(\mu\text{-}PPh_2)_2Pt^{III}(R_F)_2]$*(Pt−Pt)* (1) with OH^-, N_3^-, and OCN^-. Complex **1** shows the two Pt(III) centers in square planar environments, a Pt−Pt bond (30 valence electron count), and only one type of terminal ligand. The attack of a nucleophile to **1** is expected to occur at one of the two equivalent metal centers with rupture of the Pt−Pt bond and formation of an unsaturated Pt(II),Pt(IV) derivative.[3,28] Such a mixed-valence species can then evolve to the more stable Pt(II),Pt(II) system, via a reductive coupling.[29,30]

The addition of N^nBu_4OH to a CH_2Cl_2 solution of the Pt(III),Pt(III) **1** complex (2:1 molar ratio) gives the platinum(II) derivative $[NBu_4]_2[(R_F)_2Pt^{II}(\mu\text{-}OPPh_2)(\mu\text{-}PPh_2)Pt^{II}(R_F)_2]$ (**3**) in which the two metal centers with formal oxidation state (II) are bridged by a phosphanido and a phosphinito ligand (Scheme 3). Despite several attempts at crystallization we were not able to complete X-ray studies of the structure of complex **3** due to low quality of the crystals. However, the connectivity of

dx.doi.org/10.1021/ic401689c | Inorg. Chem. XXXX, XXX, XXX−XXX

the atoms of the anion was established unambiguously and is shown in Scheme 3.

The addition of NaN_3 to a yellow solution of **1** in acetone at room temperature, followed by addition of $[NBu_4]ClO_4$, afforded a mixture of $[NBu_4]_2[(R_F)_2Pt^{II}(\mu\text{-}N_3)(\mu\text{-}PPh_2)\text{-}Pt^{II}(R_F)_2]$ (**4a**) and $[NBu_4][(R_F)_2Pt^{II}(\mu\text{-}N_3)(\mu\text{-}PPh_2)Pt^{II}(R_F)\text{-}(PPh_2R_F)]$ (**4b**) (Scheme 3). It is notable that the four R_F ligands of the Pt(III),Pt(III) starting material are maintained in the Pt(II),Pt(II) complex **4a**, but the two metal centers are joined by a phosphanido and an azide bridging group, indicating that in all likelihood a PPh_2/N_3 reductive elimination took place (Scheme 3) with decomposition of the very unstable PPh_2N_3 formed,[31−33] along with the coordination of an azide group as end-on ($\mu_{1,1}$-N_3) mode. In **4b** the two Pt(II) centers are also joined by a phosphanido and an azide bridging groups, but three R_F and a new $PPh_2(C_6F_5)$ ligand are bonded to the platinum centers, indicating the occurrence of a PPh_2/C_6F_5 reductive coupling (Scheme 3). Complex **4a** was isolated as a pure sample (see Experimental Section), but we were not able to obtain a pure sample of complex **4b**. Nevertheless, the structure of **4b** could be inferred by comparing the characteristic spectroscopic features with those observed for the previously reported $[NBu_4][(R_F)_2Pt^{II}(\mu\text{-}I)(\mu\text{-}PPh_2)Pt^{II}(R_F)\text{-}(PPh_2R_F)]$.[19]

Finally, we have carried out the reaction of acetone solutions of **1** with KOCN, followed by addition of $[NBu_4]ClO_4$, with a method similar to the previous reaction with NaN_3. When the reaction was carried out in a 1:2 molar ratio, a mixture of products was once again obtained. In this mixture, complexes $[NBu_4]_2[(R_F)_2Pt^{II}(\mu\text{-}NCO)(\mu\text{-}PPh_2)Pt^{II}(R_F)_2]$ (**5a**) (Scheme 3) and $[NBu_4][(R_F)_2Pt^{II}(\mu\text{-}NCO)(\mu\text{-}PPh_2)Pt^{II}(R_F)(PPh_2R_F)]$ (**5b**) analogous to **4a** and **4b**, respectively, were identified by ^{31}P and ^{19}F NMR spectroscopy. All attempts to isolate samples of pure **5a** as well as to separate complex **5a** from **5b**, even using different counterions in the processes, were unsuccessful. The addition of an excess of KOCN to acetone solutions of **1** allowed the isolation of **5b** as a pure sample (although signals of other unidentified species were observed in the ^{31}P NMR spectrum of the crude reaction product, no signals due to complex **5a** were observed). However, crystals of **5a** suitable for X-ray purposes were collected from a concentrated solution of one of the mixtures of **5a** and **5b** (see Experimental Section).

The structures of complexes **4a** and **5a** were established by X-ray diffraction studies. Figures 1 and 2 show views of the corresponding complexes, and Tables 1 and 2 list a selection of relevant bond distances and angles. Complexes **4a** and **5a** display similar structures, with the only difference being one of the bridging ligands, that is N_3^- for **4a** and NCO^- for **5a**. They are dinuclear complexes in which the "$Pt(R_F)_2$" fragments are held together by a PPh_2 and a N_3^- or NCO^- bridges. The Pt atoms lie in the center of conventional square planar environments. The complexes are not planar, with the dihedral angle between the two best Pt square planes 164.1(1)° for **4a** and 163.7(1)° for **5a**. The intermetallic distance is 3.400(1) Å for **4a** and 3.372(1) Å for **5a**, excluding any type of intermetallic interaction, as expected for a dinuclear derivative with a 32 valence electron count (VEC). For both complexes, the environment of the N bridging atom is planar (see Tables 1 and 2), and the geometry of the N−N−N and N−C−O fragments are linear. The Pt−N distances in **4a**, 2.105(4) and 2.101(4) Å, are shorter than those found in the complex with the "$Pt_3(\mu\text{-}1,1,1\text{-}N_3)$" fragment,[34] slightly larger than the Pt−N distances of terminal azido platinum derivatives,[35−37] and

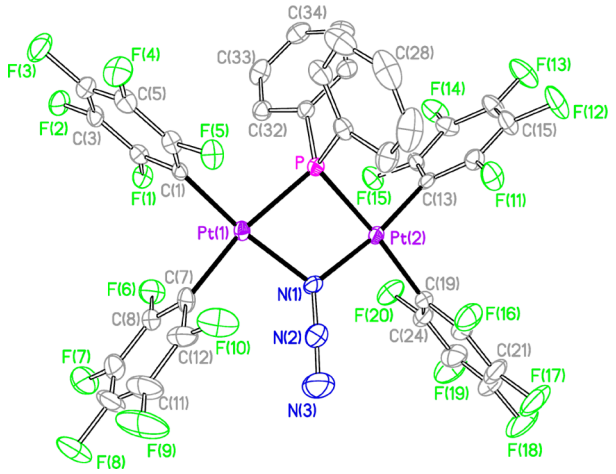

Figure 1. View of the molecular structure of the anion of the complex $[NBu_4]_2[(R_F)_2Pt^{II}(\mu\text{-}N_3)(\mu\text{-}PPh_2)Pt^{II}(R_F)_2]$ (**4a**).

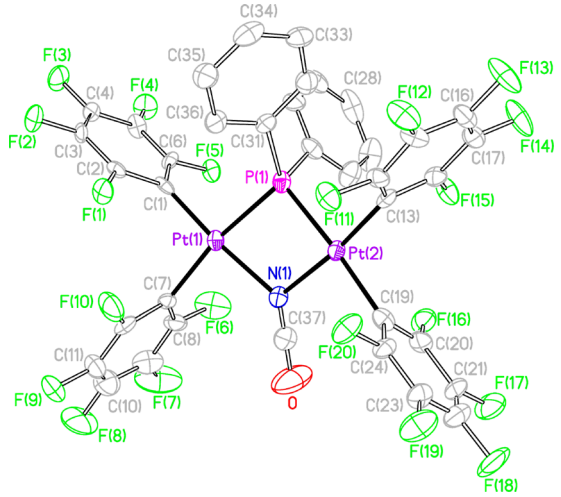

Figure 2. View of the molecular structure of the anion of the complex $[NBu_4]_2[(R_F)_2Pt^{II}(\mu\text{-}NCO)(\mu\text{-}PPh_2)Pt^{II}(R_F)_2]$ (**5a**).

similar to the Pt−N distances found in complexes with the "$Pt(\mu\text{-}1,1\text{-}N_3)Pt$" skeleton.[38] In the case of the cyanate derivative no complexes with the skeleton "$M(\mu\text{-}1,1\text{-}NCO)M$" have been characterized by X-ray diffraction (CSD search). It is to note that in both cases the two bridging ligands are bonded to the platinum centers through both a soft and a hard donor atom (P and N) of the PPh_2 and N_3^- or NCO^-, respectively.

The HRMS(−) spectrograms of complexes **3**, **4a**, and **5b** showed intense signals ascribable to the anions of the complexes with an isotope pattern superimposable to that calculated on the basis of the proposed formula.

The ^{19}F NMR spectrum of **3** (deuteroacetone solution) shows 12 signals: four signals of the same intensity (2 F each) in the *o*-F region with platinum satellites, four signal of the same intensity (2 F each) due to *m*-F atoms, and four signals assignable to the four *p*-F atoms. This pattern indicates that the four C_6F_5 groups are inequivalent, and within each ring the two *o*-F atoms (and *m*-F atoms) are equivalent. The spectra of **4a** and **5a** (deuteroacetone solution) show six signals in 2:2:2:1:2:1 intensity ratio, as expected for a complex with two types of inequivalent pentafluorophenyl rings: two rings in position *trans* to the Pt−N bonds and two rings in position

dx.doi.org/10.1021/ic401689c | Inorg. Chem. XXXX, XXX, XXX−XXX

Table 1. Selected Bond Lengths (Å) and Angles (deg) for $[NBu_4]_2[(R_F)_2Pt^{II}(\mu\text{-}N_3)(\mu\text{-}PPh_2)Pt^{II}(R_F)_2]CH_2Cl_2{\cdot}0.5n\text{-}C_6H_{14}$ ($4a{\cdot}CH_2Cl_2{\cdot}0.5n\text{-}C_6H_{14}$)

Pt(1)−C(1)	2.001(4)	Pt(1)−C(7)	2.056(4)	Pt(1)−N(1)	2.105(4)
Pt(1)−P	2.3140(11)	Pt(2)−C(13)	2.007(4)	Pt(2)−C(19)	2.062(4)
Pt(2)−N(1)	2.101(4)	Pt(2)−P	2.3067(11)	N(1)−N(2)	1.206(5)
N(2)−N(3)	1.155(6)				
C(1)−Pt(1)−C(7)	93.46(16)		C(1)−Pt(1)−N(1)	173.03(15)	
C(7)−Pt(1)−N(1)	92.62(15)		C(1)−Pt(1)−P	96.86(11)	
C(7)−Pt(1)−P	169.67(12)		N(1)−Pt(1)−P	77.05(10)	
C(13)−Pt(2)−C(19)	91.05(16)		C(13)−Pt(2)−N(1)	171.97(14)	
C(19)−Pt(2)−N(1)	96.82(15)		C(13)−Pt(2)−P	94.87(11)	
C(19)−Pt(2)−P	173.98(12)		N(1)−Pt(2)−P	77.30(10)	
Pt(2)−P−Pt(1)	94.74(4)		N(2)−N(1)−Pt(2)	126.2(3)	
N(2)−N(1)−Pt(1)	125.8(3)		Pt(2)−N(1)−Pt(1)	107.89(15)	
N(3)−N(2)−N(1)	178.5(6)				

Table 2. Selected Bond Lengths (Å) and Angles (deg) for $[NBu_4]_2[(R_F)_2Pt^{II}(\mu\text{-}NCO)(\mu\text{-}PPh_2)Pt^{II}(R_F)_2]CH_2Cl_2{\cdot}0.5n\text{-}C_6H_{14}$ ($5a{\cdot}CH_2Cl_2{\cdot}0.5n\text{-}C_6H_{14}$)

Pt(1)−C(1)	1.964(7)	Pt(1)−C(7)	2.076(7)	Pt(1)−N(1)	2.155(6)
Pt(1)−P(1)	2.313(2)	Pt(2)−C(13)	1.963(7)	Pt(2)−C(19)	2.062(8)
Pt(2)−N(1)	2.139(6)	Pt(2)−P(1)	2.293(2)	N(1)−C(37)	1.177(9)
O−C(37)	1.188(9)				
C(1)−Pt(1)−C(7)	93.3(3)		C(1)−Pt(1)−N(1)	174.6(2)	
C(7)−Pt(1)−N(1)	91.0(2)		C(1)−Pt(1)−P(1)	96.42(19)	
C(7)−Pt(1)−P(1)	170.31(19)		N(1)−Pt(1)−P(1)	79.35(16)	
C(13)−Pt(2)−C(19)	90.8(3)		C(13)−Pt(2)−N(1)	173.8(2)	
C(19)−Pt(2)−N(1)	95.2(2)		C(13)−Pt(2)−P(1)	94.0(2)	
C(19)−Pt(2)−P(1)	175.27(19)		N(1)−Pt(2)−P(1)	80.11(16)	
Pt(2)−P(1)−Pt(1)	94.13(8)		C(37)−N(1)−Pt(2)	127.7(6)	
C(37)−N(1)−Pt(1)	127.3(6)		Pt(2)−N(1)−Pt(1)	103.5(2)	
N(1)−C(37)−O	179.7(11)				

trans to the Pt−P bonds. Signals due to complexes **4b** and **5b** are unambiguously identified in the ^{19}F NMR spectra, and the data compare well with those obtained for the previously reported $[NBu_4][(R_F)_2Pt^{II}(\mu\text{-}I)(\mu\text{-}PPh_2)Pt^{II}(R_F)(PPh_2R_F)]$.[19] The ^{19}F signals due to the new ligand $PPh_2C_6F_5$ appear well separated from those due to the three R_F groups bonded to Pt,[20,24−26,39] and they can be easily assigned in our spectra. The $^{31}P\{^1H\}$ NMR spectra of **3**−**5** in deuteroacetone solution are very informative. The chemical shift of P atom of phosphanido bridging ligands in **1**, δ 281.7, decreases significantly in **3**−**5** as is to be expected due to the change of a "$M(\mu\text{-}PPh_2)_2M$" fragment with metal−metal bond into a saturated "$M(\mu\text{-}X)(\mu\text{-}PPh_2)M$" fragment without Pt−Pt bond.[25,40−42] The transformation of a phosphanido ligand into a *P,O*-bridging phosphinito (complex **3**) or a terminal $PPh_2C_6F_5$ phosphane group (complexes **4b** and **5b**) results in signals at δ 127.1, δ 13.4, and δ 12.6, respectively. All data obtained from the spectra are collected in the Experimental Section.

The detection of ^{195}Pt resonances for Pt complexes with C_6F_5 ligands is usually tricky, because of multiple $^{195}Pt-^{19}F$ couplings along with all other couplings (i.e., with ^{31}P) giving rise to very broad signals. In order to get spectra of good quality, and given that no proton is strongly scalar coupled to each platinum, we decided to carry out $^{195}Pt\{^{19}F\}$ experiments for complexes **3**, **4a**, and **5b**. Figure 5 shows the $^{195}Pt\{^{19}F\}$ spectrum of **3**, showing a doublet for Pt^2 at δ −3719 ($^1J_{Pt-P}$ = 2185 Hz) and a doublet of doublets for Pt^1 at δ −4498 ($^1J_{Pt-P}$ = 3020 and 1840 Hz). For complexes **4a** and **5b** the ^{195}Pt signals were found at δ −3381 (**4a**) and at δ −3522 and δ −3953 (**5b**). ^{195}Pt satellites originated from the geminal $^{195}Pt-^{195}Pt$ coupling were observable in the $^{195}Pt\{^{19}F\}$ spectrum of **5b**, from which a $^2J_{Pt-Pt}$ = 1310 Hz could be extracted. The chemical shifts found for **3**, **4a**, and **5b** lie in the range expected for phosphanido bridged diplatinum complexes.

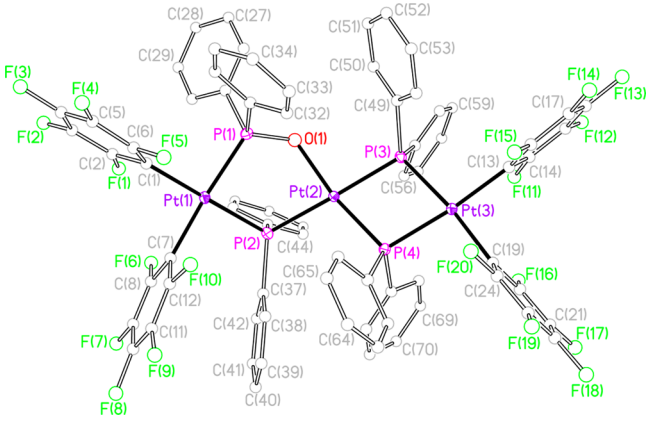

Figure 3. View of the molecular structure of the anion of the complex $[NBzMe_3]_2[(R_F)_2Pt^{II}(\mu\text{-}Ph_2PO)(\mu\text{-}PPh_2)Pt^{II}(\mu\text{-}PPh_2)_2Pt^{II}(R_F)_2]{\cdot}(\mathbf{6'})$.

The IR spectra in the solid state of pure samples of **3**, **4a**, and **5b** were recorded. The absorption in the 950 cm^{-1} region in the pentafluorophenyl derivatives is related with the oxidation state of the metal center bonded to the C_6F_5 group. This absorption appears at 947, 951, and 953 cm^{-1} in the Pt(II) complexes **3**, **4a**, and **5b**, respectively, while it appears at 964 cm^{-1} in the Pt(III) starting material **1**.[23] This red shift of the frequencies is in agreement with the change of the formal

dx.doi.org/10.1021/ic401689c | *Inorg. Chem.* XXXX, XXX, XXX−XXX

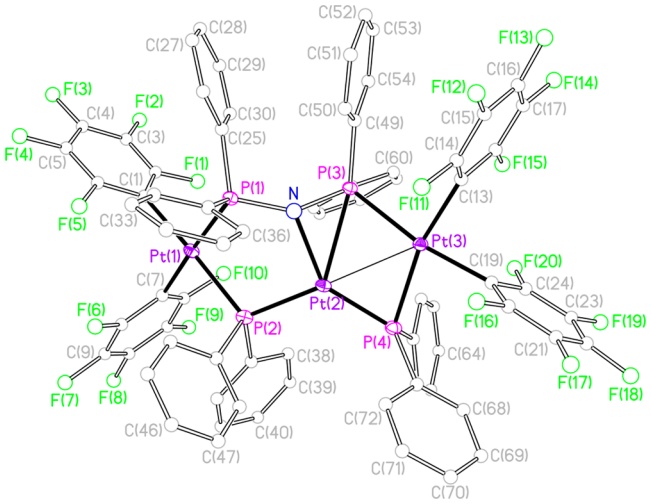

Figure 4. View of the molecular structure of the anion of the complex $[PPh_3Me][Pt_3^{II}(\mu_3\text{-}Ph_2PNPPh_2)(\mu\text{-}PPh_2)_2(R_F)_4]\cdot(7')$.

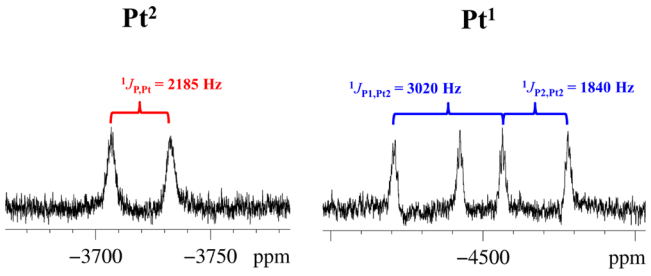

Figure 5. $^{195}Pt\{^{19}F\}$ spectrum of **3** (acetone-d_6, 293 K).

oxidation state of the platinum centers.[23] The spectra of **4a** and **5b** exhibit an strong absorption at 2067 and 2171 cm^{-1}, respectively, corresponding to the stretching vibrations of the azide and cyanate ligand.[43,44]

The reactivity exhibited by **1** toward OH^-, N_3^-, and OCN^- can be easily explained (Scheme 3) assuming that the nucleophile coordinates to one of the platinum(III) centers of **1** through the oxygen atom for the OH^- or the nitrogen atom for the N_3^- and NCO^- groups, giving rise to an anionic, unsaturated Pt(II),Pt(IV) intermediate. Taking into account that five-coordinated Pt(IV) intermediates are usually proposed in reductive elimination processes and some of them crystallographically characterized,[45−54] the unsaturated Pt(II),Pt(IV) species proposed in Scheme 3 could evolve in two different ways: (a) reductive coupling between the phosphanido bridging ligand and the added nucleophile (affording **3** and **4a**/**5a** with $PPh_2(NXY)$ elimination) or (b) coupling between the phosphanido bridging ligand and the C_6F_5 ligand initially present in the starting material (yielding **4b** and **5b**). In both cases, the intermediacy of a five-coordinated P atom, a well established fact for both phosphane and phosphanide derivatives,[40,55−61] has to be invoked.

The addition of OH^- can take place with formation of a coordinated PPh_2OH (PPh_2/OH coupling) which affords the *P,O*-bridging phosphinito complex **3** upon deprotonation by a second hydroxide (Scheme 3). Some phosphinito bridged complexes showing the Pt−P−O−Pt sequence have been structurally characterized,[62−67] and examples with both μ-phosphanido and μ-phosphinito Pt(I) derivatives have been synthesized and studied.[68−73] On the other hand, we have recently reported the synthesis of $[(PPh_2R_F)(R_F)Pt^{II}(\mu\text{-}OH)(\mu\text{-}PPh_2)Pt^{II}(dppe)][ClO_4]$[27] which seems to be formed from an undetected Pt(III),Pt(III) cationic intermediate $[(R_F)_2Pt^{III}(\mu\text{-}PPh_2)_2Pt^{III}(dppe)][ClO_4]_2$ through a PPh_2/C_6F_5 coupling and the coordination of a bridging OH, but we did not observe the PPh_2/OH coupling as in **3**. If the proposed azide or cyanate Pt(II),Pt(IV) intermediates evolve according to pathway a, a P−N bond can be formed by reductive coupling between phosphanido and azide (or cyanate) giving a coordinate PPh_2N_3 (or PPh_2NCO) which eliminates and easily decomposes.[32,33] Finally, the coordination environment of the metal centers can be completed with a $\mu_{1,1}$-N_3 ligand (or NCO), and **4a** (or **5a**) could be formed. Should pathway b be operative, the nucleophile would behave initially as a spectator, and the evolution of the proposed unsaturated intermediate of Pt(II),Pt(IV) could produce the reductive coupling between a phosphanido ligand and a pentafluorophenyl group. The coordination of the metal centers would be completed by bridging coordination of the nucleophile added affording **4b** and **5b**, i.e., a process similar to the one which produces $[NBu_4][(R_F)_2Pt^{II}(\mu\text{-}I)(\mu\text{-}PPh_2)Pt^{II}(R_F)(PPh_2R_F)]$.[19] The formation of **3**, **4a,b**, and **5a,b** mixtures indicates that the formation of a P−O bond is favored with respect the P−C coupling but the P−N bond formation competes with the P−C coupling in these intermediates.

Reaction of $[(R_F)_2Pt^{III}(\mu\text{-}PPh_2)_2Pt^{III}(\mu\text{-}PPh_2)_2Pt^{II}(R_F)_2]$*(Pt−Pt)* (2) with OH^- and N_3^-. The preparation of the trinuclear Pt(III),Pt(III),Pt(II) complex $[(R_F)_2Pt^{III}(\mu\text{-}PPh_2)_2Pt^{III}(\mu\text{-}PPh_2)_2Pt^{II}(R_F)_2]$*(Pt−Pt)* (**2**) was reported some years ago.[74] Complex **2** is also an unsaturated compound which contains two Pt(III) centers suitable to react with nucleophiles as in **1**. However, **2** displays the Pt(III) centers in two different chemical environments: the terminal Pt(III) bonded to two C_6F_5 and two PPh_2, and the central Pt(III), bonded to four phosphanido ligands. This situation could differentiate the reactivity of the two Pt(III) centers toward the nucleophiles. We have studied the reaction of **2** toward OH^- and N_3^-.

The addition of N^nBu_4OH or NaN_3 (as methanol solutions) to a CH_2Cl_2 or acetone suspension of the trinuclear Pt(III),Pt(III),Pt(II) complex **2** gives, after work-up, the trinuclear platinum(II) derivatives $[NBu_4]_2[(R_F)_2Pt^{II}(\mu\text{-}Ph_2PO)(\mu\text{-}PPh_2)Pt^{II}(\mu\text{-}PPh_2)_2Pt^{II}(R_F)_2]$ (**6**) and $[NBu_4][Pt_3^{II}(\mu_3\text{-}Ph_2PNPPh_2)(\mu\text{-}PPh_2)_2(R_F)_4]$ (**7**), respectively (Scheme 4).

Complexes **6** and **7** show the three platinum centers in formal +2 oxidation state and one PPh_2O^- group bridging two platinum centers in **6** or one $PPh_2NPPh_2^-$ group coordinated as bridging ligand to three platinum atoms in **7**. In both cases the pentafluorophenyl groups remain bonded in mutual *cis*-position to the two terminal platinum centers. Unfortunately, only low quality crystals of **6** and **7** for X-ray studies were obtained. The complete X-ray studies could be performed for the complexes $[NBzMe_3]_2[(R_F)_2Pt^{II}(\mu\text{-}Ph_2PO)(\mu\text{-}PPh_2)Pt^{II}(\mu\text{-}PPh_2)_2Pt^{II}(R_F)_2]$ (**6′**) and $[PPh_3Me][Pt_3^{II}(\mu_3\text{-}Ph_2PNPPh_2)(\mu\text{-}PPh_2)_2)(R_F)_4]$ (**7′**) (see Experimental Section). Figures 3 and 4 show views of the corresponding anions of the complexes, and Tables 3 and 4 list a selection of relevant bond distances and angles.

In the anion of **6′** (see Figure 3) the three metal atoms are disposed in an almost linear arrangement [Pt(1)−Pt(2)−Pt(3) = 156.2(1)°]. Pt(1) and Pt(2) are supported by a phosphanido, $P(2)Ph_2$, and a phosphinito, $Ph_2P(1)$−O, bridging ligands whereas Pt(2) and Pt(3) are supported by two PPh_2 groups,

dx.doi.org/10.1021/ic401689c | *Inorg. Chem.* XXXX, XXX, XXX−XXX

Scheme 4

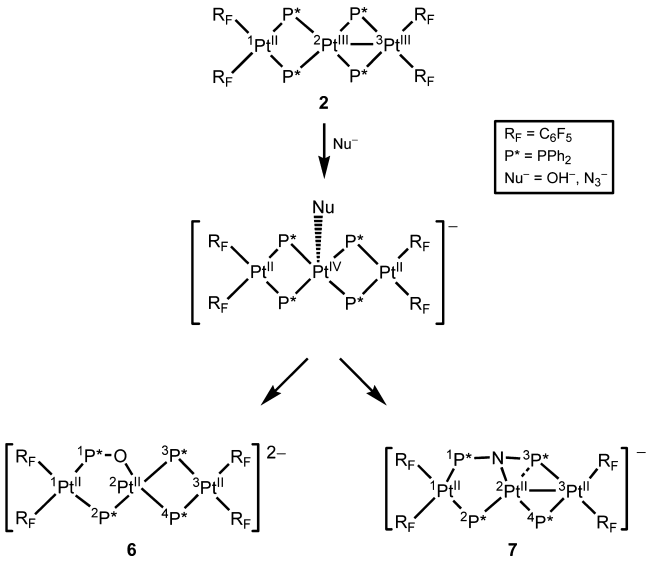

P(3) and P(4). Each terminal metal center, Pt(1) and Pt(3), is coordinated to two pentafluorophenyl groups. The three platinum atoms lie in the center of square planar environments in such a way that the core of the anion is not planar. The five membered ring formed by phosphinite P(1)−O, P(2) phosphanide, Pt(1) and Pt(2) atoms is not planar; the dihedral angle between the best C(1), C(7), Pt(1), P(1), P(2) plane and the best O, P(2), Pt(2), P(3), and P(4) plane is 39.6(1)°, and that between the best O, P(2), Pt(2), P(3), and P(4) plane and the best C(13), C(19), Pt(3), P(3), and P(4) plane is 8.6(1)°. The long intermetallic distances [Pt(1)···Pt(2) = 3.846(1) Å, Pt(2)···Pt(3) = 3.599(1) Å] discard any kind of bonding interaction between the metal centers, as expected for a saturated trinuclear platinum complex with 48 valence electron count.

The structure of the anion of **7′** is shown in Figure 4. The most remarkable feature is that it contains the bis(diphenylphosphanyl)amide ligand $(Ph_2P)_2N^-$ which has to be formed as a result of the coupling of two PPh_2^- groups and the N_3^- ligand. Below we will comment on the structural characteristics of this ligand in the anion of **7′** and its formation. The whole anion, which is trinuclear, displays two pentafluorophenyl groups coordinated to each terminal platinum center, Pt(1) and Pt(3). The phosphanido group, $P(2)Ph_2$, is bridging Pt(1) and Pt(2) centers while $P(4)Ph_2$ bridges Pt(2) and Pt(3). In addition, the metal mediated formed bis(diphenylphosphanyl)amide ligand bonds the metal centers in an unprecedented way: P(1) is bonded to Pt(1) and P(3) is bonded to Pt(3) while N and P(3) are bonded to Pt(2). The Pt(1)−P(1) and Pt(3)−P(3) distances (2.2885(9) Å and 2.3712(10) Å) are the expected for conventional Pt−P bonds. The fragment N−P(3) can be considered interacting with Pt(2) through a Pt(2)−N covalent bond and Pt(2)−P(3) weak interaction with a Pt(2)−P(3) distance of 2.6207(9) Å. Notwithstanding, considering that the N center is nearly planar (the angles around N atom equals 354.3°) and the two P(1,3)−N (distances are 1.662(3) and 1.636(3) Å, respectively) are shorter than the single-bond P−N, a π-bonding contribution to these P−N bonds should be considered and a η^2 coordination mode of the P(3)−N fragment, to Pt(2) could be invoked.[75−80] Such a type of interaction is well represented usually in lanthanoid bis(diphenylphosphanyl)amido complexes.[33,75,81−85] In **7′** the bis(diphenylphosphanyl)amide behaves as a six electron donor ligand and coordinates to the three platinum centers in an unprecedented μ_3-bridge mode.[86] This type of coordination implies that the P(3) atom is five-coordinated.[55−60] The total valence electron count of the skeleton is 46, and a Pt−Pt bond should be expected. The very different intermetallic distances (Pt(1)−Pt(2) 3.761(1) Å, Pt(2)−Pt(3) 2.7374(2) Å) are in agreement with the existence of an intermetallic bond between Pt(2) and Pt(3) centers.[87]

The two platinum(III) centers of the Pt(III),Pt(III),Pt(II) starting material **2** are different: the terminal Pt(III), which is analogous to the platinum atoms of the Pt(III),Pt(III) dinuclear complex **1**, and the central platinum(III) which is bonded to four P atoms. If it is assumed that the reaction starts with the coordination of the OH^- or N_3^- groups to a platinum(III) center, the formation of **6** and **7** seems to indicate that the coordination of the nucleophile to the central platinum(III) is preferred to the coordination on the terminal Pt(III) center. In this way trinuclear Pt(II),Pt(IV),Pt(II) intermediates could be formed. The reductive coupling between the two groups bonded to the central platinum(IV), phosphanido and hydroxide or azide, forms P−O or P−N bonds and leave the metal center in formal oxidation state (II). Thus, the formation of **6** takes place in a similar way to the formation of the dinuclear complex **3**. However, the formation of complex **7** implies a more complicated process. It could be assumed that a

Table 3. Selected Bond Lengths (Å) and Angles (deg) for $[NBzMe_3]_2[(R_F)_2Pt^{II}(\mu\text{-}Ph_2PO)(\mu\text{-}PPh_2)Pt^{II}(\mu\text{-}PPh_2)_2Pt^{II}(R_F)_2]\cdot 3Me_2CO$ (6′·3Me$_2$CO)

Pt(1)−C(1)	2.062(4)	Pt(1)−C(7)	2.062(4)	Pt(1)−P(1)	2.2835(10)
Pt(1)−P(2)	2.3137(10)	Pt(2)−O(1)	2.116(2)	Pt(2)−P(4)	2.2590(10)
Pt(2)−P(3)	2.3184(10)	Pt(2)−P(2)	2.3536(10)	Pt(3)−C(13)	2.064(4)
Pt(3)−C(19)	2.065(4)	Pt(3)−P(3)	2.3015(10)	Pt(3)−P(4)	2.3040(10)
P(1)−O(1)	1.553(3)				
C(1)−Pt(1)−C(7)	88.81(14)		C(1)−Pt(1)−P(1)	93.75(10)	
C(7)−Pt(1)−P(1)	174.84(10)		C(1)−Pt(1)−P(2)	177.61(10)	
C(7)−Pt(1)−P(2)	92.07(10)		P(1)−Pt(1)−P(2)	85.54(4)	
O(1)−Pt(2)−P(4)	169.69(6)		O(1)−Pt(2)−P(3)	94.42(7)	
P(4)−Pt(2)−P(3)	76.75(4)		O(1)−Pt(2)−P(2)	82.12(7)	
P(4)−Pt(2)−P(2)	107.46(3)		P(3)−Pt(2)−P(2)	169.99(3)	
C(13)−Pt(3)−C(19)	89.62(14)		C(13)−Pt(3)−P(3)	97.14(10)	
C(19)−Pt(3)−P(3)	173.22(10)		C(13)−Pt(3)−P(4)	172.65(9)	
C(19)−Pt(3)−P(4)	97.08(10)		P(3)−Pt(3)−P(4)	76.21(3)	

dx.doi.org/10.1021/ic401689c | Inorg. Chem. XXXX, XXX, XXX−XXX

Table 4. Selected Bond Lengths (Å) and Angles (deg) for $[PPh_3Me][Pt_3^{II}(\mu_3\text{-}Ph_2PNPPh_2)(\mu\text{-}PPh_2)_2(R_F)_4]\cdot Me_2CO\cdot n\text{-}C_6H_{14}$ (7′·$Me_2CO\cdot n\text{-}C_6H_{14}$)

Pt(1)−C(7)	2.070(4)	Pt(1)−C(1)	2.075(4)	Pt(1)−P(1)	2.2885(9)
Pt(1)−P(2)	2.3266(10)	Pt(2)−N	2.096(3)	Pt(2)−P(4)	2.1646(10)
Pt(2)−P(2)	2.2780(10)	Pt(2)−P(3)	2.6207(9)	Pt(2)−Pt(3)	2.7374(2)
Pt(3)−C(19)	2.065(4)	Pt(3)−C(13)	2.068(3)	Pt(3)−P(3)	2.3712(10)
Pt(3)−P(4)	2.3989(9)	P(1)−N	1.662(3)		
C(7)−Pt(1)−C(1)	86.18(14)		C(7)−Pt(1)−P(1)	176.54(11)	
C(1)−Pt(1)−P(1)	95.06(10)		C(7)−Pt(1)−P(2)	89.82(10)	
C(1)−Pt(1)−P(2)	175.93(10)		P(1)−Pt(1)−P(2)	88.90(3)	
N−Pt(2)−P(4)	143.29(9)		N−Pt(2)−P(2)	92.68(8)	
P(4)−Pt(2)−P(2)	123.06(4)		N−Pt(2)−P(3)	38.62(8)	
P(4)−Pt(2)−P(3)	105.52(3)		P(2)−Pt(2)−P(3)	125.82(3)	
C(19)−Pt(3)−C(13)	84.22(14)		C(19)−Pt(3)−P(3)	169.65(10)	
C(13)−Pt(3)−P(3)	87.55(10)		C(19)−Pt(3)−P(4)	81.99(10)	
C(13)−Pt(3)−P(4)	166.03(10)		P(3)−Pt(3)−P(4)	106.41(3)	
P(3)−N−P(1)	143.20(19)		P(3)−N−Pt(2)	88.29(13)	
P(1)−N−Pt(2)	122.75(15)				

reductive coupling between a bridging phosphanido ligand and the terminal azide group takes place with formation of a Pt(1)−P(1)−N−Pt(2) system. The formation of the N−P(3) has to take place with concomitant breaking off the Pt(2)−P(3) bond and elimination of N_2. The formation of the P−N bonds in some transition metal complexes has been observed,[77−79] and although the synthesis of complexes with the diphosphanylamide $(Ph_2P)_2N^-$ group is known,[33,75] the synthesis of the bis(diphenylphosphanyl)amide ligand in **7** is unprecedented: it is formally the result of transformation of two phosphanido bridging groups, one terminal azido ligand, and a Pt(IV) center into a new three-dentate ligand, $(Ph_2P)_2N^-$, a Pt(II) center, and N_2. The $(Ph_2P)_2N^-$ group has been previously used as a polydentate ligand bonded to Pt, but is usually obtained through deprotonation of bis(diphenylphosphanyl)amine (dppa), $(Ph_2P)_2NH$, and used in coordination chemistry.[75,81−83,86] In complex **7** the coordination of the bis(diphenylphosphanyl)amide $(Ph_2P)_2N^-$ is unusual because the six-electron-donor ligand bridges the three platinum centers. Although the formation of the bis(diphenylphosphanyl)amide ligand seems very striking, it is notable that the bridging $Ph_2P{-}O^-$ ligand is isoelectronic with $Ph_2P{-}N(X)^-$, X = PPh_2, and the initial processes which afford **6** and **7** are actually analogous.

The HRMS(−) spectrograms of complexes **6** and **7** showed intense signals ascribable to the anions of the complexes with an isotope pattern superimposable to that calculated on the basis of the proposed formula.

The $^{31}P\{^1H\}$ NMR spectra of **6** and **7** in deuteroacetone solution shows four signals. The signals are broad as a consequence of unresolved coupling with the ^{19}F nuclei and are in full agreement with the solid state structure. Complex **6** shows at the low field of spectrum a signal at δ 123.6 due to the P atom of the new phosphinito group (P^1 see Figure 3 for atom numbering) and a doublet (290 Hz) at δ 13.9 assignable to P atom of the phosphanido group in the "Pt(μ-P^2Ph_2)Pt" fragment. Signals due to P^3 and P^4 appear at high field, as is expected for a four-membered "Pt(μ-PPh_2)$_2$Pt" ring without metal−metal bond.[88] In the spectrum of **7**, the signals due to P atoms of phosphanido groups appear at δ 140.6 and at δ 30.7 as broad singlets and are assigned to P^4 and P^2, respectively (see Figure 4 for atom numbering). These chemical shifts are those expected for single diphenylphosphanido "Pt(μ-PPh_2)Pt" system with and without metal−metal bond, respectively. The signals due to P atoms of the new bis(diphenylphosphanyl)-amide ligand appear centered at δ 128.4 and at δ 31.7 as broad doublets ($^2J_{P1,P3} \approx 70$ Hz). The signal at δ 128.4 shows only a pair of platinum satellites and is assigned to P^1. The signal due to P^3 and centered at δ 31.7 shows, besides platinum satellites due to the coupling with Pt^3 ($^1JPt^3,P^3 \approx 1700$ Hz), satellites due to the coupling with Pt^2 in agreement with the Pt(2)···P(3) distance in solid state (2.7374(2) Å). The value of this coupling between Pt^2 and P^3 (ca. 510 Hz) is in the range of that observed in other complex in which a pentacoordinated P atom of a phosphanido group bridges three platinum centers.[59]

^{31}P EXSY experiments carried out in acetone-d_6 solution revealed that complex **7** is fluxional. In fact, the ^{31}P EXSY spectrum at 323 K (Figure 6) shows exchange cross peaks

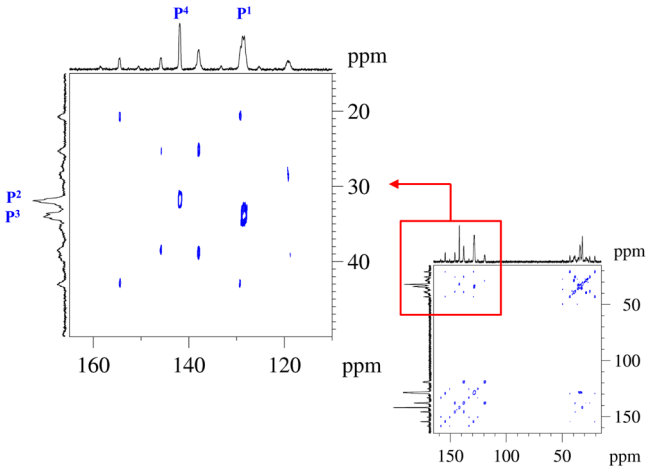

Figure 6. ^{31}P EXSY spectrum of **7** (acetone-d_6, 323 K).

between the signals at δ 128.4 and at δ 31.7 (P^1/P^3 exchange) and between the signals at δ 140.6 and at δ 30.7 (P^4/P^2 exchange). This outcome can be explained in terms of an equilibrium in which the Pt−Pt bond migrates from one side of the molecule to the other (Scheme 5). A Pt−Pt bond migration was already observed for **2** in acetone-d_6.[74] However, while in the case of **2** the fast exchange regime is attained already at room temperature, for **7** the fast exchange regime is not yet attained at 323 K.

dx.doi.org/10.1021/ic401689c | Inorg. Chem. XXXX, XXX, XXX−XXX

Scheme 5. Dynamic Behavior of 7 at 323 K

The ^{195}Pt NMR data for **6** and **7** were obtained carrying out, as in the cases of **3**, **4a**, and **5b**, ^{195}Pt{^{19}F} experiments. The signals of **6** were found at δ −4497 (Pt^1), δ −3657 (Pt^2), δ −3828 (Pt^3), while those for **7** were found at δ −4506 (Pt^1), δ −4868 (Pt^2),δ −5439 (Pt^3).

CONCLUDING REMARKS

Phosphanido groups have shown to be excellent ligands in development of molecular architecture and synthesis of specific transition metal complexes.[88,89] The strong P−M bond was thought to be the reason for the stability and the very low reactivity of polynuclear complexes containing bridging phosphanido ligands. Nevertheless, the oxidation of the metal centers has been shown to be a way to induce an unexpected reactivity on bridging phosphanido ligands.[20−22,25,90] In this work we conclude that, in the oxidized Pt(III) binuclear derivative, the phosphanido group reacts not only with the ligands bonded to the metal center in the starting material (formation of [NBu$_4$][(R$_F$)$_2$Pt^{II}(μ-X)(μ-PPh$_2$)Pt^{II}(R$_F$)-(PPh$_2$R$_F$)] **4b** and **5b**), but also with the suitable groups added to the oxidized intermediates as is demonstrated with the formation of **3**, **4a**, and **5a**. The synthesis of **6** and **7** indicates that the coordination of hydroxide or azide to the central platinum(III) of the trinuclear complex **2**, "Pt^{III}(μ-P)$_4$" fragment, is preferred to the coordination to the terminal platinum(III), "Pt^{III}(R$_F$)$_2$(μ-P)$_2$" fragment. The PPh$_2$/OH$^-$ or PPh$_2$/N$_3^-$ reductive couplings form new ligands in the coordination sphere of the platinum.

EXPERIMENTAL SECTION

General Procedures and Materials. C, H, and N analyses were performed with a Perkin-Elmer 2400 CHNS analyzer. IR spectra were recorded on a Perkin-Elmer Spectrum 100 FT-IR spectrometer (ATR in the range 250−4000 cm^{-1}). NMR spectra in solution were recorded on a Bruker AV-400 spectrometer with SiMe$_4$, CFCl$_3$, 85% H$_3$PO$_4$, and H$_2$PtCl$_6$ as external references for ^{1}H, ^{19}F, ^{31}P, and ^{195}Pt, respectively. ^{195}Pt{^{19}F} experiments were carried out setting the offset of the decoupler at the chemical shift of the *ortho*-F atoms of each complex. High resolution mass spectrometry (HRMS) was performed using a time-of-flight mass spectrometer equipped with an electrospray ion source (Bruker micrOTOF-Q II). The analyses were carried out in negative ion mode. The samples were introduced as acetonitrile solutions by continuous infusion with the aid of a syringe pump at a flow rate of 180 μL/h. The instrument was operated at end plate offset −500 V and capillary −4500 V. Nebulizer pressure was 0.3 bar (N$_2$) and the drying gas (N$_2$) flow 4 L/min. Drying gas temperature was set at 453 K. The software used for the simulations is Bruker Daltonics Data Analysis (version 4.0). Literature method was used to prepare the starting materials [(R$_F$)$_2$Pt^{III}(μ-PPh$_2$)$_2$Pt^{III}(R$_F$)$_2$][23] and [(R$_F$)$_2$Pt^{III}(μ-PPh$_2$)$_2$Pt^{II}(R$_F$)$_2$].[74]

Caution! *Azido complexes are potentially explosive, especially in the presence of organic ligands. Therefore, these compounds must be handled with care and prepared only in small amounts.*

Reaction of [(R$_F$)$_2$Pt^{III}(μ-PPh$_2$)$_2$Pt^{III}(R$_F$)$_2$](*Pt^{III}−Pt^{III}*) with N^{n}Bu$_4$OH. To a yellow solution of **1** (0.156 g, 0.110 mmol) in CH$_2$Cl$_2$ (25 mL) was added 0.220 mol of N^{n}Bu$_4$OH (0.22 mL of 1 M methanol solution). The solution was stirred at room temperature for 10 min, and the resulting pale yellow solution was evaporated to dryness. The residue was washed three times with ^{i}PrOH/hexane (1 mL/5 mL) and recrystallized from CH$_2$Cl$_2$/^{i}PrOH. Complex **3** (white solid) was filtered and washed with ^{i}PrOH (2 × 0.5 mL). Yield: 0.114 g, 54%. Anal. Found (Calcd for C$_{80}$F$_{20}$H$_{92}$N$_2$OP$_2$Pt$_2$): C, 49.67 (49.79); H, 4.80 (4.81); N 1.31 (1.45).

HRMS (−), exact mass for the dianion [C$_{48}$F$_{20}$H$_{20}$OP$_2$Pt$_2$]$^{2-}$: 721.9984 Da. Measured *m*/*z*: 721.9980 (M)$^{2-}$. ^{1}H NMR (acetone-*d*$_6$, 293 K, 400 MHz), δ: 7.69 (pseudo t, 2 H, $^3J_{H,H}$ = 8.2 Hz, *o*-H bonded to *P*Ph$_2$), 7.56 (pseudo t, 2 H, $^3J_{H,H}$ = 8.0 Hz, *o*-H bonded to *P*-O), 7.10 (t, 1 H, $^3J_{H,H}$ = 6.8 Hz, *p*-H bonded to *P*Ph$_2$), 7.04 (pseudo t, 2 H, $^3J_{H,H}$ = 7.2 Hz, *m*-H bonded to *P*Ph$_2$), 6.89 (t, 1 H, $^3J_{H,H}$ = 6.8 Hz, *p*-H bonded to *P*Ph$_2$), 6.82 (pseudo t, 2 H, $^3J_{H,H}$ = 7.2 Hz, *m*-H bonded to *P*Ph$_2$), 3.49 (m, 16H, NBu$_4^+$), 1.87 (m, 16 H, NBu$_4^+$), 1.48 (pseudo sextet, 16H, $^3J_{H,H}$ = 7.4 Hz, NBu$_4^+$), 1.02 (t, 24 H, $^3J_{H,H}$ = 7.4 Hz, NBu$_4^+$). ^{19}F NMR (acetone-*d*$_6$, 293 K, 376.5 MHz), δ: −114.1 (2 *o*-F, $^3J_{Pt,F}$ = 308 Hz), −115.2 (2 *o*-F, $^3J_{Pt,F}$ = 334 Hz), −116.4 (2 *o*-F, $^3J_{Pt,F}$ = 349 Hz), −116.7 (2 *o*-F, $^3J_{Pt,F}$ = 526 Hz), −168.7 (2 *m*-F), −169.0 (2 *m*-F), −169.2 (2 *m*-F), −169.7 (1 *p*-F), −170.3 (1 *p*-F), −170.6 (1 *p*-F), −171.7 (2 *m*-F), −173.6 (1 *p*-F). ^{31}P{^{1}H} NMR (acetone-*d*$_6$, 293 K, 162.0 MHz), δ: 127.1 ($^1J_{P,Pt1}$ = 3020 Hz, *P*-O), 0.1 ($^1J_{P,Pt2}$ = 2185, $^1J_{P,Pt1}$ = 1840 Hz, *P*Ph$_2$) ppm. ^{195}Pt{^{19}F} NMR (acetone-*d*$_6$, 293 K, 86 MHz), δ: −3719 (d, $^1J_{Pt2,P}$ = 2185 Hz, Pt^2), −4498 (dd, $^1J_{Pt1,P}$ = 3020 Hz, $^1J_{Pt1,P}$ = 1840 Hz, Pt^1).

Reaction of [(R$_F$)$_2$Pt^{III}(μ-PPh$_2$)$_2$Pt^{III}(R$_F$)$_2$](*Pt^{III}−Pt^{III}*) with NaN$_3$. To a yellow solution of **1** (0.169 g, 0.118 mmol) in acetone (30 mL) was added NaN$_3$ (0.018 g, 0.277 mmol) in MeOH (10 mL). The colorless solution was stirred, at room temperature, for 20 h and then evaporated to dryness. The residue was treated with CH$_2$Cl$_2$ (20 mL), NBu$_4$ClO$_4$ (0.081 g, 0.236 mmol) was added, and the resulting mixture was filtered through Celite. The solution was evaporated to ca. 2 mL, and ^{i}PrOH (20 mL) was added and then evaporated to ca. 5 mL. Complex **4a** crystallized as a white solid which was stirred for 30 min, filtered, and washed with cold ^{i}PrOH (2 × 0.5 mL). Yield: 0.071 g, 34%. Anal. Found (Calcd for C$_{68}$F$_{20}$H$_{82}$N$_5$PPt$_2$): C, 45.51 (46.13); H, 4.79 (4.67); N 3.63 (3.96).

In another experiment, NaN$_3$ (0.018 g, 0.277 mmol) in acetone (20 mL) was added to a yellow solution of **1** (0.171 g, 0.120 mmol) in acetone (35 mL). The mixture was worked up as in the case of **4a**, and although dark brown solids were obtained to 253 K, these solids turned into oil at room temperature. The NMR study of the oils shows the material to be a mixture in which **4a** and **4b** are identified.

Data for **4a** follow. HRMS (−), exact mass for the dianion [C$_{36}$H$_{10}$F$_{20}$N$_3$PPt$_2$]$^{2-}$: 642.4795 Da. Measured *m*/*z*: 642.4790 (M)$^{2-}$. ^{1}H NMR (acetone-*d*$_6$, 293 K, 400 MHz), δ: 7.64 (pseudo t, 2 H, $^3J_{H,H}$ = 8.3 Hz, *o*-H bonded to *P*Ph$_2$), 7.56 (m, 3 H, *m*-H + *p*-H bonded to *P*Ph$_2$), 3.49 (m, 16 H, NBu$_4^+$), 1.87 (m, 16H, NBu$_4^+$), 1.48 (pseudo sextet, 16 H, $^3J_{H,H}$ = 7.4 Hz, NBu$_4^+$), 1.02 (t, 24 H, $^3J_{H,H}$ = 7.4 Hz, NBu$_4^+$). ^{19}F NMR (acetone-*d*$_6$, 293 K, 376.5 MHz), δ: −117.5 (4 *o*-F, $^3J_{Pt,F}$ = 512 Hz), −118.0 (4 *o*-F, $^3J_{Pt,F}$ = 331 Hz), −168.1 (4 *m*-F), −168.3 (2 *p*-F), −170.9 (4 *m*-F), −171.6 (2 *p*-F). ^{31}P{^{1}H} NMR (acetone-*d*$_6$, 293 K, 162.0 MHz), δ: −75.9 ppm, $^1J_{P,Pt}$ = 2138 Hz. ^{195}Pt{^{19}F} NMR (acetone-*d*$_6$, 293 K, 86 MHz), δ: −3381 (d, $^1J_{Pt,P}$ = 2138 Hz).

Data for **4b** follow. ^{19}F NMR (acetone-*d*$_6$, 293 K, 376.5 MHz), δ: −117.6 (2 *o*-F, $^3J_{Pt,F}$ = 507 Hz), −118.3 (2 *o*-F, $^3J_{Pt,F}$ = 421 Hz), −119.0 (2 *o*-F, $^3J_{Pt,F}$ = 303 Hz), −127.6 (2 *o*-F, PPh$_2$C$_6$F$_5$), −153.7 (1 *p*-F, PPh$_2$C$_6$F$_5$), −165.0 (2 *m*-F, PPh$_2$C$_6$F$_5$), −166.8 (1 *p*-F), −167.6 (2 *m*-F), −167.8 (2 *m*-F), −168.2 (2 *m*-F), −169.7 (1 *p*-F), −170.0 (1 *p*-F). ^{31}P{^{1}H} NMR (acetone-*d*$_6$, 293 K, 162.0 MHz), δ: 13.4 ($^1J_{P,Pt}$ = 2216 Hz, $^2J_{P,P}$ = 320 Hz, PPh$_2$C$_6$F$_5$), −55.3 ($^1J_{P,Pt} \approx {}^1J_{P,Pt'} \approx$ 2148 Hz, μ-PPh$_2$) ppm.

Reaction of [(R$_F$)$_2$Pt^{III}(μ-PPh$_2$)$_2$Pt^{III}(R$_F$)$_2$](*Pt^{III}−Pt^{III}*) with KOCN. To a yellow solution of **1** (0.170 g, 0.119 mmol) in acetone (35 mL) was added KOCN (0.040 g, 0.493 mmol), and the mixture was stirred at room temperature for 20 h. The mixture was evaporated to dryness, CH$_2$Cl$_2$ (20 mL) and NBu$_4$ClO$_4$ (0.041 g, 0.120 mmol) were added, and the mixture was filtered through Celite. The solution was evaporated to ca. 2 mL; ^{i}PrOH (10 mL) was added and evaporated to ca. 5 mL. The solution was maintained in the freezer for 10 h. A small amount of a white solid crystallized which was filtered, washed with cold ^{i}PrOH (2 × 0.5 mL), and discarded. The filtrate was evaporated

dx.doi.org/10.1021/ic401689c | *Inorg. Chem.* XXXX, XXX, XXX−XXX

to ca. 3 mL and cooled ca. to 230 K, so that **5b** crystallized as a white solid which was quickly filtered and washed with cold ^{i}PrOH (2 × 0.5 mL). Yield: 0.047 g, 23%. Anal. Found (Calcd for $C_{65}F_{20}H_{56}N_2OP_2Pt_2$): C, 45.40 (45.57); H, 3.07 (3.29); N 1.73 (1.64).

To a yellow solution of **1** (0.220 g, 0.154 mmol) in acetone (35 mL) was added KOCN (0.025 g, 0.308 mmol), and the mixture was stirred for 20 h. The colorless solution was evaporated to dryness, and CH_2Cl_2 (15 mL) was added. NBu_4ClO_4 (0.053 g, 0.154 mmol) was added, and the mixture was filtered through Celite. The solution was evaporated to ca. 5 mL, and ^{i}PrOH (15 mL) was added and evaporated to 5 mL. A white solid crystallized and was filtered and washed with ^{i}PrOH (2 × 0.5 mL), 0.010 g. Three more fractions of white solid were obtained from the mother liquors. All of these four fractions contain mainly **5a** and **5b** in a molar ratio of ca. 3:1, 1:1, 1:4, and 1:6, respectively. All attempts to carry out the reaction process with a greater amount of NBu_4ClO_4 resulted in oily products that we have not been able to crystallize.

Data for **5a** follow. ^{19}F NMR (acetone-d_6, 293 K, 376.5 MHz), δ: −117.5 (4 *o*-F, $^3J_{Pt,F}$ = 538 Hz), −117.7 (4 *o*-F, $^3J_{Pt,F}$ not measured, overlapped signals), −168.0 (4 *m*-F), −168.5 (2 *p*-F), −170.9 (4 *m*-F), −171.7 (2 *p*-F). ^{31}P{^{1}H} NMR (acetone-d_6, 293 K, 162.0 MHz), δ: −72.9 ppm, $^1J_{P,Pt}$ = 2100 Hz.

Data for **5b** follow. HRMS (−), exact mass for the anion $[C_{49}H_{20}F_{20}NOP_2Pt_2]^-$: 1469.9994 Da. Measured *m*/*z*: 1469.9977 $(M)^-$. ^{1}H NMR (acetone-d_6, 293 K, 400 MHz), δ: 8.22 (dd, 2 H, $^3J_{H,H}$ = 7.6 Hz, $^3J_{H,P}$ = 12.3 Hz, *o*-H bonded to $PPh_2C_6F_5$), 7.73 (dd, 2 H, $^3J_{H,H}$ = 7.8 Hz, $^3J_{H,P}$ = 10.2 Hz, *o*-H bonded to PPh_2), from 7.66 to 7.56 (m, 3 H, *p*-H + *m*-H bonded to $PPh_2C_6F_5$), from 7.31 to 7.20 (m, 3 H, *p*-H + *m*-H bonded to PPh_2), 3.49 (m, 8 H, NBu_4^+), 1.87 (m, 8 H, NBu_4^+), 1.48 (pseudo sextet, 8 H, $^3J_{H,H}$ = 7.4 Hz, NBu_4^+), 1.02 (t, 12 H, $^3J_{H,H}$ = 7.4 Hz, NBu_4^+). ^{19}F NMR (acetone-d_6, 293 K, 376.5 MHz), δ: −117.5 (2 *o*-F, $^3J_{Pt,F}$ = 543 Hz), −118.1 (2 *o*-F, $^3J_{Pt,F}$ = 452 Hz), −118.5 (2 *o*-F, $^3J_{Pt,F}$ = 346 Hz), −127.4 (2 *o*-F, $PPh_2C_6F_5$), −153.8 (1 *p*-F, $PPh_2C_6F_5$), −165.0 (2 *m*-F, $PPh_2C_6F_5$), −166.8 (1 *p*-F), −167.7 (2 *m*-F), −168.0 (2 *m*-F), −168.3 (2 *m*-F), −169.7 (1 *p*-F), −170.0 (1 *p*-F). ^{31}P{^{1}H} NMR (acetone-d_6, 293 K, 162.0 MHz), δ: 12.6 ($^1J_{P,Pt2}$ = 2210 Hz, $^2J_{P,P}$ = 325 Hz, $PPh_2C_6F_5$), −40.5 ($^1J_{P,Pt1} \approx {}^1J_{P,Pt2} \approx$ 2100 Hz, μ-PPh_2) ppm. ^{195}Pt{^{19}F} NMR (acetone-d_6, 293 K, 86 MHz), δ: −3522 (d, $^1J_{Pt,\mu\text{-}P}$ = 2100 Hz, $^2J_{Pt,Pt}$ = 1310 Hz, Pt^1), −3953 (dd, $^1J_{Pt2,\mu\text{-}P}$ = 2100 Hz, $^1J_{Pt2,P}$ = 2210 Hz, $^2J_{Pt,Pt}$ = 1310 Hz, Pt^2).

Reaction of $[(R_F)_2Pt^{III}(\mu\text{-}PPh_2)_2Pt^{III}(\mu\text{-}PPh_2)_2Pt^{II}(R_F)_2]$*(Pt^{III}–Pt^{III})* with N^{n}Bu$_4$OH. To a red suspension of **2** (0.162 g, 0.081 mmol) in CH_2Cl_2 (15 mL) was added 0.160 mol of NBu_4OH (0.16 mL of 1.0 M methanol solution). The solution was stirred for 20 h, and the pale yellow solution was evaporated to ca. 1 mL. $CHCl_3$ (10 mL) was added, and **6** crystallized as a white solid which was filtered and washed with cold $CHCl_3$ (2 × 0.5 mL). Yield: 0.142 g, 78%. Anal. Found (Calcd for $C_{104}F_{20}H_{112}N_2OP_4Pt_3$): C, 49.99 (50.02); H, 4.12 (4.48); N 1.09 (1.12).

HRMS (−), exact mass for the anion $[C_{72}H_{40}F_{20}OP_4Pt_3]^{2-}$: 1004.5331 Da. Measured *m*/*z*: 1004.5321 $(M)^{2-}$. ^{1}H NMR (acetone-d_6, 293 K, 400 MHz), δ: 7.85 (pseudo t, 2 H, *J* = 7.1 Hz, *o*-H bonded to P^3), from 7.36 to 7.25 (m, 4 H, *o*-H bonded to P^4 and *o*-H bonded to P^1), from 7.20 to 6.98 (m, 9 H, *o*-H bonded to P^2, *m*-H + *p*-H bonded to P^3, *m*-H + *p*-H bonded to P^1, *p*-H bonded to P^4), 6.92 (pseudo t, 2 H, *J* = 7.2 Hz, *m*-H bonded to P^4), 6.84 (t, 1 H, *J* = 6.9 Hz, *p*-H bonded to P^2), 6.59 (pseudo t, 2 H, *J* = 6.9 Hz, *m*-H bonded to P^2), 3.49 (m, 16 H, NBu_4^+), 1.87 (m, 16 H, NBu_4^+), 1.48 (pseudo sextet, 16 H, $^3J_{H,H}$ = 7.4 Hz, NBu_4^+), 1.02 (t, 24 H, $^3J_{H,H}$ = 7.4 Hz, NBu_4^+). ^{19}F NMR (acetone-d_6, 293 K, 376.5 MHz), δ: from −114 to −116 (8 *o*-F), −168.6 (2 *m*-F), from −168.9 to −169.4 (6 *m*-F), −170.0 (1 *p*-F), −170.4 (1 *p*-F), −170.6 (2 *p*-F). ^{31}P{^{1}H} NMR (acetone-d_6, 293 K, 162.0 MHz), δ: 123.6 ($^1J_{P1,Pt1}$ = 2969 Hz, P^1), 13.9 ($J_{P2,Pt1}$ = 1840 Hz, $J_{P2,Pt2}$ = 1710 Hz, $^2J_{P2,P3}$ = 293 Hz, P^2), −147.9 (d, $^1J_{P4,Pt2}$ = 2857 Hz, $^1J_{P4,Pt3}$ = 1947 Hz, $^2J_{P3,P4}$ = 153 Hz, P^4), −150.5 (dd, $^1J_{P3,Pt2}$ = 1792 Hz, $^1J_{P3,Pt3}$ = 1874 Hz, $^2J_{P2,P3}$ = 293 Hz, $^2J_{P3,P4}$ = 153 Hz, P^3) ppm. ^{195}Pt{^{19}F} NMR (acetone-d_6, 293 K, 86 MHz), δ: −3657 (ddd, $^1J_{Pt2,P4}$ = 2857 Hz, $^1J_{Pt2,P3}$ = 1792 Hz, $^1J_{Pt2,P2}$ = 1740 Hz, Pt^2), −3828 (dd, $^1J_{Pt3,P4}$ = 1947 Hz, $^1J_{P3,Pt3}$ = 1874 Hz, Pt^3), −4497 (dd, $^1J_{Pt1,P1}$ = 2969 Hz, $^1J_{Pt1,P2}$ = 1840 Hz, Pt^1).

Synthesis of $[NBzMe_3]_2[(R_F)_2Pt^{II}(\mu\text{-}Ph_2PO)(\mu\text{-}PPh_2)Pt^{II}(\mu\text{-}PPh_2)_2Pt^{II}(R_F)_2]$ (6′). To a red solution of **2** (0.100 g, 0.050 mmol) in CH_2Cl_2 (25 mL) was added 0.108 mol of $NBzMe_3OH$ (0.048 mL of 40% methanol solution), and this mixture stirred for 4 h. The solution was evaporated to ca. 3 mL, and $CHCl_3$ (10 mL) was added and evaporated to ca. 3 mL. Compound **6′** crystallized as a very pale yellow solid which was filtered and washed with cold $CHCl_3$ (2 × 0.5 mL). Yield: 0.093 g, 78%.

Reaction of $[(R_F)_2Pt^{III}(\mu\text{-}PPh_2)_2Pt^{III}(\mu\text{-}PPh_2)_2Pt^{II}(R_F)_2]$*(Pt^{III}–Pt^{III})* with NaN_3. NaN_3 (0.008 g, 0.120 mmol) dissolved in methanol (5 mL) was added to a red solution of **2** (0.100 g, 0.050 mmol) in acetone (25 mL) and stirred for 20 h. The yellow solution was evaporated to dryness, and MeOH (8 mL) was added to the residue. NBu_4ClO_4 (0.035 g, 0.100 mmol) was added to the yellow solution, and **7** crystallized as a yellow solid which was filtered and washed with MeOH (2 × 0.5 mL). ^{i}PrOH (8 mL) was added to the filtrate, and evaporation to ca. 10 mL produces a second crop of **7**. Yield: 0.073 g, 65%. Anal. Found (Calcd for $C_{88}F_{20}H_{76}N_2P_4Pt_3$): C, 47.26 (46.96); H, 3.44 (3.40); N 1.15 (1.24).

HRMS (−), exact mass for the anion $[C_{72}H_{40}F_{20}NP_4Pt_3]^-$: 2007.0739 Da. Measured *m*/*z*: 2007.0680 $(M)^-$. ^{1}H NMR (acetone-d_6, 293 K, 400 MHz), δ: 7.76 (dd, 4 H, $^3J_{H,H}$ = 8.3 Hz, $^3J_{H,P}$ = 10.9 Hz, *o*-H bonded to P^3), 7.63 (dd, 4 H, $^3J_{H,H}$ = 7.7 Hz, $^3J_{H,P}$ = 9.7 Hz, *o*-H bonded to P^1), 7.41 (t, 2 H, $^3J_{H,H}$ = 6.5 Hz, *p*-H), 7.31 (t, 2 H, $^3J_{H,H}$ = 7.1 Hz, *p*-H), from 7.22 to 7.02 (m, 22 H), 6.97 (t, 2 H, $^3J_{H,H}$ = 6.5 Hz, *p*-H bonded to P^2), 6.72 (pseudo t, 4 H, *J* = 6.5 Hz, *m*-H bonded to P^2), 3.49 (m, 8 H, NBu_4^+), 1.87 (m, 8 H, NBu_4^+), 1.48 (pseudo sextet, 8H, $^3J_{H,H}$ = 7.4 Hz, NBu_4^+), 1.02 (t, 12H, $^3J_{H,H}$ = 7.4 Hz, NBu_4^+). ^{19}F NMR (acetone-d_6, 293 K, 376.5 MHz), δ: −116.3 (4 *o*-F, $^3J_{Pt,F}$ = 328 Hz), −116.7 (2 *o*-F, $^3J_{Pt,F}$ = 312 Hz), −117.5 (2 *o*-F, $^3J_{Pt,F}$ = 295 Hz), −166.1 (1 *p*-F), −166.2 (1 *p*-F), −166.7 (2 *m*-F), −167.2 (2 *m*-F), −167.9 (4 *m*-F), −168.2 (1 *p*-F), −168.8 (1 *p*-F) ppm. ^{31}P{^{1}H} NMR (acetone-d_6, 293 K, 162.0 MHz), δ: 140.6 (P^4, $^1J_{P4,Pt3}$ = 1280, $^1J_{P4,Pt2}$ = 4070 Hz), 128.4 (P^1, $^1J_{P1,Pt1}$ = 3045 Hz, $^2J_{P1,P3}$ = 70 Hz), 31.7 (P^3, $^1J_{P3,Pt3}$ = 1690 Hz, $J_{P3,Pt2}$ = 510 Hz, $^2J_{P1,P3}$ = 70 Hz), 30.7 (P^2, $^1J_{P2,Pt1}$ = 2100, $^1J_{P2,Pt2}$ = 3580 Hz) ppm. ^{195}Pt{^{19}F} NMR (acetone-d_6, 293 K, 86 MHz), δ: −4506 (dd, $^1J_{Pt1,P1}$ = 3045 Hz, $J_{Pt1,P2}$ = 2100 Hz, Pt^1), −4868 (ddd, $^1J_{Pt2,P2}$ = 3580 Hz, $^1J_{Pt2,P4}$ = 4070 Hz, $J_{Pt2,P3}$ = 510 Hz, Pt^2), −5439 (dd, $^1J_{Pt3,P3}$ = 1690 Hz, $^1J_{Pt3,P4}$ = 1280 Hz, Pt^3).

Synthesis of $[PPh_3Me][Pt_3^{II}(\mu_3\text{-}Ph_2PNPPh_2)(\mu\text{-}PPh_2)_2)(R_F)_4]$ (7′). Complex **7′** was prepared similarly to **7** from NaN_3 (0.012 g, 0.185 mmol) dissolved in methanol (7 mL), **2** (0.111 g, 0.056 mmol) in acetone (25 mL), and $[PMePh_3][ClO_4]$ (0.022 g, 0.058 mmol) as a yellow solid. Yield: 0.069 g, 54%.

X-ray Structure Determinations. Crystal data and other details of the structure analyses are presented in Supporting Information Table S1. Suitable crystals of **4a** and **5a** for X-ray diffraction studies were obtained by slow diffusion of *n*-hexane into concentrated solutions of **4a** or a **5a**/**5b** mixture, respectively, in CH_2Cl_2. Crystals of **6′** and **7′** were obtained by slow diffusion of *n*-hexane into concentrated solutions of **6′** and **7′** in acetone. Crystals were mounted at the end of quartz fibres. The radiation used in all cases was graphite monochromated Mo Kα (λ = 0.710 73 Å). X-ray intensity data were collected on an Oxford Diffraction Xcalibur diffractometer. The diffraction frames were integrated and corrected from absorption by using the CrysAlis RED program.[91] The structures were solved by Patterson and Fourier methods and refined by full-matrix least-squares on F^2 with SHELXL-97.[92] All non-hydrogen atoms were assigned anisotropic displacement parameters and refined without positional constraints, except as noted below. All hydrogen atoms were constrained to idealized geometries and assigned isotropic displacement parameters equal to 1.2 times the U_{iso} values of their attached parent atoms (1.5 times for the methyl hydrogen atoms). In the structure of **4a**·CH_2Cl_2·0.5*n*-C_6H_{14}, constraints in the geometry and the thermal parameters of the *n*-hexane molecule were applied. In the structure of **5a**·CH_2Cl_2·0.5*n*-C_6H_{14}, the data collected were weak due to the fact that the only suitable crystal was very small. This causes some problems that reflect mainly in the thermal anisotropic

dx.doi.org/10.1021/ic401689c | *Inorg. Chem.* XXXX, XXX, XXX−XXX

parameters of some atoms, for which weak restraints were applied. Moreover, one very diffuse *n*-hexane moiety (one of the solvents used in the crystallization) was found in the electron density maps, and had to be refined with half occupancy and restraints in its geometric parameters. Isotropic displacement parameters were used for all the atoms of this solvent molecule. In the structure of **7′**, one of the methyl groups of the acetone solvent molecules is disordered over two positions which were refined with 0.5 partial occupancy. Also, restraints were used in the anistropic thermal parameters of the *n*-hexane solvent molecule. Full-matrix least-squares refinement of these models against F^2 converged to final residual indices given in Table 3.

■ ASSOCIATED CONTENT

Ⓢ Supporting Information

Crystal data and other details of the structure analyses. Crystallographic data of **4a**·CH_2Cl_2·0.5*n*-C_6H_{14}, **5a**·CH_2Cl_2·0.5*n*-C_6H_{14}, **6′**·3Me_2CO, and **7′**·Me_2CO·*n*-C_6H_{14} (CIF format). This material is available free of charge via the Internet at http://pubs.acs.org.

■ AUTHOR INFORMATION

Corresponding Authors

*E-mail: cfortuno@unizar.es (C.F.).
*E-mail: p.mastrorilli@poliba.it (P.M.).

Notes

The authors declare no competing financial interest.

■ ACKNOWLEDGMENTS

This work was supported by the Spanish MICINN (DGPTC)/FEDER (Project CTQ2008-06669-C02-01/BQU), MINECO/FEDER (Project CTQ2012-35251), the Cobierno de Aragón (Grupo de Consolidado E21: Química Inorgánica y de los Compuestos Organometálicos), and the Italian MIUR (PRIN project n. 2009LR88XR). A.A. gratefully acknowledges MICINN for an FPU grant.

■ DEDICATION

Dedicated to the memory of Professor Dr. María P. García.

■ REFERENCES

(1) Matsumoto, K.; Ochiai, M. *Coord. Chem. Rev.* **2002**, *231*, 229−238.
(2) Wilson, J. J.; Lippard, S. J. *Inorg. Chem.* **2012**, *51*, 9852−9864.
(3) Canty, A. J. *Dalton Trans.* **2009**, 10409−10417.
(4) Lanci, M. P.; Remy, M. S.; Lao, D. B.; Sanford, M. S.; Mayer, J. M. *Organometallics* **2011**, *30*, 3704−3707.
(5) Dick, A. R.; Kampf, J. W.; Sanford, M. S. *Organometallics* **2005**, *24*, 482−485.
(6) Serra, D.; Cao, P.; Cabrera, J.; Padilla, R.; Rominger, F.; Limbach, M. *Organometallics* **2011**, *30*, 1885−1895.
(7) Hickman, A. J.; Sanford, M. S. *Nature* **2012**, *484*, 177−185.
(8) Powers, D. C.; Ritter, T. *Acc. Chem. Res.* **2012**, *45*, 840−850.
(9) Racowski, J. M.; Gary, J. B.; Sanford, M. S. *Angew. Chem., Int. Ed.* **2012**, *51*, 3414−3417.
(10) Julia-Hernández, F.; Arcas, A.; Vicente, J. *Chem.—Eur. J.* **2012**, *18*, 7780−7786.
(11) Tang, F.; Zhang, Y.; Rath, N. P.; Mirica, L. M. *Organometallics* **2012**, *31*, 6690−6696.
(12) Lyons, T. W.; Sanford, M. S. *Chem. Rev.* **2010**, *110*, 1147−1169.
(13) Sehnal, P.; Taylor, R. J. K.; Fairlamb, I. J. S. *Chem. Rev.* **2010**, *110*, 824−889.
(14) Xu, L. M.; Li, B. J.; Yang, Z.; Shi, Z. J. *Chem. Soc. Rev.* **2010**, *39*, 712−733.
(15) Sicilia, V.; Forniés, J.; Casas, J. M.; Martín, A.; López, J. A.; Larraz, C.; Borja, P.; Ovejero, C.; Tordera, D.; Bolink, H. *Inorg. Chem.* **2012**, *51*, 3427−3435.
(16) Ibáñez, S.; Estevan, F.; Hirva, P.; Sanaú, M.; Ubeda, M. A. *Organometallics* **2012**, *31*, 8098−8108.
(17) Mirica, L. M.; Khusnutdinova, J. R. *Coord. Chem. Rev.* **2013**, *257*, 299−314.
(18) Nielsen, M. C.; Lyngvi, E.; Schoenebeck, F. *J. Am. Chem. Soc.* **2013**, *135*, 1978−1985.
(19) Chaouche, N.; Forniés, J.; Fortuño, C.; Kribii, A.; Martín, A.; Karipidis, P.; Tsipis, A. C.; Tsipis, C. A. *Organometallics* **2004**, *23*, 1797−1810.
(20) Ara, I.; Chaouche, N.; Forniés, J.; Fortuño, C.; Kribii, A.; Tsipis, A. C. *Organometallics* **2006**, *25*, 1084−1091.
(21) Arias, A.; Forniés, J.; Fortuño, C.; Martín, A.; Latronico, M.; Mastrorilli, P.; Todisco, S.; Gallo, V. *Inorg. Chem.* **2012**, *51*, 12682−12696.
(22) Arias, A.; Forniés, F.; Fortuño, C.; Martín, A.; Mastrorilli, P.; Todisco, S.; Latronico, M.; Gallo, V. *Inorg. Chem.* **2013**, *52*, 5493−5506.
(23) Alonso, E.; Casas, J. M.; Cotton, F. A.; Feng, X. J.; Forniés, J.; Fortuño, C.; Tomás, M. *Inorg. Chem.* **1999**, *38*, 5034−5040.
(24) Forniés, J.; Fortuño, C.; Ibáñez, S.; Martín, A. *Inorg. Chem.* **2006**, *45*, 4850−4858.
(25) Ara, I.; Forniés, J.; Fortuño, C.; Ibáñez, S.; Martín, A.; Mastrorilli, P.; Gallo, V. *Inorg. Chem.* **2008**, *47*, 9069−9080.
(26) Forniés, J.; Fortuño, C.; Ibáñez, S.; Martín, A. *Inorg. Chem.* **2008**, *47*, 5978−5987.
(27) Forniés, F.; Fortuño, C.; Ibáñez, S.; Martín, A.; Mastrorilli, P.; Gallo, V. *Inorg. Chem.* **2011**, *50*, 10798−10809.
(28) Yahav-Levi, A.; Goldberg, I.; Vigalok, A.; Vedemikov, A. N. *J. Am. Chem. Soc.* **2008**, *130*, 724−731.
(29) Crespo, M.; Anderson, C. M.; Kfoury, N.; Font-Bardia, M.; Calvet, T. *Organometallics* **2012**, *31*, 4401−4404.
(30) Yahav-Levi, A.; Goldberg, I.; Vigalok, A.; Vedernikov, A. N. *Chem. Commun.* **2010**, *46*, 3324−3326.
(31) A mixture of **1** (0.152 g, 0.106 mmol) in acetone and NaN_3 (0.016 g, 0.246 mmol) in methanol was stirred for 20 h at room temperature and evaporated to dryness. The ^{31}P NMR spectrum (acetone solution) of the solid showed the signal due to the anion of **4a** along with other signals (from +70 to +10 ppm) which did not show platinum satellites. The spectrum indicates that several phosphorous containing species are present in the solid, and this should be in agreement with the evolution of the unstable PPh_2N_3 formed.
(32) Böske, J.; Niecke, E.; Ocando-Mavarez, E.; Majoral, J. P.; Bertrand, G. *Inorg. Chem.* **1986**, *25*, 2695−2698.
(33) Bebbington, M. W. P.; Bourissou, D. *Coord. Chem. Rev.* **2009**, *253*, 1248−1261.
(34) Atam, M.; Muller, U. *J. Organomet. Chem.* **1974**, *71*, 435−441.
(35) Mackay, F. S.; Farrer, N. J.; Salassa, L.; Tai, H. C.; Deeth, R. J.; Moggach, S. A.; Wood, P. A.; Parsons, S.; Sadler, P. J. *Dalton Trans.* **2009**, 2315−2325.
(36) Mukhopadhyay, B. G.; Mukhopadhyay, S.; da Silva, M.; Charmier, M. A. J.; Pombeiro, A. J. L. *Dalton Trans.* **2009**, 4778−4785.
(37) Smolenski, P.; Mukhopadhyay, S.; Silva, M.; Charmier, M. A. J.; Pombeiro, A. J. L. *Dalton Trans.* **2008**, 6546−6555.
(38) Platinum complexes with azide groups coordinated in a terminal mode are well-known, and a complex in which a N_3^- group bridges three platinum centers, μ-1,1,1-N_3, was characterized a long time ago, but only recently have such species been prepared and complexes with a "Pt(μ-1,1-N_3)Pt" skeleton characterized by x-ray: Arias, A.; Forniés, J.; Fortuño, C.; Martín, A. *Inorg. Chim. Acta* **2013**, *407*, 189−196.
(39) Falvello, L. R.; Forniés, J.; Fortuño, C.; Martín, A.; Martínez-Sariñena, A. P. *Organometallics* **1997**, *16*, 5849−5856.
(40) Alonso, E.; Forniés, J.; Fortuño, C.; Martín, A.; Orpen, A. G. *Organometallics* **2000**, *19*, 2690−2697.
(41) Forniés, J.; Fortuño, C.; Gil, R.; Martín, A. *Inorg. Chem.* **2005**, *44*, 9534−9541.

(42) Alonso, E.; Forniés, J.; Fortuño, C.; Martín, A.; Rosair, G. M.; Welch, A. J. *Inorg. Chem.* **1997**, *36*, 4426−4431.
(43) Stamatatos, T. C.; Papaefstathiou, G. S.; MacGillivray, L. R.; Escuer, A.; Vicente, R.; Ruiz, E.; Perlepes, S. P. *Inorg. Chem.* **2007**, *46*, 8843−8850.
(44) Habib, M.; Karmakar, T. K.; Aromí, G.; Ribas-Ariño, J.; Fun, H.-K.; Chantrapromma, S.; Chandra, S. K. *Inorg. Chem.* **2008**, *47*, 4109−4117.
(45) Fekl, U.; Goldberg, K. I. *J. Am. Chem. Soc.* **2002**, *124*, 6804−6805.
(46) Zhao, S.-B.; Wu, G.; Wang, S. *Organometallics* **2008**, *27*, 1030−1033.
(47) Zhao, S.-B.; Cui, Q.; Wang, S. *Organometallics* **2010**, *29*, 998−1003.
(48) Crumton-Bregel, D. M.; Goldberg, K. I. *J. Am. Chem. Soc.* **2003**, *125*, 9442−9456.
(49) Fekl, U.; Kaminsky, W.; Goldberg, K. I. *J. Am. Chem. Soc.* **2003**, *125*, 15286−15287.
(50) Karshtedt, D.; McBee, J. L.; Bell, A. T.; Tilley, T. D. *Organometallics* **2006**, *25*, 1801−1811.
(51) Kloek, S. M.; Goldberg, K. I. *J. Am. Chem. Soc.* **2007**, *129*, 3460−3461.
(52) Sangtrirutnugul, P.; Tilley, T. D. *Organometallics* **2008**, *27*, 2223−2230.
(53) West, N. M.; White, P. S.; Templeton, J. L.; Nixon, J. F. *Organometallics* **2009**, *28*, 1425−1434.
(54) McBee, J. L.; Tilley, T. D. *Organometallics* **2009**, *28*, 3947−3952.
(55) Welsch, S.; Nohra, B.; Peresypkina, E. V.; Lescop, C.; Scheer, M.; Réau, R. *Chem.—Eur. J.* **2009**, *15*, 4685−4703.
(56) Braunstein, P.; Boag, N. M. *Angew. Chem., Int. Ed.* **2001**, *40*, 2427−2433.
(57) Leca, F.; Sauthier, M.; Deborde, V.; Toupet, L.; Réau, R. *Chem.—Eur. J.* **2003**, *9*, 3785−3795.
(58) Alonso, E.; Forniés, J.; Fortuño, C.; Martín, A.; Orpen, A. G. *Chem. Commun.* **1996**, 231−232.
(59) Alonso, E.; Forniés, J.; Fortuño, C.; Martín, A.; Orpen, A. G. *Organometallics* **2003**, *22*, 2723−2728.
(60) Alonso, E.; Forniés, F.; Fortuño, C.; Lledós, A.; Martín, A.; Nova, A. *Inorg. Chem.* **2009**, *48*, 7679−7690.
(61) Chaouche, N.; Forniés, J.; Fortuño, C.; Kribii, A.; Martín, A. *J. Organomet. Chem.* **2007**, *692*, 1168−1172.
(62) Burrows, A. D.; Mahon, M. F.; Palmer, M. T. *J. Chem. Soc., Dalton Trans.* **2000**, 1669−1677.
(63) Slawin, A. M. Z.; Wainwright, M.; Woollins, J. D. *New J. Chem.* **2000**, *24*, 69−71.
(64) Alcock, N. W.; Bergamini, P.; Gomes-Carniero, T. M.; Jackson, R. D.; Nicholls, J.; Orpen, A. G.; Pringle, P. G.; Sostero, S.; Traverso, O. *J. Chem. Soc., Chem. Commun.* **1990**, 980−982.
(65) Matt, D.; Ingold, F.; Balegroune, F.; Grandjean, D. *J. Organomet. Chem.* **1990**, *399*, 349−360.
(66) Lin, I. J. B.; Lai, J. S.; Liu, L.-K.; Wen, Y. S. *J. Organomet. Chem.* **1990**, *399*, 361−364.
(67) Powell, J.; Horvath, M. J.; Lough, A. *J. Chem. Soc., Dalton Trans.* **1996**, 1679−1685.
(68) Gallo, V.; Latronico, M.; Mastrorilli, P.; Nobile, C. F.; Polini, F.; Re, N.; Englert, U. *Inorg. Chem.* **2008**, *47*, 4785−4795.
(69) Latronico, M.; Polini, F.; Gallo, V.; Mastrorilli, P.; Calmuschi-Cula, B.; Englert, U.; Re, N.; Repo, T.; Räisänen, M. *Inorg. Chem.* **2008**, *47*, 9779−9796.
(70) Latronico, M.; Mastrorilli, P.; Gallo, V.; Dell'Anna, M.; Creati, F.; Re, N.; Englert, U. *Inorg. Chem.* **2011**, *50*, 3539−3558.
(71) Mastrorilli, P.; Latronico, M.; Gallo, V.; Polini, F.; Re, N.; Marrone, A.; Gobetto, R.; Ellena, S. *J. Am. Chem. Soc.* **2010**, *132*, 4752−4765.
(72) Latronico, M.; Sanchez, S.; Rizzuti, A.; Gallo, V.; Polini, F.; Lalinde, E.; Mastrorilli, P. *Dalton Trans.* **2013**, *42*, 2502−2511.
(73) Gallo, V.; Latronico, M.; Mastrorilli, P.; Nobile, C. F.; Suranna, G. P.; Ciccarella, G.; Englert, U. *Eur. J. Inorg. Chem.* **2005**, 4607−4616.
(74) Alonso, E.; Casas, J. M.; Forniés, J.; Fortuño, C.; Martín, A.; Orpen, A. G.; Tsipis, C. A.; Tsipis, A. C. *Organometallics* **2001**, *20*, 5571−5582.
(75) Fei, Z.; Dyson, P. J. *Coord. Chem. Rev.* **2005**, *249*, 2056−2074.
(76) Nagashima, H.; Sue, T.; Oda, T.; Kanemitsu, A.; Matsumoto, T.; Motoyama, Y.; Sunada, Y. *Organometallics* **2006**, *25*, 1987−1994.
(77) Baranger, A. M.; Bergman, R. G. *J. Am. Chem. Soc.* **1994**, *116*, 3822−3835.
(78) Morello, L.; Yu, P.; Carmichael, C. D.; Patrick, B. O.; Fryzuk, M. D. *J. Am. Chem. Soc.* **2005**, *127*, 12796−12797.
(79) Älvarez, M. A.; García, M. E.; Ruiz, M. A.; Toyos, A.; Vega, F. *Inorg. Chem.* **2013**, *52*, 3942−3952.
(80) Cordero, B.; Gómez, V.; Platero-Prats, A. E.; Revés, M.; Echeverría, J.; Cremades, E.; Barragán, F.; Älvarez, S. *Dalton Trans.* **2008**, 2832−2838.
(81) Gamer, M. T.; Roesky, P. W. *Inorg. Chem.* **2004**, *43*, 4903−4906.
(82) Roesky, P. W. *Inorg. Chem.* **2006**, *45*, 798−802.
(83) Said, M.; Hughes, D. L.; Bochmann, M. *Polyhedron* **2006**, *25*, 843−852.
(84) Datta, S.; Gamer, M. T.; Roesky, P. W. *Dalton Trans.* **2008**, 2839−2843.
(85) Haehnel, M.; Hansen, S.; Spannenberg, A.; Arndt, P.; Beweries, T.; Rosenthal, U. *Chem.—Eur. J.* **2012**, *18*, 10546−10553.
(86) Usón, R.; Laguna, A.; Laguna, M.; Gimeno, M. C.; Jones, P. G.; Fittschen, C.; Sheldrick, G. M. *J. Chem. Soc., Chem. Commun.* **1986**, 509−510.
(87) Forniés, J.; Fortuño, C.; Ibáñez, S.; Martín, A.; Mastrorilli, P.; Gallo, V.; Tsipis, A. *Inorg. Chem.* **2013**, *52*, 1942−1953.
(88) Mastrorilli, P. *Eur. J. Inorg. Chem.* **2008**, 4835−4850.
(89) Berenguer, J. R.; Chaouche, N.; Forniés, J.; Fortuño, C.; Martín, A. *New J. Chem.* **2006**, *30*, 473−478.
(90) Forniés, J.; Fortuño, C.; Ibáñez, S.; Martín, A.; Tsipis, A. C.; Tsipis, C. A. *Angew. Chem., Int. Ed.* **2005**, *44*, 2407−2410.
(91) *CrysAlisRED; Program for X-ray CCD Camera Data Reduction, Version 1.171.32.19*; Oxford Diffraction Ltd.: Oxford, U.K., 2008.
(92) Sheldrick, G. M. *SHELXL-97 A Program for Crystal Structure Determination*; University of Gottingen: Gottingen, Germany, 1997.

dx.doi.org/10.1021/ic401689c | *Inorg. Chem.* XXXX, XXX, XXX−XXX

Inorganica Chimica Acta 407 (2013) 189–196

Contents lists available at ScienceDirect

Inorganica Chimica Acta

journal homepage: www.elsevier.com/locate/ica

From a di- and trinuclear phosphanido fragment to tetra- and hexanuclear platinum(II) complexes ☆

Andersson Arias [a], Juan Forniés [a], Consuelo Fortuño [b,*], Antonio Martín [a]

[a] Departamento de Química Inorgánica, Instituto de Síntesis Química y Catálisis Homogénea (ISQCH), Universidad de Zaragoza-C.S.I.C., Facultad de Ciencias, Campus San Francisco, E-50009 Zaragoza, Spain

[b] Departamento de Química Inorgánica, Instituto de Síntesis Química y Catálisis Homogénea (ISQCH), Universidad de Zaragoza-C.S.I.C., Escuela de Ingeniería y Arquitectura, Ed. Torres Quevedo, Campus Río Ebro, E-50018 Zaragoza, Spain

ARTICLE INFO

Article history:
Received 9 May 2013
Received in revised form 15 July 2013
Accepted 25 July 2013
Available online 1 August 2013

Keywords:
Phosphanido ligand
Platinum
Polynuclear complex
Single crystal X-ray diffraction

ABSTRACT

The di- and trinuclear derivatives $[(R_F)_2Pt(\mu\text{-}PPh_2)_2Pt(CH_3CN)_2]$, **1**, $[(R_F)_2Pt(\mu\text{-}PPh_2)_2Pt(\mu\text{-}PPh_2)_2Pt(CH_3CN)_2]$, **2**, ($R_F = C_6F_5$) behave as synthons of di- and trinuclear fragments. Addition of azide and oxalate ions to **1** and **2**, even in an excess, provides a way to isolate the tetranuclear and hexanuclear platinum complexes $[NBu_4]_2[\{(R_F)_2Pt\{(\mu\text{-}PPh_2)_2Pt\}_n(\mu\text{-}1,1\text{-}N_3)\}_2]$ ($n = 1$, **3**; 2, **5**), $[NBu_4]_2[\{(R_F)_2Pt(\mu\text{-}PPh_2)_2Pt\}_2(\mu\text{-}C_2O_4\text{-}\kappa^2O,O'\text{:}\ \kappa^2O'',O''')\}]$, **4**, and $[NBu_4]_2[\{(R_F)_2Pt(\mu\text{-}PPh_2)_2Pt(\mu\text{-}PPh_2)_2Pt\}_2(\mu\text{-}C_2O_4\text{-}\kappa^2O,O'\text{:}\ \kappa^2O'',O''')\}]$, **6**. The structures of **3**–**6**, determined by single crystal X-ray diffraction, show a linear arrangement of the platinum centres maintained through "$Pt(\mu\text{-}PPh_2)_2Pt$" and "$Pt(\mu\text{-}1,1\text{-}N_3)_2Pt$" or "$Pt(\mu\text{-}C_2O_4\text{-}\kappa^2O,O'\text{:}\ \kappa^2O'',O''')Pt$" bridging fragments. Finally, addition of KCN to **2** affords the trinuclear $[NBu_4]_2[(R_F)_2Pt(\mu\text{-}PPh_2)_2Pt(\mu\text{-}PPh_2)_2Pt(CN)_2]$, **7**, in which two cyanido groups are bonded to the platinum centre in a terminal way.

1. Introduction

Polynuclear complexes with phosphanido groups as bridging ligands have drawn great attention [2–5] and initially two well-known characteristics of the phosphanido ligands were well established: their flexibility, which allows them to support a great variety of structural situations, and the stability of M–P bond. These characteristics were believed to be the cause of the usual maintenance of the polynuclear "$Pt(\mu\text{-}PPh_2)_nPt$" fragment in the reaction processes [6–11]. Although processes such as conversion of the phosphanido groups in other ligands [1,12–17], migration of the phosphanido ligand from one metal centre to another [18–20], or modification of the coordination mode [21,22] are well known today, the stability of the "$Pt(\mu\text{-}PPh_2)_nPt$" fragment is a very useful tool in the synthetic design of new types of complexes. In the course of our current research on phosphanido derivatives, we have prepared $[(R_F)_2Pt(\mu\text{-}PPh_2)_2Pt(S)_2]$ ($R_F = C_6F_5$, S = $(CH_3)_2CO$, CH_3CN) [23,24]. These complexes easily lose the S ligands while the strong Pt–C and Pt–P bonds are maintained and the R_F and PPh_2 groups act as blocking ligands, protecting the coordination sites at the metal centre, and thus behaving as neutral dinuclear building blocks with "open-coordination sites" at 90°. Addition of a bidentate linker ligand, such as cyanido, allows the synthesis of complexes of higher nuclearity. Hence, we reported the first platinum(II) derivatives in which only the phosphanido and cyanido groups act as bridging ligands between the metal centres of hexa- and octanuclear compounds [24]. In this paper we describe the reactions of the dinuclear and/or trinuclear $[(R_F)_2Pt\{(\mu\text{-}PPh_2)_2Pt\}_n(CH_3CN)_2]$ ($n = 1$, **1**; 2, **2**) [24,25] complexes with azido and oxalato, which result in the formation of new tetra- and hexanuclear complexes in which the platinum centres are held together through ligands with only P and N or P and O donor atoms.

2. Experimental section

2.1. General considerations

C, H, and N analyses were performed with a Perkin-Elmer 2400 analyzer. IR spectra were recorded on a Perkin-Elmer Spectrum 100 FT-IR spectrometer. NMR spectra in solution were recorded on a Bruker Avance 400 spectrometer with $SiMe_4$, $CFCl_3$ and 85% H_3PO_4 as external references for ^1H, ^{19}F and ^{31}P, respectively. Literature methods were used to prepare the starting materials $[(R_F)_2Pt(\mu\text{-}PPh_2)_2Pt(CH_3CN)_2]$ [24] and $[(R_F)_2Pt(\mu\text{-}PPh_2)_2Pt(\mu\text{-}PPh_2)_2Pt(CH_3CN)_2]$ [25].

☆ Polynuclear Homo- or Heterometallic Palladium(II)–Platinum(II) Pentafluorophenyl Complexes Containing Bridging Diphenylphosphido Ligands 32. For part 31 see reference [1].

* Corresponding author. Tel.: +34 976 762559.
E-mail addresses: aariasa@unizar.es (A. Arias), juan.fornies@unizar.es (J. Forniés), cfortuno@unizar.es (C. Fortuño), tello@unizar.es (A. Martín).

0020-1693/$ - see front matter © 2013 Elsevier B.V. All rights reserved.
http://dx.doi.org/10.1016/j.ica.2013.07.048

2.2. Caution

Due to the fact that azido complexes are potentially explosive, especially in the presence of organic ligands, these compounds must be handled with care and prepared only in small amounts.

2.3. Synthesis of $[NBu_4]_2[\{(R_F)_2Pt(\mu\text{-}PPh_2)_2Pt(\mu\text{-}1,1\text{-}N_3)\}_2]$, **3**

To a colorless solution of $[(R_F)_2Pt(\mu\text{-}PPh_2)_2Pt(CH_3CN)_2]$ **1** (0.121 g, 0.103 mmol) in acetone (15 mL) was added NaN_3 (0.064 g, 0.989 mmol) and the mixture was stirred at room temperature for 20 h. $[NBu_4]ClO_4$ (0.070 g, 0.206 mmol) was added and the mixture was evaporated to dryness. CH_2Cl_2 (15 mL) was added to the residue and filtered through Celite. The resulting yellow solution was evaporated to ca. 1 mL, *i*-PrOH (10 mL) was added and the mixture was evaporated to ca. 6 mL. Complex **3** crystallized as a pale yellow solid, which was filtered, washed with *i*-PrOH (2×0.5 mL) and air dried, 0.085 g, 60% yield. *Anal.* Calc. for $C_{104}H_{112}F_{20}N_8P_4Pt_4$: C, 45.49; H, 4.09; N, 4.06. Found: C, 45.69; H, 4.21; N, 4.20%. IR: 780, 771 (X-sensitive C_6F_5 group); 2063 $\nu(N_3)$ cm^{-1}. ^1H NMR (295 K, $(CD_3)_2CO$, 400 MHz): δ 7.77 (broad m, 16 *o*-H, C_6H_5), 7.21 to 7.12 (m, 24 *m*- + *p*-H, C_6H_5), 3.45 (m, 16 CH_2, NBu_4), 1.83 (m, 16 CH_2, NBu_4), 1.43 (pseudosextet, 16 CH_2, NBu_4), 0.98 (t, 24 CH_3, NBu_4). ^{19}F NMR (295 K, $(CD_3)_2CO$, 376.5 MHz): δ −116.3 (m, 8 *o*-F, ^3JPt,F = 323 Hz), −168.6 (m, 8 *m*-F), −169.6 (t, 4 *p*-F). $^{31}P\{^1H\}$ NMR (acetone-*d6*, 293 K, 162.0 MHz), δ: −143.5 (broad s, $^1J_{Pt,P}$ = 2505 and 1907 Hz) ppm.

2.4. Synthesis of $[NBu_4]_2[\{(R_F)_2Pt(\mu\text{-}PPh_2)_2Pt(\mu\text{-}PPh_2)_2Pt(\mu\text{-}1,1\text{-}N_3)\}_2]$, **4**

Complex **4** was prepared similarly to **3** $\{[(R_F)_2Pt(\mu\text{-}PPh_2)_2Pt(\mu\text{-}PPh_2)_2Pt(CH_3CN)_2]$, **2**, (0.151 g, 0.086 mmol), NaN_3 (0.055 g, 0.852 mmol) and $[NBu_4]ClO_4$ (0.059 g, 0.173 mmol)$\}$ as a pale yellow solid. 0.127 g, 76% yield. *Anal.* Calc. for $C_{152}H_{152}F_{20}N_8P_8Pt_6$: C, 46.94; H, 3.94; N, 2.88. Found: C, 47.06; H, 3.92; N, 2.98%. IR: 776, 767 (X-sensitive C_6F_5 group); 2066 $\nu(N_3)$ cm^{-1}. ^1H NMR (295 K, $(CD_3)_2CO$, 400 MHz): δ 7.41 (broad m, 16 *o*-H, C_6H_5), 7.13 (m, 8 *p*-H, C_6H_5), 7.04 (broad m, 16 *o*-H, C_6H_5), 7.00 (m, 16 *m*-H, C_6H_5), 6.82 (m, 8 *p*-H, C_6H_5), 6.65 (m, 16 *m*-H, C_6H_5), 3.45 (m, 16 CH_2, NBu_4), 1.83 (m, 16 CH_2, NBu_4), 1.43 (pseudosextet, 16 CH_2, NBu_4), 0.98 (t, 24 CH_3, NBu_4). ^{19}F NMR (295 K, $(CD_3)_2CO$, 376.5 MHz): δ −115.1 (m, 8 *o*-F, ^3JPt,F = 326 Hz), −169.0 (m, 8 *m*-F), −170.3 (t, 4 *p*-F). $^{31}P\{^1H\}$ NMR (acetone-*d6*, 293 K, 162.0 MHz), δ: −112.3 ($^1J_{Pt,P} \approx 1632$ and 1782 Hz, P^A, *P* trans to C_6F_5), −134.0 ($^1J_{Pt,P} \approx 1728$ and 2434 Hz, P^X) ppm. J_{AX} = 301 Hz, $J_{AX'}$ = 11 Hz, $J_{AA'}$ = 152 Hz, $J_{XX'}$ = 121 Hz. The P–P coupling constants have been derived from the XX′ part analysis because of these signals are sharper than the observed in the AA′ part. For a AA′XX′ spin system, ten signals could be observed for each part. Since eight of the signals can be identified in the XX′ part of the spectrum, the $|J_{PP}|$ values given before can be calculated.

2.5. Synthesis of $[NBu_4]_2[\{(R_F)_2Pt(\mu\text{-}PPh_2)_2Pt\}_2(\mu\text{-}C_2O_4\text{-}\kappa^2O,O':\kappa^2O'',O''')]$, **5**

Complex **5** was prepared similarly to **3** $\{[(R_F)_2Pt(\mu\text{-}PPh_2)_2Pt(CH_3CN)_2]$, **1**, (0.200 g, 0.170 mmol), $K_2C_2O_4{\cdot}H_2O$ (0.016 g, 0.087 mmol) and $[NBu_4]ClO_4$ (0.058 g, 0.170 mmol)$\}$ as a pale yellow solid. 0.180 g, 77% yield. *Anal.* Calc. for $C_{106}F_{20}H_{112}N_2O_4P_4Pt_4$: C, 46.09; H, 4.08; N, 1.01. Found: C, 46.42; H, 4.30; N, 1.01%. IR: 781, 773 (X-sensitive C_6F_5 group); 1604 $\nu(C{\equiv}O)$ cm^{-1}. ^1H NMR (295 K, $(CD_3)_2CO$, 400 MHz): δ 7.73 (m, 16 *o*-H, C_6H_5), 7.20 (m, 8 *p*-H, C_6H_5), 7.13 (m, 16*m*-H, C_6H_5), 3.44 (m, 16 CH_2, NBu_4), 1.83 (m, 16 CH_2, NBu_4), 1.43 (pseudosextet, 16 CH_2, NBu_4), 0.98 (t, 24 CH_3, NBu_4). ^{19}F NMR (295 K, $(CD_3)_2CO$, 376.5 MHz): δ −116.5 (broad m, 8 *o*-F, ^3JPt,F = 326 Hz), −166.4 (m, 8 *m*-F), −169.0 (t, 4 *p*-F). $^{31}P\{^1H\}$ NMR (acetone-*d6*, 293 K, 162.0 MHz), δ: −144.2 (broad s, $^1J_{Pt,P}$ = 2640 and 1953 Hz) ppm

2.6. Synthesis of $[NBu_4]_2[\{(R_F)_2Pt(\mu\text{-}PPh_2)_2Pt(\mu\text{-}PPh_2)_2Pt\}_2(\mu\text{-}C_2O_4\text{-}\kappa^2O,O':\kappa^2O'',O''')]$, **6**

Complex **6** was prepared similarly to **3** $\{[(R_F)_2Pt(\mu\text{-}PPh_2)_2Pt(\mu\text{-}PPh_2)_2Pt(CH_3CN)_2]$, **2**, (0.150 g, 0.086 mmol), $K_2C_2O_4{\cdot}H_2O$ (0.030 g, 0.160 mmol) and $[NBu_4]ClO_4$ (0.059 g, 0.172 mmol)$\}$ as a pale yellow solid. 0.123 g, 74% yield. *Anal.* Calc. for $C_{154}F_{20}H_{152}N_2O_4P_8Pt_6$: C, 47.51; H, 3.94; N, 0.72. Found: C, 47.74; H, 3.60; N, 0.88%. IR: 778, 770 (X-sensitive C_6F_5 group); 1605 $\nu(C{=}O)$ cm^{-1}. ^1H NMR (295 K, $(CD_3)_2CO$, 400 MHz): δ 7.31 (broad m, 16 *o*-H, C_6H_5), 7.13 (m, 8 *p*-H, C_6H_5), 7.11 (broad m, 16 *o*-H, C_6H_5), 7.01 (t, 16 *m*-H, C_6H_5), 6.84 (t, 8 *p*-H, C_6H_5), 6.67 (t, 16 *m*-H, C_6H_5), 3.45 (m, 16 CH_2, NBu_4), 1.83 (m, 16 CH_2, NBu_4), 1.44 (pseudosextet, 16 CH_2, NBu_4), 0.98 (t, 24 CH_3, NBu_4). ^{19}F NMR (295 K, $(CD_3)_2CO$, 376.5 MHz): δ −115.2 (m, 8 *o*-F, ^3JPt,F = 329 Hz), −168.9 (m, 8 *m*-F), −170.1 (t, 4 *p*-F). $^{31}P\{^1H\}$ NMR (acetone-*d6*, 293 K, 162.0 MHz), δ: −112.4 ($^1J_{Pt,P} \approx 1645$ and 1769 Hz, P^A, *P* trans to C_6F_5), −132.4 ($^1J_{Pt,P} \approx 1729$ and 2595 Hz, P^X) ppm. J_{AX} = 300 Hz, $J_{AX'}$ = 8 Hz, $J_{AA'}$ = 156 Hz, $J_{XX'}$ = 126 Hz. The P–P coupling constants have been derived from the XX′ part analysis because of these signals are sharper than the observed in the AA′ part. For a AA′XX′ spin system, ten signals could be observed for each part. Since eight of the signals can be identified in the XX′ part of the spectrum, the $|J_{PP}|$ values given before can be calculated.

2.7. Synthesis of $[NBu_4]_2[(R_F)_2Pt(\mu\text{-}PPh_2)_2Pt(\mu\text{-}PPh_2)_2Pt(CN)_2]$, **7**

To a suspension of **2** (0.506 g, 0.170 mmol) in acetone (40 mL) was added KCN (0.090 g, 1.382 mmol) and the mixture was stirred at room temperature for 12 h. The resulting suspension was filtered, $[NBu_4]ClO_4$ (0.199 g, 0.582 mmol) was added and the mixture was evaporated to ca. 3 mL. *i*-PrOH (15 mL) was added and a pale yellow solid crystallized. The mixture was evaporated to ca. 15 mL. and a pale yellow solid, **7**, was filtered off, washed with of *i*-PrOH (2×1 mL) and vacuum dried. **7**, 0.553 g, 87% yield. *Anal.* Calc. for $C_{94}H_{112}F_{10}N_4P_4Pt_3$: C, 51.39; H, 5.14; N, 2.55. Found: C, 50.92; H, 5.42; N, 2.56%. IR: 777, 769 (X-sensitive C_6F_5 group); 2117 $\nu(C{\equiv}N)$ cm^{-1}. ^1H NMR (295 K, $(CD_3)_2CO$, 400 MHz): δ 7.53 (broad m, 8 *o*-H, C_6H_5), 7.14 (broad m, 8 *o*-H, C_6H_5), 7.03 (t, 4 *p*-H, C_6H_5), 6.96 (t, 8 *m*-H, C_6H_5), 6.83 (t, 4 *p*-H, C_6H_5), 6.67 (t, 8 *m*-H, C_6H_5), 3.40 (m, 16 CH_2, NBu_4), 1.77 (m, 16 CH_2, NBu_4), 1.39 (pseudosextet, 16 CH_2, NBu_4), 0.95 (t, 24 CH_3, NBu_4). ^{19}F NMR (295 K, $(CD_3)_2CO$, 376.5 MHz): δ −114.9 (m, 4 *o*-F, ^3JPt,F = 335 Hz), −169.1 m, (4 *m*-F), -170.1 (t, 2 *p*-F). $^{31}P\{^1H\}$ NMR (acetone-*d6*, 293 K, 162.0 MHz), δ: −113.0 ($^1J_{Pt,P} \approx 1603$ and 1732 Hz, P^A, *P* trans to C_6F_5), −146.5 ($^1J_{Pt,P} \approx 1648$ and 1768 Hz, P^X) ppm. J_{AX} = 285 Hz, $J_{AX'}$ = 16 Hz, $J_{AA'}$ = 130 Hz, $J_{XX'}$ = 125 Hz. The P–P coupling constants have been derived from the XX′ part analysis because of these signals are sharper than the observed in the AA′ part. The ten signals are identified in the XX′ part and the earlier $|J_{PP}|$ values can be calculated.

2.8. Crystallographic details

Crystal data and other details of the structure analyses are presented in Table 1. Suitable crystals for X-ray diffraction studies were obtained by slow diffusion of: *n*-hexane into concentrated solutions of the complexes in 3 mL of Me_2CO (**3** and **5**), petroleum ether into concentrated solutions of complex **4** in 3 mL of Me_2CO and a MeOH/*n*-hexane (1:1) mixture into concentrated solutions of complex **6′** in 3 mL of CH_2Cl_2. Crystals were mounted at the end of quartz fibres. The radiation used in all cases was graphite

Table 1
Crystal data and structure refinement for complexes $[NBu_4]_2[\{(R_F)_2Pt(\mu\text{-}PPh_2)_2Pt(\mu\text{-}1,1\text{-}N_3)\}_2]\cdot 1.3Me_2CO\cdot 0.3n\text{-}C_6H_{14}$ (**3**·1.3Me$_2$CO·0.3*n*-C$_6$H$_{14}$), $[NBu_4]_2[\{(R_F)_2Pt(\mu\text{-}PPh_2)_2Pt(\mu\text{-}PPh_2)_2Pt(\mu\text{-}1,1\text{-}N_3)\}_2]\cdot 2Me_2CO\cdot 2n\text{-}C_5H_{12}$ (**4**·2Me$_2$CO·2*n*-C$_5$H$_{12}$), $[NBu_4]_2[\{(R_F)_2Pt(\mu\text{-}PPh_2)_2Pt\}_2(\mu\text{-}C_2O_4\text{-}\kappa^2O,O':\kappa^2O'',O''')]\cdot 4Me_2CO$ (**5**·4Me$_2$CO), and $N(PPh_3)_2)_2[\{(R_F)_2Pt(\mu\text{-}PPh_2)_2\text{-}Pt(\mu\text{-}PPh_2)_2Pt\}_2(\mu\text{-}C_2O_4\text{-}\kappa^2O,O':\kappa^2O'',O''')]\cdot 0.7CH_2Cl_2\cdot x$MeOH (**6′**·0.7CH$_2Cl_2$·*x*MeOH).

	3·1.3Me$_2$CO·0.3*n*-C$_6$H$_{14}$	**4**·2Me$_2$CO·2*n*-C$_5$H$_{12}$	**5**·4Me$_2$CO	**6′**·1.4CH$_2$Cl$_2$·*x*MeOH
Formula	$C_{104}H_{112}F_{20}N_8P_4Pt_4$ 1.3Me$_2$CO·0.3*n*-C$_6$H$_{14}$	$C_{152}H_{152}F_{20}N_8P_8Pt_6$ 2Me$_2$CO·2*n*-C$_5$H$_{12}$	$C_{106}H_{112}F_{20}N_2O_4P_4Pt_4$ 4Me$_2$CO	$C_{194}H_{140}F_{20}N_2O_4P_{12}Pt_6$ 0.7CH$_2$Cl$_2$·*x*MeOH
M_t	2859.61	4149.56	2994.53	4603.55
Crystal system	monoclinic	triclinic	triclinic	triclinic
Space group	*C*2/*c*	P$\bar{1}$	P$\bar{1}$	P$\bar{1}$
a (Å)	45.6260(5)	11.6836(8)	12.6049(6)	14.3212(2)
b (Å)	23.8283(3)	12.9431(5)	13.9590(10)	16.3216(2)
c (Å)	20.7786(2)	29.9205(9)	18.4014(6)	21.8189(3)
α (°)	90	90.076(3)	78.919(4)	102.328(1)
β (°)	91.0483(9)	100.661(4)	80.161(3)	101.313(1)
γ (°)	90	114.603(5)	69.917(5)	95.261(1)
V (Å^3)	22586.5(4)	4027.3(3)	2964.8(3)	4837.92(11)
Z	8	1	1	1
D_{calc} (g cm^{-3})	1.682	1.711	1.677	1.580
T (K)	100(1)	100(1)	100(1)	100(1)
μ (mm^{-1})	5.079	5.348	4.844	4.530
F(000)	11205	2036	1474	2236
2θ (°)	8.2–54.0	8.2–53.0	7.5–54.1	8.3–57.8
Collected reflections	123096	44474	34403	104912
Unique reflections	24551	16617	12778	104912
Data/restraints/parameters	24551/158/1508	16617/60/955	15556/17/1045	23266/4/1105
R_{int}	0.0634	0.0578	0.0176	0.0462
R_1, wR_2[a] [$I > 2\sigma(I)$]	0.0389, 0.0690	0.0385, 0.0725	0.0176, 0.0441	0.0402, 0.0998
R_1, wR_2[a] (all data)	0.0691, 0.0731	0.0720, 0.0764	0.0215, 0.0455	0.0712, 0.1039
Goodness-of-fit (GOF) on F^2[b]	1.020	0.883	1.073	1.052
Largest difference peak/hole (e Å^{-3})	1.63/−1.12	1.65/−1.73	1.08/−0.71	4.49/−1.13

[a] $R_1 = \Sigma(|F_o| - |F_c|)/\Sigma|F_o|$. $wR_2 = [\Sigma w (F_o^2 - F_c^2)^2/\Sigma w(F_o^2)^2]^{1/2}$.
[b] Goodness-of-fit = $[\Sigma w (F_o^2 - F_c^2)^2/(n_{obs} - n_{param})]^{1/2}$.

monochromated Mo Kα (λ = 0.71073 Å). X-ray intensity data were collected on an Oxford Diffraction Xcalibur diffractometer. The diffraction frames were integrated and corrected from absorption by using the CRYSALIS RED program [26]. The structures were solved by Patterson and Fourier methods and refined by full-matrix least squares on F^2 with SHELXL-97 [27]. All non-hydrogen atoms were assigned anisotropic displacement parameters and refined without positional constraints, except as noted below. All hydrogen atoms were constrained to idealized geometries and assigned isotropic displacement parameters equal to 1.2 times the *U*iso values of their attached parent atoms (1.5 times for the methyl hydrogen atoms). In the structure of **3**·1.3Me$_2$CO·0.3*n*-C$_6$H$_{14}$, one of the NBu_4^+ cations is disordered over two sets of positions that were refined with partial occupancy 0.5/0.5. Restraints were applied in the geometry and thermal parameters of some of the atoms of these disordered moieties. For **4**·2Me$_2$CO·2*n*-C$_5$H$_{12}$, due to the poor quality of the only available crystals, the intensity of the data was small, especially at higher angles. Despite the fact that the structure could be unambiguously established and that the final indexes are quite reasonable, the low intensity of the data is reflected by the amount of residual electron density points of low intensity, but above 1 e Å−3, with clearly no chemical meaning. For **6′**·0.7CH$_2$Cl$_2$·*x*MeOH, a partially disordered molecule of CH_2Cl_2 is present, and its chlorine atoms were refined with partial occupancy 0.5/0.2, and restraints in its geometric parameters and anisotropic displacement parameters were used. Furthermore, a great amount of very diffuse electron density was found. It was not possible to model this density in any logical chemical species, but it seems to correspond to very disordered molecules of methanol, one of the solvents used in the crystallization. This diffuse electron density was treated with the SQUEEZE procedure, as implemented in the PLATON computer crystallographic program [28]. Full-matrix least-squares refinement of these models against F^2 converged to the final residual indexes given in Table 5.

3. Results and discussion

3.1. Reaction of 1 and 2 with azide or oxalate

The addition of an excess of NaN_3 to acetone solutions of the dinuclear or trinuclear platinum(II) phosphanido complexes $[(R_F)_2Pt(\mu\text{-}PPh_2)_2Pt(CH_3CN)_2]$ [24] **1** or $[(R_F)_2Pt(\mu\text{-}PPh_2)_2Pt(\mu\text{-}PPh_2)_2Pt(CH_3CN)_2]$ [25] **2** results in a substitution reaction and the formation of the azido complexes. In spite of the fact that an excess of the azido ligand has been used, we have not detected the formation of the corresponding dianionic complexes with two terminal azido groups coordinated to the platinum centres $[(R_F)_2Pt(\mu\text{-}PPh_2)_2Pt(N_3)_2]^{2-}$ or $[(R_F)_2Pt(\mu\text{-}PPh_2)_2Pt(\mu\text{-}PPh_2)_2Pt(N_3)_2]^{2-}$ but rather only complexes with bridging azido ligands. As will be discussed further on, the azido group is coordinated to the platinum centres in a μ-1,1-N_3 bridging mode so that the tetranuclear $[NBu_4]_2[\{(R_F)_2Pt(\mu\text{-}PPh_2)_2Pt(\mu\text{-}1,1\text{-}N_3)\}_2]$, **3** or hexanuclear $(NBu_4)_2[\{(R_F)_2Pt(\mu\text{-}PPh_2)_2Pt(\mu\text{-}PPh_2)_2Pt(\mu\text{-}1,1\text{-}N_3)\}_2]$, **4** derivatives are obtained respectively.

The azide anion N_3^- is known to coordinate to the metal centres in both terminal and bridging modes [29–32]. The coordination of the azido group to a platinum centre as a terminal monodentate ligand is well known [33–36] but in our case the tetranuclear or hexanuclear complexes **3** and **4** in which the azido groups coordinate as a μ-1,1-N_3 bridging ligand. Considering that azido is a common pseudohalide bridging ligand, this behavior is analogous to that observed in the synthesis of tetranuclear and hexanuclear chlorido complexes $[\{(R_F)_2Pt(\mu\text{-}PPh_2)_2Pt(\mu\text{-}Cl)\}_2]^{2-}$ [37] and $[\{(R_F)_2Pt(\mu\text{-}PPh_2)_2Pt(\mu\text{-}PPh_2)_2Pt(\mu\text{-}Cl)\}_2]^{2-}$ [25]. As far as we know, complexes with a "Pt(μ-1,1-N_3)Pt" skeleton have not been structurally characterized by X-ray diffraction (CSD and ICSD) and the only azido bridging platinum complex structurally characterized shows the azido ligand coordinated in a (μ-1,1,1-N_3) mode to the Pt atoms [38]. Nevertheless a great number of nickel complexes

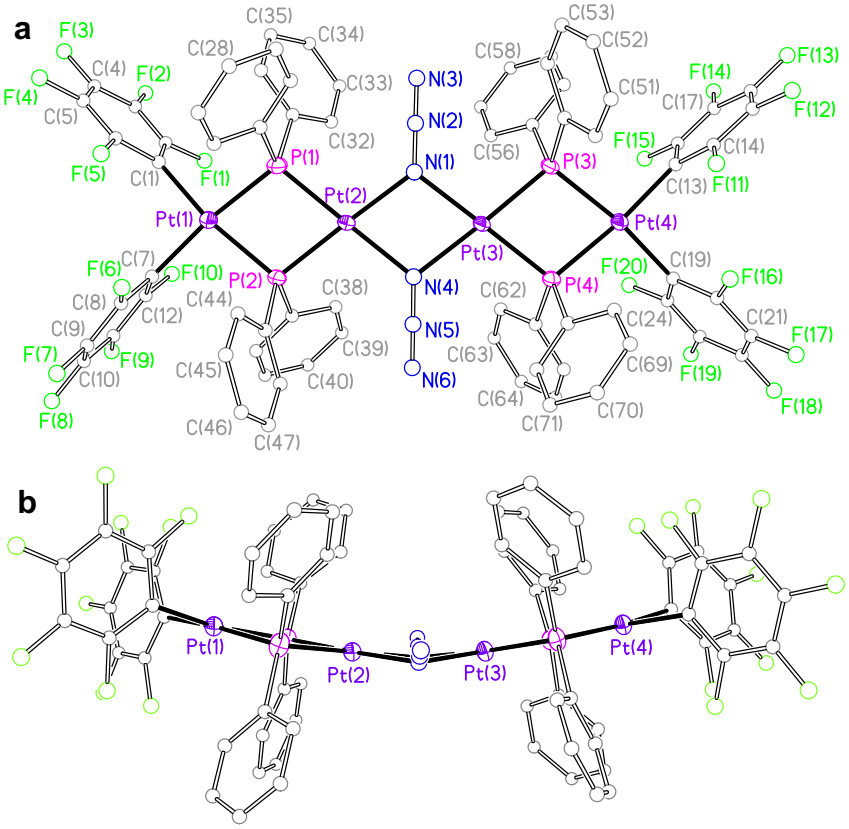

Fig. 1. Two views of the molecular structure of anion of the complex $[NBu_4]_2[\{(R_F)_2Pt(\mu\text{-}PPh_2)_2Pt(\mu\text{-}1,1\text{-}N_3)\}_2]$ (**3**).

with bridging azido ligands [29,39,40] are known and some palladium complexes showing the "$Pd(\mu\text{-}1,1\text{-}N_3)_xPd$" fragment have been also reported [41–43].

The structures of complexes **3** and **4** have been established by X-ray diffraction measurements. Figs. 1 and 2 show views of the corresponding anions, and Tables 2 and 3 list a selection of relevant bond distances and angles. The crystal structure confirms the tetranuclear and hexanuclear nature of the anions of **3** and **4**, respectively. In the case of **4**, the complex anion shows the symmetry caused by an inversion centre located in the middle of the molecule. The anion complexes can be regarded as an array of square planar platinum units sharing edges. The innermost bridging systems between the Pt atoms are made up of two azido groups, while the remaining outermost ones are constituted by two phosphanido ligands. The coordination sphere of each of the outermost Pt centres is completed by two pentafluorophenyl groups in a mutually *cis* position. The four metal atoms have a roughly linear arrangement, the Pt(1)–Pt(2)–Pt(3) and Pt(2)–Pt(3)–Pt(4) angles being 169.2(1)° and 169.4(1)° respectively in **3**, and Pt(1)–Pt(2)–Pt(3) and Pt(2)–Pt(3)–Pt(3′) angles of 177.3(1)° and 169.7(1)° respectively in **4**. The intermetallic separation is longer between the phosphanido-bridged metals (range 3.550(1)-3.578(1) Å) than between the azido- bridged Pt (3.374(1) Å for **3** and 3.381(1) Å for **4**). The azido ligands bridge the central platinum atoms symmetrically and all Pt–N distances and Pt–N–N angles are very similar. The disposition of the array of the three N atoms in each ligand is linear, with an almost planar environment of the bridging N atoms and, in both cases, the Pt–N–Pt angles in **3** and **4** are minor than the Pt–N–N ones.

The overall relative disposition of the square planes of the Pt centres displays some differences in **3** and **4**. Thus, in **3**, both "$(R_F)_2Pt(\mu\text{-}PPh_2)_2Pt(\mu\text{-}1,1\text{-}N_3)_2$" halves are essentially planar (the dihedral angle between the Pt(1) and Pt(2) best planes is 7.3(1)° and between the Pt(3) and Pt(4) best planes is 4.2(1)°), while the complex is bent on the imaginary vector N(1)–N(4), the dihedral angle between the Pt(2) and Pt(3) best planes being 16.2(1)° (see Fig. 1b). The lines formed by the three nitrogen atoms of each azido ligand are not contained in their respective Pt(2)–Pt(3)–N(1,4) planes, but are slightly inward-bent (angles between the perpendicular to the Pt(2)–Pt(3)–N(1,4) and the azide line is 70.7(4)° for N(1) azide and 69.6(2)° for N(4) azide). On the other hand, in **4** the Pt(3)–N(1)–N(1′)–Pt(3′) core is planar, and the azide vectors are contained in this plane (see Fig. 2b). The coordination environments of Pt(3) and Pt(3′) are coplanar, while the square planes of the Pt(1) and Pt(2) and Pt(1′) and Pt(2′) centres are bent (dihedral angle plane Pt(1)-plane Pt(2) 28.9(1)°; dihedral angle plane Pt(2)-plane Pt(3) 22.8(1)°), probably due to the steric hindrances of the diphenylphosphido ligands, thus establishing a kind of zigzag configuration (see Fig. 2b).

In an attempt to obtain dinuclear or trinuclear anions we have treated solutions of **1** or **2** in acetone with an excess of $K_2C_2O_4$ but in both cases the tetranuclear $[NBu_4]_2[\{(R_F)_2Pt(\mu\text{-}PPh_2)_2Pt\}_2(\mu\text{-}C_2O_4\text{-}\kappa^2O,O':\kappa^2O'',O''')]$, **5**, or hexanuclear $[NBu_4]_2[\{(R_F)_2Pt(\mu\text{-}PPh_2)_2Pt(\mu\text{-}PPh_2)_2Pt\}_2(\mu\text{-}C_2O_4\text{-}\kappa^2O,O':\kappa^2O'',O''')]$, **6**, were respectively obtained after work-up of the mixture[1]. Complexes **5** and **6** are the result of the substitution of the acetonitrile ligands and the coordination of the oxalato group through the four oxygen atoms to two di- or trinuclear fragments in a chelating and bridging mode. Since we were not able to obtain crystals of **6** suitable for X-ray purposes we prepared $(N(PPh_3)_2)_2[\{(R_F)_2Pt(\mu\text{-}PPh_2)_2Pt(\mu\text{-}PPh_2)_2Pt\}_2(\mu\text{-}C_2O_4\text{-}\kappa^2O,O':\kappa^2O'',O''')]$, **6′**, using an analogous procedure to that used for **6**, adding bis(triphenylphosphine)iminium as the cation instead of tetrabutyl ammonium.

[1] As was suggested by one of the referees, we have added $K_2C_2O_4$ (0.031 g, 0.168 mmol) to an acetone solution of complex **5** (0.043 g, 0.016 mmol) and the mixture has been refluxed for 4 h. The evaporation to dryness gives a white solid, the ^{19}F and ^{31}P NMR spectra ($(CD_3)_2CO$) of which show signals due only to, complex **5**.

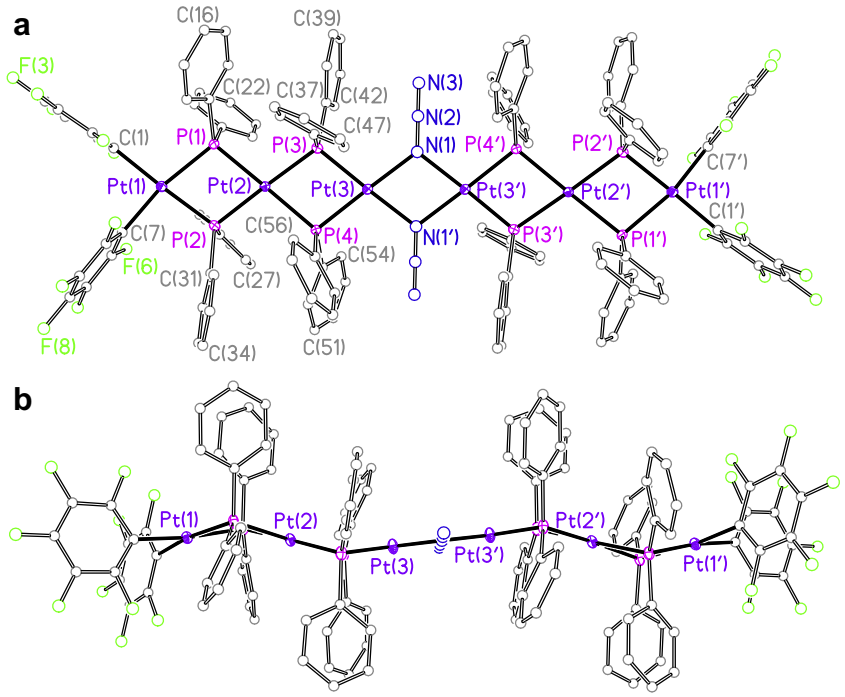

Fig. 2. Two views of the molecular structure of anion of the complex $[NBu_4]_2[\{(R_F)_2Pt(\mu\text{-}PPh_2)_2Pt(\mu\text{-}PPh_2)_2Pt(\mu\text{-}1,1\text{-}N_3)\}_2]$ (**4**).

Table 2
Selected bond lengths (Å) and angles (°) for $[NBu_4]_2[\{(R_F)_2Pt(\mu\text{-}PPh_2)_2Pt(\mu\text{-}1,1\text{-}N_3)\}_2]\cdot 1.3Me_2CO\cdot 0.3n\text{-}C_6H_{14}$ (**3**·1.3Me_2CO·0.3*n*-C_6H_{14}).

Pt(1)–C(1)	2.055(5)	Pt(1)–C(7)	2.074(5)
Pt(1)–P(1)	2.288(2)	Pt(1)–P(2)	2.300 (2)
Pt(2)–N(1)	2.125(4)	Pt(2)–N(4)	2.149(4)
Pt(2)–P(2)	2.262(1)	Pt(2)–P(1)	2.264(2)
Pt(3)–N(1)	2.133(4)	Pt(3)–N(4)	2.157(4)
Pt(3)–P(4)	2.260(1)	Pt(3)–P(3)	2.268(1)
Pt(4)–C(2)	2.068(5)	Pt(4)–C(1)	2.077(5)
Pt(4)–P(4)	2.296(1)	Pt(4)–P(3)	2.298(2)
N(1)–N(2)	1.226(6)	N(2)–N(3)	1.144(6)
N(4)–N(5)	1.230(6)	N(5)–N(6)	1.132(6)
C(1)–Pt(1)–C(7)	90.7(2)	C(1)–Pt(1)–P(1)	97.1(2)
C(7)–Pt(1)–P(1)	171.7(2)	C(1)–Pt(1)–P(2)	169.6(2)
C(7)–Pt(1)–P(2)	96.9(2)	P(1)–Pt(1)–P(2)	75.9(5)
N(1)–Pt(2)–N(4)	75.0(2)	N(1)–Pt(2)–P(2)	177.8(1)
N(4)–Pt(2)–P(2)	103.6(1)	N(1)–Pt(2)–P(1)	104.3(1)
N(4)–Pt(2)–P(1)	179.2(1)	P(2)–Pt(2)–P(1)	77.1(5)
N(1)–Pt(3)–N(4)	74.7(2)	N(1)–Pt(3)–P(4)	179.2(1)
N(4)–Pt(3)–P(4)	104.5(1)	N(1)–Pt(3)–P(3)	103.5(1)
N(4)–Pt(3)–P(3)	176.3(1)	P(4)–Pt(3)–P(3)	77.3(5)
C(19)–Pt(4)–C(13)	89.6(2)	C(19)–Pt(4)–P(4)	96.9(1)
C(13)–Pt(4)–P(4)	173.4(1)	C(19)–Pt(4)–P(3)	172.0(2)
C(13)–Pt(4)–P(3)	97.7(1)	P(4)–Pt(4)–P(3)	76.0(5)
Pt(2)–P(1)–Pt(1)	103.6(6)	Pt(2)–P(2)–Pt(1)	103.3(5)
Pt(3)–P(3)–Pt(4)	103.2(6)	Pt(3)–P(4)–Pt(4)	103.5(6)
N(2)–N(1)–Pt(2)	126.1(4)	N(2)–N(1)–Pt(3)	124.2(3)
Pt(2)–N(1)–Pt(3)	104.8(2)	N(3)–N(2)–N(1)	179.2(7)
N(5)–N(4)–Pt(2)	125.5(3)	N(5)–N(4)–Pt(3)	125.7(3)
Pt(2)–N(4)–Pt(3)	103.2(2)	N(6)–N(5)–N(4)	178.5(6)

Table 3
Selected bond lengths (Å) and angles (°) for $[NBu_4]_2[\{(R_F)_2Pt(\mu\text{-}PPh_2)_2Pt(\mu\text{-}PPh_2)_2\text{-}Pt(\mu\text{-}1,1\text{-}N_3)\}_2]\cdot 2Me_2CO\cdot 2n\text{-}C_5H_{12}$ (**4**·2Me_2CO·2*n*-C_5H_{12}).

Pt(1)–C(7)	2.076(6)	Pt(1)–C(1)	2.096(5)
Pt(1)–P(2)	2.291(2)	Pt(1)–P(1)	2.323(2)
Pt(2)–P(4)	2.336(2)	Pt(2)–P(2)	2.336(2)
Pt(2)–P(3)	2.345(2)	Pt(2)–P(1)	2.361(2)
Pt(3)–N(1)	2.128(5)	Pt(3)–N(1′)	2.131(4)
Pt(3)–P(3)	2.247(2)	Pt(3)–P(4)	2.254(2)
C(7)–Pt(1)–C(1)	88.8(2)	C(7)–Pt(1)–P(2)	94.2(2)
C(1)–Pt(1)–P(2)	173.7(2)	C(7)–Pt(1)–P(1)	168.7(2)
C(1)–Pt(1)–P(1)	101.7(2)	P(2)–Pt(1)–P(1)	75.8(5)
P(4)–Pt(2)–P(2)	104.3(5)	P(4)–Pt(2)–P(3)	74.0(5)
P(2)–Pt(2)–P(3)	177.9(6)	P(4)–Pt(2)–P(1)	177.1(6)
P(2)–Pt(2)–P(1)	74.2(5)	P(3)–Pt(2)–P(1)	107.5(5)
N(1)–Pt(3)–N(1′)	74.9(2)	N(1)–Pt(3)–P(3)	103.4(1)
N(1′)–Pt(3)–P(3)	178.1(1)	N(1)–Pt(3)–P(4)	178.2(2)
N(1′)–Pt(3)–P(4)	104.1(1)	P(3)–Pt(3)–P(4)	77.5(5)
Pt(1)–P(1)–Pt(2)	99.4(6)	Pt(1)–P(2)–Pt(2)	101.1(6)
Pt(3)–P(3)–Pt(2)	101.3(6)	Pt(3)–P(4)–Pt(2)	101.4(6)
N(2)–N(1)–Pt(3)	128.2(4)	N(2)–N(1)–Pt(3′)	126.3(4)
Pt(3)–N(1)–Pt(3′)	105.1(2)	N(3)–N(2)–N(1)	179.5(9)

The symmetry transformation used to generate equivalent primed atoms is $-x,-y,-z$.

The structures of complexes **5** and **6′** have been established by an X-ray diffraction study. Figs. 3 and 4 show views of the corresponding anion of the complexes and Tables 4 and 5 list a selection of relevant bond distances and angles. The anions of **5** and **6′** are symmetric tetra and hexanuclear complexes, respectively. In both cases, the anions have a crystallographically imposed inversion centre. The anions are formed by an array of square planar platinum units that share one or two edges. At the centre of each anion there is an oxalato ligand, bonded in a $\mu\text{-}C_2O_4\text{-}\kappa^2O,O':\kappa^2O'',O'''$ mode, bridging the innermost platinum atoms. The rest of the links between the metal centres are established by phosphanido ligands. The external Pt centres complete their coordination sphere with two *cis* pentafluorophenyl groups. The four (**5**) or six (**6′**) platinum atoms are in a linear disposition, with Pt–Pt–Pt angles ranging from 169.7(1)° to 177.3(1)°. The oxalato ligands are planar and coplanar with the best square plane of the Pt bonded to it (dihedral angle coordination plane Pt(2)-plane C_2O_4 is 3.1(1)° for **5**; dihedral angle coordination plane Pt(3)-plane C_2O_4 is 3.8(1)° for **6′**). The Pt–O distances are very similar in both complexes (see Tables 4 and 5) and the four C–O distances are also equal (average value 1.253 Å). In complexes **5** and **6′** the four O atoms of each oxalato group are coordinated to platinum centres and consequently the four C–O distances of these first characterized "Pt $\mu\text{-}C_2O_4\text{-}\kappa^2O,O':\kappa^2$

$O'',O''')$Pt" systems are equal and the value (average value 1.253 Å) is similar to those found in complexes with other "M(μ-C_2O_4-κ^2-$O,O':\kappa^2O'',O''')$M" systems [44–46].

As for **3** and **4**, there are some differences in the relative disposition of the square planes of the Pt centres for **5** and **6′**. Thus, while in **5** the core formed by the metal atoms, the P and C atoms bonded to them and the oxalato ligand are essentially planar (the dihedral angle between the Pt(1) and Pt(2) best planes is 4.6(1)° and between the best Pt(2) plane and the oxalato ligand is 3.1(1)°) (see Fig. 3b), in **6′** there is a perceptible bending between the Pt(1) and Pt(2) best planes (32.0(1)°) and Pt(2) and Pt(3) best planes (18.7(1)°) (see Fig. 4b) probably due, as in **4**, to the steric hindrance of the phosphanido ligands.

The coordination of the oxalato ligand to an M centre (M = Ni, Pd, Pt) as a chelate and terminal ligand is well established for the Ni triad. The coordination as a chelate and bridging ligand is found in many nickel complexes, but only in a few cases has the "Pd(μ-C_2O_4-$\kappa^2O,O':\kappa^2O'',O''')$Pd" fragment [44,47,48] been described and as far as we know complexes with a "Pt(μ-C_2O_4-$\kappa^2O,O':\kappa^2O'',O''')$Pt" fragment have not been structurally characterized by X-ray diffraction (CSD and ICSD) while some palladium [49] or platinum-based metallacycles [50] with an oxalato group as a didentate bridging ligand have been 'reported.

3.2. Spectroscopic properties

The ^{19}F NMR spectra of **3**–**6** (see Experimental) show three signals with intensities in the ratio 2:2:1. One of them, with platinum satellites, is characteristic of the *o*-F atoms, and the other two signals at higher field are due to *m*-F and *p*-F atoms. This ^{19}F NMR pattern indicates that all C_6F_5 moieties are equivalent in solution. The ^{1}H NMR spectra of **3**–**6** (see Experimental) show the signals due to PPh_2 and NBu_4^+ groups and their intensity ratio is that expected given the anionic nature of each complex. The ^{31}P{^{1}H} NMR spectra of **3** and **5** show one signal at −143.5 and −144.2 ppm, respectively, for the four equivalent P atoms with platinum satellites. The high-field chemical shifts are in agreement with the presence of "$(R_F)_2Pt^1(\mu\text{-}PPh_2)_2Pt^2$" fragments with non bonding platinum-platinum distances and the two values of $^1J_{Pt,P}$ in each complex can be unambiguously assigned: the coupling with the platinum centre bonded to nitrogen or oxygen, $^1J_{Pt2,P}$, is greater than the coupling with the platinum centre bonded to C_6F_5 groups, $^1J_{Pt1,P}$. The P atoms in **4** and **6** ("$(R_F)_2Pt^1(\mu\text{-}P^{A,A'}Ph_2)_2Pt^2(\mu\text{-}P^{X,X'}Ph_2)_2Pt^{3}$") appear as an AA′XX′ spin system in the high-field region for the isotopomers without ^{195}Pt. The AA′ part is broader than its XX′ counterpart indicating that A and A′ have to be assigned to the P atoms trans to C_6F_5 groups. Both signals show platinum satellites from which two values of $^1J_{Pt,P}$ are measured. The two values of $^1J_{Pt,P(A)}$ are very similar (about 1700 Hz) but the two values of $^1J_{Pt,P(X)}$ are different (about 1700 and 2500 Hz), indicating that the coupling with the Pt^3 platinum atom of the "Pt(μ-N_3)$_2$Pt" or "Pt(μ-C_2O_4)Pt" fragments is greater than with the Pt^2 atom. These different values of $^1J_{Pt,P}$ are in good agreement with those observed earlier in similar fragments [25,37,51].

The relevant feature of the IR spectra of **3** and **4** is the presence of a sharp absorption at 2063 and 2066 cm^{-1} respectively, which is assigned to the asymmetric stretching vibration of the ligand N_3^- and is consistent with the presence of only one type of azido bridge in the complexes [52,53]. The oxalato ligand in **5** and **6** shows absorptions at 1604 and 1605 cm^{-1} [44]. In all cases the absorptions observed in the 800 cm^{-1} region, due the X-sensitive mode of the C_6F_5 groups, are in agreement with the presence of the "*cis*-M$(C_6F_5)_2$" fragments [54,55].

3.3. Reaction of 2 with cyanide

As mentioned above, neither the azido nor the oxalato ligands are able to act as terminal ligands in the platinum phosphanido

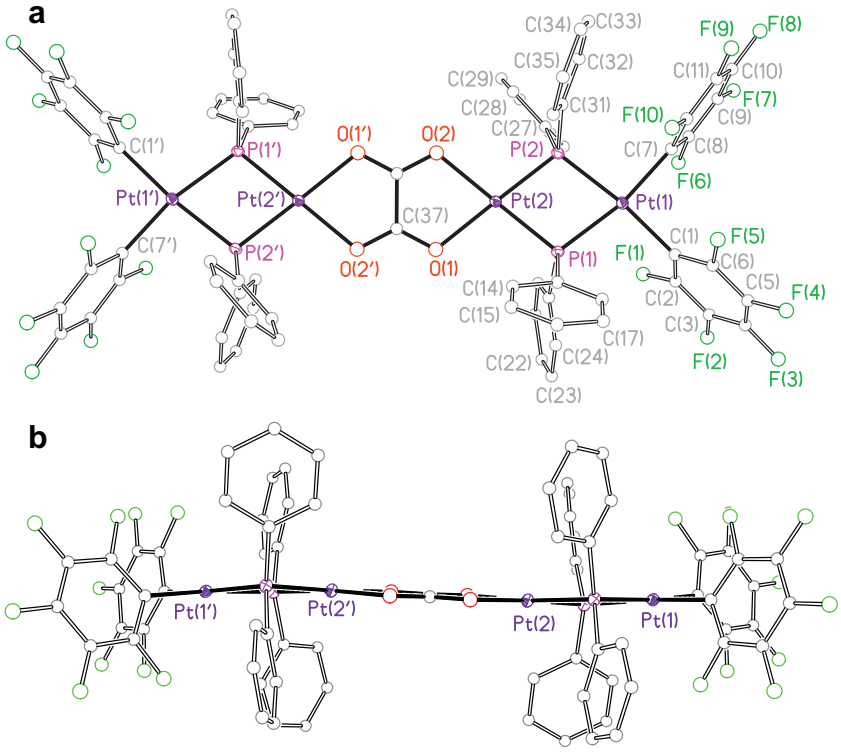

Fig. 3. Two views of the molecular structure of anion of the complex $[NBu_4]_2[\{(R_F)_2Pt(\mu\text{-}PPh_2)_2Pt\}_2(\mu\text{-}C_2O_4\text{-}\kappa^2O,O':\kappa^2O'',O''')]$ (**5**).

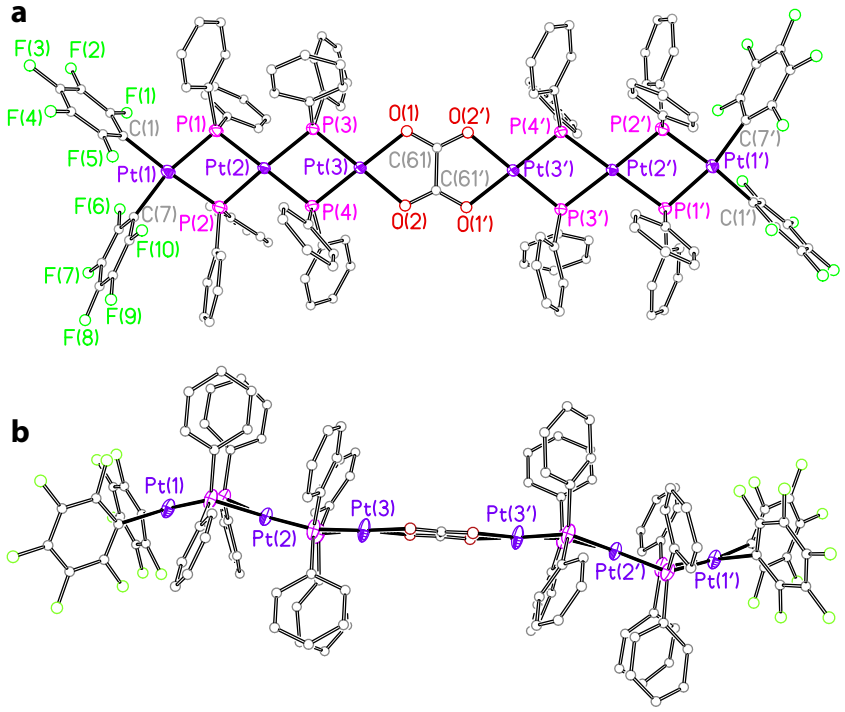

Fig. 4. Two views of the molecular structure of anion of the complex $(N(PPh_3)_2)_2[\{(R_F)_2Pt(\mu\text{-}PPh_2)_2Pt(\mu\text{-}PPh_2)_2Pt\}_2(\mu\text{-}C_2O_4\text{-}\kappa^2O,O':\kappa^2O'',O''')]$ (**6′**).

Table 4
Selected bond lengths (Å) and angles (°) for $[NBu_4]_2[\{(R_F)_2Pt(\mu\text{-}PPh_2)_2Pt\}_2(\mu\text{-}C_2O_4\text{-}\kappa^2O,O':\kappa^2O'',O''')]\cdot 4Me_2CO$ (**5**·4Me$_2$CO).

Pt(1)–C(7)	2.073(2)	Pt(1)–C(1)	2.080(2)
Pt(1)–P(2)	2.286(6)	Pt(1)–P(1)	2.301(6)
Pt(2)–O(2)	2.158(1)	Pt(2)–O(1)	2.159(2)
Pt(2)–P(2)	2.233(6)	Pt(2)–P(1)	2.239(6)
O(1)–C(37)	1.250(2)	O(2)–C(37′)	1.259(3)
C(37)–C(37′)	1.559(4)		
C(7)–Pt(1)–C(1)	91.9(8)	C(7)–Pt(1)–P(2)	94.4(6)
C(1)–Pt(1)–P(2)	172.6(6)	C(7)–Pt(1)–P(1)	168.5(6)
C(1)–Pt(1)–P(1)	99.1(6)	P(2)–Pt(1)–P(1)	74.8(2)
O(2)–Pt(2)–O(1)	78.2(6)	O(2)–Pt(2)–P(2)	102.6(4)
O(1)–Pt(2)–P(2)	175.0(4)	O(2)–Pt(2)–P(1)	177.5(4)
O(1)–Pt(2)–P(1)	102.3(4)	P(2)–Pt(2)–P(1)	77.1(2)
Pt(2)–P(1)–Pt(1)	103.7(2)	Pt(2)–P(2)–Pt(1)	104.2 (2)
C(37)–O(1)–Pt(2)	113.4(1)	C(37′)–O(2)–Pt(2)	113.0(1)
O(1)–C(37)–O(2′)	124.7(2)	O(1)–C(37)–C(37′)	117.7(2)

The symmetry transformation used to generate equivalent primed atoms is $-x,-y,-z$.

Table 5
Selected bond lengths (Å) and angles (°) for $(N(PPh_3)_2)_2[\{(R_F)_2Pt(\mu\text{-}PPh_2)_2Pt(\mu\text{-}PPh_2)_2\text{-}Pt\}_2(\mu\text{-}C_2O_4\text{-}\kappa^2O,O':\kappa^2O'',O''')]\cdot 1.4CH_2Cl_2\cdot x$MeOH (**6′**·0.7CH$_2Cl_2$·$x$MeOH).

Pt(1)–C(7)	2.069(6)	Pt(1)–C(1)	2.110(6)
Pt(1)–P(2)	2.304(1)	Pt(1)–P(1)	2.314(1)
Pt(2)–P(4)	2.345(1)	Pt(2)–P(3)	2.348(1)
Pt(2)–P(2)	2.349(1)	Pt(2)–P(1)	2.363(1)
Pt(3)–O(2)	2.137(3)	Pt(3)–O(1)	2.151(3)
Pt(3)–P(3)	2.228(1)	Pt(3)–P(4)	2.230(1)
O(1)–C(61)	1.257(6)	O(2)–C(61′)	1.247(6)
C(61)–C(61′)	1.551(1)		
C(7)–Pt(1)–C(1)	92.0(2)	C(7)–Pt(1)–P(2)	91.9(2)
C(1)–Pt(1)–P(2)	173.1(2)	C(7)–Pt(1)–P(1)	167.5(2)
C(1)–Pt(1)–P(1)	100.5(2)	P(2)–Pt(1)–P(1)	75.6(5)
P(4)–Pt(2)–P(3)	73.5(4)	P(4)–Pt(2)–P(2)	105.9(5)
P(3)–Pt(2)–P(2)	173.3(5)	P(4)–Pt(2)–P(1)	179.2(6)
P(3)–Pt(2)–P(1)	106.8(5)	P(2)–Pt(2)–P(1)	73.9(5)
O(2)–Pt(3)–O(1)	78.3 (1)	O(2)–Pt(3)–P(3)	176.5(1)
O(1)–Pt(3)–P(3)	102.5(9)	O(2)–Pt(3)–P(4)	101.0(1)
O(1)–Pt(3)–P(4)	178.4(1)	P(3)–Pt(3)–P(4)	78.1(5)
Pt(1)–P(1)–Pt(2)	99.4(5)	Pt(1)–P(2)–Pt(2)	100.1(5)
Pt(3)–P(3)–Pt(2)	102.4(5)	Pt(3)–P(4)–Pt(2)	102.4(5)
C(61)–O(1)–Pt(3)	112.6(3)	C(61′)–O(2)–Pt(3)	113.9(3)
O(2′)–C(61)–O(1)	124.9(5)	O(2′)–C(61)–C(61′)	117.1(6)
O(1)–C(61)–C(61′)	117.9(6)		

The symmetry transformation used to generate equivalent primed atoms is $-x,-y,-z$.

complexes forming the asymmetric dinuclear or trinuclear $[(R_F)_2Pt(\mu\text{-}PPh_2)_2Pt(L_2)]^{2-}$ or $[(R_F)_2Pt(\mu\text{-}PPh_2)_2Pt(\mu\text{-}PPh_2)_2PtL_2]^{2-}$ complexes (L_2^{2-} = 2 N_3^-, $C_2O_4^{2-}$). However the reaction of **2** with an excess of KCN in acetone yields the asymmetric trinuclear derivative $[NBu_4]_2[(R_F)_2Pt(\mu\text{-}PPh_2)_2Pt(\mu\text{-}PPh_2)_2Pt(CN)_2]$, **7**, with the CN groups (νCN stretching mode at 2117 cm^{-1}) acting as terminal ligands[56,57] and two NBu_4^+ groups as counterion. In agreement with this proposal the ^{1}H NMR spectrum in deuteroacetone solution shows the signals due to phenyl group atoms and those due to NBu_4^+ in the adequate ratio (40:72) while for complexes **4** and **6** this ratio is 40:36. The NMR spectroscopic features of **7** are similar to those observed for **4** and **6**. It is noteworthy that the two values of $^1J_{Pt,P(A)}$, 1603 and 1732 Hz, and the two values of $^1J_{Pt,P(X)}$, 1648 and 1768 Hz, indicate that in complex **7** the coupling with the platinum atom bonded to cyanido is in the same range as that for platinum bonded to the pentafluorophenyl and phosphanido groups, as was previously observed in the dinuclear $[NBu_4]_2[(R_F)_2Pt(\mu\text{-}PPh_2)_2Pt(CN)_2]$ [24].

4. Conclusions

The straightforward coordination process of the dinuclear or trinuclear synthons **1** and **2** with different ligands can afford di-, tri-, tetra- and hexanuclear platinum derivatives. Nevertheless the nuclearity of the new complexes obtained cannot be established *a priori*. It should be noted that although the cyanido, azido and oxalato groups are able to act as terminal ligands, only the cyanido ligand bonds the platinum atom of **1** and **2** in a terminal way whereas the azido and oxalato in complexes **3**–**6** bond two platinum centres affording tetra- or hexanuclear derivatives.

The platinum centres in complexes **3**–**6** display a linear arrangement in which only phosphanido (P donor) and azido (N donor) or oxalato (O donor) ligands support the metal centres. As far as we are aware, these complexes are the first cases of "$Pt(\mu\text{-}1,1\text{-}N_3)_2Pt$" (complexes **3** and **4**) and "$Pt(\mu\text{-}C_2O_4\text{-}\kappa^2O,O':\kappa^2O'',O''')Pt$" fragments (complexes **5** and **6**).

Acknowledgements

This work was supported by the Spanish MICINN (DGPTC)/FEDER (Project CTQ2008-06669-C02-01/BQU), MINECO/FEDER (Project CTQ2012-35251) and the Gobierno de Aragón (Grupo Consolidado E21: Química Inorgánica y de los Compuestos Organometálicos). A. A. gratefully acknowledges MICINN for a FPU grant.

Appendix A. Supplementary material

CCDC 936740–936743 contains the supplementary crystallographic data for complexes **3**–**6**. These data can be obtained free of charge from The Cambridge Crystallographic Data Centre via www.ccdc.cam.ac.uk/data_request/cif. Supplementary data associated with this article can be found, in the online version, at http://dx.doi.org/10.1016/j.ica.2013.07.048.

References

[1] A. Arias, J. Forniés, C. Fortuño, A. Martín, P. Mastrorilli, S. Todisco, M. Latronico, V. Gallo, Inorg. Chem. 52 (2013) 5493.
[2] P. Mastrorilli, Eur. J. Inorg. Chem. (2008) 4835.
[3] R. Bender, C. Okio, R. Welter, P. Braunstein, Dalton Trans. (2009) 4901.
[4] C. Cavazza, F. Fabrizi de Biani, T. Funaioli, P. Leoni, F. Marchetti, L. Marchetti, P. Zanello, Inorg. Chem. 48 (2009) 1385.
[5] V. Gallo, M. Latronico, P. Mastrorilli, C.F. Nobile, G.P. Suranna, G. Ciccarella, U. Englert, Eur. J. Inorg. Chem. (2005) 4607.
[6] A. Albinati, F. Balzanot, F. Fabrizi de Biani, P. Leoni, G. Manca, L. Marchetti, S. Rizzato, U.G. Barretta, Inorg. Chem. 49 (2010) 3714.
[7] M. Latronico, F. Polini, V. Gallo, P. Mastrorilli, B. Calmuschi-Cula, U. Englert, N. Re, T. Repo, M. Räisänen, Inorg. Chem. 47 (2008) 9779.
[8] C. Archambault, R. Bender, P. Braunstein, Y. Dusausoy, J. Chem. Soc., Dalton Trans. (2002) 4084.
[9] I. Ara, N. Chaouche, J. Forniés, C. Fortuño, A. Kribii, A.C. Tsipis, C.A. Tsipis, Inorg. Chim. Acta 358 (2005) 1377.
[10] E. Alonso, J. Forniés, C. Fortuño, A. Martín, G.M. Rosair, A.J. Welch, Inorg. Chem. 36 (1997) 4426.
[11] A. Albinati, P. Leoni, F. Marchetti, L. Marchetti, M. Pasquali, S. Rizzato, Eur. J. Inorg. Chem. (2008) 4092.
[12] A. Albinati, V. Filippi, P. Leoni, L. Marchetti, M. Pasquali, V. Passarelli, Chem. Commun. (2005) 2155.
[13] N. Chaouche, J. Forniés, C. Fortuño, A. Kribii, A. Martín, P. Karipidis, A.C. Tsipis, C.A. Tsipis, Organometallics 23 (2004) 1797.
[14] J. Forniés, C. Fortuño, S. Ibáñez, A. Martín, A.C. Tsipis, C.A. Tsipis, Angew. Chem., Int. Ed. 44 (2005) 2407.
[15] C. Archambault, R. Bender, P. Braunstein, A. Decian, J. Fischer, Chem. Commun. (1996) 2729.
[16] J. Forniés, C. Fortuño, S. Ibáñez, A. Martín, Inorg. Chem. 45 (2006) 4850.
[17] A. Arias, J. Forniés, C. Fortuño, A. Martín, M. Latronico, P. Mastrorilli, S. Todisco, V. Gallo, Inorg. Chem. 51 (2012) 12682.
[18] E. Alonso, J. Forniés, C. Fortuño, A. Martín, A.G. Orpen, Organometallics 22 (2003) 2723.
[19] E. Alonso, J. Forniés, C. Fortuño, A. Martín, A.G. Orpen, Organometallics 19 (2000) 2690.
[20] L.R. Falvello, J. Forniés, C. Fortuño, F. Durán, A. Martín, Organometallics 21 (2002) 2226.
[21] E. Alonso, F. Forniés, C. Fortuño, A. Lledós, A. Martín, A. Nova, Inorg. Chem. 48 (2009) 7679.
[22] N. Chaouche, J. Forniés, C. Fortuño, A. Kribii, A. Martín, J. Organomet. Chem. 692 (2007) 1168.
[23] E. Alonso, J. Forniés, C. Fortuño, M. Tomás, J. Chem. Soc., Dalton Trans. (1995) 3777.
[24] I. Ara, N. Chaouche, J. Forniés, C. Fortuño, A. Kribii, A. Martín, Eur. J. Inorg. Chem. (2005) 3894.
[25] I. Ara, J. Forniés, C. Fortuño, S. Ibáñez, A. Martín, P. Mastrorilli, V. Gallo, Inorg. Chem. 47 (2008) 9069.
[26] CRYSALISRED Program for X-ray CCD camera data reduction, Version 1.171.32.19, Oxford Diffraction Ltd., Oxford, UK, 2008.
[27] G.M. Sheldrick, SHELXL-97 a program for crystal structure determination ed., University of Gottingen, Germany, 1997.
[28] A.L. Spek, Acta Crystallogr., Sect. D 65 (2009) 148.
[29] A. Escuer, G. Aromí, Eur. J. Inorg. Chem. (2006) 4721.
[30] T.C. Stamatatos, G.S. Papaefstathiou, L.R. MacGillivray, A. Escuer, R. Vicente, E. Ruiz, S.P. Perlepes, Inorg. Chem. 46 (2007) 8843.
[31] S. Sasmal, S. Sarkar, N. Aliaga-Alcalde, S. Mohanta, Inorg. Chem. 50 (2011) 5687.
[32] C. Papatriantafyllopoulou, T.C. Stamatatos, W. Wernsdorfer, S.J. Teat, A.J. Tasiopoulos, A. Escuer, S.P. Perlepes, Inorg. Chem. 49 (2010) 10486.
[33] P. Smolenski, S. Mukhopadhyay, M.F.C. Guedes da Silva, M.A.J. Charmier, A.J.L. Pombeiro, Dalton Trans. (2008) 6546.
[34] F.S. Mackay, N.J. Farrer, L. Salassa, H.-C. Tai, R.J. Deeth, S.A. Moggach, P.A. Wood, S. Parsons, P.J. Sadler, Dalton Trans. (2009) 2315.
[35] L. Ronconi, P.J. Sadler, Chem. Commun. (2008) 235.
[36] K. Sutter, J. Autschbach, J. Am. Chem. Soc. 134 (2012) 13374.
[37] J. Forniés, C. Fortuño, R. Navarro, F. Martínez, A.J. Welch, J. Organomet. Chem. 394 (1990) 643.
[38] M. Atam, U. Muller, J. Organomet. Chem. 71 (1974) 435.
[39] A. Roth, A. Buchholz, M. Rudolph, E. Schütze, E. Kothe, W. Plass, Chem. Eur. J. 14 (2008) 1571.
[40] B. Sun, X. Chen, Z. Li, L. Zhang, Q. Zhao, New J. Chem. (2010) 190.
[41] W.P. Fehlhammer, L.F. Dahl, J. Am. Chem. Soc. 94 (1972) 3377.
[42] E.T. Almeida, A.E. Mauro, A.M. Santana, S.R. Ananias, A.V.G. Netto, J.G. Ferreira, R.H.A. Santos, Inorg. Chem. Commun. 10 (2007) 1394.
[43] A.M. Santana, J.G. Ferreira, A.C. Moro, S.C. Lemos, A.E. Mauro, A.V.G. Netto, R.C.G. Frem, R.H.A. Santos, Inorg. Chem. Commun. 14 (2011) 83.
[44] M.J. Arendse, G.K. Anderson, N.P. Rath, Polyhedron 20 (2001) 2495.
[45] P. Govindaswamy, D. Linder, J. Lacour, G. Süss-Fink, B. Therrien, Dalton Trans. (2007) 4457.
[46] J.L. Shaw, G.T. Yee, G. Wang, D.E. Benson, C. Gokdemir, C.J. Ziegler, Inorg. Chem. 44 (2005) 5060.
[47] T. Kawato, T. Uechi, H. Koyama, H. Kanatomi, Inorg. Chem. 23 (1984) 764.
[48] R. Krämer, K. Polborn, W. Beck, J. Organomet. Chem. 441 (1992) 333.
[49] W. He, F. Liu, C. Duan, Z. Guo, S. Zhou, Y. Liu, L. Zhu, Inorg. Chem. 40 (2001) 7065.
[50] N. Das, A. Ghosh, A.M. Arif, P.J. Stang, Inorg. Chem. 44 (2005) 7130.
[51] J. Forniés, C. Fortuño, S. Ibáñez, A. Martín, P. Mastrorilli, V. Gallo, Inorg. Chem. 50 (2011) 10798.
[52] R. Bisbas, S. Mukherjee, P. Kar, A. Ghosh, Inorg. Chem. 51 (2012) 8150.
[53] M. Habib, T.K. Karmakar, G. Aromí, J. Ribas-Ariño, H.-K. Fun, S. Chantrapromma, S.K. Chandra, Inorg. Chem. 47 (2008) 4109.
[54] E.J. Maslowsky, Vibrational Spectra of Organometallic Compounds, Wiley, New York, 1997.
[55] R. Usón, J. Forniés, Adv. Organomet. Chem. 28 (1988) 219.
[56] K. Nakamoto, Infrared and Raman Spectra of Inorganic and Coordination Compounds, Part B: Applications in Coordination, Organometallic and Bioinorganic Chemistry, Wiley, New York, 1997.
[57] Vavra, I. Potocnák, E. Cizmár, M. Kajnaková, M. Dušek, H. Schmidt, M. Ozerov, S. Zvyagin, L. Dlhán and R. Boca, (2011).

Apartado E

Resumen con los objetivos, aportaciones y metodología. Conclusiones y referencias

En este apartado se recoge un resumen individual de cada una de las publicaciones (Apartados **E1**–**E5**). En cada caso, se comienza planteando los objetivos y se continúa explicando la metodología utilizada que ha dado lugar a los resultados presentados. El trabajo expuesto es el resultado de las aportaciones del doctorando bajo la orientación de la Directora de Tesis, exceptuando la resolución de todas las estructuras cristalinas por estudios de difracción de rayos-X, llevada a cabo por el Dr. Antonio Martín Tello, y algunos estudios específicos de espectroscopia de RMN llevados a cabo en el grupo del profesor Piero Mastrorilli, que se indican en forma oportuna en cada caso. A continuación de este breve resumen, se recogen en forma conjunta las conclusiones de todo el trabajo de investigación (Apartado **E6**) y sus referencias (Apartado **E7**).

E1. Formación de enlace P–C a través de acoplamiento reductor entre grupos fosfanuro y benzoquinolinato. Aislamiento de complejos de la secuencia Pt(II)/Pt(IV)/Pt(II)

Andersson Arias, Juan Forniés, Consuelo Fortuño y Antonio Martín. Mario Latronico, Piero Mastrorilli, Stefano Todisco y Vito Gallo. *Inorg. Chem.*, **2012**, 51, 12682–12696

Objetivo: Diseño y síntesis de cuatro nuevos fosfanuro-derivados asimétricos con fórmula general $[NBu_4][(C_6F_5)_2M(\mu\text{-}PPh_2)_2M'(C\text{^}N)]$ (C^N = 7,8-benzoquinolinato (bzq). M = M' = Pt, **1**; M = Pt, M' = Pd, **2**; M = Pd, M' = Pt, **3**; M = M' = Pd, **4**) para estudiar su comportamiento frente a I_2.

Metodología utilizada y resultados más relevantes: La síntesis se ha llevado a cabo mediante la reacción de fosfanuro-derivados de fórmula *cis*-$Li_2[M(C_6F_5)_2(PPh_2)_2]$[40] con complejos binucleares simétricos de tipo $[\{M'(\mu\text{-}Cl)(C\text{^}N)\}_2]$ (relación molar 1:0.5) en thf. En esta reacción, el fosfanuro-derivado actúa como ligando bidentado, causando la ruptura del sistema $(\mu\text{-}Cl)_2$ y el desplazamiento del ligando halogenuro. De las mezclas correspondientes, se aislaron los complejos **1**–**4** como sólidos amarillos, usando la sal NBu_4ClO_4 para favorecer la cristalización de los derivados (Esquema 5).

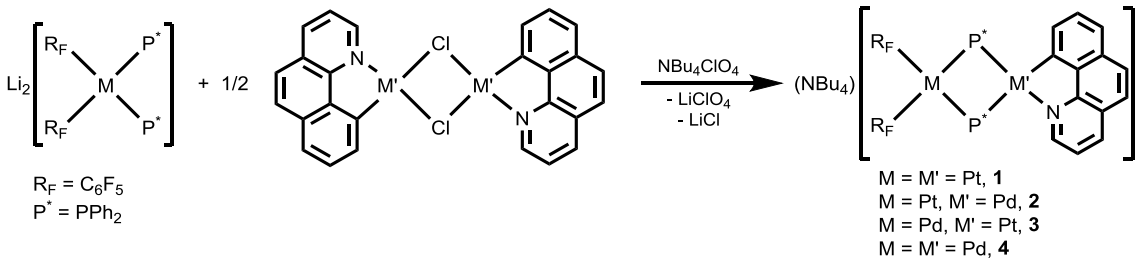

Esquema 5

Los compuestos fueron caracterizados por análisis elemental, espectroscopia de IR, espectrometría de masas de alta resolución (HRMS) y espectroscopia de RMN multinuclear. Los espectros de IR de los complejos **1**–**4** en estado sólido confirmaron la presencia de los ligandos, mientras que los espectrogramas de HRMS(–) mostraron, para cada derivado, picos intensos correspondientes al anión, $[M]^-$, con un patrón isotópico superponible al calculado en base a las fórmulas propuestas.

Los espectros de RMN de $^{31}P\{^1H\}$ de los compuestos **1**–**4** consisten en dos dobletes mutuamente acoplados (sistema de spin AX), con satélites de ^{195}Pt para los derivados **1**–**3**. Los valores de desplazamiento químico observados en estos compuestos están en el rango entre δ -58.0 y δ -118.9 (Tabla 1). Se ha establecido que de forma general los valores de desplazamientos químicos de ^{31}P en grupos $\mu\text{-}PPh_2$ disminuyen a medida que aumenta el número atómico de arriba hacia abajo en una triada[69,72] y en acuerdo con esto, los desplazamientos químicos aumentan al pasar de **1** (Pt_2) a **2**, **3** (PtPd) y **4** (Pd_2). Como se ha

señalado previamente, las señales correspondientes a un sistema $M(\mu\text{-}PPh_2)_2M'$ sin enlace metal–metal, se observan generalmente a mayor campo que las correspondientes a un sistema $M(\mu\text{-}PPh_2)M'$, con un solo grupo difenilfosfanuro actuando como puente entre dos centros que no presentan enlace metal–metal. El valor de δ -58.0 es el más alto encontrado en complejos que contienen el sistema $M(\mu\text{-}PPh_2)_2M'$ y es cercano a aquellos encontrados en complejos con el sistema $M(\mu\text{-}PPh_2)M'$ sin enlace metal–metal.[15] La asignación de las constantes de acoplamiento entre P y Pt se realizó inequívocamente mediante la comparación de los espectros de RMN de $^{31}P\{^1H\}$ y $^{195}Pt\{^1H\}$. La asignación de las señales de ^{31}P se realizó en base al ligando *trans* al átomo de P. En estos derivados se observa que los valores más bajos de ^1JPt,P (1320 Hz para **1** y 1213 Hz para **3**) corresponden a los acoplamientos entre P^2 y Pt^2 (P *trans* al átomo de C del ligando 7,8-benzoquinolinato; numeración atómica en Tabla 1), mientras que los valores más altos (2810 Hz para **1** y 2658 Hz para **3**) corresponden a la constante ^1JPt^2,P^1 (P *trans* a átomo de N del ligando bzq); estos valores de ^1JPt,P se han observado previamente en derivados en los que el grupo difenilfosfanuro se encuentra en posición *trans* respecto a un átomo de N.[88,89] Finalmente, las constantes de acoplamiento entre los átomos de P y el centro de Pt^1 en los complejos **1** y **2** están en el rango de 1530 a 1937 Hz. Los espectros de RMN de $^{195}Pt\{^1H\}$ de los complejos **1–3** constan de señales finas para los átomos de Pt unidos al grupo bzq (Pt^2) y de multipletes anchos, debido a diversos acoplamientos con núcleos de ^{19}F no equivalentes, para los átomos unidos a los anillos C_6F_5 (Pt^1).

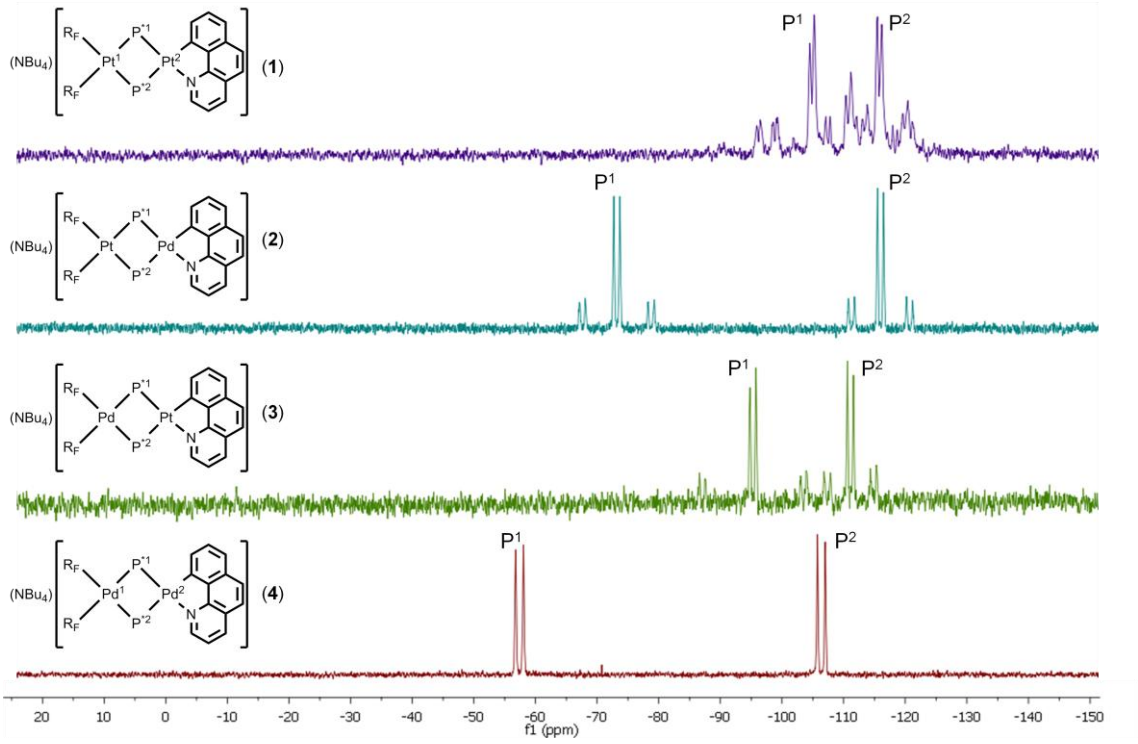

Figura 1. Espectros de RMN de $^{31}P\{^1H\}$ de los derivados **1–4**.

Tabla 1. Datos de RMN de ^{31}P y ^{195}Pt de **1–11** en acetona deuterada (δ en ppm, *J* en Hz).

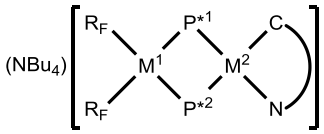

1-4

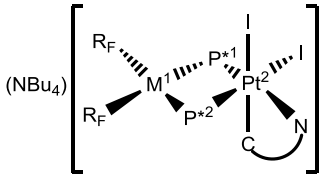

5, **9**

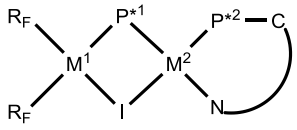

6-8, **10**

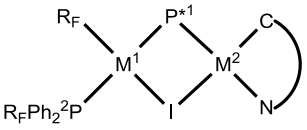

11

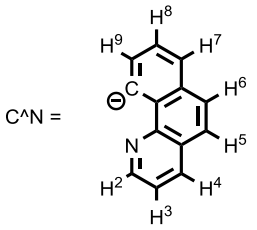

M = Pd, Pt
$R_F = C_6F_5$
P* = PPh_2

Complejo	δP^1	δP^2	^2JP^1,P^2	^1JPt^1,P^1	^1JPt^2,P^1	JPt^1,P^2	^1JPt^2,P^2	δPt^1	δPt^2
1	-107.9	-118.9	116	1937	2810	1646	1320	-3889[a]	-3717[a]
2	-78.8	-116.6	160	1806		1530		-3909	
3	-95.9	-111.7	160		2658		1213		-3738
4	-58.0	-107.0	204						
5	-115.5	-107.5	126	2032	1807	2189	1270	-3806[b]	-2917[b]
9	-97.7	-89.1	161		1680		1121		-2966
6	-11.4	14.2	2	1846	2513	37	4435	-4238	-4397
7	55.2	37.5	40	1864		97		-4315	
8	66.0	42.3	36						
10	7.9	18.6	2		2542		4307		-4416
11	-5.4	8.7	381		3317				n.d.

[a] ^2JPt,Pt = 541 Hz. [b] ^2JPt,Pt = ca. 100 Hz

Los espectros de RMN de ^{19}F de los derivados **1**–**4**, registrados en acetona deuterada a temperatura ambiente, muestran en todos los casos, dos señales correspondientes a los átomos de *o*-F de los dos grupos C_6F_5 (rango entre δ -110 y δ -115), así como dos señales correspondientes a *m*-F (rango entre δ -166 y δ -167) y dos señales correspondientes a *p*-F (rango entre δ -168 y δ -169), en acuerdo con la presencia de dos grupos C_6F_5 que no son equivalentes entre sí, y en los que las dos mitades de cada anillo se hacen equivalentes en disolución. La mayoría de señales homólogas están parcialmente solapadas, lo que es un indicativo de la similitud de los entornos químicos de los dos grupos C_6F_5.

Los espectros de RMN de ^1H (mono y bidimensionales) de los derivados **1**–**4**, además de confirmar la naturaleza aniónica de los complejos, permitieron la asignación de todas las señales de los átomos de hidrógeno. Los cuatro espectros monodimensionales son casi superponibles, siendo la principal diferencia la resonancia del protón M'–N–CHC (H^2 en Tabla 1), que es de aproximadamente 8.6 ppm cuando M' es Pt (derivados **1** y **3**) y de 8.4 ppm cuando M' es Pd (derivados **2** y **4**).

Los compuestos **1**–**4** reaccionan con I_2 (relación molar 1:1) y los productos resultantes dependen tanto de los derivados de partida como del disolvente en el que se lleva a cabo la reacción (Esquema 6).

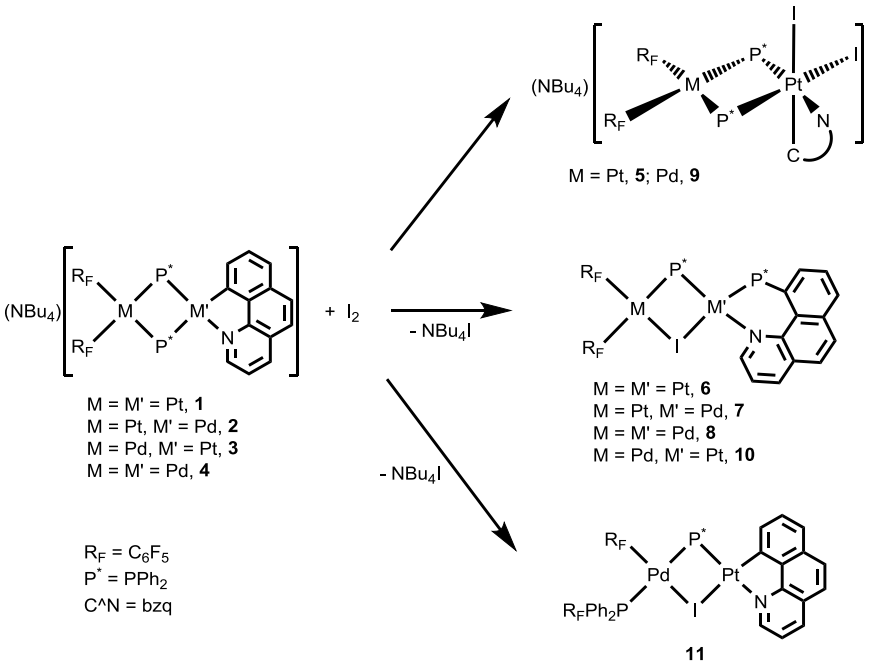

Esquema 6

En un procedimiento general, se agregó una disolución de I_2 en CH_2Cl_2, gota a gota, a una disolución del complejo dinuclear de fórmula $[NBu_4][(C_6F_5)_2M(\mu\text{-}PPh_2)_2M'(C\text{^}N)]$, también en CH_2Cl_2, en relación molar 1:1. Para el derivado **1**, la disolución se mantuvo en agitación durante 20 horas a temperatura ambiente, y mediante la adición de 2-propanol, se aisló una mezcla de los derivados $[NBu_4][(C_6F_5)_2Pt^{II}(\mu\text{-}PPh_2)_2Pt^{IV}(C\text{^}N)I_2]$ (**5**) y $[(C_6F_5)_2Pt^{II}(\mu\text{-}PPh_2)(\mu\text{-}I)Pt^{II}(Ph_2P\text{–}bzq)]$ (**6**) (Esquema 6). El compuesto **5** es un derivado que contiene un centro de Pt(II) y uno de Pt(IV) con una configuración OC-6-42 (solo se muestra uno del par de isómeros en el Esquema 6) y **6** es un complejo de Pt(II),Pt(II) en el que los dos centros metálicos se encuentran unidos por un grupo difenilfosfanuro y uno ioduro, y que presenta un ligando aminofosfano bidentado, resultante del acoplamiento entre un grupo $\mu\text{-}PPh_2$ y el ligando bzq, con formación de enlace P–C (Esquema 6). Cuando se realizó la adición de I_2 a **1** en acetona, solo se obtuvo el derivado **5**, lo que sugiere que este podría ser un precursor de **6** y que el proceso de acoplamiento reductor no está favorecido en acetona. De hecho, disoluciones de **5** en acetona deuterada son estables durante dos semanas a temperatura ambiente, mientras que disoluciones en diclorometano deuterado evolucionan en el mismo periodo de tiempo a una mezcla de **5** y **6** (casi 70% de **6**).

Los compuestos **2** (M = Pt, M' = Pd) y **4** (M = M' = Pd) reaccionan con I_2 bajo condiciones similares produciendo solo la cristalización de los aminofosfano-derivados $[(C_6F_5)_2M^{II}(\mu\text{-}PPh_2)(\mu\text{-}I)Pd^{II}(Ph_2P\text{–}bzq)]$ (M = Pt, **7**; Pd, **8**) (Esquema 6). En un intento de detectar un intermedio de Pt(II),Pd(IV) análogo al derivado **5**, se llevó a cabo la adición de I_2 a **2** (relación

molar 1:1) en acetona a 213 K y se evaporó a sequedad, obteniendo un sólido naranja. Los espectros de RMN de $^{31}P\{^{1}H\}$ registrados en acetona deuterada, tanto a 213 K como a temperatura ambiente identifican este sólido como una mezcla de principalmente el derivado **7** y el derivado tetranuclear $[NBu_4]_2[\{(C_6F_5)_2Pt^{II}(\mu\text{-}PPh_2)_2Pd^{II}(\mu\text{-}I)\}_2]$, descrito previamente;[73] sin embargo, no se detectan señales atribuibles a un intermedio de Pt(II),Pd(IV).

Finalmente, se agregó una disolución de I_2 en CH_2Cl_2 sobre una del derivado **3** (M = Pd, M' = Pt), también en CH_2Cl_2 (relación molar 1:1), se dejó en agitación durante 20 horas y se evaporó la reacción a sequedad, obteniendo un sólido amarillo. La espectroscopia de RMN multinuclear, en acetona deuterada, indica que este sólido es una mezcla de productos en la que se pueden identificar los derivados $[NBu_4][(C_6F_5)_2Pd^{II}(\mu\text{-}PPh_2)_2Pt^{IV}(C\text{^}N)I_2]$ (**9**), $[(C_6F_5)_2Pd^{II}(\mu\text{-}PPh_2)(\mu\text{-}I)Pt^{II}(Ph_2P\text{–}bzq)]$ (**10**) y $[(C_6F_5)(Ph_2P\text{–}C_6F_5)Pd^{II}(\mu\text{-}PPh_2)(\mu\text{-}I)Pt^{II}(C\text{^}N)]$ (**11**) (Esquema 6). Todos los intentos de separar esta mezcla fueron infructuosos.

No se pudieron obtener cristales del compuesto **5** que fueran adecuados para estudios de difracción de rayos-X, por lo que se preparó el derivado $[N(PPh_3)_2][(C_6F_5)_2Pt^{II}(\mu\text{-}PPh_2)_2Pt^{IV}(C\text{^}N)I_2]$ (**5'**) a través de dos pasos: (a) la síntesis del compuesto $[N(PPh_3)_2][(C_6F_5)_2Pt^{II}(\mu\text{-}PPh_2)_2Pt^{II}(C\text{^}N)]$ (**1'**), en un procedimiento análogo al usado para la síntesis de los complejos **1**–**4**, empleando $[N(PPh_3)_2]Cl$ en vez de NBu_4ClO_4, y (b) la adición de I_2 al derivado **1'** (relación molar 1:1).

Las estructuras de los derivados **5'**–**8** se han establecido mediante estudios de difracción de rayos-X. La estructura cristalina de **5'** confirma su naturaleza binuclear, con dos centros de Pt unidos por dos ligandos difenilfosfanuro (Figura 2, izquierda. Por claridad, en todas las estructuras moleculares establecidas por difracción de rayos-X presentadas en esta Memoria, únicamente se muestran las etiquetas de los átomos más relevantes). La distancia intermetálica observada, de 3.571(1) Å, descarta cualquier posibilidad de interacción entre los centros de platino. El entorno del centro de Pt(1) es típico para este metal en estado de oxidación II, es decir, en el centro de un entorno plano cuadrado, formado por los dos ligandos C_6F_5 mutuamente *cis* y los grupos fosfanuro puentes (Figura 2, izquierda). Por otra parte, el entorno del centro de Pt(2) es octaédrico, como cabe esperar para un centro de Pt(IV) y presenta una configuración OC-6-42. Las posiciones de coordinación de este centro metálico están ocupadas de la siguiente forma: en el plano ecuatorial, por los dos ligandos $\mu\text{-}PPh_2$, un ligando ioduro y el átomo de N del ligando bzq; y en las posiciones apicales, por otro grupo ioduro y el átomo de C del ligando bidentado.

Los complejos **6**–**8** son isoestructurales, y en la Figura 2 (derecha) se muestra la estructura molecular del derivado **6** a manera de representación de los tres. Estos derivados presentan un fragmento "*cis*-$M(C_6F_5)_2$" (M = Pt en **6** y **7**; M = Pd en **8**) y un fragmento "$M(Ph_2P\text{–}bzq)$" (M = Pt en **6**; M = Pd en **7** y **8**) unidos entre sí por un ligando ioduro y uno difenilfosfanuro. El centro metálico del fragmento "*cis*-$M(C_6F_5)_2$" presenta un entorno de coordinación plano cuadrado esencialmente plano, mientras que el entorno de coordinación

plano cuadrado del centro metálico unido al ligando aminofosfano se desvía significativamente de la planaridad (Pt(2) en complejo **6**. Figura 2, derecha). Esta distorsión puede deberse a la tensión provocada por la coordinación bidentada del ligando aminofosfano. Las tres estructuras confirman el acoplamiento de los ligandos iniciales difenilfosfanuro y 7,8-benzoquinolinato, con formación de enlace P–C, en el que el nuevo ligando forma un metalaciclo no plano de 6 miembros con el centro metálico al que se une. Finalmente, la diferencia principal entre las estructuras **6**–**8** es la distancia intermetálica, que es mayor para el complejo **6** (3.255(1) Å) y muy similar para los otros dos derivados (3.081(1) Å en **7** y 3.078(1) Å en **8**).

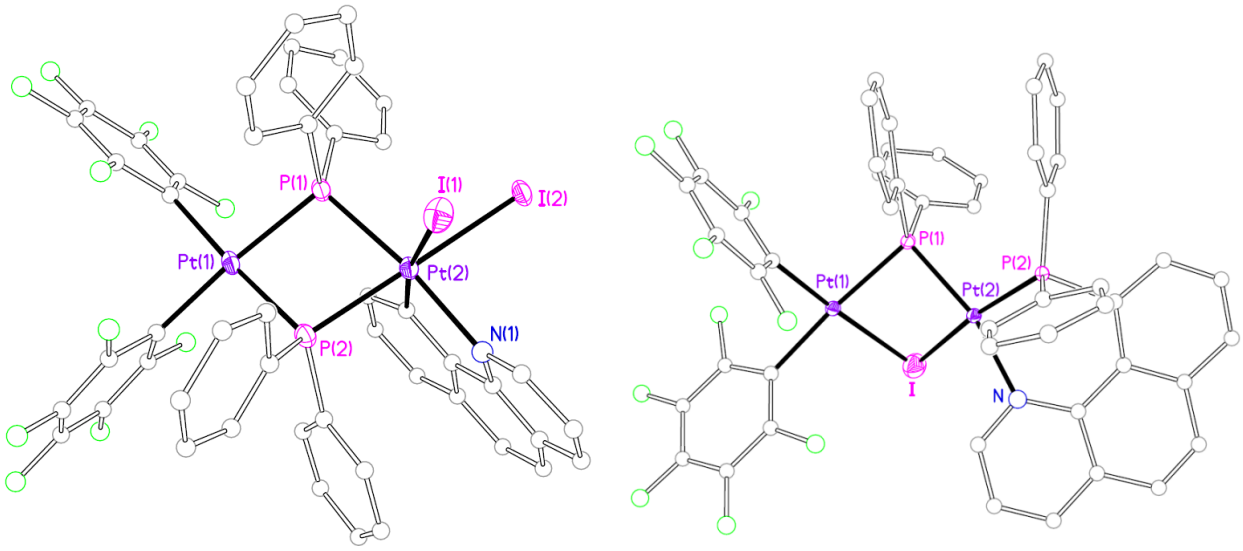

Figura 2. Vista de la estructura molecular del anión del compuesto $[N(PPh_3)_2][(C_6F_5)_2Pt^{II}(\mu\text{-}PPh_2)_2Pt^{IV}(C\text{^}N)I_2]$ (**5'**) (izquierda) y del complejo $[(C_6F_5)_2Pt^{II}(\mu\text{-}PPh_2)(\mu\text{-}I)Pt^{II}(Ph_2P\text{–}bzq)]$ (**6**) (derecha).

El espectro de RMN de $^{31}P\{^1H\}$ del derivado **5** consiste en dos dobletes, centrados a δ -107.5 y a δ -115.5, cada uno flanqueado por satélites de ^{195}Pt provenientes de los isotopómeros que contienen uno o dos átomos de ^{195}Pt. La comparación de los datos de los espectros de RMN de $^{31}P\{^1H\}$, HMQC ^1H–^{31}P, NOESY ^1H y $^{195}Pt\{^1H\}$ permite asignar la señal a δ -107.5 al átomo P(2) (numeración atómica en Figura 2, izquierda) y la de δ -115.5 a P(1), así como las constantes de acoplamiento de estos átomos con los centros de platino. Los valores de $^1JPt^1,P^1$ y $^1JPt^1,P^2$ encontrados en **5** son de 2032 y 2189 Hz, respectivamente, mientras que los valores de acoplamiento entre los átomos de P y el centro de Pt(IV) son de 1807 ($^1JPt^2,P^1$) y 1270 Hz ($^1JPt^2,P^2$), respectivamente (Tabla 1). Estos valores están en acuerdo con datos publicados en la bibliografía en los que se ha encontrado que las constantes de acoplamiento Pt–P en derivados de Pt(IV) con ligandos fosfano son aproximadamente de dos tercios en magnitud a las de sus precursores de Pt(II).[90,91]

La combinación de datos de los espectros de RMN de HMQC $^{1}H–^{31}P$, HMQC $^{1}H–^{195}Pt$, NOESY ^{1}H y COSY ^{1}H permitió identificar todas las señales del grupo bzq, así como diferenciar los hidrógenos *ortho*, *metha* y *para* de cada uno de los cuatro grupos fenilo presentes en el derivado **5**. El espectro de RMN de ^{19}F de **5** a 200 K muestra diez señales, una por cada átomo de F del compuesto, lo que indica que los dos anillos C_6F_5 no son equivalentes y que a esta temperatura, la estructura del derivado en disolución se asemeja a la del estado sólido. Al registrar el espectro a temperatura ambiente, dos señales de *o*-F y dos de *m*-F colapsan entre sí, mientras que las otras permanecen separadas unas de otras, lo que indica que al aumentar la temperatura, solamente uno de los anillos C_6F_5 gira alrededor del eje C–Pt lo suficientemente rápido en la escala de tiempo de RMN como para hacer equivalentes las dos mitades del anillo. Finalmente, el espectro de RMN de $^{195}Pt\{^{1}H\}$ muestra dos señales, un multiplete (por diversos acoplamientos con átomos de ^{19}F) centrado en δ -3806 y un doblete de dobletes centrado en δ -2917, asignado al centro de Pt(2) (Tabla 1). Esta señal experimenta un desplazamiento hacia campo bajo de 800 ppm al pasar del derivado **1** de Pt(II), al **5** de Pt(IV), lo que está en acuerdo con la mayoría de datos encontrados en la bibliografía.[92]

Los espectros multinucleares de RMN de los complejos **6**–**8** y **10** son concluyentes para establecer sus estructuras y concuerdan con el estudio de estado sólido de los derivados. Para los derivados **6**–**8** y **10**, la señal correspondiente al átomo de fósforo del grupo aminofosfano (P^2 en Tabla 1) aparece a menor campo que la señal correspondiente en los productos de partida **1**–**4**, como consecuencia de la transformación del ligando difenilfosfanuro en un ligando aminofosfano. Por otra parte, la señal correspondiente al átomo de fósforo del grupo difenilfosfanuro en estos complejos, también se desplaza hacia campo bajo respecto a la señal correspondiente en los productos de partida **1**–**4**, como cabe esperar al pasar de un sistema de tipo $M(\mu\text{-}PPh_2)_2M$ a uno $M(\mu\text{-}PPh_2)(\mu\text{-}X)M$ (X = I) en derivados saturados de platino o paladio. Por su parte, los espectros de RMN de ^{19}F de los complejos **6**–**8** muestran tres señales (relación de intensidad 2:2:1) para cada anillo C_6F_5, indicando que estos dos grupos no son equivalentes y que en disolución las dos mitades de cada anillo sí lo son.

Para el derivado **9**, análogo a **5**, las resonancias de ^{31}P se hallan a δ -97.7 (P^1; ^{1}JPt,P = 1680 Hz) y δ -89.1 (P^2; ^{1}JPt,P = 1121 Hz) y la señal de RMN de ^{195}Pt se encuentra a δ -2966 (Tabla 1). A su vez, la identificación del complejo **11** como $[(C_6F_5)(Ph_2P–C_6F_5)Pd^{II}(\mu\text{-}PPh_2)(\mu\text{-}I)Pt^{II}(C\text{^}N)]$ se logró mediante la comparación de sus espectros de RMN de $^{31}P\{^{1}H\}$ y de ^{19}F con los del compuesto $[NBu_4][(C_6F_5)(Ph_2P–C_6F_5)Pd^{II}(\mu\text{-}PPh_2)(\mu\text{-}I)Pt^{II}(C_6F_5)_2]$ previamente preparado en nuestro grupo.[72] La asignación del enlace Pt–N como *trans* al átomo de P y no al de I (Esquema 6) se realiza en base al gran valor de ^{1}JPt,P obtenido de los espectros de RMN (3317 Hz).

De esta forma, la reacción entre I_2 y compuestos de fórmula $[NBu_4][(C_6F_5)_2M(\mu\text{-}PPh_2)_2M'(C\text{^}N)]$ puede considerarse de forma general como una adición oxidante sobre el centro metálico unido al ligando 7,8-benzoquinolinato, M' –en caso del derivado homonuclear de platino pudo aislarse el intermedio **5**–, seguida de un acoplamiento reductor entre un grupo

difenilfosfanuro y el ligando bzq. En acuerdo con esto, la adición de I_2 sobre los dos derivados homonucleares **1** y **4** produce el acoplamiento reductor con formación del ligando aminofosfano y no con formación de $Ph_2P–C_6F_5$.

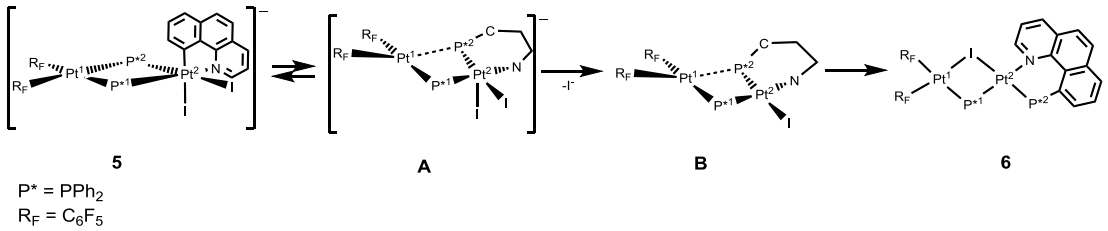

Esquema 7

Se ha propuesto el proceso que se muestra en el Esquema 7 para describir la transformación del intermedio **5** en el aminofosfano-derivado **6**, que iniciaría con la inserción del átomo P^2 en el enlace Pt^2–C para dar el intermedio **A** con el centro Pt^2 pentacoordinado. Este intermedio puede experimentar la disociación de un grupo ioduro para dar el intermedio **B** que a través de la ruptura del enlace Pt^1–P^2, rotación sobre el eje P^1–Pt^2–N y coordinación a modo de puente del ligando ioduro, se transforma finalmente en **6**. La eliminación de ioduro a través de un proceso disociativo se comprobó por comparación de los espectros de RMN de ^{31}P de dos disoluciones de **5** en diclorometano deuterado, sin y con exceso de ioduro (agregado como 5 equivalentes de NBu_4I): mientras que la conversión de **5** en **6** en ausencia de ioduro externo fue de 25% en 64 horas, la disolución que contenía **5** y NBu_4I mostró en el mismo tiempo, solamente señales de **5**. La geometría del centro Pt^2 pentacoordinado en el intermedio **A** (Esquema 7) podría ser en principio de bipirámide trigonal, con los dos ligandos ioduro mutuamente *trans*, o de pirámide de base cuadrada, con los grupos ioduro mutuamente *cis*. La presencia de señales de intercambio entre dos grupos fenilos, cada uno perteneciente a un ligando difenilfosfanuro diferente, en el espectro de RMN de EXSY ^1H del intermedio **5** registrado en acetona deuterada a temperatura ambiente, apunta a que la geometría de este centro es de pirámide de base cuadrada, la única que permitiría el intercambio de estos dos grupos fenilo a través de la posición apical del centro metálico.

Es necesario destacar que los experimentos de RMN que han llevado a la propuesta de procesos dinámicos y mecanismos de reacción se han llevado a cabo en el grupo del profesor Piero Mastrorilli.

E2. Formación de enlace P–O inducido oxidativamente a través de acoplamiento reductor entre grupos fosfanuro y acetilacetonato, 8-hidroxiquinolinato y *o*-picolinato

Andersson Arias, Juan Forniés, Consuelo Fortuño y Antonio Martín. Piero Mastrorilli, Stefano Todisco, Mario Latronico y Vito Gallo. *Inorg. Chem.*, **2013**, 52(9), 5493–5506

Objetivo: Diseño y síntesis de cinco nuevos fosfanuro-derivados binucleares asimétricos de paladio y platino (II) de fórmula general $[NBu_4][(C_6F_5)_2M(\mu\text{-}PPh_2)_2M'(N\text{^}O)]$, en los que N^O es un ligando N,O- dador coordinado en forma bidentada al centro metálico y estudio de reactividad frente a I_2 de estos cinco compuestos y del derivado $[NBu_4][(C_6F_5)_2Pt(\mu\text{-}PPh_2)_2Pt(acac)]$[56] (acac = acetilacetonato), previamente sintetizado en nuestro grupo.

Metodología utilizada y resultados más relevantes: La síntesis de los cinco nuevos fosfanuro-derivados con fórmula $[NBu_4][(C_6F_5)_2M(\mu\text{-}PPh_2)_2M'(N\text{^}O)]$ (N^O = 8-hidroxiquinolinato (hq); M = M' = Pt, **12**; M = M' = Pd, **13**; M = Pt, M' = Pd, **14**. N^O = *o*-picolinato (pic); M = M' = Pt, **15**; M = Pt, M' = Pd, **16**) se realizó a través de dos vías distintas: la síntesis de los productos **12**, **15** y **16** se llevó a cabo mediante la eliminación de de los ligandos cloruro puentes de los correspondientes derivados tetranucleares $[NBu_4]_2[\{(C_6F_5)_2Pt(\mu\text{-}PPh_2)_2M(\mu\text{-}Cl)\}_2]$,[40] (M = Pd, Pt) y el tratamiento de las especies resultantes con el correspondiente ligando O,N- dador (Esquema 8a). Por otra parte, los compuestos **13** y **14** se sintetizaron mediante la reacción de los fosfanuro-derivados de fórmula *cis*-$Li_2[M(C_6F_5)_2(PPh_2)_2]$ (M = Pd, Pt)[40] con el complejo binuclear simétrico de fórmula $[\{Pd(\mu\text{-}Cl)(hq)\}_2]$ (Esquema 8b), un procedimiento análogo al usado para la síntesis de los compuestos **1**–**4** (Apartado E1).

Los derivados sintetizados fueron caracterizados por análisis elemental, HRMS y espectroscopia de IR y RMN. La espectroscopia de IR de los derivados **12**–**16** en estado sólido no aporta gran información estructural pero sí confirma la presencia de los ligandos en los respectivos complejos. Los espectros de RMN de ^{19}F de los compuestos se registraron en acetona deuterada; en estos derivados, los dos grupos C_6F_5 no son equivalentes pero los entornos químicos de los dos anillos son muy similares y algunos núcleos de ^{19}F son casi isócronos. Los espectros de RMN de $^{31}P\{^1H\}$ son más informativos y muestran en todos los casos las dos señales correspondientes a los dos átomos de P no equivalentes localizadas a campo alto, entre δ -100 y δ -145, como cabe esperar de fragmentos de tipo "$M(\mu\text{-}PPh_2)_2M$" (M = Pt, Pd) que no presentan enlace metal–metal.

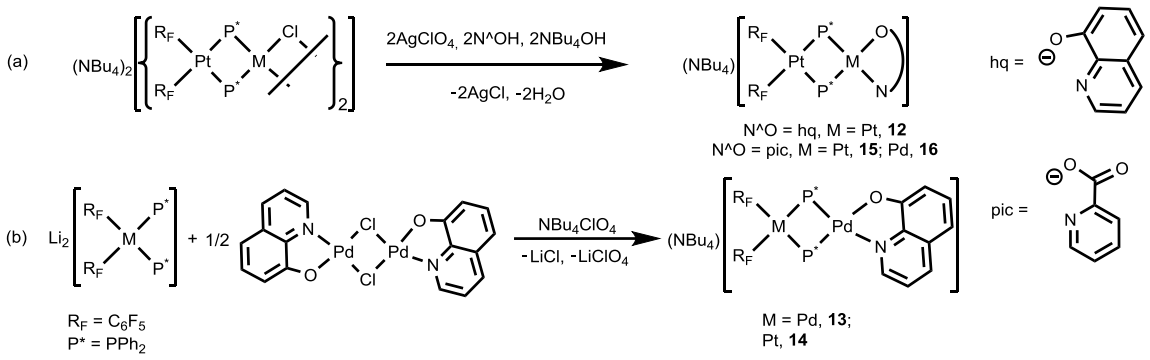

Esquema 8

Tabla 2. Datos de RMN de ^{31}P y ^{195}Pt de **12**–**16** y de **18**–**23** en acetona deuterada (δ en ppm, *J* en Hz).

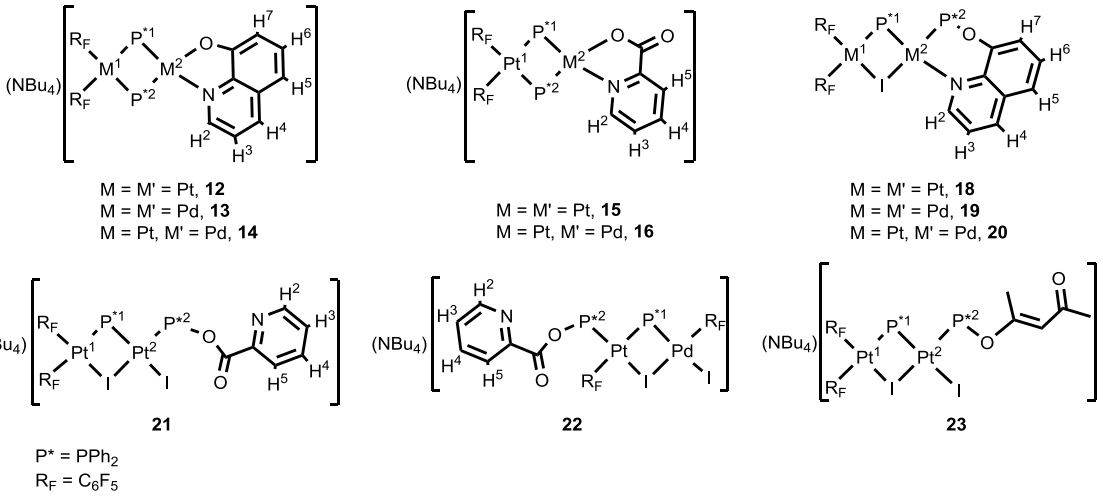

Derivado	δP^1	δP^2	^2JP^1,P^2	^1JPt^1,P^1	^1JPt^2,P^1	JPt^1,P^2	^1JPt^2,P^2	δPt^1	δPt^2
12	-137.2	-140.4	157	1892	2436	1876	2441	-3903[a]	-3450[a]
13	-100.4	-106.0	263						
14	-119.0	-124.5	216	1739		1719		-3901	
15	-139.1	-141.6	160	1900	2420	1903	2532	-3911[b]	-3542[b]
16	-121.2	-125.6	220	1766		1737		-3905	
18	-19.9	86.0		1903	2373	49	5025	-4250[c]	-4420[c]
19	55.4	122.9	32						
20	50.1	119.3	37	1928		119		-4317	
21	-71.3	80.6		2005	2215		5179	-4045[d]	-3572[d]
21-hid	-76.4	67.2	13	2042	2320		5019	-4050	-3520
22	-45.8	84.6	8	1654			5088	-4436	
23	-88.5	81.6	21	2030	2291	29	5216	-4020[e]	-3500[e]

[a] ^2JPt,Pt = 289 Hz. [b] ^2JPt,Pt = 284 Hz. [c] ^2JPt,Pt = 1220 Hz. [d] ^2JPt,Pt = 1280 Hz. [e] ^2JPt,Pt = 1283 Hz.

La asignación de cada señal de RMN de ^{31}P a cada átomo de P de los grupos difenilfosfanuro (Tabla 2) se realizó comparando los datos obtenidos de los espectros de RMN de HMQC ^{1}H–^{31}P y NOESY ^{1}H: los espectros de HMQC ^{1}H–^{31}P permiten identificar los hidrógenos *ortho* de los anillos fenilos de los grupos difenilfosfanuro, mientras que el efecto

NOE encontrado entre la señal de los hidrógenos N–C–H (H^2 en Tabla 2) y la de los hidrógenos *ortho* más próximos a estos, permite identificar plenamente el grupo difenilfosfanuro *trans* al átomo de O (P^2 en Tabla 2). La asignación de las constantes de acoplamiento entre P y Pt se hizo por comparación de los espectros de RMN de $^{31}P\{^1H\}$ y de $^{195}Pt\{^1H\}$. Los espectros de RMN de $^{195}Pt\{^1H\}$ de los compuestos **12**, **14**–**16**, muestran multipletes anchos a aproximadamente δ -3900 para los átomos de Pt unidos a los anillos C_6F_5; para los derivados **12** y **15**, estos espectros también muestran señales a δ -3450 y δ -3542, respectivamente, correspondientes al centro de Pt unido al ligando bidentado N^O (Pt^2 en Tabla 2). Finalmente, la comparación de los datos de RMN de ^1H (mono y bidimensional), permitió la asignación de todas las señales de RMN de los hidrógenos presentes en los compuestos **12**–**16**.

Se ha llevado a cabo la adición de I_2 sobre los nuevos compuestos sintetizados **12**–**16**, así como sobre el derivado aniónico binuclear $[NBu_4][(C_6F_5)_2Pt(\mu\text{-}PPh_2)_2Pt(acac)]$ (**17**), que contiene el ligando O,O- dador acetilacetonato coordinado en forma bidentada.[56] La adición se realizó en forma análoga a la realizada sobre los compuestos **1**–**4** (Apartado E1), es decir, sobre disoluciones en CH_2Cl_2 de los fosfanuro-derivados, en relación molar 1:1, a temperatura ambiente y dejando en agitación aproximadamente 20 horas. El resultado de la reacción entre I_2 y los compuestos **12**–**17** son los fosfanuro-derivados **18**–**23**, cuyas estructuras dependen tanto del ligando presente en el sustrato de partida como de los centros metálicos (Esquema 9).

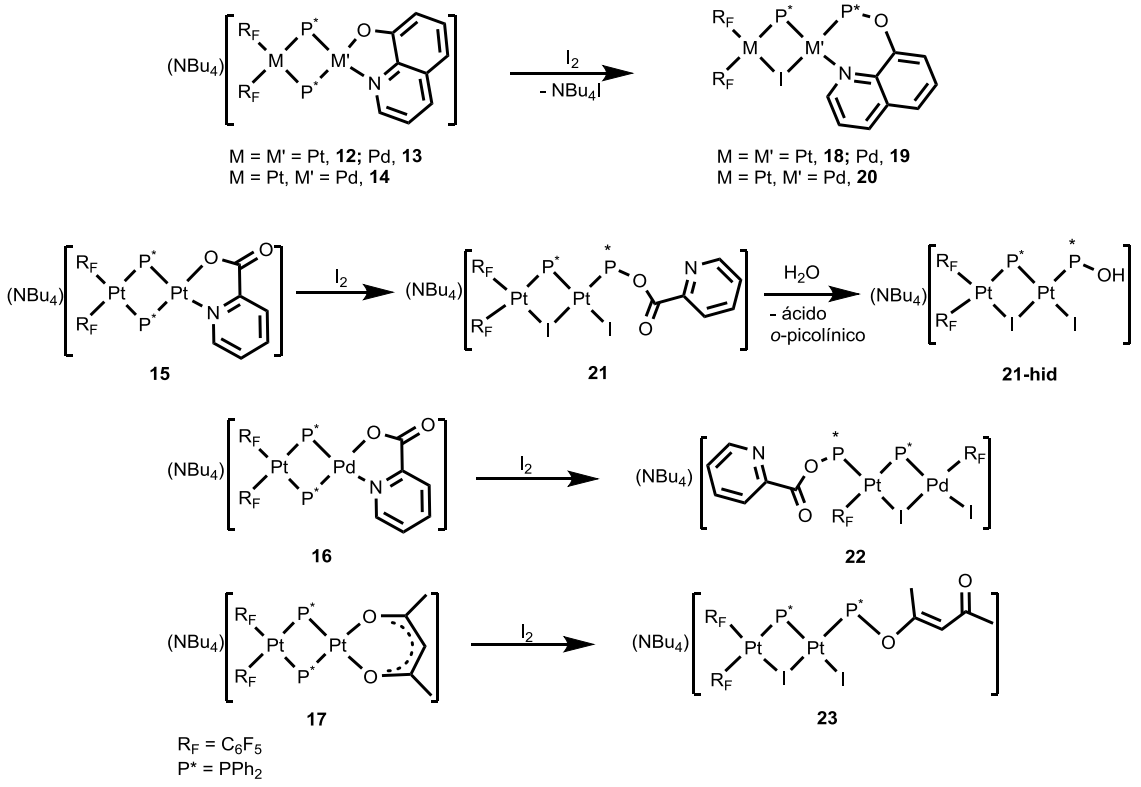

Esquema 9

Los fosfanuro-derivados **18**–**23** tienen un núcleo común constituido por un fragmento "M(μ-PPh_2)(μ-I)M'", y un ligando fosfano coordinado, que es el resultado del acoplamiento entre un grupo μ-PPh_2 y el ligando hq, pic o acac, con formación de enlace P–O (Esquema 9). En los complejos **18**–**20**, el nuevo ligando Ph_2P–hq se coordina de forma bidentada, a través de los átomos de P y N, al centro metálico M', mientras que en los derivados **21**–**23**, los grupos Ph_2P–pic o Ph_2P–acac actúan como ligandos monodentados (κ-P) y un grupo ioduro completa la esfera de coordinación de uno de los centros metálicos (Esquema 9). El derivado **21** es muy sensible a la humedad, hidrolizándose cuantitativamente en disolventes no anhidros, para dar lugar al producto **21-hid** (Esquema 9). Finalmente, la adición de I_2 sobre el derivado **16** da lugar a la coordinación del ligando Ph_2P–pic formado al centro de Pt y la migración de un grupo C_6F_5 del centro de Pt al de Pd (Esquema 9).

La caracterización estructural de los productos **18**, **20**, **22** y **23** se ha establecido mediante estudios de difracción de rayos-X (Figuras 3 y 4), que confirman la naturaleza binuclear de los complejos y la presencia del fragmento común "M(μ-PPh_2)(μ-I)M". Las distancias intermetálicas observadas en estos derivados (3.306(1) Å para **18**, 3.142(1) Å para **20**, 3.347(1) Å para **22** y 3.601(2) Å para **23**) están en acuerdo con la ausencia de enlace metal–metal, como cabe esperar en estos complejos saturados de 32 electrones de valencia. En cada complejo, los átomos metálicos presentan entornos de coordinación planos cuadrados distorsionados que comparten un lado común y con el fragmento "M(μ-PPh_2)(μ-I)M" mostrando una geometría no plana. Finalmente, las estructuras moleculares muestran que, tal como se ha señalado antes, en los fosfanuro-derivados **18** y **20**, neutros, el nuevo ligando Ph_2P–hq se coordina de forma bidentada, mientras que en **22** y **23**, aniónicos, los nuevos ligandos Ph_2P–pic y Ph_2P–acac actúan como ligandos monodentados (κ-P). En el derivado **22**, uno de los dos grupos C_6F_5 migra hacia el átomo de Pd –que completa su entorno de coordinación con un ligando ioduro–, mientras que el grupo Ph_2P–pic se coordina de forma monodentada (κ-P) al átomo de Pt.

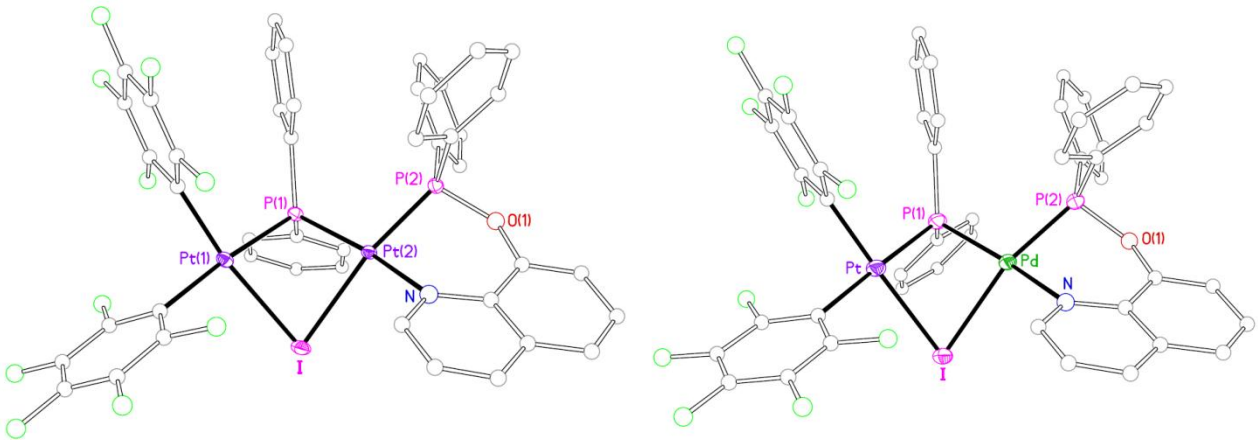

Figura 3. Vista de la estructura molecular del complejo [$(C_6F_5)_2Pt^{II}$(μ-PPh_2)(μ-I)Pt^{II}(Ph_2P–hq)] (**18**) (izquierda) y del complejo [$(C_6F_5)_2Pt^{II}$(μ-PPh_2)(μ-I)Pd^{II}(Ph_2P–hq)] (**20**) (derecha).

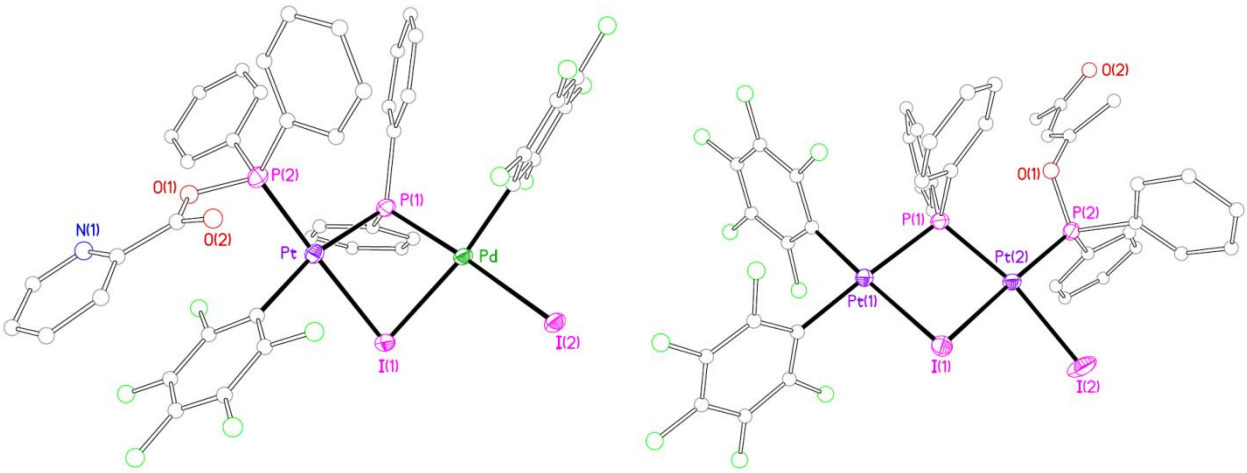

Figura 4. Vista de la estructura molecular de los aniones de los derivados [NBu_4][(Ph_2P–pic)(C_6F_5)Pt^{II}(μ-PPh_2)(μ-I)Pd^{II}(C_6F_5)I] (**22**) (izquierda) y [NBu_4][(C_6F_5)$_2Pt^{II}$(μ-PPh_2)(μ-I)Pt^{II}(Ph_2P–acac)I] (**23**) (derecha).

Los espectros de RMN de $^{31}P\{^1H\}$ de los fosfanuro-derivados **18**–**23**, registrados en acetona deuterada, muestran las señales correspondientes al átomo de P del grupo fosfano (Ph_2P–hq, Ph_2P–pic, Ph_2P–acac) a campo bajo respecto a las de sus respectivos productos de partida (Tabla 2), en el rango entre δ 80.6 y δ 122.9. De igual forma, las señales correspondientes a los grupos difenilfosfanuro del fragmento "M(μ-PPh_2)(μ-I)M" de los derivados **18**–**23**, aparecen a menor campo (entre δ 55.4 y δ -88.5) que las señales correspondientes a sus respectivos productos de partida, que contienen el fragmento "M(μ-PPh_2)$_2$M" (entre δ -100.4 y δ -144.6[56]). Este comportamiento es análogo al observado al comparar las señales de los aminofosfano-derivados **6**–**8**, **10** y **11** con las de sus respectivos productos de partida que contienen el ligando bzq, **1**–**4** (Apartado E1).

Los espectros de RMN de ^{19}F de los derivados **18**–**23**, registrados en acetona deuterada, muestran en todos los casos, dos señales correspondientes a los átomos de *o*-F, así como dos señales correspondientes a *m*-F y dos señales correspondientes a *p*-F, en acuerdo con la presencia de dos grupos C_6F_5 que no son equivalentes entre sí, y en los que las dos mitades de cada anillo se hacen equivalentes en disolución. Los espectros de RMN de ^1H (mono y bidimensionales) de los productos **18**–**23** muestran las señales correspondientes a los nuevos ligandos fosfano, a los grupos difenilfosfanuro y en el caso de los derivados iónicos **21**–**23**, del contraión NBu_4^+, en la relación de intensidad apropiada. Además, se observa un desplazamiento hacia menor campo de la señal correspondiente al átomo M'–N–CH (H^2 en Tabla 2) al pasar de los difenilfosfanuro-derivados **12**–**16** (en el rango entre δ 8.12 y δ 7.63) a los aminofosfano-derivados **18**–**22** (en el rango entre δ 10.53 y δ 8.60). El espectro de RMN de ^1H del derivado **23** muestra dos señales correspondientes a los dos grupos CH_3 no equivalentes y una correspondiente al hidrógeno CH del ligando Ph_2P–acac.

Los espectros de RMN de $^{195}Pt\{^{1}H\}$ de los derivados **18** y **20**–**23** muestran multipletes anchos en el rango entre δ -4020 y δ -4436 para el átomo de Pt^1 (Tabla 2). Para los derivados **18**, **21** y **23**, los espectros muestran también señales definidas a δ -4420, -3572 y -3500, respectivamente, para el átomo Pt^2 (Tabla 2). La constante de acoplamiento Pt–Pt en estos derivados está en el rango entre 1220 y 1283 Hz, valores cuatro veces mayores que las halladas en sus respectivos productos de partida, hecho que puede estar asociado al cambio del sistema de ligandos puentes entre los centros metálicos, al pasar de un fragmento "$M(\mu\text{-}PPh_2)_2M$" a uno "$M(\mu\text{-}PPh_2)(\mu\text{-}I)M$".

Teniendo en cuenta los resultados obtenidos con los derivados **1**–**4**, que contienen el grupo 7,8-benzoquinolinato (Apartado E1), la formación de los productos **18**–**23** puede ser el resultado de una oxidación inicial de los fosfanuro-derivados **12**–**17** con I_2 en CH_2Cl_2, seguida de un acoplamiento reductor entre uno de los grupos $\mu\text{-}PPh_2$ y el ligando bidentado O,N- u O,O- dador. La adición de I_2 puede dar lugar a un complejo de tipo M(II),M(IV), análogo al intermedio **5** (Apartado E1), o a un complejo insaturado de tipo M(III)–M(III) (Esquema 3, Apartado C), que podrían evolucionar, a través de acoplamiento reductor con formación de enlace P–O, hacia los productos **18**–**23** que presentan ligando fosfano.

Dado que para el fosfanuro-derivado binuclear de Pt **1** ha sido posible interrumpir el proceso de acoplamiento entre el grupo fosfanuro y el ligando bzq realizando la adición de I_2 en acetona, lo que permitió aislar el intermedio **5**, y que este intermedio es lo suficientemente estable como para mantenerse en disoluciones en CH_2Cl_2 con exceso de ioduro (Apartado E1), se ha estudiado la adición de I_2 a los derivados binucleares de Pt **12**, **15** y **17** en acetona deuterada, a 268 K y en presencia de cuatro equivalentes de NBu_4I.

Bajo estas condiciones, fueron necesarios tres equivalentes de I_2 para transformar el derivado **12** en una nueva especie, **12-ox** (>90%), que se mostró estable por al menos una semana; los espectros de RMN de $^{31}P\{^{1}H\}$ y $^{195}Pt\{^{1}H\}$ son concluyentes para identificar esta especie como un intermedio de tipo M(II),M(IV) análogo al fosfanuro-derivado **5** (Apartado E1), con el centro de Pt que está unido a los dos grupos C_6F_5 en un entorno de coordinación plano cuadrado y el otro, unido al ligando hq, con entorno octaédrico y dos grupos ioduro coordinados en mutua posición *cis* (Esquema 10). El espectro de RMN de $^{195}Pt\{^{1}H\}$ de **12-ox** a 268 K muestra dos señales centradas a δ -2385 y δ -3774; de estas, la primera es un doblete de dobletes asignable al átomo Pt^2 (numeración atómica en Esquema 10). El desplazamiento hacia campo bajo de esta señal en más de 1000 ppm respecto a la de su producto de partida (δ -3450), un comportamiento análogo al observado al oxidar con I_2 el fosfanuro-derivado **1** al intermedio **5** (Apartado E1), está en acuerdo con que el átomo Pt^2 de **12-ox** es un centro de Pt(IV) octaédrico. La señal a δ -3774 es un multiplete ancho debido a los múltiples acoplamientos ^{195}Pt–^{19}F y se asigna al átomo de Pt^1.

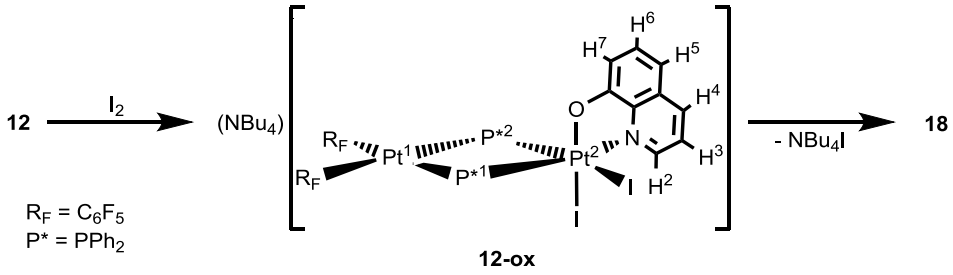

Esquema 10

La comparación de los datos de RMN de HMQC $^{1}H–^{31}P$, COSY ^{1}H y NOESY ^{1}H indica que la estructura del derivado **12-ox** es análoga a la del intermedio aislado **5**, con las posiciones de coordinación del átomo de Pt^{2}(IV) octaédrico ocupadas de la siguiente forma: en el plano ecuatorial, por los dos ligandos μ-PPh_2, un ligando ioduro y el átomo de N del ligando hq; y en las posiciones apicales, por otro grupo ioduro y el átomo de O del ligando bidentado (Esquema 10). El espectro de RMN de $^{31}P\{^{1}H\}$ del derivado **12-ox** a 268 K muestra dos señales centradas a δ -107.5 y δ -84.3 (^{2}JP,P = 116 Hz), de las que la señal a mayor campo es asignada al átomo de P *trans* al átomo de N del ligando bidentado (P^{1}, Esquema 10), en forma análoga a la asignación de señales de RMN de ^{31}P del intermedio **5** (Apartado E1).

La estabilidad de **12-ox** en acetona en presencia de ioduro apunta a que el mecanismo de transformación del derivado **12** en el complejo **18** (Esquema 10) puede ser similar al propuesto en la transformación del compuesto **1** en **6** (Apartado E1). Por otra parte, al realizar la adición de I_2 al derivado **12** (relación molar 1:1) en acetona deuterada a 298 K y en ausencia de ioduro, se observó mediante espectroscopia de RMN de ^{31}P que tras la adición, la mezcla contiene principalmente el derivado **12-ox** (además de trazas de **12** y **18**) que, tras 48 horas, se transforma en el complejo **18** en casi un 61%. El espectro de RMN de $^{31}P\{^{1}H\}$ también muestra señales asignables a dos especies: el compuesto tetranuclear $[NBu_4]_2[\{(C_6F_5)_2Pt(\mu\text{-}PPh_2)_2Pt(\mu\text{-}I)\}_2]$ (preparado previamente en nuestro grupo de investigación[73]) y el derivado $[NBu_4][(C_6F_5)_2Pt(\mu\text{-}PPh_2)(\mu\text{-}I)(Ph_2P–I)I]$, con señales asignables a δ 13.4 (^{2}JP,P = 10 Hz; ^{1}JPt,P = 4852 Hz) y δ -63.1(^{2}JP,P = 10 Hz; ^{1}JPt,P = 1980 Hz; ^{1}JPt,P = 2194 Hz) y que puede corresponder con el pico con *m*/*z* = 1474.7291 (masa exacta para la fórmula propuesta = 1474.7306 Da) encontrado en el espectrograma de HRMS(–) de la mezcla de reacción. Finalmente, todos los intentos de aislar el derivado **12-ox** han sido infructuosos.

El seguimiento de la reacción del derivado **15** con I_2 (3 equivalentes) en presencia de NBu_4I (4 equivalentes) en acetona deuterada a 268 K, permitió detectar inmediatamente después de la adición de los reactivos, el intermedio **15-ox** (Esquema 11), con una estructura similar a la de **12-ox**. Las señales de RMN de ^{31}P de este intermedio de Pt(II),Pt(IV) se encuentran a δ -99.5 (P^{1}, Esquema 11) y δ -77.5 (P^{2}), y el desplazamiento químico del centro de Pt^{2}(IV) octaédrico es de δ -2501. Al realizar la adición de I_2 sobre el derivado **15** (relación molar 1:1) en thf deuterado anhidro, a 298 K y en ausencia de NBu_4I, se observó la formación inmediata de **15-ox**, que se transforma progresivamente en un intermedio, **21***, con señales de

RMN de ^{31}P a δ 93.1 (^{1}JPt,P = 4993 Hz) y δ -20.4 (^{1}JPt,P = 2257 Hz; ^{1}JPt,P = 1906 Hz), que evoluciona en aproximadamente una hora hacia el derivado **21**. La similitud de las características de RMN de ^{31}P entre la especie **21*** y el derivado **18** sugiere que el intermedio **21*** podría tener una estructura análoga a este complejo; por tanto, la obtención del producto final **21** a partir del intermedio **21*** podría ser el resultado del desplazamiento del átomo de N coordinado al centro de Pt^2 por ioduro (Esquema 11).

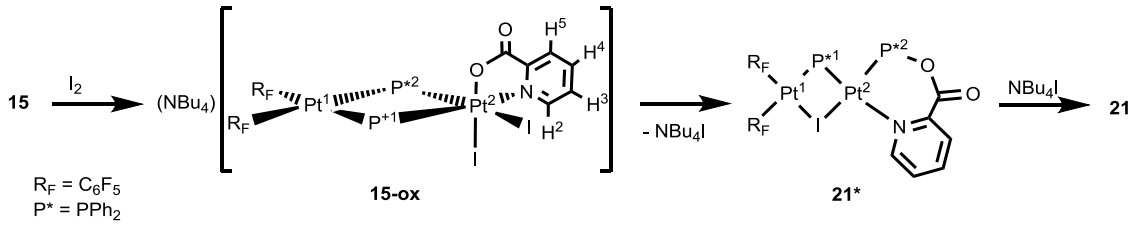

Esquema 11

Al realizar el seguimiento de la reacción entre el compuesto **17** y I_2 (3 equivalentes) en acetona deuterada, a 268 K y en presencia de NBu_4I (4 equivalentes), se observa en el espectro de RMN de $^{31}P\{^{1}H\}$ la transformación del derivado **17** en dos nuevas especies; una de ellas, caracterizada por dos dobletes mutuamente acoplados (^{2}JP,P = 102 Hz) a δ -73.4 (P^1, Esquema 12) y δ -81.6 (P^2), y características de RMN de ^{31}P análogas a las de las especies **12-ox** y **15-ox**, se identifica como el derivado **17-ox**-*cis* (Esquema 12). La otra especie, caracterizada por un singlete a δ -88.5 con satélites correspondientes a dos centros de ^{195}Pt no equivalentes (^{1}JPt,P = 2160 Hz; ^{1}JPt,P = 1570 Hz), es presumiblemente un derivado de tipo Pt(II),Pt(IV) en el que los dos grupos ioduro se coordinan en las posiciones apicales del átomo Pt^2(IV), **17-ox**-*trans* (Esquema 12). En acuerdo con estas asignaciones, el espectro de RMN de $^{195}Pt\{^{1}H\}$ de esta mezcla de reacción muestra un doblete de dobletes a δ -2024 asignable al átomo de Pt^2(IV) del derivado **17-ox**-*cis*, un triplete a δ -2834 asignable al átomo de Pt^2(IV) de la especie **17-ox**-*trans* y un multiplete ancho a δ -3746 asignable al solapamiento de las señales de los átomos de Pt^1(II) de ambos derivados.

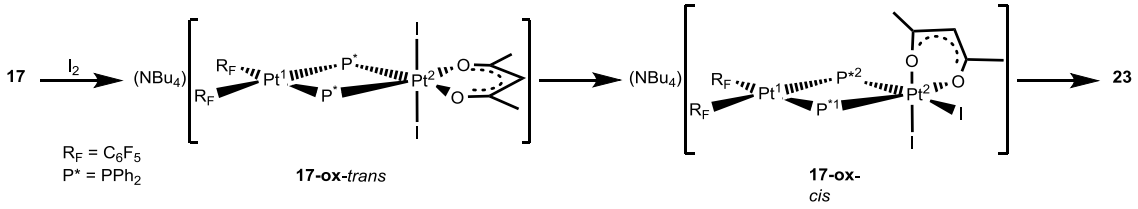

Esquema 12

A esta temperatura (268 K), el intermedio **17-ox**-*trans* se transforma cuantitativamente en **17-ox**-*cis*, que se mantiene estable al menos por una semana en estas condiciones; de hecho, este derivado no evoluciona hacia el producto **23** al aumentar la temperatura a 298 K, manteniendo el exceso de NBu_4I. Al realizar el seguimiento de la reacción de I_2 y el compuesto **17** en acetona deuterada, a 298 K y en ausencia de NBu_4I, se observa de forma inmediata la formación de **17-ox**-*cis* y **17-ox**-*trans*, que evolucionan rápidamente al derivado **23**.

Con toda esta información, la formación de los productos **18**–**23** puede entenderse a través de un proceso similar al observado en la formación de los derivados **6**–**8** y **10** (Apartado E1): la adición de I_2 a los compuestos **12**–**17** produce un intermedio binuclear en el que uno de los centros metálicos presenta un estado de oxidación II y el otro, estado de oxidación IV; la disociación de un ligando ioduro y el acoplamiento entre un grupo μ-PPh_2 y el ligando bidentado O,N- u O,O- dador da lugar al nuevo ligando fosfano, con formación de enlace P–O. Finalmente, aunque los derivados **18**–**23** han podido ser aislados como sólidos puros, el acoplamiento entre un grupo μ-PPh_2 y el ligando bidentado no es el único proceso que tiene lugar en la reacción; se han observado diferentes especies formadas por reacciones laterales –algunas de las cuales han sido identificadas– que pueden ser el resultado de otro tipo de acoplamiento reductor entre los ligandos.

Es necesario destacar que los experimentos de RMN que han llevado a la caracterización de intermedios y a la propuesta de mecanismos de reacción se han llevado a cabo en el grupo del profesor Piero Mastrorilli.

E3. Comportamiento dador de fosfanuro-derivados aniónicos y asimétricos de platino y paladio

Andersson Arias, Juan Forniés, Consuelo Fortuño y Antonio Martín. Piero Mastrorilli, Vito Gallo, Mario Latronico y Stefano Todisco. *Eur. J. Inorg. Chem.* doi: 10.1002/ejic.20130088

Objetivo: Una vez estudiado el comportamiento frente a I_2 de los nuevos derivados aniónicos binucleares sintetizados, estudiar el comportamiento de este tipo de compuestos hacia otro agente oxidante.

Metodología utilizada y resultados más relevantes: Se ha llevado a cabo la adición de la sal de plata (I) $[Ag(OClO_3)PPh_3]$ a los derivados aniónicos asimétricos $[NBu_4][(C_6F_5)_2Pt(\mu\text{-}PPh_2)_2Pt(bzq)]$ (**1**), $[NBu_4][(C_6F_5)_2Pt(\mu\text{-}PPh_2)_2Pd(bzq)]$ (**2**), $[NBu_4][(C_6F_5)_2Pt(\mu\text{-}PPh_2)_2Pt(hq)]$ (**12**), $[NBu_4][(C_6F_5)_2Pt(\mu\text{-}PPh_2)_2Pd(hq)]$ (**14**), $[NBu_4][(C_6F_5)_2Pt(\mu\text{-}PPh_2)_2Pt(C_6F_5)(tht)]$[40] (**24**) (tht = tetrahidrotiofeno), $[NBu_4][(C_6F_5)_2Pt(\mu\text{-}PPh_2)_2Pt(pic)]$ (**15**) y $[NBu_4][(C_6F_5)_2Pt(\mu\text{-}PPh_2)_2Pd(pic)]$ (**16**) (en CH_2Cl_2, relación molar 1:1).

En ninguno de los casos se ha observado la oxidación de los centros metálicos de los complejos binucleares aniónicos, sino la coordinación del centro de Ag(I) a los aniones de los productos de partida, dando lugar a los derivados neutros trinucleares **25**–**31** (Esquema 13). En estos complejos, la coordinación del centro de plata se produce, en estado sólido, a los dos centros metálicos (derivados **25**–**29**) o a un átomo de oxígeno del ligando bidentado unido a uno de estos centros (derivados **30** y **31**) (Esquema 13).

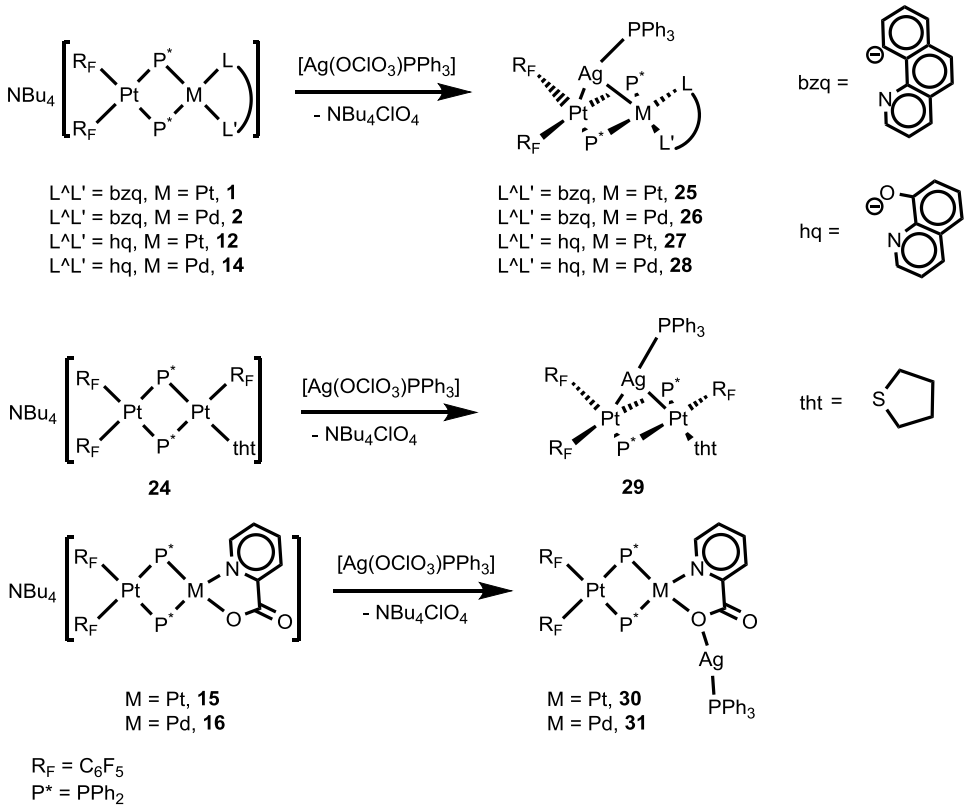

Esquema 13

Las estructuras moleculares en estado sólido de los complejos **25**, **27**–**31** se han establecido mediante estudios de difracción de rayos-X. Las estructuras de los derivados **25**, **27**–**29** son similares y en los cuatro casos los complejos pueden considerarse como compuestos por dos subunidades: un fragmento "$(C_6F_5)_2Pt(\mu\text{-}PPh_2)_2M(L)(L')$" (M = Pd, Pt; L, L' = C, N, O, S) y un fragmento "$AgPPh_3$", unidos a través de enlaces Pt–Ag y M–Ag. La Figura 5 muestra las estructuras moleculares de los complejos **27** y **29** a manera de ejemplo de este tipo de derivados. En esta, se observa que los centros de platino presentan entornos de coordinación planos cuadrados que comparten el lado conformado por los átomos de P de los dos grupos $\mu\text{-}PPh_2$. Uno de los centros metálicos completa su esfera de coordinación con dos grupos C_6F_5 en posición mutuamente *cis*, mientras el otro centro lo hace coordinándose ya sea al ligando bidentado (derivado **27**) o a un grupo C_6F_5 y al ligando neutro tht (derivado **29**) (Figura 5). Las distancias intermetálicas Pt···Pt o Pt···Pd observadas en los derivados **25**, **27**–**29**, que se encuentran en un rango entre 3.408(1) y 3.472(1) Å, son suficientemente largas para descartar cualquier posibilidad de interacción entre los dos centros metálicos.[16,19,73,87,93,94]

En cada complejo **25**, **27**–**29**, el ángulo diedro entre los planos de los dos centros metálicos Pt,M (M = Pt, Pd), calculado por el método de mínimos cuadrados, se encuentra en el rango entre 35.7(1) (complejo **29**) y 40.7(1)º (complejo **25**), resultando en una estructura de tipo "libro abierto". El centro metálico de plata se ubica en el lado interior del libro y está unido a los otros dos centros metálicos. Las distancias Pt/Pd–Ag se encuentran en el rango entre 2.7723(7) y 2.8889(3) Å, que son similares a las observadas en otros derivados análogos con

enlaces Pt(II)–Ag(I).[18,95-97] A su vez, el centro de plata completa su entorno de coordinación trigonal con el átomo de fósforo del ligando trifenilfosfano. Los átomos Pt, M, Ag, P (PPh_3) son coplanares y el entorno trigonal de Ag es asimétrico; de esta forma, el fragmento "$AgPPh_3$" se coordina al fragmento "$(C_6F_5)_2Pt(\mu\text{-}PPh_2)_2M(L)(L')$" de tal forma que el ligando PPh_3 se inclina ya sea hacia el ligando bidentado (derivados **25**, **27** y **28**) o hacia el ligando C_6F_5 y el grupo tht (derivado **29**). Esta inclinación es más pronunciada en los complejos con ligando bidentado (**25**, **27** y **28**) debido probablemente a que la coordinación coplanar de este grupo al centro M (Pt, Pd) conlleva a un menor impedimento estérico que la coordinación de los grupos C_6F_5 y tht, casi perpendicular al plano de coordinación del centro M (Pt) (derivado **27**, Figura 5).

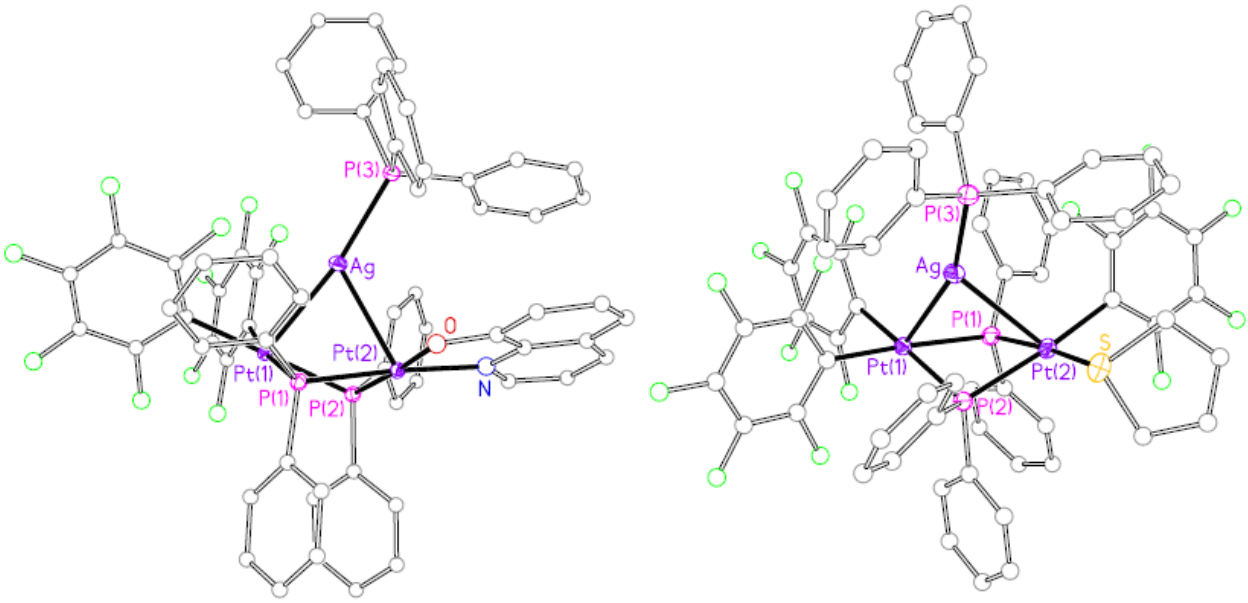

Figura 5. Vistas de las estructuras moleculares de los complejos $[(C_6F_5)_2Pt^{II}(\mu\text{-}PPh_2)_2(\mu\text{-}AgPPh_3)Pt^{II}(hq)]$ (**27**) (izquierda) y $[(C_6F_5)_2Pt^{II}(\mu\text{-}PPh_2)_2(\mu\text{-}AgPPh_3)Pt^{II}(C_6F_5)(tht)]$ (**29**) (derecha).

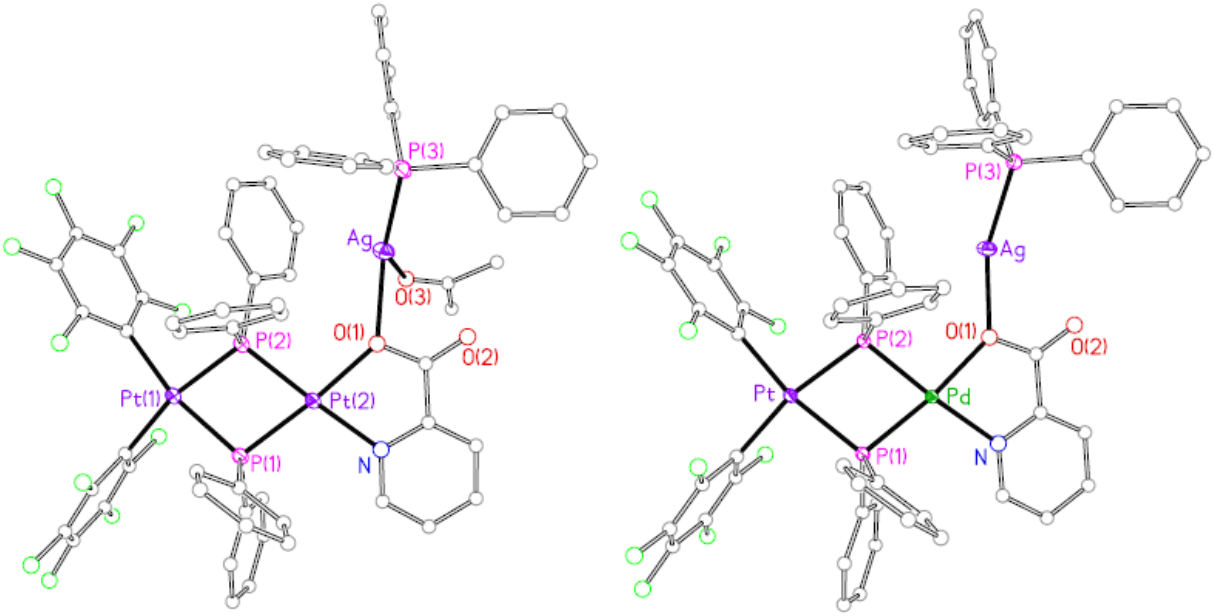

Figura 6. Vistas de las estructuras moleculares de los complejos $[(C_6F_5)_2Pt^{II}(\mu\text{-}PPh_2)_2Pt^{II}(pic\text{-}Ag(Me_2CO)PPh_3]$ (**30'**) (izquierda) y $[(C_6F_5)_2Pt^{II}(\mu\text{-}PPh_2)_2Pd^{II}(pic\text{-}AgPPh_3)]$ (**31**) (derecha).

Los cristales adecuados para los estudios de difracción de rayos-X de casi todos los complejos fueron obtenidos a partir de disoluciones en CH_2Cl_2; la excepción es el complejo **30**, para el cual no fue posible obtener cristales adecuados para estudios de rayos-X a partir de disoluciones en CH_2Cl_2 pero sí en acetona. Los cristales estudiados eran efectivamente del derivado **30** pero con una molécula de acetona coordinada al centro de plata (**30'**). Así, las estructuras moleculares de **30'** y **31** son muy similares, con la diferencia del entorno de coordinación de los centros de plata. La Figura 6 muestra las estructuras moleculares en estado sólido de los derivados **30'** y **31**.

Las estructuras de **30'** y **31** son diferentes de las estructuras de **25**, **27**–**29**. Aunque también son el resultado de la interacción de dos fragmentos, "$(C_6F_5)_2Pt(\mu\text{-}PPh_2)_2M(pic)$" (M = Pd, Pt) y "$AgPPh_3$", ambos fragmentos están conectados exclusivamente por un enlace Ag–O(1) (Figura 6) y no se observan interacciones Pt–Ag o Pd–Ag en ningún caso; tampoco se observan interacciones entre el centro de Ag y el otro átomo de oxígeno del ligando *o*-picolinato (O(2), Figura 6). Como se ha mencionado antes, el entorno de coordinación de los centros de Ag es diferente en cada complejo. En la estructura **30'**, el centro de plata se coordina además de al átomo O(1) del ligando *o*-picolinato y al átomo P(3) del grupo PPh_3, a un átomo de O de una molécula de acetona que actúa como ligando (Figura 6, izquierda), presentando de esta forma un entorno casi plano con forma de T distorsionada. A su vez, en la estructura del complejo **31**, el centro de Ag se coordina únicamente al átomo O(1) del ligando *o*-picolinato y al átomo P(3) del grupo PPh_3 (Figura 6, derecha). Respecto a las características estructurales del fragmento "$(C_6F_5)_2Pt(\mu\text{-}PPh_2)_2M(pic)$" (M = Pd, Pt), son análogas a las observadas en los derivados **25**, **27** y **28**, con ángulos diedros entre los planos de los dos centros metálicos Pt,M

(M = Pt, Pd), calculados por el método de mínimos cuadrados, de 29.1(1)º (**30'**) y de 30.2(1)º (**31**), con lo que estos fragmentos también pueden describirse como estructuras de "libro abierto". Aunque se podría pensar que este tipo de estructuras se favorece para facilitar interacciones de tipo Ag–M (Pt, Pd), las estructuras de **30'** y **31** demuestran que las interacciones M–Ag no parecen tener un papel decisivo en este hecho.

Tabla 3. Datos de RMN de ^{31}P y ^{195}Pt de **25**–**33** en diclorometano deuterado (δ en ppm, *J* en Hz).

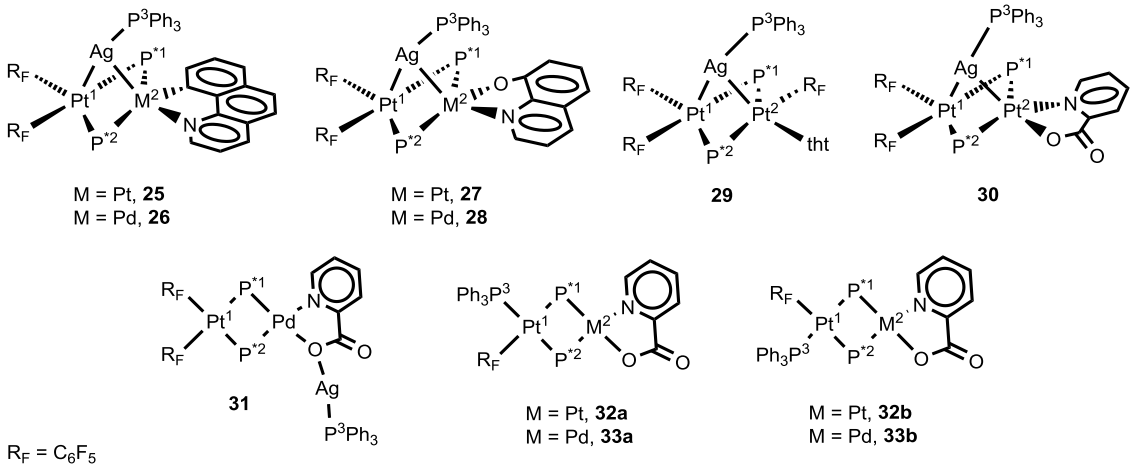

M = Pt, **25**
M = Pd, **26**

M = Pt, **27**
M = Pd, **28**

29

30

31

M = Pt, **32a**
M = Pd, **33a**

M = Pt, **32b**
M = Pd, **33b**

$R_F = C_6F_5$
P* = PPh_2

Complejo	δP^1	δP^2	$^2J_{P1,P2}$	$^1J_{P1,Pt1}$	$^1J_{P1,Pt2}$	$^1J_{P2,Pt1}$	$^1J_{P2,Pt2}$	δPt^1	δPt^2	δP^3	$^1J_{P3,^{107}Ag}$	$^1J_{P3,^{109}Ag}$
25	-88.0	-93.3	57	1478	2378	1254	1089	-3337[a]	-3426[a]	4.0	630	726
26	-60.2	-98.3	86	1359		1184		-3315		7.5	629	723
27	-124.5	-119.7	100	1465	2094	1506	2070	-3351[b]	-3177[b]	8.8	653	752
28	-104.7	-102.4	150	1387		1436		-3438		11.8	667	772
29[b]	-110.6	-125.2	81	1423	2031	1292	1412	-3337	-3655	7.7	701	806
30	-122.2	-127.1	102	1481	2271	1473	2113	-3335[c]	-3275[c]	9.2	664	764
31	-108.5	-111.3	193	1644		1613		-3920[c]		16.6	713	822
32a	-135.2	-126.2	160	1773	2635	1964	2752	-4200	-3502	22.0[d]		
32b	-134.2	-146.2	164	1979	2800	1661	2470	-4200	-3541	22.8[e]		
33a	-114.6	-110.5	213	1666		1776		-4240		19.9[f]		
33b	-116.2	-127.2	221	1822		1614		-4250		20.1[g]		

[a] $^1J_{Pt2,Ag}$ = ca. 250 Hz, $^2J_{Pt1,Pt2}$ = ca. 400 Hz, $^2J_{P3,Pt2}$ = 280 Hz; T = 268 K. [b] T = 213 K. [c] T = 243 K.
[d] $^2J_{P3,P2}$ = 349 Hz; $^1J_{P3,Pt1}$ = 2255 Hz. [e] $^2J_{P3,P1}$ = 345 Hz; $^1J_{P3,Pt1}$ = 2245 Hz. [f] $^2J_{P3,P2}$ = 326 Hz; $^1J_{P3,Pt}$ = 2304 Hz.
[g] $^2J_{P3,P1}$ = 336 Hz; $^1J_{P3,Pt}$ = 2298 Hz.

El comportamiento en disolución de los derivados **25**–**31**, mediante espectroscopia de RMN multinuclear a diversas temperaturas (disoluciones en diclorometano deuterado), se ha estudiado en el grupo del profesor Piero Mastrorilli. La Tabla 3 muestra los datos de RMN de ^{31}P y ^{195}Pt de los complejos **25**–**31**. Los espectros de RMN de ^{31}P{^{1}H} de los derivados **25**–**31**, registrados a 298 K, muestran a campo alto, en el rango entre δ -125 y δ -60, dos dobletes mutuamente acoplados, asignables a los átomos de P de los dos grupos μ-PPh_2, y una señal compleja a menor campo, entre δ 4.0 y δ 16.6, asignable al átomo de P del grupo PPh_3 unido a

Ag; esta señal consiste de la superposición de los dobletes debidos al acoplamiento del átomo de P con los isótopos ^{107}Ag y ^{109}Ag. Todas las señales de ^{31}P son anchas a temperatura ambiente, debido tanto a pequeños acoplamientos con núcleos de ^{19}F como a procesos dinámicos observados.

Los espectros de RMN de ^{195}Pt{^{1}H} de los derivados **25**–**28** muestran, cada uno, una señal muy ancha, en el rango entre δ -3315 y δ -3438, asignable al átomo de Pt unido a los dos grupos C_6F_5 (Pt^1, Tabla 3), y una señal más fina, a δ -3426 (derivado **25**) y δ -3177 (derivado **27**), correspondiente al centro de platino unido al ligando bidentado (Pt^2, Tabla 3). Al comparar los valores de estos desplazamientos con los de sus respectivos productos de partida **1**, **2**, **12** y **14** (δPt^1 = ca. -3900; δPt^2 = -3717 (derivado **1**), -3450 (derivado **12**); Tablas 1 y 2), se observa que en todos los casos, la adición del grupo $AgPPh_3$ resulta en un desplazamiento de las señales a menor campo, lo que es consistente con el comportamiento dador de los átomos de platino en derivados con enlaces Pt–Ag. Un comportamiento similar se observa al comparar los desplazamientos químicos del complejo **29** (δPt^1 = -3337; δPt^2 = -3655) con los de su producto de partida, **24** (δPt^1 = -3821; δPt^2 = -3911).

Por otra parte, en el espectro de RMN de ^{195}Pt{^{1}H} del derivado **31** (registrado a 243 K), la señal del átomo de Pt^1 se observa a δ -3920, un valor muy similar al de su producto de partida, **16** (δPt^1 = -3905; Tabla 2) y muy diferente al encontrado para los derivados **25**–**29**, sugiriendo que el entorno químico del centro Pt^1 del derivado **31** es diferente al de los derivados **25**–**29**, en acuerdo con las diferencias encontradas en las estructuras en estado sólido de estos derivados (Figuras 5 y 6). Finalmente, las señales de RMN de ^{195}Pt del complejo **30** (δPt^1 = -3335; δPt^2 = -3275) experimentan un desplazamiento a menor campo respecto a los desplazamientos químicos de su producto de partida, **15** (δPt^1 = -3911; δPt^2 = -3542), en forma análoga a la experimentada en los derivados **25**–**29**; esta observación sugiere que la estructura del complejo **30** en disolución puede ser similar a la de los derivados **25**–**29**, con el fragmento "$AgPPh_3$" actuando como puente entre los dos centros metálicos, y no como su estructura en estado sólido, con el centro de Ag unido a un átomo de oxígeno del grupo *o*-picolinato.

El estudio de RMN en disolución de los complejos **25**–**31** se completó con experimentos ^{1}H, ^{19}F, COSY ^{1}H, HMQC ^{1}H–^{31}P, NOESY ^{1}H, EXSY ^{1}H, EXSY ^{31}P, EXSY ^{19}F y HOESY ^{1}H–^{19}F a diferentes temperaturas. El análisis de estos datos permitió discernir el comportamiento de estos complejos en disolución.

El análisis de estos datos ha permitido concluir que las estructuras en estado sólido de los derivados **25**–**29** se mantienen en disolución, es decir, que constan de los fragmentos "$(C_6F_5)_2Pt(\mu\text{-}PPh_2)_2M(L)(L')$" y "$AgPPh_3$" unidos por los enlaces Pt–Ag y M–Ag. Además, se ha observado en estos derivados un comportamiento dinámico en disolución consistente en el movimiento del fragmento "$AgPPh_3$", que pasa de la parte superior a la inferior de los

complejos, tal como se recoge en el Esquema 14. Este comportamiento dinámico puede explicarse a través de la ruptura y nueva formación de los enlaces Ag–Pt/M.

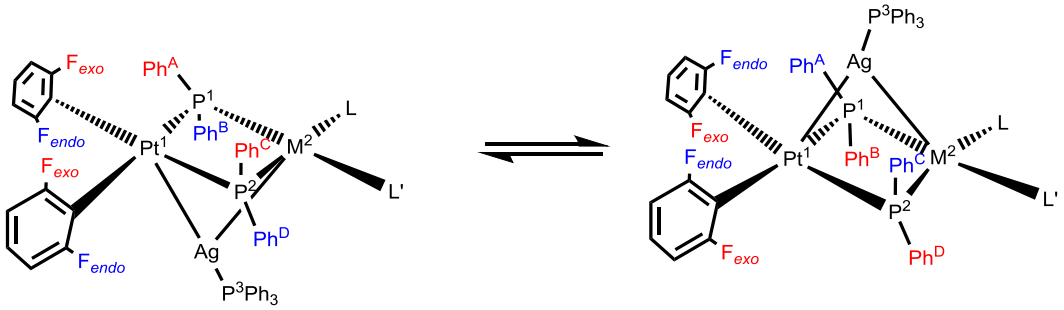

Esquema 14

Por otra parte, el comportamiento del complejo **31** en disolución es diferente al observado en los derivados **25**–**29**. En este complejo, los experimentos de RMN de EXSY ^{1}H, EXSY ^{31}P y EXSY ^{19}F revelan un intercambio entre los dos grupos difenilfosfanuro puentes, así como entre los dos grupos C_6F_5. Una explicación factible de lo observado en disolución es el intercambio de las posiciones de los átomos de N y O unidos al centro de Pd, posiblemente por ruptura y nueva formación del enlace Pd–O, como se muestra en el Esquema 15.

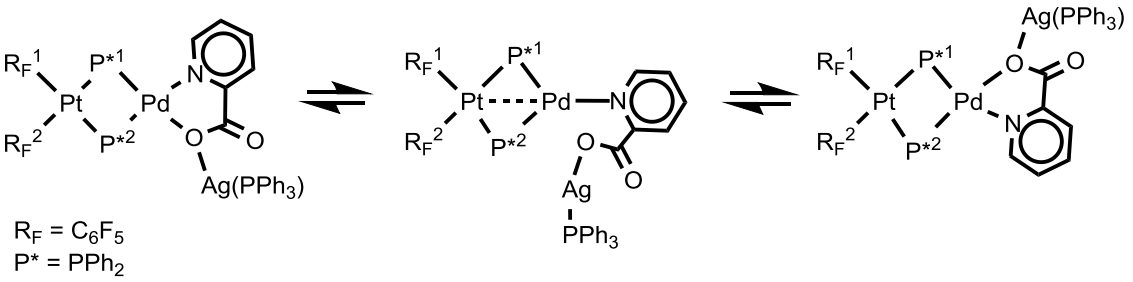

Esquema 15

Finalmente, el espectro de RMN de ^{1}H del derivado **30**, registrado a 298 K, muestra, además de las señales de los grupos pic y PPh_3, un grupo de señales correspondientes a los dos anillos fenilo unidos al átomo P^1 y otro grupo de señales correspondientes a los dos anillos unidos a P^2 (numeración atómica en Tabla 3); sin embargo, no se observaron picos de intercambio en los espectros de RMN de EXSY ^{1}H, EXSY ^{31}P y EXSY ^{19}F, como sí ocurre en los espectros del derivado **31**. Aunque estos resultados negativos deben interpretarse con cuidado y no prueban la ausencia de intercambios entre los átomos P^1 y P^2, así como entre los dos grupos C_6F_5, al sumarlos con el análisis de los espectros de RMN de ^{195}Pt, apuntan a que el derivado **30** tiene un comportamiento en disolución análogo al de los derivados **25**–**29** y no al del complejo **31**. De esta forma, para el derivado **30** puede proponerse una estructura en disolución análoga a la de los complejos **25**–**29**, con el fragmento "$AgPPh_3$" actuando como puente entre los dos centros metálicos (Tabla 3).

El comportamiento de los derivados **30** y **31** en disolución puede racionalizarse admitiendo que, para estas especies, son posibles las dos estructuras en disolución, ya sea con el fragmento "$AgPPh_3$" actuando como puente entre los centros metálicos o unido a un

átomo de oxígeno del grupo pic (Esquema 16); en el caso del complejo homonuclear de Pt, la forma estable es aquella con el fragmento "$AgPPh_3$" actuando como puente entre los centros metálicos y el equilibrio se desplaza hacia la derecha, mientras que en el derivado de Pt y Pd, la forma más estable es aquella con este fragmento unido al átomo de oxígeno. Este comportamiento en disolución está en acuerdo con el menor número de complejos que presentan enlace Pd–Ag respecto a los que presentan enlace Pt–Ag.[98-101]

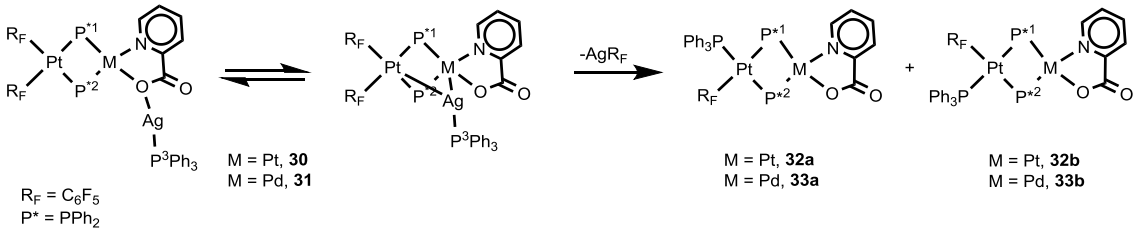

Esquema 16

Finalmente, los aductos de M–Ag (M= Pt, Pd) son, en muchas ocasiones, inestables en disolución y descomponen. El seguimiento de este proceso de descomposición para los complejos **30** y **31** mostró la formación de los derivados **32** y **33**, respectivamente (sus datos de RMN de ^{31}P y ^{195}Pt se muestran en la Tabla 3), en los que uno de los grupos C_6F_5 ha sido reemplazado por PPh_3 (Esquema 16); de esta forma, los derivados **30** y **31** pueden considerarse como intermedios en la formación de los complejos **32** y **33**.

E4. Adición de nucleófilos a fosfanuro-derivados de Pt(III): Formación de enlaces P–C, P–N y P–O

Andersson Arias, Juan Forniés, Consuelo Fortuño, Susana Ibañez y Antonio Martín. Piero Mastrorilli, Vito Gallo y Stefano Todisco. *Inorg. Chem.* doi: 10.1021/ic401689c

En los Apartados E1 y E2 se describe cómo la adición de I_2 a los nuevos fosfanuro-derivados binucleares de Pt/Pd(II) sintetizados, produce el acoplamiento entre uno de los grupos PPh_2 y otro ligando, con formación de enlaces P–C, P–O o P–I, dando lugar a derivados de Pt/Pd(II) que presentan un nuevo ligando fosfano; se ha demostrado que esta reacción ocurre a través de intermedios binucleares de tipo M(II),M'(IV) (M, M' = Pd, Pt), que al experimentar el acoplamiento reductor, se transforman en los productos finales de M(II),M'(II). Por otra parte, en el Apartado C se ha señalado que la adición de I_2 a derivados bi y trinucleares con fórmulas generales $[(C_6F_5)_2M(\mu\text{-}PPh_2)_2M'L_2]^{n-}$ y $[(C_6F_5)_2Pt(\mu\text{-}PPh_2)_2M(\mu\text{-}PPh_2)_2Pt(C_6F_5)_2]^{2-}$ (M, M' = Pd, Pt), da lugar a derivados con centros metálicos en estado de oxidación formal II que presentan un nuevo ligando fosfano y enlaces P–C o P–P, a través de intermedios de tipo M(III)–M'(III) y Pt(III)–M(III),Pt(II).

De estas experiencias se ha concluido que la coordinación del nucleófilo I^- a un intermedio de tipo M(III)–M(III) (A, Esquema 17) o la eliminación de un grupo ioduro de un intermedio de tipo M(II),M(IV) (B, Esquema 17), produce un intermedio insaturado de tipo M(II),M(IV) que evoluciona a través de acoplamiento reductor con formación de nuevos enlaces (Esquema 17). Además de estos estudios, poco se conoce acerca del comportamiento de fosfanuro-derivados de tipo M(III)–M(III) y su papel en la formación de acoplamientos reductores.

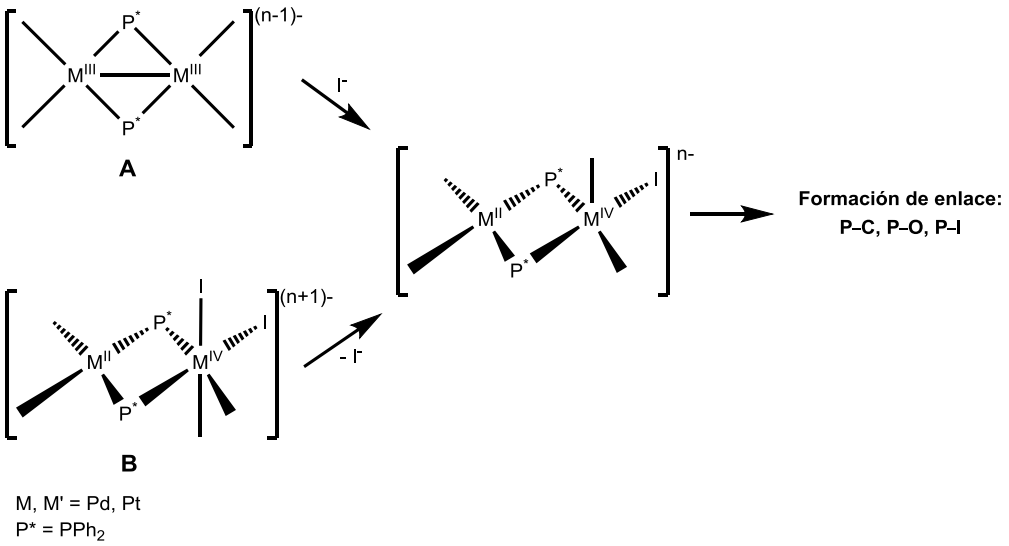

Esquema 17

Objetivo: Estudiar la reacción entre los fosfanuro-derivados $[(C_6F_5)_2Pt^{III}(\mu\text{-}PPh_2)_2Pt^{III}(C_6F_5)_2]$(Pt–Pt) (**34**) y $[(C_6F_5)_2Pt^{III}(\mu\text{-}PPh_2)_2Pt^{III}(\mu\text{-}PPh_2)_2Pt^{II}(C_6F_5)_2](Pt^{III}–Pt^{III})$ (**35**), obtenidos previamente en nuestro grupo de investigación,[55,69] y nucleófilos diferentes a I^-, con el objeto de establecer la capacidad de estos complejos de formar nuevos acoplamientos y enlaces.

Metodología utilizada y resultados más relevantes: El fosfanuro-derivado **34** muestra dos centros de Pt(III) en entornos planos cuadrados, enlace metal–metal y solo un tipo de ligando terminal (C_6F_5). El ataque de un nucleófilo a este sustrato es previsible que ocurra sobre uno de los dos centros metálicos, con ruptura de enlace Pt–Pt y formación de una especie insaturada de Pt(II),Pt(IV)[49,102] que evolucione hacia un derivado de Pt(II),Pt(II) a través de acoplamiento reductor.[103,104]

La adición de NBu_4OH a una disolución del complejo **34** en CH_2Cl_2 (relación molar 2:1) da lugar al derivado $[NBu_4]_2[(C_6F_5)_2Pt^{II}(\mu\text{-}Ph_2P–O)(\mu\text{-}PPh_2)Pt^{II}(C_6F_5)_2]$ (**36**), en el que los dos centros de Pt(II) están unidos por un ligando fosfanuro y uno fosfinito (Esquema 18. Solo se muestra el anión del derivado). A pesar de diversos intentos de cristalización, la pobre calidad de los cristales obtenidos no permitió completar los estudios de difracción de rayos-X de la estructura del producto **36**; sin embargo, la conectividad de los átomos del anión fue establecida sin ambigüedad y es la que se muestra en el Esquema 18.

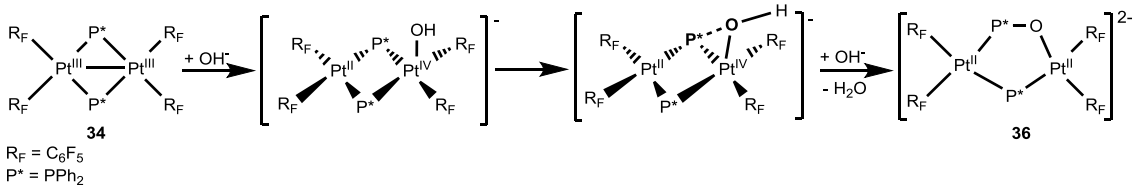

Esquema 18

La adición de NaN_3 a una disolución del derivado **34** en acetona a temperatura ambiente da lugar, usando NBu_4^+ como contraión, a mezclas en las que se identifican los derivados $[NBu_4]_2[(C_6F_5)_2Pt^{II}(\mu\text{-}N_3)(\mu\text{-}PPh_2)Pt^{II}(C_6F_5)_2]$ (**37a**) y $[NBu_4][(C_6F_5)_2Pt^{II}(\mu\text{-}N_3)(\mu\text{-}PPh_2)Pt^{II}(C_6F_5)(Ph_2P–C_6F_5)]$ (**37b**) (Esquema 19. Solo se muestran los aniones de los derivados). El derivado **37a** mantiene los mismos cuatro ligandos terminales que su producto de partida, **34**. Sin embargo, se observa (Esquema 19) que los dos centros metálicos están unidos por un ligando fosfanuro y uno azido, indicando que probablemente ha tenido lugar una eliminación reductora PPh_2/N_3, con descomposición del grupo inestable $Ph_2P–N_3$ formado,[105,106] y la coordinación de un grupo azido, que actúa como puente entre los dos centros metálicos a través de uno de sus átomos de N terminales (μ-1,1-N_3). Por otra parte, en el derivado **37b** se observa la formación del ligando $Ph_2P–C_6F_5$, indicando que ha tenido lugar un acoplamiento reductor PPh_2/C_6F_5 (Esquema 19). El derivado **37a** ha podido ser aislado puro realizando la reacción en una mezcla acetona/metanol, pero no pudo ser obtenida una muestra pura de **37b**; sin embargo, la estructura de este derivado pudo inferirse por comparación de sus

características espectroscópicas con las del producto análogo $[NBu_4][(C_6F_5)_2Pt^{II}(\mu\text{-}I)(\mu\text{-}PPh_2)Pt^{II}(C_6F_5)(Ph_2P\text{–}C_6F_5)]$, previamente sintetizado en nuestro grupo.[72]

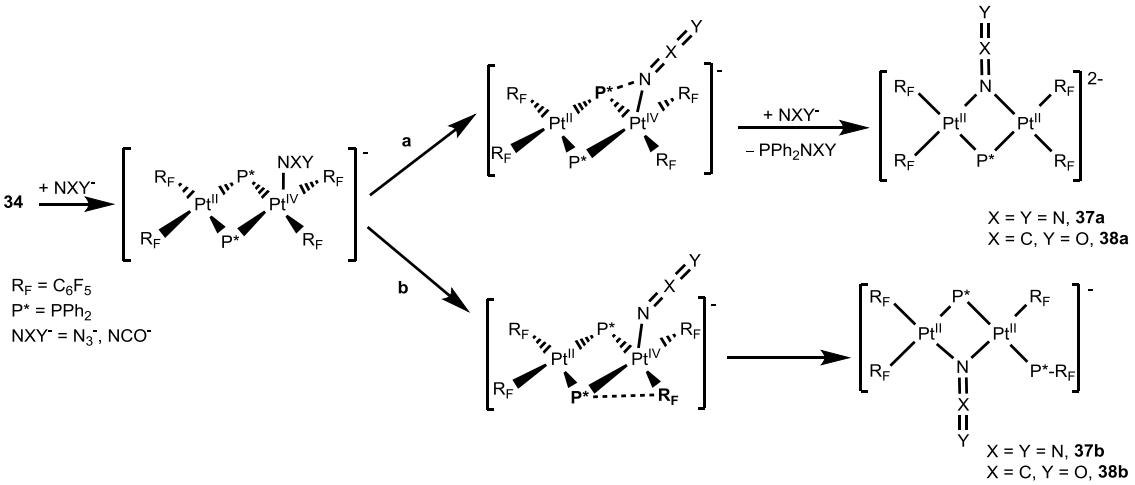

Esquema 19

Finalmente, la adición de KNCO a una disolución del complejo **34** en acetona a temperatura ambiente y en relación molar 2:1, da lugar, usando NBu_4^+ como contraión, a mezclas en las que se identifican los derivados $[NBu_4]_2[(C_6F_5)_2Pt^{II}(\mu\text{-}NCO)(\mu\text{-}PPh_2)Pt^{II}(C_6F_5)_2]$ (**38a**) y $[NBu_4][(C_6F_5)_2Pt^{II}(\mu\text{-}NCO)(\mu\text{-}PPh_2)Pt^{II}(C_6F_5)(Ph_2P\text{–}C_6F_5)]$ (**38b**) (Esquema 19), análogos a **37a** y **37b**, respectivamente. Al realizar la reacción con un exceso de KNCO, puede aislarse el derivado **38b**, mientras que **38a** no se detecta en la mezcla de reacción. Todos los intentos de obtener una muestra pura de **38a** o de separar las mezclas de **38a** y **38b** han sido infructuosos. Sin embargo, ha sido posible obtener cristales del derivado **38a** adecuados para estudios de difracción de rayos-X a partir de disoluciones concentradas de mezclas conteniendo **38a** y **38b**.

Las estructuras de los derivados **37a** y **38a** se han establecido mediante estudios de difracción de rayos-X y las estructuras de los aniones de ambos compuestos se muestran en la Figura 7. Los dos derivados aniónicos muestran estructuras similares, con la única diferencia en uno de los ligandos puentes, que es N_3 en el caso del derivado **37a** y NCO en el de **38a**. Son estructuras binucleares no planas en las que los átomos de Pt(II) presentan entornos planos cuadrados, con distancias intermetálicas que excluyen cualquier posibilidad de interacciones entre los dos centros (3.400(1) Å para **37a** y 3.372(1) Å para **38a**). En ambos aniones el entorno del átomo de N puente es plano y la geometría de los fragmentos N–N–N y N–C–O es lineal.

Se han registrado espectros de IR en estado sólido de muestras puras de los derivados **36**, **37a** y **38b**. La absorción en la región de 950 cm^{-1} en derivados que presentan el grupo C_6F_5 unido a un centro metálico, está relacionada con el estado de oxidación del átomo metálico. Esta absorción aparece a 947, 951 y 953 cm^{-1} en los derivados de Pt(II) **36**, **37a** y **38b**, respectivamente, mientras que aparece a 964 cm^{-1} en el complejo de Pt(III) **34**. Esta

disminución de la frecuencia de absorción está en acuerdo con el descenso en el estado de oxidación formal de los centros de platino.[55]

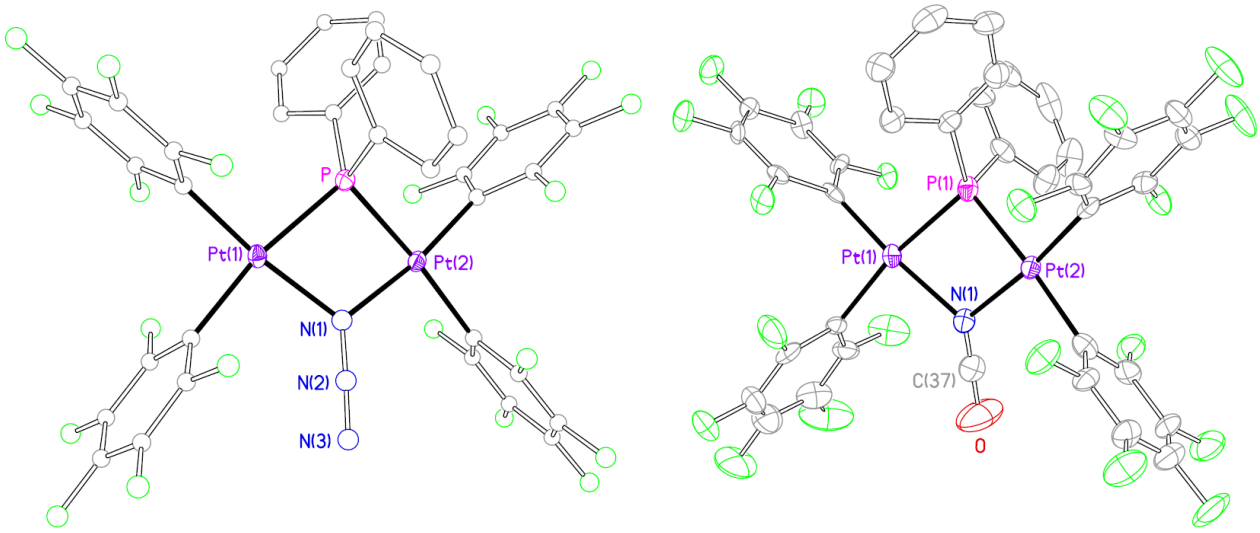

Figura 7. Vista de la estructura molecular de los aniones de los compuestos $[NBu_4]_2[(C_6F_5)_2Pt^{II}(\mu\text{-}N_3)(\mu\text{-}PPh_2)Pt^{II}(C_6F_5)_2]$ (**37a**) (izquierda) y $[NBu_4]_2[(C_6F_5)_2Pt^{II}(\mu\text{-}NCO)(\mu\text{-}PPh_2)Pt^{II}(C_6F_5)_2]$ (**38a**) (derecha).

El espectro de RMN de ^{19}F del derivado **36** (disolución en acetona deuterada) muestra doce señales: cuatro señales de la misma intensidad en la región de *o*-F, cuatro asignables a los átomos de *m*-F y cuatro asignables a *p*-F; este patrón indica la existencia de cuatro grupos C_6F_5 no equivalentes y que en cada uno de estos, las dos mitades del anillo son equivalentes. Los espectros de los derivados **37a** y de **38a** (disoluciones en acetona deuterada) muestran seis señales con un patrón que indica dos tipos de grupos C_6F_5 no equivalentes en los que las mitades de cada anillo sí lo son. Las señales de RMN de ^{19}F de los compuestos **37b** y **38b** han sido identificadas sin ambigüedad y son comparables a las obtenidas para el derivado $[NBu_4][(C_6F_5)_2Pt^{II}(\mu\text{-}I)(\mu\text{-}PPh_2)Pt^{II}(C_6F_5)(Ph_2P\text{–}C_6F_5)]$, previamente sintetizado en nuestro grupo.[72]

El desplazamiento químico de los átomos de P de los dos grupos $\mu\text{-}PPh_2$ del complejo **34**, δ 281.7, disminuye considerablemente al pasar a los derivados **36**–**38**, como cabe esperar debido a la transformación de un fragmento "$M(\mu\text{-}PPh_2)_2M$" que presenta enlace metal–metal, en un fragmento "$M(\mu\text{-}PPh_2)(\mu\text{-}X)M$" sin enlace metal–metal. A su vez, la transformación de un ligando $\mu\text{-}PPh_2$ en un grupo fosfinito P,O-puente (compuesto **36**) o en el grupo fosfano terminal $Ph_2P\text{–}C_6F_5$ (derivados **37b** y **38b**) resulta en señales a δ 127.1, 13.4 y 12.6, respectivamente.

La reactividad exhibida por el complejo **34** hacia OH^-, N_3^- y NCO^- puede explicarse asumiendo que el nucleófilo se coordina a uno de los centros de Pt(III) a través del átomo de O del grupo OH o de N de los grupos N_3 o NCO, dando lugar a intermedios insaturados de

Pt(II),Pt(IV) (Esquemas 18 y 19). Teniendo en cuenta que complejos intermedios de Pt(IV) pentacoordinado se proponen usualmente en procesos de eliminación reductora, y algunos han sido caracterizados cristalográficamente,[107-112] estos intermedios podrían evolucionar a través de dos vías: a) el acoplamiento reductor entre uno de los grupos μ-PPh_2 y el nucleófilo coordinado (dando lugar a los derivados **36**, **37a** y **38a**), o b) el acoplamiento reductor entre uno de los grupos μ-PPh_2 y un grupo C_6F_5 (obteniendo los derivados **37b** y **38b**). En ambos casos, puede plantearse la existencia de un intermedio con un átomo de P pentacoordinado (Esquemas 18 y 19), un hecho bien establecido en la química de derivados de fosfanos y fosfanuros.[11,14-17,113-115]

De esta forma, la adición del nucleófilo OH^- al derivado **34** puede dar lugar a un acoplamiento reductor entre un grupo μ-PPh_2 y el grupo OH, con formación de un ligando Ph_2P–OH coordinado, que al ser desprotonado por un segundo anión OH^-, da lugar al ligando fosfinito P,O-puente observado (Esquema 18). Si los intermedios de Pt(II),Pt(IV) de azido o cianato propuestos evolucionan de acuerdo a la vía a), pueden dar lugar a la formación de los ligandos Ph_2P–N_3 o Ph_2P–NCO, respectivamente, con formación de enlace P–N; estos ligandos son eliminados y descomponen fácilmente[105] y el entorno de coordinación de los centros metálicos se completa con un grupo μ-N_3 o μ-NCO, respectivamente, dando lugar a los derivados **37a** y **38a**. Por otra parte, si estos intermedios evolucionan a través de la vía b), el nucleófilo coordinado actuaría inicialmente como espectador y el acoplamiento reductor podría tener lugar entre un grupo μ-PPh_2 y uno C_6F_5, con formación del ligando Ph_2P–C_6F_5; el cambio en la forma de coordinación del nucleófilo, de ligando terminal a ligando puente, completa la esfera de coordinación de ambos centros metálicos, dando lugar a los derivados **37b** y **38b**.

Finalmente, la formación del derivado **36** y de las mezclas de productos **37a-b** y **38a-b**, indica que en estos intermedios insaturados de Pt(II),Pt(IV), la formación de enlace P–O está favorecida respecto a la formación de enlace P–C; sin embargo, la formación de enlace P–N es competitiva con la formación de enlace P–C.

Por otra parte, se ha realizado la adición de los nucleófilos OH^- y N_3^- al derivado trinuclear insaturado $[(C_6F_5)_2Pt^{III}(\mu\text{-}PPh_2)_2Pt^{III}(\mu\text{-}PPh_2)_2Pt^{II}(C_6F_5)_2](Pt^{III}\text{–}Pt^{III})$ (**35**).[69] Este derivado, al igual que **34**, muestra dos centros de Pt(III) susceptibles de reaccionar con nucleófilos; sin embargo, los dos centros tienen dos entornos químicos diferentes: el átomo de Pt(III) terminal está unido a dos ligandos C_6F_5 y a dos grupos μ-PPh_2, mientras que el centro de Pt(III) central está unido a cuatro grupos μ-PPh_2, situación que puede condicionar la reactividad de los dos centros de Pt(III) hacia los nucleófilos.

La adición de NBu_4OH y de NaN_3 (como disoluciones en metanol) a suspensiones del complejo **35**, en CH_2Cl_2 y acetona, respectivamente, da lugar, después del tratamiento adecuado de las mezclas de reacción, a los derivados trinucleares de Pt(II) $[NBu_4]_2[(C_6F_5)_2Pt^{II}(\mu\text{-}Ph_2P\text{–}O)(\mu\text{-}PPh_2)Pt^{II}(\mu\text{-}PPh_2)_2Pt^{II}(C_6F_5)_2]$ (**39**) y $[NBu_4][Pt_3^{II}(\mu_3$-

$Ph_2PNPPh_2)(\mu\text{-}PPh_2)_2(C_6F_5)_4]$ (**40**), respectivamente (Esquema 20. Solo se muestran los aniones de los derivados).

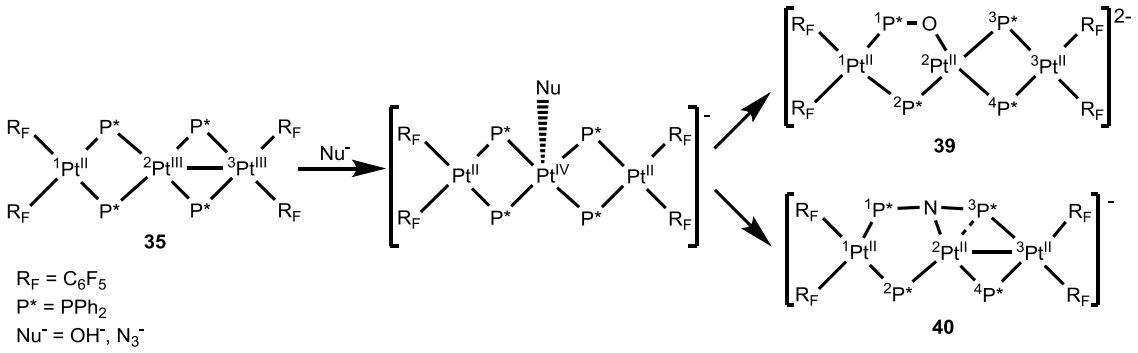

Esquema 20

Los productos **39** y **40** muestran tres centros de platino en estado de oxidación formal II y dos nuevos ligandos puentes: un grupo $Ph_2P–O$ actúa como puente entre dos centros de platino en el derivado **39**, mientras que en el derivado **40**, un grupo bis(difenilfosfanil)amida, $(PPh_2)_2N$, formado durante el transcurso de la reacción, se coordina a los centros metálicos de forma muy inusual: como ligando puente a los tres centros de platino. En ambos casos los grupos C_6F_5 se mantienen coordinados a los átomos de Pt terminales en mutua posición *cis*.

La formación de los compuestos **39** y **40** parece indicar que la coordinación de los nucleófilos es preferida sobre el átomo de Pt(III) central del complejo **35** que sobre el Pt(III) terminal. De esta forma, podrían formarse intermedios de tipo Pt(II),Pt(IV),Pt(II), que mediante acoplamiento reductor, con formación de enlaces P–O y P–N, dan lugar a los productos finales **39** y **40** de tipo Pt(II),Pt(II),Pt(II). El proceso de formación del derivado **39** es análogo al del producto **36**; sin embargo, la formación del derivado **40** implica un proceso más complicado, que podría explicarse a través de dos etapas consecutivas: 1) formación de un acoplamiento reductor entre el grupo $\mu\text{-}P(1)Ph_2$ y el grupo N_3 coordinado como ligando terminal, con ruptura del enlace P(1)–Pt(2) y formación del sistema Pt(1)–P(1)–N–Pt(2) (numeración atómica en Esquema 20); y 2) ruptura del enlace formal P(3)–Pt(2), formación del enlace P(3)–N y eliminación de N_2. Aunque la síntesis de complejos con el ligando $(PPh_2)_2N$ es conocida,[116] la formación de este grupo en el derivado **40** no tiene precedentes: es formalmente el resultado de la transformación de dos grupos difenilfosfanuro puentes, un ligando azido terminal y un centro de Pt(IV) en un nuevo ligando tridentado, un centro de Pt(II) y N_2.

Dado que no fue posible obtener cristales de los derivados **39** y **40** adecuados para estudios de difracción de rayos-X, se han sintetizado los compuestos $[NBzMe_3]_2[(C_6F_5)_2Pt^{II}(\mu\text{-}Ph_2P–O)(\mu\text{-}PPh_2)Pt^{II}(\mu\text{-}PPh_2)_2Pt^{II}(C_6F_5)_2]$ (**39'**) y $[PPh_3Me][Pt_3^{II}(\mu_3\text{-}Ph_2PNPPh_2)(\mu\text{-}PPh_2)_2(C_6F_5)_4]$ (**40'**); las estructuras moleculares de los aniones de estos derivados se han establecido por estudios de difracción de rayos-X y se muestran en la Figura 8.

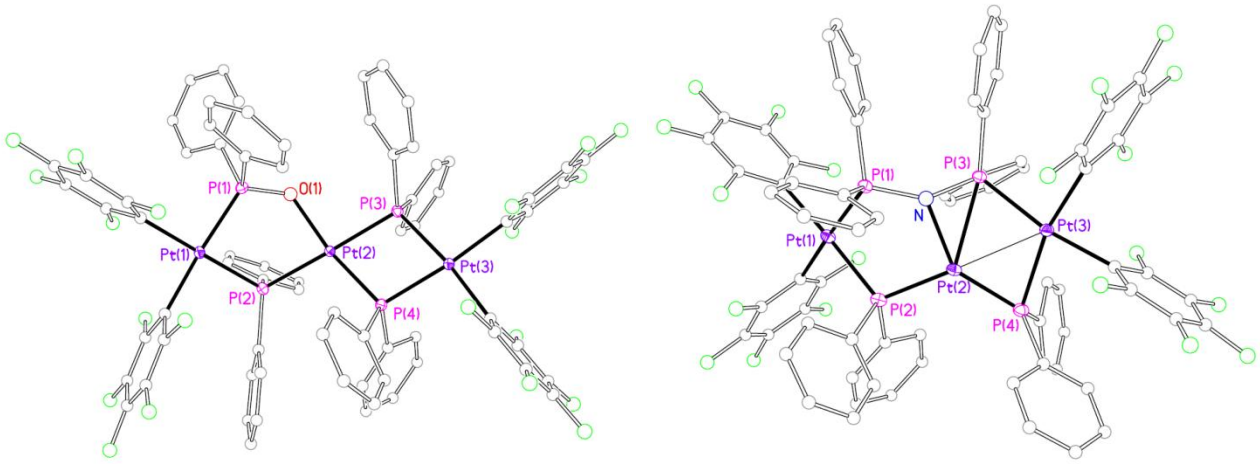

Figura 8. Vista de la estructura molecular de los aniones de los compuestos $[NBzMe_3]_2[(C_6F_5)_2Pt^{II}(\mu\text{-}Ph_2P\text{–}O)(\mu\text{-}PPh_2)Pt^{II}(\mu\text{-}PPh_2)_2Pt^{II}(C_6F_5)_2]$ (**39'**) (izquierda) y $[PPh_3Me][Pt_3^{II}(\mu_3\text{-}Ph_2PNPPh_2)(\mu\text{-}PPh_2)_2(C_6F_5)_4]$ (**40'**) (derecha).

En el anión del derivado **39'** se observan tres centros de platino, de los que Pt(1) y Pt(2) están unidos por un grupo PPh_2 y uno fosfinito, mientras que Pt(2) y Pt(3) lo están a través de dos grupos PPh_2 (Figura 8, izquierda). Los tres centros de platino presentan entornos de coordinación planos cuadrados dispuestos de forma tal que el anión no es plano, y a distancias intermetálicas (distancia Pt(1)···Pt(2) = 3.846(1) Å; Pt(2)···Pt(3) = 3.599(1) Å) que excluyen cualquier posibilidad de interacción entre ellos.

La característica más destacable del anión del derivado **40'** es la presencia del ligando $(PPh_2)_2N$, que actúa como puente entre los tres centros metálicos. El ligando se une al centro de Pt(1) a través del átomo P(1) y al centro de Pt(3) con el átomo P(3) (Figura 8, derecha). La unión al centro de Pt(2) podría considerarse formada por un enlace covalente Pt(2)–N y una interacción débil Pt(2)···P(3) (distancia Pt(2)···P(3) = 2.6207(9) Å); sin embargo, considerando que el centro de N es casi plano (la suma de los ángulos alrededor de N es de 354.3º) y que las distancias N–P del ligando $(PPh_2)_2N$ (distancia N–P(1) = 1.662(3) Å; N–P(3) = 1.636(3) Å) son más cortas que las de un enlace sencillo N–P (ca. 1.78 Å[117]), puede considerarse una contribución π a estos enlaces P–N y así, un modo de coordinación η^2 del fragmento P(3)–N al centro Pt(2).[116,118-121] El conteo total de electrones de valencia es 46, por lo que cabe esperar un enlace Pt–Pt; la diferencia observada entre las dos distancias intermetálicas (distancia Pt(1)···Pt(2) = 3.761(1) Å; Pt(2)–Pt(3) = 2.7374(2) Å) está en acuerdo con la existencia de un enlace Pt(2)–Pt(3).[19]

Los espectros de RMN de $^{31}P\{^1H\}$ de los derivados **39** y **40** (disoluciones en acetona deuterada) muestran cuatro señales anchas que concuerdan con las estructuras en estado sólido. En el espectro del compuesto **39** se observa a campo bajo una señal a δ 123.6 asignada al átomo de P del nuevo ligando fosfinito (P^1, Esquema 20) y un doblete a δ 13.9 asignable al grupo $\mu\text{-}P(2)Ph_2$; a campo alto se observan las señales asignables a los átomos P^3

y P^4, como cabe esperar para un sistema "Pt(μ-PPh_2)$_2$Pt" que no presenta enlace metal–metal. A su vez, en el espectro del derivado **40**, las señales correspondientes a los dos grupos difenilfosfanuro puentes se encuentran a δ 140.6 y δ 30.7, asignadas a los átomos P^4 y P^2, respectivamente (numeración atómica en Esquema 20), siendo estos desplazamientos químicos los esperados para un sistema "Pt(μ-PPh_2)Pt" con y sin enlace metal–metal, respectivamente. Las señales correspondientes a los átomos de P del ligando $(PPh_2)_2N$ aparecen como dos dobletes anchos ($^2JP^1,P^3$ ≈ 70 Hz) centrados a δ 128.4 y a δ 31.7; la señal a δ 128.4 muestra solo un par de satélites de platino y es asignada a P^1, mientras que la señal a δ 31.7 muestra satélites de platino debido a dos centros de ^{195}Pt no equivalentes, lo que está en acuerdo con la distancia Pt(2)···P(3) encontrada en la estructura en estado sólido de **40'** (2.6207(9) Å).

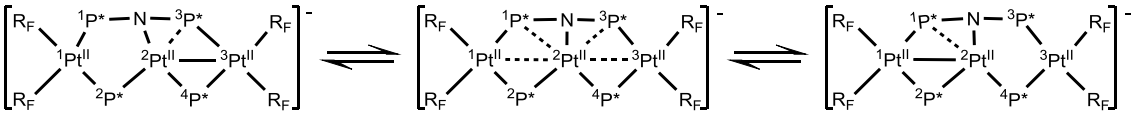

$R_F = C_6F_5$
$P^* = PPh_2$

Esquema 21

Finalmente, el experimento EXSY ^{31}P del derivado **40** a 323 K ha revelado un intercambio entre los átomos P^1 y P^3, así como entre P^2 y P^4. Estos resultados pueden explicarse a través de un intermedio que supone la deslocalización electrónica entre los centros de Pt y entre los átomos de P del ligando $(PPh_2)_2N$ (Esquema 21). En este intermedio propuesto, los átomos P^1 y P^3 son equivalentes, así como P^2 y P^4.

E5. De fragmentos fosfanuros bi y trinucleares a complejos tetra y hexanucleares de Pt(II)

Andersson Arias, Juan Forniés, Consuelo Fortuño, Antonio Martín. *Inorg. Chim. Acta*, **2013**, 407, 189–196

En el Apartado E2 se describe un método de síntesis de derivados binucleares asimétricos que consiste en la eliminación de los dos ligandos cloruro puentes –como AgCl– de derivados tetranucleares de tipo $[NBu_4]_2[\{(C_6F_5)_2Pt(\mu\text{-}PPh_2)_2M(\mu\text{-}Cl)\}_2]$ (M = Pd, Pt),[40] y el tratamiento de las especies resultantes con el correspondiente ligando O,N- dador (Esquema 8a). El primer paso de este método da lugar a especies binucleares de tipo $[(C_6F_5)_2Pt(\mu\text{-}PPh_2)_2M(S)_2]$ (S = disolvente dador), en las que las dos posiciones de coordinación que quedan libres por la eliminación de los ligandos cloruro, se completan con la coordinación del disolvente dador. En nuestro grupo de investigación ha sido posible aislar complejos de este tipo, obteniendo entre otros, el derivado binuclear de platino $[(C_6F_5)_2Pt(\mu\text{-}PPh_2)_2Pt(NCCH_3)_2]$[88] (**41**), empleando acetonitrilo como disolvente dador. Por otra parte, una modificación de este método, empleando un paso intermedio, ha permitido aislar el derivado trinuclear de platino $[(C_6F_5)_2Pt(\mu\text{-}PPh_2)_2Pt(\mu\text{-}PPh_2)_2Pt(NCCH_3)_2]$[89] (**42**).

Estos derivados neutros **41** y **42** pierden fácilmente el ligando CH_3CN, por lo que la adición de nuevos ligandos daría lugar a nuevos derivados bi o trinucleares, neutros o aniónicos, dependiendo de la naturaleza de los grupos entrantes; por ejemplo, la adición del anión cianuro (CN^-) al complejo **41**, da lugar al derivado $[NBu_4]_2[(C_6F_5)_2Pt(\mu\text{-}PPh_2)_2Pt(CN)_2]$, previamente aislado en nuestro grupo de investigación.[88]

Objetivo: Obtener nuevos derivados bi y trinucleares dianiónicos en los que los grupos azido (N_3), oxalato (C_2O_4) y cianuro (CN) actúen como ligandos terminales.

Metodología utilizada y resultados más relevantes: La adición de los aniones N_3^- y $C_2O_4^{2-}$ (como sales de NaN_3 y $K_2C_2O_4$) a los derivados **41** y **42**, incluso añadiéndolos en exceso, no permite aislar las sales de los complejos bi o trinucleares dianiónicos de tipo $[(C_6F_5)_2Pt(\mu\text{-}PPh_2)_2Pt(L_2)]^{2-}$ y $[(C_6F_5)_2Pt(\mu\text{-}PPh_2)_2Pt(\mu\text{-}PPh_2)_2Pt(L_2)]^{2-}$ ($L_2 = 2N_3$; C_2O_4), sino las sales de complejos tetra y hexanucleares en los que el grupo entrante actúa como ligando puente entre los dos átomos de platino centrales (Esquema 22).

Así, la adición de un exceso de NaN_3 a disoluciones en acetona de los derivados **41** y **42** resulta, tras el tratamiento de las mezclas de reacción, en la sustitución de los ligandos CH_3CN y formación de complejos que contienen el ligando N_3; sin embargo, no se ha detectado la formación de complejos dianiónicos con dos grupos azido terminales, sino de los derivados que presentan dos grupos azido puentes con modo de coordinación μ-1,1-N_3, $[NBu_4]_2[\{(C_6F_5)_2Pt(\mu\text{-}PPh_2)_2Pt(\mu\text{-}1,1\text{-}N_3)\}_2]$ (**43**) y $[NBu_4]_2[\{(C_6F_5)_2Pt(\mu\text{-}PPh_2)_2Pt(\mu\text{-}PPh_2)_2Pt(\mu\text{-}1,1\text{-}N_3)\}_2]$ (**45**) (Esquema 22).

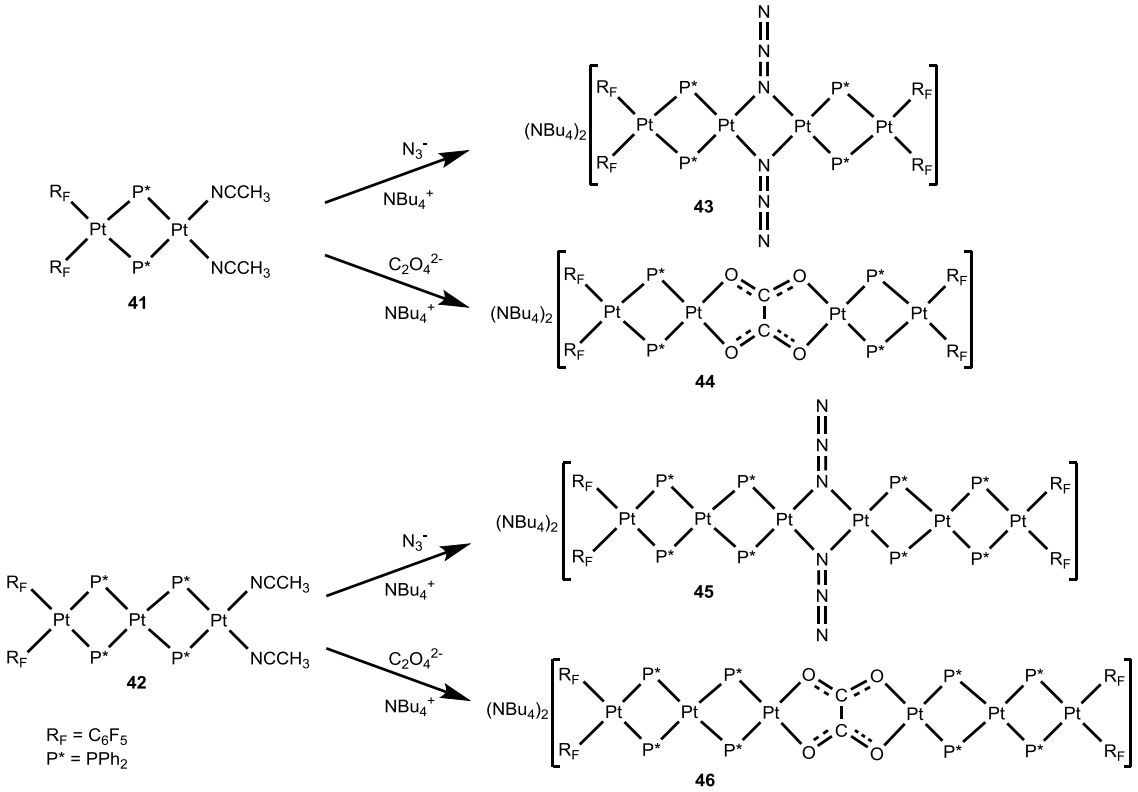

Esquema 22

El anión N_3^- puede coordinarse a los centros metálicos como ligando terminal o como puente,[122-125] y se conocen complejos de Pt en los que este ligando se coordina en forma terminal monodentada;[126-129] sin embargo, en el caso de los derivados **41** y **42**, si se forman los aniones $[(C_6F_5)_2Pt(\mu\text{-}PPh_2)_2Pt(N_3)_2]^{2-}$ y $[(C_6F_5)_2Pt(\mu\text{-}PPh_2)_2Pt(\mu\text{-}PPh_2)_2Pt(N_3)_2]^{2-}$, estos no cristalizan, sino que evolucionan a los derivados **43** y **45**, respectivamente, con un modo de coordinación $\mu\text{-}1,1\text{-}N_3$ del ligando central. Este modo de coordinación no es común en derivados de platino; de hecho, aunque se conocen un gran número de complejos de níquel con ligandos azido puentes[122,130,131] y han sido publicados algunos complejos de paladio que muestran el fragmento "$Pd(\mu\text{-}1,1\text{-}N_3)_xPd$",[132-134] hasta el momento de la publicación de los resultados resumidos en este apartado –en cuanto a lo que conocemos–, ningún complejo con el fragmento "$Pt(\mu\text{-}1,1\text{-}N_3)_2Pt$" ha sido caracterizado estructuralmente mediante estudios de difracción de rayos-X. El único complejo de platino con ligandos azido puentes caracterizado cristalográficamente muestra un modo de coordinación $\mu\text{-}1,1,1\text{-}N_3$ a los centros de Pt.[135]

Las estructuras moleculares de los derivados **43** y **45** se han establecido mediante estudios de difracción de rayos-X, y en las Figuras 9 y 10 se muestran dos vistas de las estructuras de los aniones de los respectivos compuestos. Las estructuras cristalinas confirman la naturaleza tetra y hexanuclear de los aniones de **43** y **45**, respectivamente. El anión del derivado **45** es simétrico debido a un centro de inversión localizado en el centro del mismo. Ambos aniones pueden ser considerados como una secuencia de unidades de Pt en entornos planos cuadrados que comparten un lado con las unidades adyacentes. El sistema de ligandos puentes entre los átomos de Pt centrales está conformado por dos grupos azido en modo de

coordinación μ-1,1-N_3, y los demás átomos de Pt contiguos están unidos por grupos μ-PPh_2. Finalmente, la esfera de coordinación de los dos centros de Pt más externos se completa con dos grupos C_6F_5 en posición mutuamente *cis* (Figuras 9 y 10).

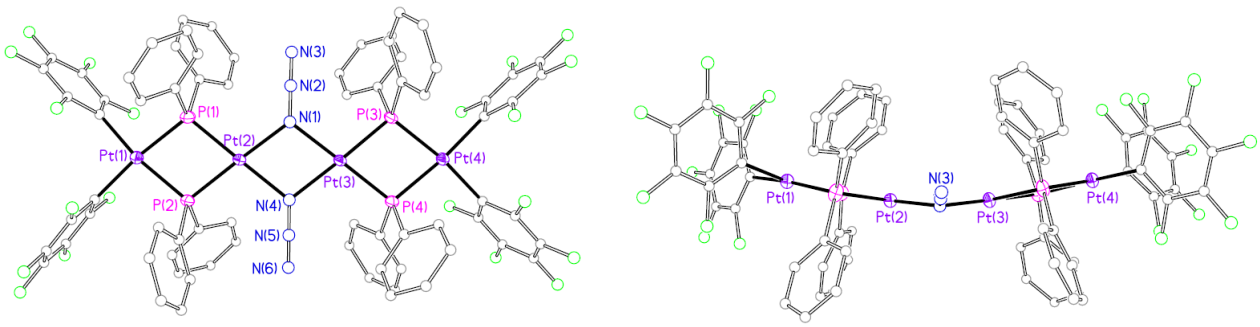

Figura 9. Dos vistas de la estructura molecular del anión del derivado $[NBu_4]_2[\{(C_6F_5)_2Pt(\mu\text{-}PPh_2)_2Pt(\mu\text{-}1,1\text{-}N_3)\}_2]$ (**43**).

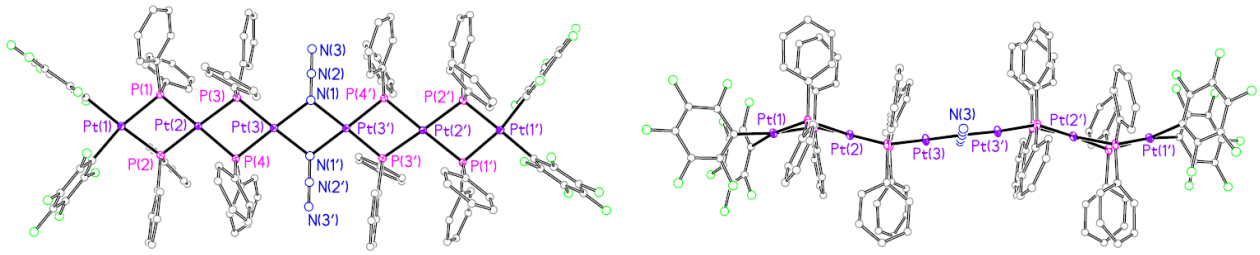

Figura 10. Dos vistas de la estructura molecular del anión del derivado $[NBu_4]_2[\{(C_6F_5)_2Pt(\mu\text{-}PPh_2)_2Pt(\mu\text{-}PPh_2)_2Pt(\mu\text{-}1,1\text{-}N_3)\}_2]$ (**45**).

Las distancias encontradas entre los centros de Pt adyacentes en ambas estructuras (rango entre 3.374(1) y 3.578(1) Å) descartan cualquier interacción intermetálica, como cabe esperar para derivados saturados de Pt(II) en entornos planos cuadrados. Además, en ambas estructuras, los dos grupos μ-N_3 se coordinan simétricamente a los centros de Pt y la disposición de los tres átomos de N en los ligandos es lineal, con un entorno casi plano de los átomos de N que actúan como puentes.

Finalmente, a pesar de todas las similitudes encontradas, la disposición relativa de las unidades de platino en entornos planos cuadrados es diferente en los aniones de los derivados **43** y **45**. Así, en la estructura del derivado **43**, las dos mitades son esencialmente planas, el anión se encuentra doblado a lo largo del eje imaginario N(1)–N(4) y ambos ligandos azido se encuentran ligeramente inclinados respecto a los planos Pt(2)–N(1)–Pt(3) o Pt(2)–N(4)–Pt(3) (Figura 9, derecha). Sin embargo, en la estructura del derivado **45**, el esqueleto central del anión formado por los átomos Pt(3)–N(1)–N(1')–Pt(3') es plano y los ligandos μ-N_3 son

coplanares con este, mientras que la disposición general de las unidades de platino adopta una configuración en zigzag (Figura 10, derecha).

En forma similar, la adición de un exceso de $K_2C_2O_4$ a disoluciones de los derivados **41** y **42** en acetona, tras el tratamiento de las mezclas de reacción, resulta en la cristalización de los derivados tetra y hexanucleares $[NBu_4]_2[\{(C_6F_5)_2Pt(\mu\text{-}PPh_2)_2Pt\}_2(\mu\text{-}C_2O_4\text{-}\kappa^2O,O':\kappa^2O'',O''')]$ (**44**) y $[NBu_4]_2[\{(C_6F_5)_2Pt(\mu\text{-}PPh_2)_2Pt(\mu\text{-}PPh_2)_2Pt\}_2(\mu\text{-}C_2O_4\text{-}\kappa^2O,O':\kappa^2O'',O''')]$ (**46**), respectivamente (Esquema 22). La coordinación del grupo oxalato a centros de Ni, Pd y Pt está bien establecida, actuando tanto como grupo terminal o como ligando bidentado. Por otra parte, la coordinación de este grupo como ligando quelato y puente ha sido encontrada en muchos compuestos de níquel, pero solo algunos complejos con el fragmento "$Pd(\mu\text{-}C_2O_4\text{-}\kappa^2O,O':\kappa^2O'',O''')Pd$" han sido publicados[136-138] y hasta el momento de la publicación de los resultados resumidos en este apartado –en cuanto a lo que conocemos–, ningún complejo con el fragmento "$Pt(\mu\text{-}C_2O_4\text{-}\kappa^2O,O':\kappa^2O'',O''')Pt$" ha sido caracterizado estructuralmente mediante estudios de difracción de rayos-X.

Debido a que no ha sido posible obtener cristales del producto **46** adecuados para estudios de difracción de rayos-X, se ha preparado el derivado $[N(PPh_3)_2]_2[\{(C_6F_5)_2Pt(\mu\text{-}PPh_2)_2Pt(\mu\text{-}PPh_2)_2Pt\}_2(\mu\text{-}C_2O_4)]$ (**46'**), utilizando el catión bis(trifenilfosfano)iminio ($N(PPh_3)_2^+$) en lugar de NBu_4^+. Las estructuras de los derivados **44** y **46'** se han establecido mediante estudios de difracción de rayos-X, y en las Figuras 11 y 12 se muestran dos vistas de las estructuras de los aniones de los respectivos compuestos.

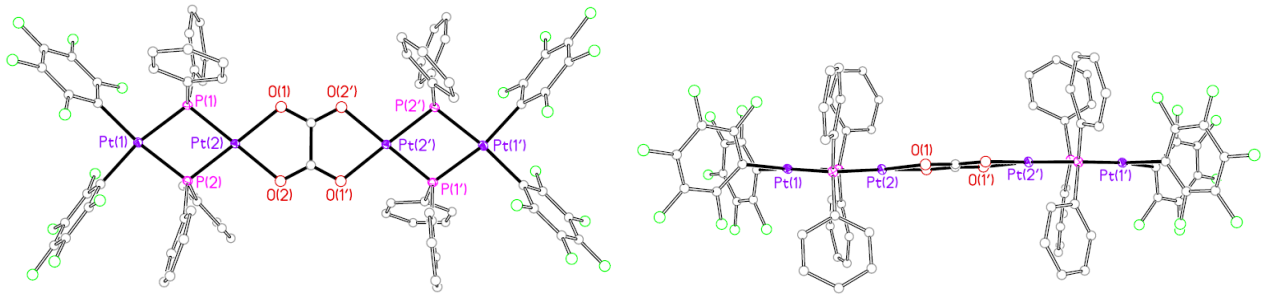

Figura 11. Dos vistas de la estructura molecular del anión del derivado $[NBu_4]_2[\{(C_6F_5)_2Pt(\mu\text{-}PPh_2)_2Pt\}_2(\mu\text{-}C_2O_4)]$ (**44**).

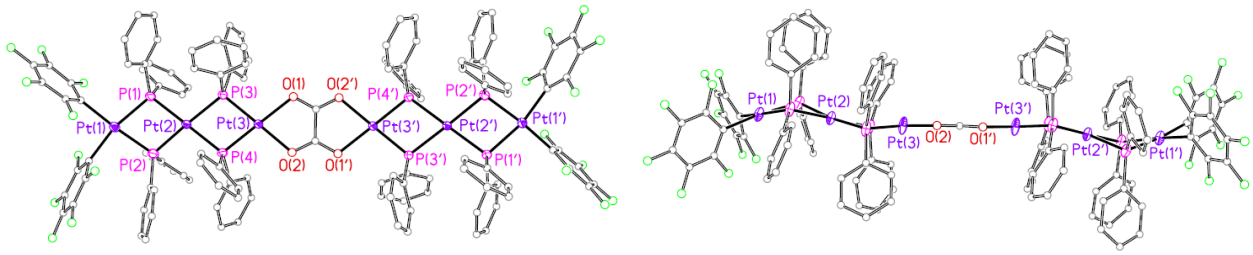

Figura 12. Dos vistas de la estructura molecular del anión del derivado $[N(PPh_3)_2]_2[\{(C_6F_5)_2Pt(\mu\text{-}PPh_2)_2Pt(\mu\text{-}PPh_2)_2Pt\}_2(\mu\text{-}C_2O_4)]$ (**46'**).

Los aniones de los derivados **44** y **46'** son simétricos; en ambos, las estructuras tienen un centro de inversión y las dos mitades de los complejos son equivalentes. Los complejos, al igual que en los derivados **43** y **45**, están formados por una secuencia de unidades de Pt en entornos planos cuadrados que comparten un lado con las unidades adyacentes. En el centro de los aniones de los derivados **44** y **46'**, el grupo oxalato, con modo de coordinación $\mu\text{-}C_2O_4\text{-}\kappa^2O,O':\kappa^2O'',O'''$, une los dos átomos de Pt centrales, mientras que los demás centros de Pt adyacentes están unidos por grupos $\mu\text{-}PPh_2$. Los átomos de Pt externos completan su esfera de coordinación con dos grupos C_6F_5 con mutua posición *cis* (Figuras 11 y 12).

De la misma forma que en los aniones de los compuestos **43** y **45**, las distancias encontradas entre los centros de Pt contiguos de los derivados **44** y **46'** (en un rango entre 3.567(1) y 3.569(1) Å), excluyen cualquier posibilidad de interacciones intermetálicas. Los ligandos $\mu\text{-}C_2O_4$ son planos y coplanares con el plano de coordinación de los centros metálicos unidos a ellos (Figuras 11 y 12). Finalmente, las distancias Pt–O observadas son similares en ambos complejos (rango entre 2.137(3) y 2.1594(15) Å), al igual que las cuatro distancias C–O (rango entre 1.247(6) y 1.259(3) Å).

Al igual que entre los derivados **43** y **45**, también existen diferencias entre las estructuras de los aniones de los derivados **44** y **46'**. Así, mientras que el esqueleto formado por los centros de platino, los átomos unidos a estos y el ligando central del anión de **44** es esencialmente plano (Figura 11, derecha), la disposición general de las unidades de platino del derivado **46'** adopta una configuración en zigzag (Figura 12, derecha). Estas diferencias encontradas al pasar de los derivados tetranucleares a sus homólogos hexanucleares puede deberse al impedimento estérico causado por los grupos difenilfosfanuro.

Finalmente, la adición de un exceso de KCN a una disolución del complejo **42** en acetona, tras el tratamiento de la mezcla de reacción, da lugar al derivado trinuclear $[NBu_4]_2[(C_6F_5)_2Pt(\mu\text{-}PPh_2)_2Pt(\mu\text{-}PPh_2)_2Pt(CN)_2]$ (**47**), con los dos grupos CN actuando como ligandos terminales (Esquema 23).

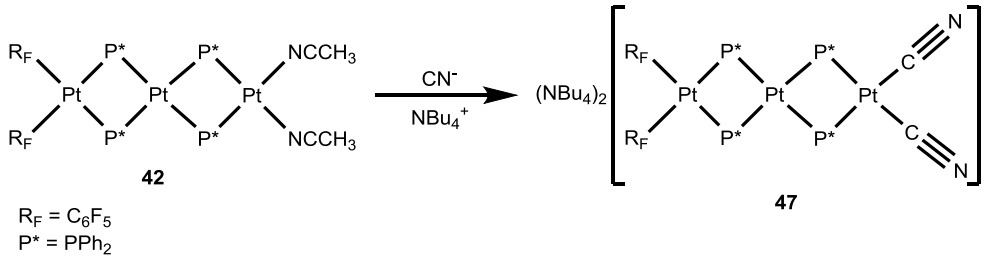

42 **47**

$R_F = C_6F_5$
$P^* = PPh_2$

Esquema 23

No ha sido posible obtener cristales del derivado **47** adecuados para realizar estudios de difracción de rayos-X; sin embargo, la caracterización por análisis elemental y espectroscopia de IR y RMN, permite asignar a este compuesto la estructura que se muestra en el Esquema 23. El espectro de IR de este derivado muestra una absorción a 2117 cm^{-1}, asignable a la frecuencia de tensión del grupo CN actuando como ligando terminal.[139] Además, aunque las características de los espectros de RMN de ^{19}F y ^{31}P del derivado **47** son análogas a las de los derivados **45** y **46**, el espectro de RMN de ^{1}H en acetona deuterada muestra una diferencia: mientras que para los derivados **45** y **46** la relación de intensidades entre los grupos μ-PPh_2 y NBu_4^+ es 40:36, consistente con complejos hexanucleares dianiónicos, para el derivado **47**, esta relación es 40:72, consistente con un complejo trinuclear dianiónico.

E6. Conclusiones

- El desarrollo de la química de complejos con ligandos fosfanuros está relacionado con las características particulares de los mismos, siendo las más conocidas la gran flexibilidad de los sistemas "$M(\mu\text{-}PR_2)_xM$" y la estabilidad de los enlaces M–P. Hoy en día hay que añadir que estos ligandos son capaces de estabilizar complejos de paladio y platino en diferentes estados de oxidación formal: I, II, III y IV.

- Los métodos de síntesis de nuevos complejos de tipo $[(C_6F_5)_2M^{II}(\mu\text{-}PPh_2)_2M'^{II}(L)(L')]^{n-}$ (M, M' = Pd, Pt) están ahora bien establecidos. Esto permite el diseño y la preparación de nuevos derivados con características y propiedades específicas que puedan ser empleados como sustratos adecuados sobre los que ensayar procesos determinados.

- La adición de I_2 sobre los derivados aniónicos **1**–**4** de fórmula $[NBu_4][(C_6F_5)_2M^{II}(\mu\text{-}PPh_2)_2M'^{II}(C\text{^}N)]$ (M, M' = Pd, Pt; C^N = bzq) transcurre con adición oxidante de iodo sobre uno de los centros metálicos, y en general, con acoplamiento reductor entre un grupo difenilfosfanuro y el ligando bzq, con formación del nuevo ligando Ph_2P–C^N coordinado en forma bidentada. Solo en el caso del compuesto $[NBu_4][(C_6F_5)_2Pd^{II}(\mu\text{-}PPh_2)_2Pt^{II}(C\text{^}N)]$ (**3**) se observa también la formación de Ph_2P–C_6F_5.

- La adición de I_2 sobre los derivados aniónicos **12**–**16** de fórmula $[NBu_4][(C_6F_5)_2M^{II}(\mu\text{-}PPh_2)_2M'^{II}(O\text{^}N)]$ (M, M' = Pd, Pt) transcurre con adición oxidante de iodo sobre el centro M'(II) y acoplamiento reductor entre un grupo difenilfosfanuro y el ligando O^N, con formación del nuevo ligando coordinado Ph_2P–O^N. Durante estos procesos se han identificado complejos con difeniliodofosfano (Ph_2P–I), indicando que el acoplamiento entre un grupo difenilfosfanuro y el ligando ioduro también es operativo.

- La oxidación de los difenilfosfanuro-derivados de tipo $[(C_6F_5)_2Pt^{II}(\mu\text{-}PPh_2)_2Pt^{II}(L\text{^}L')]^-$ permite identificar y –en el caso del derivado **1**– aislar los intermedios de reacción, que resultan ser complejos en estado de oxidación mixto de tipo $[(C_6F_5)_2Pt^{II}(\mu\text{-}PPh_2)_2Pt^{IV}(L\text{^}L')I_2]^-$. En general, estos procesos de adición oxidante y acoplamiento reductor pueden describirse como nuevas secuencias de tipo Pt(II),Pt(II)/Pt(II),Pt(IV)/Pt(II),Pt(II).

- Los ligandos difenilfosfanuro en derivados de paladio y platino (II) no actúan simplemente como grupos que mantienen fragmentos de tipo "$M(\mu\text{-}PR_2)_xM$", sino que, en condiciones de reacción adecuadas, pueden ser transformados en otros ligandos, a través de procesos que, hoy en día, pueden ser convenientemente diseñados. Con anterioridad se había observado la formación de los ligandos Ph_2P–C_6F_5 y Ph_2P–PPh_2 a través de procesos de adición oxidante y acoplamiento reductor. La síntesis de los

nuevos ligandos Ph_2P–bzq (derivados **6**–**8** y **10**), Ph_2P–hq (**18**–**20**), Ph_2P–pic (**21** y **22**) y Ph_2P–acac (**23**), apunta a que estas nuevas secuencias de tipo Pt(II),Pt(II)/Pt(II),Pt(IV)/Pt(II),Pt(II) constituyen una excelente vía de formación de ligandos Ph_2P–X específicos.

- Los nuevos derivados binucleares asimétricos preparados de tipo $[(C_6F_5)_2Pt^{II}(\mu\text{-}PPh_2)_2M^{II}(L\text{^}L')]^-$ (M = Pd, Pt; L^L' = bzq, hq, pic) no se oxidan en presencia de sales de plata (I). En las condiciones ensayadas, disoluciones en diclorometano y a temperatura ambiente, se obtienen en todos los casos, aductos entre los fragmentos "$(C_6F_5)_2Pt^{II}(\mu\text{-}PPh_2)_2M^{II}(L\text{^}L')$" y "$AgPPh_3$".

- La determinación estructural de los aductos mediante estudios de difracción de rayos-X establece que, en estado sólido, la unión de ambos fragmentos se lleva a cabo a través de dos enlaces Ag–Pt/M (M = Pd, Pt) (complejos **25**–**29**), o a través del ligando bidentado, con formación de enlace Ag–O (derivados **30** y **31**). La información estructural de los complejos en disolución, obtenida mediante espectroscopia de RMN, está en acuerdo con las estructuras en estado sólido, excepto en el caso del derivado **30**. Los datos de RMN de **30** son compatibles con que, en disolución, el centro de Ag está enlazado a los dos centros dadores de Pt, como en los complejos **25**–**29**. Estos resultados apuntan a una energía de estabilización muy similar de ambos tipos de isómeros.

- La adición de ioduro sobre el fosfanuro-derivado simétrico insaturado $[(C_6F_5)_2Pt^{III}(\mu\text{-}PPh_2)_2Pt^{III}(C_6F_5)_2]$ mostró hace unos años que transcurría con acoplamiento entre un grupo $\mu\text{-}PPh_2$ y un ligando C_6F_5. La adición de distintos nucleófilos (hidróxido, azida y cianato) ha demostrado ahora que no solo puede ocurrir este tipo de acoplamiento, sino que también puede observarse el acoplamiento entre un grupo fosfanuro y el nucleófilo añadido. Los resultados obtenidos indican que en este tipo de derivados, el acoplamiento con el grupo hidróxido (formación de enlace P–O) está favorecido sobre el acoplamiento con el grupo C_6F_5 (formación de enlace P–C); sin embargo, la formación de enlace P–C es competitiva con la formación de enlace P–N.

- Finalmente, en el intento de sintetizar derivados aniónicos de platino con alta carga negativa y con los ligandos azido y oxalato coordinados en forma terminal, se obtuvieron los complejos **43**–**46**, de mayor nuclearidad y que contienen los fragmentos "$Pt(\mu\text{-}1,1\text{-}N_3)_2Pt$" y "$Pt(\mu\text{-}C_2O_4\text{-}\kappa^2O,O':\kappa^2O'',O''')Pt$". Este modo de coordinación no había sido observado con anterioridad para complejos de este metal. Este hecho pone de manifiesto una vez más que, a pesar de los avances en el diseño de métodos de síntesis específicos, la química es una ciencia experimental.

E7. Referencias

(1) Mastrorilli, P. *European Journal of Inorganic Chemistry* **2008**, *2008*, 4835.

(2) Handler, A.; Peringer, P.; Muller, E. P. *Journal of the Chemical Society, Dalton Transactions* **1990**, *0*, 3725.

(3) Wicht, D. K.; Kourkine, I. V.; Lew, B. M.; Nthenge, J. M.; Glueck, D. S. *Journal of the American Chemical Society* **1997**, *119*, 5039.

(4) Wicht, D. K.; Paisner, S. N.; Lew, B. M.; Glueck, D. S.; Yap, G. P. A.; Liable-Sands, L. M.; Rheingold, A. L.; Haar, C. M.; Nolan, S. P. *Organometallics* **1998**, *17*, 652.

(5) Wicht, D. K.; Kovacik, I.; Glueck, D. S.; Liable-Sands, L. M.; Incarvito, C. D.; Rheingold, A. L. *Organometallics* **1999**, *18*, 5141.

(6) Zhuravel, M. A.; Glueck, D. S.; Zakharov, L. N.; Rheingold, A. L. *Organometallics* **2002**, *21*, 3208.

(7) Turculet, L.; McDonald, R. *Organometallics* **2007**, *26*, 6821.

(8) Gloaguen, Y.; Jacobs, W.; de Bruin, B.; Lutz, M.; van der Vlugt, J. I. *Inorganic Chemistry* **2013**, *52*, 1682.

(9) Bender, R.; Braunstein, P.; Dedieu, A.; Dusausoy, Y. *Angewandte Chemie International Edition in English* **1989**, *28*, 923.

(10) Corrigan, J. F.; Doherty, S.; Taylor, N. J.; Carty, A. J. *Journal of the American Chemical Society* **1992**, *114*, 7557.

(11) Alonso, E.; Fornies, J.; Fortuno, C.; Martin, A.; Orpen, A. G. *Chemical Communications* **1996**, *0*, 231.

(12) Falvello, L. R.; Forniés, J.; Fortuño, C.; Martín, A.; Martínez-Sariñena, A. P. *Organometallics* **1997**, *16*, 5849.

(13) Englich, U.; Hassler, K.; Ruhlandt-Senge, K.; Uhlig, F. *Inorganic Chemistry* **1998**, *37*, 3532.

(14) Alonso, E.; Forniés, J.; Fortuño, C.; Martín, A.; Orpen, A. G. *Organometallics* **2000**, *19*, 2690.

(15) Alonso, E.; Forniés, J.; Fortuño, C.; Martín, A.; Orpen, A. G. *Organometallics* **2003**, *22*, 2723.

(16) Chaouche, N.; Forniés, J.; Fortuño, C.; Kribii, A.; Martín, A. *Journal of Organometallic Chemistry* **2007**, *692*, 1168.

(17) Alonso, E.; Forniés, J.; Fortuño, C.; Lledós, A.; Martín, A.; Nova, A. *Inorganic Chemistry* **2009**, *48*, 7679.

(18) Forniés, J.; Fortuño, C.; Ibáñez, S.; Martín, A.; Mastrorilli, P.; Gallo, V. *Inorganic Chemistry* **2011**, *50*, 10798.

(19) Forniés, J.; Fortuño, C.; Ibáñez, S.; Martín, A.; Mastrorilli, P.; Gallo, V.; Tsipis, A. *Inorganic Chemistry* **2013**, *52*, 1942.

(20) Harley, A. D.; Whittle, R. R.; Geoffroy, G. L. *Organometallics* **1983**, *2*, 60.

(21) Brauer, D. J.; Hessler, G.; Knueppel, P. C.; Stelzer, O. *Inorganic Chemistry* **1990**, *29*, 2370.

(22) Harley, A. D.; Guskey, G. J.; Geoffroy, G. L. *Organometallics* **1983**, *2*, 53.

(23) Burkhardt, E. W.; Mercer, W. C.; Geoffrey, G. L. *Inorganic Chemistry* **1984**, *23*, 1779.

(24) Yu, Y. F.; Gallucci, J.; Wojcicki, A. *Journal of the American Chemical Society* **1983**, *105*, 4826.

(25) Geoffroy, G. L.; Rosenberg, S.; Shulman, P. M.; Whittle, R. R. *Journal of the American Chemical Society* **1984**, *106*, 1519.

(26) Carty, A. J.; Mott, G. N.; Taylor, N. J.; Yule, J. E. *Journal of the American Chemical Society* **1978**, *100*, 3051.

(27) Dixon, K. R.; Rattray, A. D. *Inorganic Chemistry* **1978**, *17*, 1099.

(28) Meij, R.; Stufkens, D. J.; Vrieze, K.; Brouwers, A. M. F.; Overbeek, A. R. *Journal of Organometallic Chemistry* **1978**, *155*, 123.

(29) Mott, G. N.; Carty, A. J. *Inorganic Chemistry* **1979**, *18*, 2926.

(30) Cartwright, S. J.; Dixon, K. R.; Rattray, A. D. *Inorganic Chemistry* **1980**, *19*, 1120.

(31) Petersen, J. L.; Stewart, R. P. *Inorganic Chemistry* **1980**, *19*, 186.

(32) Carty, A. J.; MacLaughlin, S. A.; Taylor, N. J. *Journal of Organometallic Chemistry* **1981**, *204*, C27.

(33) Garrou, P. E. *Chemical Reviews* **1981**, *81*, 229.

(34) Carty Arthur, J. In *Catalytic Aspects of Metal Phosphine Complexes*; AMERICAN CHEMICAL SOCIETY: 1982; Vol. 196, p 163.

(35) Mercer, W. C.; Geoffroy, G. L. *Organometallics* **1985**, *4*, 1418.

(36) Mercer, W. C.; Whittle, R. R.; Burkhardt, E. W.; Geoffroy, G. L. *Organometallics* **1985**, *4*, 68.

(37) Jones, R. A.; Wright, T. C.; Atwood, J. L.; Hunter, W. E. *Organometallics* **1983**, *2*, 470.

(38) Rosen, R. P.; Hoke, J. B.; Whittle, R. R.; Geoffroy, G. L.; Hutchinson, J. P.; Zubieta, J. A. *Organometallics* **1984**, *3*, 846.

(39) Targos, T. S.; Rosen, R. P.; Whittle, R. R.; Geoffroy, G. L. *Inorganic Chemistry* **1985**, *24*, 1375.

(40) Forniés, J.; Fortuño, C.; Navarro, R.; Martínez, F.; Welch, A. J. *Journal of Organometallic Chemistry* **1990**, *394*, 643.

(41) Miyaura, N.; Suzuki, A. *Chemical Reviews* **1995**, *95*, 2457.

(42) Zeni, G.; Larock, R. C. *Chemical Reviews* **2006**, *106*, 4644.

(43) Sehnal, P.; Taylor, R. J. K.; Fairlamb, I. J. S. *Chemical Reviews* **2010**, *110*, 824.

(44) Ariafard, A.; Hyland, C. J. T.; Canty, A. J.; Sharma, M.; Brookes, N. J.; Yates, B. F. *Inorganic Chemistry* **2010**, *49*, 11249.

(45) Canty, A. J.; Gardiner, M. G.; Jones, R. C.; Rodemann, T.; Sharma, M. *Journal of the American Chemical Society* **2009**, *131*, 7236.

(46) Ibáñez, S.; Estevan, F.; Hirva, P.; Sanaú, M.; Úbeda, M. A. *Organometallics* **2012**, *31*, 8098.

(47) Powers, D. C.; Lee, E.; Ariafard, A.; Sanford, M. S.; Yates, B. F.; Canty, A. J.; Ritter, T. *Journal of the American Chemical Society* **2012**, *134*, 12002.

(48) Whitfield, S. R.; Sanford, M. S. *Organometallics* **2008**, *27*, 1683.

(49) Canty, A. J. *Dalton Transactions* **2009**, *0*, 10409.

(50) Mirica, L. M.; Khusnutdinova, J. R. *Coordination Chemistry Reviews* **2013**, *257*, 299.

(51) Connelly, N. G.; Geiger, W. E. *Chemical Reviews* **1996**, *96*, 877.

(52) Song, L.; Trogler, W. C. *Angewandte Chemie International Edition in English* **1992**, *31*, 770.

(53) Albano, V. G.; Azzaroni, F.; Iapalucci, M. C.; Longoni, G.; Monari, M.; Mulley, S.; Proserpio, D. M.; Sironi, A. *Inorganic Chemistry* **1994**, *33*, 5320.

(54) Ebihara, M.; Iiba, M.; Matsuoka, H.; Okuda, C.; Kawamura, T. *Journal of Organometallic Chemistry* **2004**, *689*, 146.

(55) Alonso, E.; Casas, J. M.; Cotton, F. A.; Feng, X.; Forniés, J.; Fortuño, C.; Tomas, M. *Inorganic Chemistry* **1999**, *38*, 5034.

(56) Alonso, E.; Forniés, J.; Fortuño, C.; Martín, A.; Orpen, A. G. *Organometallics* **2003**, *22*, 5011.

(57) Uson, R.; Fornies, J.; Tomas, M.; Casas, J. M.; Cotton, F. A.; Falvello, L. R.; Feng, X. *Journal of the American Chemical Society* **1993**, *115*, 4145.

(58) Cotton, F. A.; Gu, J.; Murillo, C. A.; Timmons, D. J. *Journal of the American Chemical Society* **1998**, *120*, 13280.

(59) Matsumoto, K.; Ochiai, M. *Coordination Chemistry Reviews* **2002**, *231*, 229.

(60) Iwatsuki, S.; Mizushima, C.; Morimoto, N.; Muranaka, S.; Ishihara, K.; Matsumoto, K. *Inorganic Chemistry* **2005**, *44*, 8097.

(61) Cotton, F. A.; Koshevoy, I. O.; Lahuerta, P.; Murillo, C. A.; Sanaú, M.; Ubeda, M. A.; Zhao, Q. *Journal of the American Chemical Society* **2006**, *128*, 13674.

(62) Powers, D. C.; Geibel, M. A. L.; Klein, J. E. M. N.; Ritter, T. *Journal of the American Chemical Society* **2009**, *131*, 17050.

(63) Ariafard, A.; Hyland, C. J. T.; Canty, A. J.; Sharma, M.; Yates, B. F. *Inorganic Chemistry* **2011**, *50*, 6449.

(64) Penno, D.; Estevan, F.; Fernández, E.; Hirva, P.; Lahuerta, P.; Sanaú, M.; Úbeda, M. A. *Organometallics* **2011**, *30*, 2083.

(65) Romero, M. J.; Rodríguez, A.; Fernández, A.; López-Torres, M.; Vázquez-García, D.; Vila, J. M.; Fernández, J. J. *Polyhedron* **2011**, *30*, 2444.

(66) Sicilia, V.; Forniés, J.; Casas, J. M.; Martín, A.; López, J. A.; Larraz, C.; Borja, P.; Ovejero, C.; Tordera, D.; Bolink, H. *Inorganic Chemistry* **2012**, *51*, 3427.

(67) Wilson, J. J.; Lippard, S. J. *Inorganic Chemistry* **2012**, *51*, 9852.

(68) Sicilia, V.; Borja, P.; Casas, J. M.; Fuertes, S.; Martín, A. *Journal of Organometallic Chemistry* **2013**, *731*, 10.

(69) Alonso, E.; Casas, J. M.; Forniés, J.; Fortuño, C.; Martín, A.; Orpen, A. G.; Tsipis, C. A.; Tsipis, A. C. *Organometallics* **2001**, *20*, 5571.

(70) Forniés, J.; Fortuño, C.; Ibáñez, S.; Martín, A. *Inorganic Chemistry* **2008**, *47*, 5978.

(71) Forniés, J.; Fortuño, C.; Ibáñez, S.; Martín, A.; Tsipis, A. C.; Tsipis, C. A. *Angewandte Chemie* **2005**, *117*, 2459.

(72) Chaouche, N.; Forniés, J.; Fortuño, C.; Kribii, A.; Martín, A.; Karipidis, P.; Tsipis, A. C.; Tsipis, C. A. *Organometallics* **2004**, *23*, 1797.

(73) Ara, I.; Chaouche, N.; Forniés, J.; Fortuño, C.; Kribii, A.; Tsipis, A. C. *Organometallics* **2006**, *25*, 1084.

(74) Archambault, C.; Bender, R.; Braunstein, P.; De Cian, A.; Fischer, J. *Chemical Communications* **1996**, *0*, 2729.

(75) Cabeza, J. A.; del Río, I.; Riera, V.; García-Granda, S.; Sanni, S. B. *Organometallics* **1997**, *16*, 1743.

(76) Albinati, A.; Filippi, V.; Leoni, P.; Marchetti, L.; Pasquali, M.; Passarelli, V. *Chemical Communications* **2005**, *0*, 2155.

(77) Fahey, D. R.; Mahan, J. E. *Journal of the American Chemical Society* **1976**, *98*, 4499.

(78) Dubois, R. A.; Garrou, P. E.; Lavin, K. D.; Allcock, H. R. *Organometallics* **1986**, *5*, 460.

(79) Shulman, P. M.; Burkhardt, E. D.; Lundquist, E. G.; Pilato, R. S.; Geoffroy, G. L.; Rheingold, A. L. *Organometallics* **1987**, *6*, 101.

(80) Ang, H. G.; Kwik, W. L.; Leong, W. K.; Johnson, B. F. G.; Lewis, J.; Raithby, P. R. *Journal of Organometallic Chemistry* **1990**, *396*, C43.

(81) Bender, R.; Braunstein, P.; Dedieu, A.; Ellis, P. D.; Huggins, B.; Harvey, P. D.; Sappa, E.; Tiripicchio, A. *Inorganic Chemistry* **1996**, *35*, 1223.

(82) García, G.; García, M. E.; Melón, S.; Riera, V.; Ruiz, M. A.; Villafañe, F. *Organometallics* **1997**, *16*, 624.

(83) Shiu, K.-B.; Jean, S.-W.; Wang, H.-J.; Wang, S.-L.; Liao, F.-L.; Wang, J.-C.; Liou, L.-S. *Organometallics* **1997**, *16*, 114.

(84) Zhuravel, M. A.; Moncarz, J. R.; Glueck, D. S.; Lam, K.-C.; Rheingold, A. L. *Organometallics* **2000**, *19*, 3447.

(85) Heyn, R. H.; Görbitz, C. H. *Organometallics* **2002**, *21*, 2781.

(86) Mizuta, T.; Onishi, M.; Nakazono, T.; Nakazawa, H.; Miyoshi, K. *Organometallics* **2002**, *21*, 717.

(87) Forniés, J.; Fortuño, C.; Ibáñez, S.; Martín, A. *Inorganic Chemistry* **2006**, *45*, 4850.

(88) Ara, I.; Chaouche, N.; Forniés, J.; Fortuño, C.; Kribii, A.; Martín, A. *European Journal of Inorganic Chemistry* **2005**, *2005*, 3894.

(89) Ara, I.; Forniés, J.; Fortuño, C.; Ibáñez, S.; Martín, A.; Mastrorilli, P.; Gallo, V. *Inorganic Chemistry* **2008**, *47*, 9069.

(90) Bennett, M. A.; Bhargava, S. K.; Ke, M.; Willis, A. C. *Journal of the Chemical Society, Dalton Transactions* **2000**, *0*, 3537.

(91) Yahav, A.; Goldberg, I.; Vigalok, A. *Organometallics* **2005**, *24*, 5654.

(92) Pregosin, P. S. *Coordination Chemistry Reviews* **1982**, *44*, 247.

(93) Alonso, E.; Forniés, J.; Fortuño, C.; Martín, A.; Orpen, A. G. *Organometallics* **2001**, *20*, 850.

(94) Forniés, J.; Fortuño, C.; Ibáñez, S.; Martín, A.; Romero, P.; Mastrorilli, P.; Gallo, V. *Inorganic Chemistry* **2010**, *50*, 285.

(95) Moret, M.-E.; Chen, P. *Journal of the American Chemical Society* **2009**, *131*, 5675.

(96) Fornies, J.; Ibanez, S.; Lalinde, E.; Martin, A.; Moreno, M. T.; Tsipis, A. C. *Dalton Transactions* **2012**, *41*, 3439.

(97) Falvello, L. R.; Forniés, J.; Fortuño, C.; Durán, F.; Martín, A. *Organometallics* **2002**, *21*, 2226.

(98) Bauer, J.; Braunschweig, H.; Dewhurst, R. D. *Chemical Reviews* **2012**, *112*, 4329.

(99) Kessler, F.; Szesni, N.; Maaß, C.; Hohberger, C.; Weibert, B.; Fischer, H. *Journal of Organometallic Chemistry* **2007**, *692*, 3005.

(100) Braunstein, P.; Frison, C.; Oberbeckmann-Winter, N.; Morise, X.; Messaoudi, A.; Bénard, M.; Rohmer, M.-M.; Welter, R. *Angewandte Chemie International Edition* **2004**, *43*, 6120.

(101) Liu, Y.; Lee, K. H.; Vittal, J. J.; Hor, T. S. A. *Journal of the Chemical Society, Dalton Transactions* **2002**, 2747.

(102) Yahav-Levi, A.; Goldberg, I.; Vigalok, A.; Vedernikov, A. N. *Journal of the American Chemical Society* **2007**, *130*, 724.

(103) Crespo, M.; Anderson, C. M.; Kfoury, N.; Font-Bardia, M.; Calvet, T. *Organometallics* **2012**, *31*, 4401.

(104) Yahav-Levi, A.; Goldberg, I.; Vigalok, A.; Vedernikov, A. N. *Chemical Communications* **2010**, *46*, 3324.

(105) Bebbington, M. W. P.; Bourissou, D. *Coordination Chemistry Reviews* **2009**, *253*, 1248.

(106) Boeske, J.; Niecke, E.; Ocando-Mavarez, E.; Majoral, J. P.; Bertrand, G. *Inorganic Chemistry* **1986**, *25*, 2695.

(107) Fekl, U.; Goldberg, K. I. *Journal of the American Chemical Society* **2002**, *124*, 6804.

(108) McBee, J. L.; Tilley, T. D. *Organometallics* **2009**, *28*, 3947.

(109) Sangtrirutnugul, P.; Tilley, T. D. *Organometallics* **2008**, *27*, 2223.

(110) West, N. M.; White, P. S.; Templeton, J. L.; Nixon, J. F. *Organometallics* **2009**, *28*, 1425.

(111) Zhao, S.-B.; Cui, Q.; Wang, S. *Organometallics* **2009**, *29*, 998.

(112) Zhao, S.-B.; Wu, G.; Wang, S. *Organometallics* **2008**, *27*, 1030.

(113) Braunstein, P.; Boag, N. M. *Angewandte Chemie International Edition* **2001**, *40*, 2427.

(114) Leca, F.; Sauthier, M.; Deborde, V.; Toupet, L.; Réau, R. *Chemistry – A European Journal* **2003**, *9*, 3785.

(115) Welsch, S.; Nohra, B.; Peresypkina, E. V.; Lescop, C.; Scheer, M.; Réau, R. *Chemistry – A European Journal* **2009**, *15*, 4685.

(116) Fei, Z.; Dyson, P. J. *Coordination Chemistry Reviews* **2005**, *249*, 2056.

(117) Cordero, B.; Gomez, V.; Platero-Prats, A. E.; Reves, M.; Echeverria, J.; Cremades, E.; Barragan, F.; Alvarez, S. *Dalton Transactions* **2008**, 2832.

(118) Alvarez, M. A.; García, M. E.; Ruiz, M. A.; Toyos, A.; Vega, M. F. *Inorganic Chemistry* **2013**, *52*, 3942.

(119) Baranger, A. M.; Bergman, R. G. *Journal of the American Chemical Society* **1994**, *116*, 3822.

(120) Morello, L.; Yu, P.; Carmichael, C. D.; Patrick, B. O.; Fryzuk, M. D. *Journal of the American Chemical Society* **2005**, *127*, 12796.

(121) Nagashima, H.; Sue, T.; Oda, T.; Kanemitsu, A.; Matsumoto, T.; Motoyama, Y.; Sunada, Y. *Organometallics* **2006**, *25*, 1987.

(122) Escuer, A.; Aromí, G. *European Journal of Inorganic Chemistry* **2006**, *2006*, 4721.

(123) Papatriantafyllopoulou, C.; Stamatatos, T. C.; Wernsdorfer, W.; Teat, S. J.; Tasiopoulos, A. J.; Escuer, A.; Perlepes, S. P. *Inorganic Chemistry* **2010**, *49*, 10486.

(124) Sasmal, S.; Sarkar, S.; Aliaga-Alcalde, N. r.; Mohanta, S. *Inorganic Chemistry* **2011**, *50*, 5687.

(125) Stamatatos, T. C.; Papaefstathiou, G. S.; MacGillivray, L. R.; Escuer, A.; Vicente, R.; Ruiz, E.; Perlepes, S. P. *Inorganic Chemistry* **2007**, *46*, 8843.

(126) Mackay, F. S.; Farrer, N. J.; Salassa, L.; Tai, H.-C.; Deeth, R. J.; Moggach, S. A.; Wood, P. A.; Parsons, S.; Sadler, P. J. *Dalton Transactions* **2009**, 2315.

(127) Ronconi, L.; Sadler, P. J. *Chemical Communications* **2008**, 235.

(128) Smolenski, P.; Mukhopadhyay, S.; Guedes da Silva, M. F. C.; Charmier, M. A. J.; Pombeiro, A. J. L. *Dalton Transactions* **2008**, 6546.

(129) Sutter, K.; Autschbach, J. *Journal of the American Chemical Society* **2012**, *134*, 13374.

(130) Roth, A.; Buchholz, A.; Rudolph, M.; Schütze, E.; Kothe, E.; Plass, W. *Chemistry – A European Journal* **2008**, *14*, 1571.

(131) Sun, B.; Chen, X.; Li, Z.; Zhang, L.; Zhao, Q. *New Journal of Chemistry* **2010**, *34*, 190.

(132) de Almeida, E. T.; Mauro, A. E.; Santana, A. M.; Ananias, S. R.; Netto, A. V. G.; Ferreira, J. G.; Santos, R. H. A. *Inorganic Chemistry Communications* **2007**, *10*, 1394.

(133) Fehlhammer, W. P.; Dahl, L. F. *Journal of the American Chemical Society* **1972**, *94*, 3377.

(134) Santana, A. M.; Ferreira, J. G.; Moro, A. C.; Lemos, S. C.; Mauro, A. E.; Netto, A. V. G.; Frem, R. C. G.; Santos, R. H. A. *Inorganic Chemistry Communications* **2011**, *14*, 83.

(135) Atam, M.; Müller, U. *Journal of Organometallic Chemistry* **1974**, *71*, 435.

(136) Arendse, M. J.; Anderson, G. K.; Rath, N. P. *Polyhedron* **2001**, *20*, 2495.

(137) Kawato, T.; Uechi, T.; Koyama, H.; Kanatomi, H.; Kawanami, Y. *Inorganic Chemistry* **1984**, *23*, 764.

(138) Krämer, R.; Polborn, K.; Beck, W. *Journal of Organometallic Chemistry* **1992**, *441*, 333.

(139) Nakamoto, K. In *Handbook of Vibrational Spectroscopy*; John Wiley & Sons, Ltd: 2006.

Apéndice

Factor de impacto de las revistas y área temática (**"Chemistry, Inorganic and Nuclear"** de ISI WoK) correspondientes a las publicaciones que se recogen en la Memoria de Tesis Doctoral:

Título: “Formation of P-C Bond through Reductive Coupling between Bridging Phosphido and Benzoquinolinate Groups. Isolation of Complexes of the Pt(II)/Pt(IV)/Pt(II) Sequence”.
Autores: Andersson Arias, Juan Forniés, Consuelo Fortuño, Antonio Martín, Mario Latronico, Piero Mastrorilli, Stefano Todisco, Vito Gallo.
Revista: *Inorganic Chemistry* 2012, 51, 12682-12696. Factor de Impacto: 4.593; 5/43 de la categoría "Chemistry, Inorganic and Nuclear" de ISI WoK.

Título: “Oxidatively Induced P-O Bond Formation through Reductive Coupling between Phosphido and Acetylacetonate, 8-Hydroxyquinolinate, and Picolinate Groups”
Autores: Andersson Arias, Juan Forniés, Consuelo Fortuño, Antonio Martín, Piero Mastrorilli, Stefano Todisco, Mario Latronico, Vito Gallo.
Revista: *Inorganic Chemistry* 2013, 52, 5493-5506. Factor de Impacto: 4.593; 5/43 de la categoría "Chemistry, Inorganic and Nuclear" de ISI WoK.

Título: “Donor Behaviour of Anionic and Asymmetric Phosphanido Derivatives of Platinum and Palladium”
Autores: Andersson Arias, Juan Forniés, Consuelo Fortuño, Antonio Martín, Piero Mastrorilli, Vito Gallo, Mario Latronico, Stefano Todisco.
Revista: *European Journal of Inorganic Chemistry*, doi: 10.1002/ejic.20130088. Factor de Impacto: 3.120; 11/43 de la categoría "Chemistry, Inorganic and Nuclear" de ISI WoK.

Título: “Addition of Nucleophiles to Phosphanido Derivatives of Pt(III): Formation of P-C, P-N and P-O Bonds”
Autores: Andersson Arias, Juan Forniés, Consuelo Fortuño, Susana Ibáñez, Antonio Martín, Piero Mastrorilli, Vito Gallo, Stefano Todisco.
Revista: *Inorganic Chemistry*, doi: 10.1021/ic401689c. Factor de Impacto: 4.593; 5/43 de la categoría "Chemistry, Inorganic and Nuclear" de ISI WoK.

Título: “From a di- and trinuclear phosphanido fragment to tetra- and hexanuclear platinum(II) complexes”
Autores: Andersson Arias, Juan Forniés, Consuelo Fortuño, Antonio Martín,
Revista: *Inorganica Chimica Acta* 2013, 407, 189-196. Factor de Impacto: 1.687; 22/43 de la categoría "Chemistry, Inorganic and Nuclear" de ISI WoK.

Justificación de la contribución del doctorando al trabajo que ha dado lugar a la Tesis que lleva por título "*Complejos polinucleares de paladio y platino con el grupo difenilfosfanuro: diseño, síntesis, caracterización y reactividad*" y presentada por **Andersson Arias Aguilar**.

Los objetivos de investigación de este trabajo han sido la síntesis de fosfanuro-derivados de Pd (II) y Pt(II) del tipo $[NBu_4]_n[(R_F)_2Pt(\mu\text{-}PPh_2)_2M(L)(L')]$ (M = Pd, Pt; $R_F = C_6F_5$) y el estudio de su reactividad frente a agentes oxidantes para profundizar en el conocimiento de los procesos de transformación del grupo difenilfosfanuro actuando como ligando puente. Para ello, se han diseñado, sintetizado y caracterizado de forma inequívoca los distintos fosfanuro-derivados conteniendo el fragmento "$(R_F)_2Pt(\mu\text{-}PPh_2)_2M$" y se ha estudiado la reactividad de muchos de ellos frente a dos agentes potencialmente oxidantes: yodo y sales de plata (I).

En el estudio realizado, además de la caracterización de las especies obtenidas, se han identificado, y en algunos casos incluso aislado, algunos de los intermedios de reacción. De manera que los objetivos de investigación que se propusieron para este trabajo se han cumplido completamente y los resultados obtenidos han sido plenamente satisfactorios.

La síntesis, caracterización y estudio de la reactividad llevado a cabo le han planteado al doctorando dificultades que ha logrado resolver con éxito en su quehacer diario y ha obtenido así resultados excelentes que han dado lugar a cinco publicaciones en revistas científicas.

Los procesos sintéticos llevados a cabo han sido muy largos y laboriosos, de manera que han consumido una gran parte del trabajo y dedicación del doctorando. Muchas de las reacciones y manipulaciones necesarias para el desarrollo del trabajo presentado se han llevado a cabo bajo argón utilizando técnicas de Schlenk. La caracterización de los derivados obtenidos se ha llevado a cabo mediante una combinación de técnicas analíticas y espectroscópicas entre las que se encuentran: análisis elementales, espectroscopia de IR y de RMN multinuclear. En los casos en los que se han obtenido monocristales adecuados y el interés de la sustancia así lo aconsejaba, se ha determinado la estructura en estado sólido mediante estudios de difracción de rayos-X. Con todo ello, el doctorando ha adquirido el conocimiento necesario para llevar a cabo el trabajo en síntesis avanzada y caracterización estructural de los compuestos obtenidos, así como elaborar una adecuada discusión de resultados y planteamiento de nuevos experimentos. Es decir, a la finalización de este trabajo, el doctorando dispone de una elevada formación científica.

Durante el desarrollo de este trabajo se ha colaborado con el grupo del Prof. Piero Mastrorilli del Politécnico de Bari (Italia), un grupo que centra parte de su investigación en la química de fosfanuros de platino (I) y muy experto en técnicas de RMN multinuclear. Los experimentos de RMN en disolución que han llevado a la propuesta de procesos dinámicos y mecanismos de reacción, así como a la caracterización completa de algunos derivados y los HRMS, se han llevado a cabo por el grupo de Bari. El planteamiento de objetivos, el diseño, síntesis y caracterización estructural en disolución y en sólido de los nuevos derivados, así como el estudio de la reactividad que se recoge en la Memoria, se ha llevado a cabo en los

laboratorios de Zaragoza. Teniendo en cuenta que el doctorando es el único no Doctor de nuestro grupo de Zaragoza, la contribución del doctorando a esta investigación y a las publicaciones presentadas en esta Memoria ha sido decisiva.

En resumen, y como se ha mencionado en los párrafos anteriores, hay que señalar que:

1) Los trabajos presentados en esta Memoria **se ajustan perfectamente** al Proyecto de Tesis presentado con anterioridad,
2) los resultados obtenidos han dado lugar a **cinco publicaciones** en revistas científicas,
3) el doctorando ha **adquirido una elevada formación científica**, y
4) la **contribución** del doctorando a los resultados ha sido **decisiva**.

Zaragoza, a 1 de octubre de 2013.

Fdo: Consuelo Fortuño Turmo